STANFORD UNIVERSITY

Guidance and Control Laboratory

DAA/ AMES

SUDAAR #553

THE DESIGN OF MULTIRATE DIGITAL CONTROL SYSTEMS

by

Martin Conrad Berg
Stanford University
Guidance & Control Laboratory
Department of Aeronautics & Astronautics
Stanford, CA 94305

Research Supported by
The NASA Dryden Flight Research Center
Grant NSG-4002

March 1986

Abstract

As technology in digital hardware advances, commensurate advances in the performance of digital compensators will be expected to follow. To meet these performance demands, engineers are resorting to complex design configurations that include multiple sensors and control effectors. For such a system, to obtain the best performance at a fixed level of real-time computation load, it is often necessary to sample the signals for the various sensors and control effectors at different rates. Surprisingly, methods for synthesizing digital compensators are well-developed only for the special case where all sampling rates are the same.

The successive loop closures synthesis method is the only method for multirate (MR) synthesis in common use. It is an ad-hoc method in that cross-coupling effects between control loops are dealt with as cross-loop disturbances.

For single-rate (SR) systems, algorithms that solve for steady-state optimal quadratic regulators and steady-state Kalman estimators are popular for synthesizing multivariable compensators. Recently, extensions of these algorithms have been developed that handle MR sampling policies. A disadvantage of this method is that the optimal compensators tend to be unnecessarily complex.

A new method for MR synthesis is introduced in this work. It requires a gradient-search solution to a constrained optimization problem. Some advantages of this method are that the control laws for all control loops are synthesized simultaneously, taking full advantage of all cross-coupling effects (which is the principal advantage of the optimal control law synthesis method), and that simple, low-order compensator structures are easily accommodated (which is the principal advantage of the successive loop closures synthesis method). An algorithm and an associated computer program for solving the constrained optimization problem are described.

The successive loop closures, optimal control, and constrained optimization synthesis methods are applied to two example design problems. A series of compensator pairs are synthesized for each example problem. Each pair consists of one MR compensator and one SR compensator that are designed to satisfy the same performance objectives with sampling rates such that the computation loads for their real-time operation are the same. Except for cases involving very fast sampling rates compared to the characteristic frequencies of the desired closed-loop poles, the MR compensators are shown to consistently out-perform their SR counterparts.

The successive loop closures, optimal control, and constrained optimization synthesis methods are compared, in the context of the two example design problems. For the mass-spring-mass problem, where good rejection of random disturbances is the performance objective, the successive loop closures synthesis method is shown to be ideal. For the two link robot arm problem, the constrained optimization synthesis method is shown to be a good method for synthesizing a second-order compensator to control the tip position.

For the two link robot arm problem, an optimal MR compensator provides the best responses to tip positioning commands in terms of speed and overshoot. But this compensator is periodically time varying and consequently the computation load for its real-time operation is high. It is shown that such periodicity is not a prerequisite for good performance. A time-invariant MR compensator with virtually identical performance characteristics is synthesized using the constrained optimization synthesis method.

Acknowledgements

I sincerely thank my advisor, Professor J. David Powell, for his support and guidance throughout the course of my research at Stanford.

I also thank the other members of my reading committee, Professors Arthur E. Bryson, Jr. and Gene F. Franklin, for their thorough review and constructive comments.

For their financial support, I very much appreciate the help of the NASA Dryden Flight Research Center under Grant NSG-4002.

For the unique research environment that they create, I wish to thank the entire faculty of the Guidance and Control Laboratory at Stanford.

I especially thank my fellow students for their constant support and friendship. My interactions with them have contributed more to my experiences here than they will ever know.

For the support and encouragement that caused me to consider this opportunity years ago, I thank Professor Kurt R. Galle at the University of Washington and Dr. Uy-Loi Ly at the Boeing Company.

Finally, I thank my parents, whose support and encouragement I carry with me always. This thesis is dedicated to them.

Table of Contents

List of Figures

Page

List of Tables

Page

Chapter 1

Introduction

This chapter contains four sections. Section 1.1 discusses the motivation for this research. Section 1.2 is a summary of related works from the literature. Section 1.3 is an outline of the thesis. Section 1.4 lists the principal contributions of this research.

§1.1 Purpose. As technology in digital hardware advances, commensurate advances in the performance of digital compensators will be expected to follow. To meet these performance demands, engineers are resorting to complex design configurations that include multiple sensors and control effectors. For such a system, to obtain the best performance at a fixed level of real-time computation load, it is often necessary to sample the signals for the various sensors and control effectors at different rates. Surprisingly, methods for synthesizing digital compensators are well-developed only for the special case where all sampling rates are the same.

The purpose of this research was to develop new understanding in the area of multirate (MR) synthesis. In this document, we consider three methods for MR synthesis: (1) the successive loop closures synthesis method; (2) the optimal control law synthesis method; and (3) the constrained optimization synthesis method.

The one-loop-at-a-time successive loop closures synthesis method is virtually the only method for MR synthesis in common use. It is an ad-hoc method in that cross-coupling effects between control loops are dealt with as cross-loop disturbances.

An advantage of the optimal control law synthesis method is that the control laws for all control loops are synthesized simultaneously, taking full advantage of all cross coupling effects. A disadvantage of this method is that the optimal compensators tend to be unnecessarily complex.

The constrained optimization synthesis method is a new method that we developed as part of this research. It requires a gradient-search solution to a constrained optimzation problem. Some advantages of this method are that the control laws for all control loops are synthesized simultaneously, taking full advantage of all cross-coupling effects (which is the principal advantage of the optimal control law synthesis method), and that simple, low-order compensator structures are easily accommodated (which is the principal advantage of the successive loop closures synthesis method).

§1.2 Related Literature. In an exhaustive survey of some 50 technical papers, Walton (1981) describes advances in the analysis and synthesis of MR systems from 1953 to 1981. In the early fifties, digital control systems were invariably single-input, single-output systems. Multirate sampling got its start at this time as an analysis tool. The idea was to attach a "phantom" sampler to the input or output port of such a system, and operate it at some integer multiple of the basic sampling rate to detect inter-sample ripple.

Sklansky (1955a, 55b) developed the "frequency decomposition" method for determining a transfer function that describes the input-output behavior of a such a system. Shortly thereafter, Kranc (1955, 56, 57a, 57b, 57c) developed the "switch

decomposition" method, which is an extension of the frequency decomposition method that allows sampling rates with ratios that are rational numbers. Chapter 9 of Ragazzini and Franklin (1958) includes an execllent discussion of the frequency decomposition and switch decomposition methods. A multi-input, multi-output generalization of the switch decomposition method was recently developed by Whitbeck and Didaleusky (1980, 81).

While, in principle, these methods provide a means to determine a transfer function that describes the input-output behavior of MR systems, in practice they are extremely cumbersome. Ragazzini and Franklin (1958) discuss an application of the switch decomposition method to a single-input, single-output system having two samplers with sampling periods T and T/n. The resulting transfer function includes n parallel forward paths, each with delay and advance operators. Rao (1979) uses switch decomposition to design a compensator for a color videotape recorder, but the applications are limited to single loops with two samplers and sampling rates related by a small integer. What Rao describes as a "heuristic" overall approach is yet another example of the use of the successive loop closures synthesis method.

The first treatment of MR systems from a state-space perspective appeared in an excellent paper by Kalman and Bertram (1959). This paper presents a method for formulating a discrete state model to represent a MR sampled data system. For the general case of multiple sampling rates, the discrete state model is time-varying. For the special case where, for every pair of sampling rates, the ratio of the sampling rates is a rational number, the discrete state model is periodically time-varying.

Amit and Powell (1980, 81) were the first to fully capitalize on Kalman and Bertram's contribution. They developed a computer program to solve the steady-state optimal quadratic regulator and the steady-state Kalman estimator synthesis problems for a MR sampled data system using eigenvector decomposition.

Glasson *et al.* (1979, 80, 81, 82) developed a computer program for determining the same steady-state optimal regulator and steady-state Kalman estimator solutions by a different method. They obtained the solutions by propagating the Riccati difference equations to steady-state, which is a computationally costly approach compared to eigenvector decomposition. As an example, they design an optimal MR compensator to control the lateral dynamics of the space shuttle during reentry (Glasson and Dawd, 1981).

A disadvantage of optimal MR compensators is that the steady-state regulator and Kalman estimator gain matrices are periodically time-varying. However, in a study involving a simple mass-spring-mass system and fifty different steady-state optimal regulator designs, Amit and Powell (1980, 1981) found only a few cases where the performance of an optimal MR regulator was significantly better than that of its time-invariant averaged-gains approximation.

The successive loop closures synthesis method is an indirect approach to MR synthesis in that a MR compensator is determined by successively closing a series of SR control loops. It is an ad-hoc method in that cross-coupling effects between control loops are dealt with as cross-loop disturbances. Except in connection with applications, the successive loop closures synthesis method has received little attention in the literature. Walton (1981) does not mention it. Albanes (1981), Chrétien (1982), Penchuck (1983), and Rao (1979) describe some applications of the successive loop closures synthesis method to practical design problems.

The constrained optimization synthesis method, which is the new method that was developed in connection with this work, is an outgrowth of the work of Amit and Powell (1980, 1981) on optimal MR compensators. The idea is to solve the steady-state optimal MR quadratic regulator problem, but with the solution constrained to be a linear, constant-gain, state feedback control law.

Broussard and Halyo (1984) developed an algorithm to solve an almost identical optimization problem. A problem with their approach is that it cannot handle control laws that fail to stabilize the closed-loop system. Thus, the designer must determine a stabilizing guess for the control law before the numerical search can begin and special logic must be used to (hopefully) avoid destabilizing control laws during the search.

To avoid these difficulties, we chose a different approach. The algorithm that we developed relies on a gradient search. The gradients are calculated exactly, using a closed-form expression, and a finite-time performance index is used so that a stablizing initial guess for the control law is not required. The idea of using a finite-time performance index is due to Ly (1982), from his work developing the SANDY algorithm for synthesizing robust analog compensators.

An important additional advantage of our method is that it accommodates linear constraints on the elements of the feedback gain matrices. This is an important feature because, by adding compensator states to the state vector and constraining certain feedback gain elements to fixed values, compensators of arbitrary structure and dynamic order can be synthesized.

§1.3 Thesis Outline. Chapter 2 deals with discretization. It is largely a review of material in Amit (1980). Section 2.1 presents a method for generating a discrete state model to represent a MR sampled data system. Section 2.2 presents a method for generating the discrete equivalent to an analog quadratic performance index for a MR sample data system.

Chapter 3 presents a review of the successive loop closures and optimal control law synthesis methods. The successive loop closures synthesis method is discussed in Section 3.1. We derive the equations for the steady-state optimal MR quadratic regulator and the steady-state MR Kalman estimator in Section 3.2.

The constrained optimization synthesis method is the subject of Chapter 4. Section 4.1 discusses the motivation that led to the development of the method. A formal statement of the constrained optimization problem is presented in Section 4.2. An algorithm for determining a solution is presented in Section 4.3. The solution algorithm requires explicit calculations of the value of a performance index and of the gradient of this performance index with respect to the compensator parameters. Closed-form expressions for calculating this value and gradient are derived in Sections 4.4 and 4.5, respectively. Section 4.6 describes some features of the constrained optimization synthesis method that make it a powerful tool for synthesizing low-order compensators.

Chapters 5 and 6 deal with applications. Chapter 5 deals with a mass-spring-mass (MKM) system, where good rejection of random disturbances is the performance objective. Chapter 6 deals with a two link robot arm (TLA) system, where fast servo control of the tip position is the performance objective. These studies demonstrate: (1) some potential performance benefits of MR compensation over SR compensation, for the same real-time computation load; and (2) some relative merits of the three synthesis methods.

The conclusions of this research and the recommendations for further research are presented in Chapter 7.

§1.4 Contributions. The primary contributions of this research are:

1. The constrained optimization synthesis method for synthesizing MR or SR digital compensators. The advantages of this method are: (1) the control laws for all control loops are synthesized simultaneously, taking full advantage of all cross-coupling effects; and (2) the compensator structure is arbitrary, and simple, low-order compensator structures are easily accommodated. The constrained optimization synthesis method relys on a gradient search to

determine a control law that minimizes a quadratic performance index. The gradients are calculated exactly, using a closed-form expression, and a finite-time performance index is used so that a stabilizing initial guess for the control laws is not required.

2. Design studies involving applications of the successive loop closures, optimal control, and constrained optimization synthesis methods that demonstate: (1) some potential performance benefits of MR compensation over SR compensation, for the same real-time computation load; and (2) some relative merits of the three synthesis methods. The design studies involve two representative design problems, so that the results are applicable to a large class of systems.

Chapter 2

Discretization

This chapter deals with discretization. It is largely a review of material in Amit (1980). Section 2.1 presents a method for generating a discrete state model to represent a MR sampled data system. Section 2.2 looks at the stability of the resulting discrete state model. Section 2.3 presents a method for generating the discrete equivalent to an analog quadratic performance index for a MR sampled data system. The presentations refer to a particular MR sampling policy. As presented, however, the methods are quite general and extensions to accommodate more complicated sampling policies are noted.

§2.1 Discretization of an Analog Plant. In their excellent paper, Kalman and Bertram (1959) describe a method for generating a discrete state model to represent a MR sampled data system. For the general case of a linear, time-invariant, analog plant and multiple sampling rates, the discrete state model is time-varying. For the special case of a linear, time-invariant, analog plant and multiple sampling rates where, for every pair of sampling rates, the ratio of the sampling rates is a rational number, the discrete state model is periodically time-varying. We shall deal exclusively with sampling policies that result in a discrete state model that

is periodically time-varying. This class of sampling policies actually includes more than just the special case where every sampling-rates ratio is a rational number; for details see Kalman and Bertram (1959).

An example MR sampling policy is shown in Figure 2.1. The time lines show the sampling schedules for four samplers. For sampler #1, the sampling period is $24T$, and the first sample is taken at time $1T$. For samplers #2, #3, and #4, the sampling periods are $4T$, $3T$, and T, respectively, and the first samples are taken at time 0.

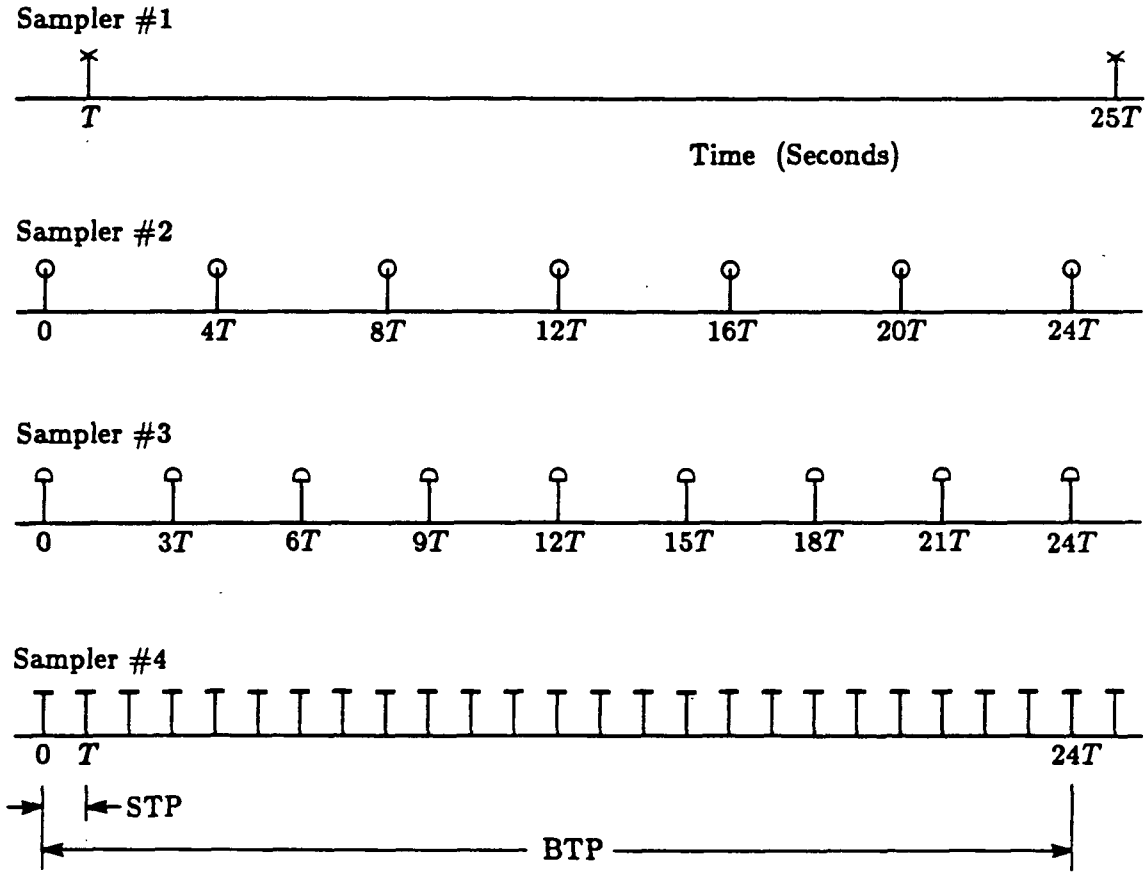

Figure 2.1 Example MR Sampling Policy.

When Kalman and Bertram's method is applied, the period of repetition of the discrete state model is the same as the period of repetition of the sampling

policy. We shall call this period of repetition the BTP (basic time period). For the sampling policy in Figure 2.1, the BTP is $24T$. Another characteristic time of importance in MR sampling policies is the STP (shortest time period). For the sampling policy in Figure 2.1, the STP is T. When Kalman and Bertram's method is applied, the STP of the sampling policy is the time step for the discrete state model. (For more complicated sampling policies, it may be advantageous to apply Kalman and Bertram's method in a slightly different way, and split the BTP into STPs of unequal lengths. For further information, see Kalman and Bertram (1959).)

To apply Kalman and Bertram's method to the sampling policy of Figure 2.1, let P represent the number of STPs per BTP. A sampler is "fast" if it is active at every STP. A sampler is "slow" if it is not active at every STP. We define P diagonal "switching matrices" that describe the sampling schedules for the slow samplers. The ith diagonal element of the nth switching matrix is 1 or 0, depending upon whether the ith sampler is active or inactive, respectively, at the start of the nth STP. For the sampling policy in Figure 2.1, the switching matrices are:

$$S(0) = S(12) = \text{Diag}(0,1,1)\,, \tag{1}$$

$$S(1) = \text{Diag}(1,0,0)\,, \tag{2}$$

$$\begin{aligned} S(2) &= S(5) = S(7) = S(10) = S(11) = S(13) \\ &= S(14) = S(17) = S(19) = S(22) = S(23) = \text{Diag}(0,0,0)\,, \end{aligned} \tag{3}$$

$$S(3) = S(6) = S(9) = S(15) = S(18) = S(21) = \text{Diag}(0,0,1)\,, \tag{4}$$

$$S(4) = S(8) = S(16) = S(20) = \text{Diag}(0,1,0)\,, \tag{5}$$

where $\text{Diag}(d_1, \ldots, d_n)$ is a diagonal matrix with diagonal elements $d_1, d_2, \ldots, d_n$.

We assume that the analog plant is represented by the state equation

$$\dot{p}(t) = F\,p(t) + \bar{G}\,\bar{u}(t) + \tilde{G}\,\tilde{u}(t) + G_w\,w(t)\,, \tag{6}$$

for $t \geq 0$, where

$$\bar{u}(t) = [\, u_1(t) \quad u_2(t) \quad u_3(t) \,]^{\mathrm{T}} , \tag{7}$$

and $p(t)$ is the state vector, $u_1(t)$, $u_2(t)$, and $u_3(t)$ are scalar control inputs, $\tilde{u}(t)$ is a vector control input, and $w(t)$ is the process noise input vector. The process noise input vector $w(t)$ is assumed to be stationary, zero-mean, gaussian white noise of intensity W, so that

$$\mathrm{E}\{w(t)\, w^{\mathrm{T}}(\tau)\} = W\, \delta(t-\tau) , \tag{8}$$

where $\mathrm{E}\{\cdot\}$ is the expected value operator, and $\delta(\cdot)$ is the Dirac delta function.

We assume that the sampling policy is applied such that $u_i(t)$ is generated via a zero-order hold according to the sampling schedule for sampler #i, for $i = 1, 2, 3$, and $\tilde{u}(t)$ is generated via a vector zero-order hold according to the sampling schedule for sampler #4. Let

$$\Phi \triangleq \mathrm{e}^{FT} , \tag{9}$$

$$\bar{\Gamma} \triangleq \int_0^T \mathrm{e}^{Ft}\, dt\, \bar{G} , \tag{10}$$

$$\tilde{\Gamma} \triangleq \int_0^T \mathrm{e}^{Ft}\, dt\, \tilde{G} . \tag{11}$$

(For a numerical algorithm to solve for Φ, $\bar{\Gamma}$, and $\tilde{\Gamma}$ given values for F, $\bar{G}$, $\tilde{G}$, and T, see Van Loan (1978).) Let $I_{\bar{u}}$, $I_{\tilde{u}}$, and I_p be identity matrices with the same number of rows and columns as there are elements in $\bar{u}(t)$, $\tilde{u}(t)$, and $p(t)$, respectively. The state equation for the discrete state model is then

$$x(m, n+1) = A(n)\, x(m,n) + B(n)\, u(m,n) + B_w\, w(m,n) , \tag{12}$$

for $m = 0, 1, \ldots$ and $n = 0, 1, \ldots, P-1$, where

$$x(m,n) \triangleq [\, p^{\mathrm{T}}(m,n) \quad h_1(m,n) \quad h_2(m,n) \quad h_3(m,n) \,]^{\mathrm{T}} , \tag{13}$$

$$u(m,n) \triangleq [\, u_1(m,n) \quad u_2(m,n) \quad u_3(m,n) \quad \tilde{u}^{\mathrm{T}}(m,n) \,]^{\mathrm{T}} , \tag{14}$$

$$w(m,n) \triangleq \int_{(mP+n)T}^{(mP+n+1)T} e^{F((mP+n+1)T-t)}\, G_w\, w(t)\, dt\,, \tag{15}$$

$$A(n) \triangleq \begin{bmatrix} \Phi & \bar{\Gamma}\,(I_{\bar{u}} - S(n)) \\ 0 & (I_{\bar{u}} - S(n)) \end{bmatrix}, \tag{16}$$

$$B(n) \triangleq \begin{bmatrix} \bar{\Gamma}\, S(n) & \tilde{\Gamma} \\ S(n) & 0 \end{bmatrix}, \tag{17}$$

$$B_w \triangleq \begin{bmatrix} I_p \\ 0 \end{bmatrix}. \tag{18}$$

In (13), $p(m,n)$ represents the state $p(t)$ of the analog plant at the $(mP+n)$th sampling instant. In the same equation, $h_i(m,n)$ represents the analog control input $u_i(t)$, for $i=1,\ 2,\ 3$, at the $(mP+n)$th sampling instant. In (14), $u_i(m,n)$ is the discrete control input that generates $h_i(m,n)$, for $i=1,\ 2,\ 3$. In the same equation, $\tilde{u}(m,n)$ represents the analog control input $\tilde{u}(t)$ at the $(mP+n)$th sampling instant. In (15), $w(m,n)$ represents the effect of the analog process noise that occurs between the $(mP+n-1)$th and $(mP+n)$th sampling instants on the state of the analog plant at the $(mP+n)$th sampling instant. The sequence $w(m,n)$ is a stationary, zero-mean, gaussian, purely random sequence with covariance W_{D}, where

$$W_{\mathrm{D}} = \int_0^T e^{F\,t}\, G_w\, W\, G_w^{\mathrm{T}}\, e^{F^{\mathrm{T}}\,t}\, dt\,. \tag{19}$$

(For a numerical algorithm to solve for W_{D} given values for F, G_w, W, and T, see Van Loan (1978).)

The discrete state model in (12) through (19) is complete, except for the measurement equation. Fortunately, a MR measurement scheme is no more difficult to handle than a SR one, except that the sampling schedules for *all* samplers must be taken into account when determining the STP and BTP of the sampling policy. The discrete measurement equation that corresponds to the discrete state equation in (12) is

$$y(m,n) = H(n)\, x(m,n) + v(m,n)\,, \tag{20}$$

where $y(m,n)$ represents the discrete measurement vector at the $(mP+n)$th sampling instant, and $v(m,n)$ represents the discrete measurement noise vector at the $(mP+n)$th sampling instant. If the sampler for the ith sensor is active at the $(mP+n)$th sampling instant, to yield a scalar measurement

$$y_i(m,n) = H_i\, x(m,n) + v_i(m,n)\,, \tag{21}$$

where $v_i(m,n)$ is measurement noise, then the ith row of $H(n)$ is H_i. If the sampler for the ith sensor is inactive at the $(mP+n)$th sampling instant, then the ith row of $H(n)$ is zero. The discrete measurement noise vector $v(m,n)$ is assumed to be a periodically stationary, zero-mean, gaussian, purely random sequence with covariance $V(n)$, so that

$$\mathrm{E}\{v(k,l)\, v^{\mathrm{T}}(m,n)\} = V(n)\, \delta(kP+l, mP+n)\,, \tag{22}$$

where

$$\delta(i,j) \triangleq \begin{cases} 1 & \text{if } i=j\,; \\ 0 & \text{if } i \neq j\,. \end{cases} \tag{23}$$

§2.2 Closed-Loop BTP State Transition Matrix. For the discrete state model in (12), suppose that the control input vector $u(m,n)$ satisfies

$$u(m,n) = -C(n)\, x(m,n)\,. \tag{24}$$

Let

$$\Phi_{\mathrm{BTP}} \triangleq \Big(A(P-1) - B(P-1)C(P-1)\Big) * \cdots * \Big(A(0) - B(0)C(0)\Big)\,. \tag{25}$$

We shall refer to the time-invariant matrix Φ_{BTP} as the "closed-loop BTP state transition matrix" for the system. The eigenvalues of Φ_{BTP} indicate whether the closed-loop system is stable in the BTP-to-BTP sense. Note that a time-invariant

analog to Φ_{BTP} for the STP-to-STP state transitions does not exist, because the discrete state equation is time-varying from one STP to the next.

§2.3 Discretization of an Analog Performance Index. For the MR sampled data system composed of the analog plant in (6) plus the MR sampling policy in Figure 2.1, the analog performance index to be considered is

$$\tilde{J}(N) \triangleq \mathrm{E}\Big\{\frac{1}{2NPT}\int_0^{NPT}\begin{bmatrix}p(t)\\u(t)\end{bmatrix}^{\mathrm{T}}\begin{bmatrix}\tilde{Q} & 0\\0 & \tilde{R}\end{bmatrix}\begin{bmatrix}p(t)\\u(t)\end{bmatrix}dt\Big\}, \tag{26}$$

where

$$u(t) \triangleq [\,\bar{u}^{\mathrm{T}}(t) \quad \tilde{u}^{\mathrm{T}}(t)\,]^{\mathrm{T}}\,. \tag{27}$$

In (26), $\mathrm{E}\{\cdot\}$ is the expected value operator, T is the STP for the sampling policy, P is the number of STPs per BTP for the sampling policy, $\tilde{Q}$ is a symmetric, positive semidefinite matrix, and $\tilde{R}$ is a symmetric, positive definite matrix.

For the analog plant in (6), let

$$p(m,n,t) \triangleq p((mP+n)T+t)\,, \tag{28}$$

$$\bar{u}(m,n,t) \triangleq \bar{u}((mP+n)T+t)\,, \tag{29}$$

$$\tilde{u}(m,n,t) \triangleq \tilde{u}((mP+n)T+t)\,. \tag{30}$$

Using the properties of the expected value operator, (26) can be written

$$\tilde{J}(N) = \frac{1}{2NPT}\sum_{m=0}^{N-1}\sum_{n=0}^{P-1} j(m,n)\,, \tag{31}$$

where

$$j(m,n) = \mathrm{E}\Big\{\int_0^T\begin{bmatrix}p(m,n,t)\\\bar{u}(m,n,t)\\\tilde{u}(m,n,t)\end{bmatrix}^{\mathrm{T}}\begin{bmatrix}\tilde{Q} & 0\\0 & \tilde{R}\end{bmatrix}\begin{bmatrix}p(m,n,t)\\\bar{u}(m,n,t)\\\tilde{u}(m,n,t)\end{bmatrix}dt\Big\}. \tag{32}$$

But $p(m,n,t)$, $\bar{u}(m,n,t)$, and $\tilde{u}(m,n,t)$ are easily written in terms of the discrete state, control input, and process noise input vectors in (12). Letting

$$\Phi(t) \triangleq \mathrm{e}^{Ft}\,, \tag{33}$$

$$\bar{\Gamma}(t) \triangleq \int_0^t e^{F\tau}\, d\tau\, \bar{G}\,, \tag{34}$$

$$\tilde{\Gamma}(t) \triangleq \int_0^t e^{F\tau}\, d\tau\, \tilde{G}\,, \tag{35}$$

$$\tilde{w}(t_2,t_1) \triangleq \int_{t_1}^{t_2} e^{F(t_2-\tau)} w(\tau)\, d\tau\,, \tag{36}$$

we obtain

$$\begin{bmatrix} p(m,n,t) \\ \bar{u}(m,n,t) \\ \tilde{u}(m,n,t) \end{bmatrix} = \begin{bmatrix} \Phi(t) & \bar{\Gamma}(t)\,(I_{\bar{u}} - S(n)) \\ 0 & (I_{\bar{u}} - S(n)) \\ 0 & 0 \end{bmatrix} x(m,n) + \begin{bmatrix} \bar{\Gamma}(t)\,S(n) & \tilde{\Gamma}(t) \\ S(n) & 0 \\ 0 & I_{\tilde{u}} \end{bmatrix} u(m,n) + \begin{bmatrix} \tilde{w}((mP+n)T+t,(mP+n)T) \\ 0 \end{bmatrix}, \tag{37}$$

for $0 < t \leq T$.

Let

$$K(n) \triangleq \begin{bmatrix} I_p & 0 & 0 & 0 \\ 0 & (I_{\bar{u}} - S(n)) & S(n) & 0 \\ 0 & 0 & 0 & I_{\tilde{u}} \end{bmatrix}, \tag{38}$$

$$Q_{\mathrm{D}} \triangleq \int_0^T \begin{bmatrix} \Phi(t) & \bar{\Gamma}(t) & \tilde{\Gamma}(t) \\ 0 & I_{\bar{u}} & 0 \\ 0 & 0 & I_{\tilde{u}} \end{bmatrix}^{\mathrm{T}} \begin{bmatrix} \tilde{Q} & 0 \\ 0 & \tilde{R} \end{bmatrix} \begin{bmatrix} \Phi(t) & \bar{\Gamma}(t) & \tilde{\Gamma}(t) \\ 0 & I_{\bar{u}} & 0 \\ 0 & 0 & I_{\tilde{u}} \end{bmatrix} dt\,. \tag{39}$$

(For a numerical algorithm to solve for Q_{D} given values for F, $\bar{G}$, $\tilde{G}$, $\tilde{Q}$, $\tilde{R}$, and T, see Van Loan (1978).) From (32), substituting for $p(m,n,t)$, $\bar{u}(m,n,t)$, and $\tilde{u}(m,n,t)$ using (37), and taking advantage of the fact that

$$\mathrm{E}\left\{\tilde{w}((mP+n)T+t,(mP+n)T) \begin{bmatrix} x(m,n) \\ u(m,n) \end{bmatrix}^{\mathrm{T}}\right\} = 0\,, \tag{40}$$

for $0 < t \leq T$, we obtain

$$j(m,n) = \mathrm{E}\left\{ \begin{bmatrix} x(m,n) \\ u(m,n) \end{bmatrix}^{\mathrm{T}} \begin{bmatrix} Q(n) & N(n) \\ N^{\mathrm{T}}(n) & R(n) \end{bmatrix} \begin{bmatrix} x(m,n) \\ u(m,n) \end{bmatrix} + \int_0^T \tilde{w}^{\mathrm{T}}((mP+n)T+t,(mP+n)T)\, \tilde{Q}\, \tilde{w}((mP+n)T+t,(mP+n)T)\, dt \right\}, \tag{41}$$

where

$$\begin{bmatrix} Q(n) & N(n) \\ N^{\mathrm{T}}(n) & R(n) \end{bmatrix} = K^{\mathrm{T}}(n)\, Q_{\mathrm{D}}\, K(n)\,. \tag{42}$$

Except for multiplying Q_D by $K^T(n)$ and $K(n)$, for $n=0, 1, \ldots, P-1$, we see from (42), (38), and (39) that it is no more difficult to determine the $Q(n)$, $N(n)$, and $R(n)$ than it is to determine the corresponding matrices Q, N, and R in the SR case. (See Katz (1974) for the corresponding SR development.) Furthermore, for the purpose of synthesizing a feedback control law that minimizes $\tilde{J}(N)$, the positive semidefinite integral term in (41) can be dropped. This leaves the simpler performance index

$$J(N) \triangleq \mathrm{E}\left\{\frac{1}{2NPT}\sum_{m=0}^{N-1}\sum_{n=0}^{P-1}\begin{bmatrix}x(m,n)\\u(m,n)\end{bmatrix}^T\begin{bmatrix}Q(n) & N(n)\\N^T(n) & R(n)\end{bmatrix}\begin{bmatrix}x(m,n)\\u(m,n)\end{bmatrix}\right\}. \quad (43)$$

Chapter 3

Review of Existing Synthesis Methods

This chapter presents a review of two popular methods for MR synthesis. The successive loop closures synthesis method is discussed in Section 3.1. It is virtually the only method for MR synthesis in common use. The optimal control law synthesis method is discussed in Section 3.2. The equations that define the steady-state optimal MR quadratic regulator and the steady-state MR Kalman estimator are derived from the corresponding equations for a time-varying SR problem.

§3.1 Successive Loop Closures. The successive loop closures synthesis method is an indirect approach to MR synthesis in that a MR compensator is determined by successively closing a series of SR control loops. To design the $(n+1)$th control loop, the approximation is often made that the first n loops respond instantaneously. This approximation is often not necessary: If the sampling rates for the different control loops are integer multiples of one another, and if the control loops are closed in order according to sampling rate, from fastest sampling to slowest, then it is a simple matter to obtain an exact representation of the plant with the first n loops closed for use in designing the $(n+1)$th loop.

Consider an analog plant represented by the state equation

$$\dot{p}(t) = F\,p(t) + \tilde{G}\,\tilde{u}(t) + \bar{G}\,\bar{u}(t)\,, \tag{1}$$

where $p(t)$ is the state vector, and $\tilde{u}(t)$ and $\bar{u}(t)$ are the control input vectors. Suppose that the $\tilde{u}$ loop is closed first, at a sampling rate $1/T$, using the discrete control law

$$\tilde{u}(k) = -\tilde{C}\,p(k)\,. \tag{2}$$

If the $\bar{u}$ loop is to operate at a slower sampling rate $1/PT$, where P is a positive, nonzero integer, then the state model for the $\bar{u}$ loop design is

$$p(k+1) = (A - \tilde{B}\tilde{C})^P\,p(k) + \bar{B}\,\bar{u}(k)\,, \tag{3}$$

where

$$A \triangleq \mathrm{e}^{FT}, \qquad \tilde{B} \triangleq \int_0^T \mathrm{e}^{Ft}\,dt\tilde{G}\,, \qquad \bar{B} \triangleq \int_0^{PT} \mathrm{e}^{Ft}\,dt\bar{G}\,. \tag{4}$$

Dynamic compensation is handled just as easily. For the analog plant in (1), suppose that the state model that describes the $\tilde{u}$ control loop is:

$$\tilde{c}(k+1) = \tilde{A}_{\tilde{c}}\,\tilde{c}(k) + \tilde{A}_p\,p(k) + \tilde{B}_{\tilde{u}}\,\tilde{u}(k)\,, \tag{5}$$

$$\tilde{u}(k) = -\tilde{C}_{\tilde{c}}\,\tilde{c}(k) - \tilde{C}_p\,p(k)\,, \tag{6}$$

where $\tilde{c}(k)$ is the compensator state vector. The state equation for the $\bar{u}$ loop design is then

$$\begin{bmatrix} p(k+1) \\ \tilde{c}(k+1) \end{bmatrix} = \begin{bmatrix} A - \tilde{B}\,\tilde{C}_p & -\tilde{B}\,\tilde{C}_{\tilde{c}} \\ \tilde{A}_p - \tilde{B}_{\tilde{u}}\,\tilde{C}_p & \tilde{A}_{\tilde{c}} - \tilde{B}_{\tilde{u}}\,\tilde{C}_{\tilde{c}} \end{bmatrix}^P \begin{bmatrix} p(k) \\ \tilde{c}(k) \end{bmatrix} + \begin{bmatrix} \bar{B} \\ 0 \end{bmatrix} \bar{u}(k)\,. \tag{7}$$

§3.2 Optimal Control. In this section, the equations that define the steady-state optimal MR quadratic regulator and the steady-state MR Kalman estimator are derived. The developments are not rigorous. They are a useful supplement to the works of Glasson *et al.* (1979, 80, 81, 82) and of Amit and Powell (1980, 81).

We start with the finite-time optimal MR control law synthesis problem, because the equations for the finite-time optimal MR quadratic regulator and the finite-time MR Kalman estimator are easily determined from the corresponding equations for a time-varying SR system. The equations for the steady-state optimal MR quadratic regulator and the steady-state MR Kalman estimator are then easily determined from the corresponding finite-time equations.

Finite Time Case. An open-loop MR sampled-data plant is assumed to be represented by the discrete state model:

$$x(m,n+1) = A(n)\,x(m,n) + B(n)\,u(m,n) + w(m,n)\,, \tag{8}$$

$$y(m,n) = H(n)x(m,n) + v(m,n)\,, \tag{9}$$

for $m=0,\ 1,\ \ldots$ and $n=0,\ 1,\ \ldots,\ P-1$, where P is the number of STPs per BTP for the sampling policy, $x(m,n)$, $u(m,n)$, $w(m,n)$, $y(m,n)$, and $v(m,n)$ are the discrete state, control input, process noise input, measurement output, and sensor noise input vectors, respectively.

The initial state $x(0,0)$ is assumed to be a zero-mean, gaussian random vector with covariance X_0. The process noise and measurement noise vectors $w(m,n)$ and $v(m,n)$ are assumed to be zero-mean, gaussian, purely random sequences, with covariances $W(n)$ and $V(n)$, respectively, so that

$$\mathrm{E}\{w(k,l)\,w^{\mathrm{T}}(m,n)\} = W(n)\,\delta(kP+l, mP+n)\,, \tag{10}$$

$$\mathrm{E}\{v(k,l)\,v^{\mathrm{T}}(m,n)\} = V(n)\,\delta(kP+l, mP+n)\,, \tag{11}$$

where $\mathrm{E}\{\cdot\}$ is the expected value operator, and

$$\delta(i,j) \triangleq \begin{cases} 1 & \text{if } i=j\,; \\ 0 & \text{if } i\neq j\,. \end{cases} \tag{12}$$

The process noise, measurement noise, and initial state are assumed to be mutually uncorrelated.

Given the measurements $y(0,0)$, $y(0,1)$, ..., $y(N-1,P-1)$, the finite-time optimal control law synthesis problem is to determine a control sequence $u(0,0)$, $u(0,1)$, ..., $u(N-1,P-1)$ that minimizes the performance index

$$J(N) \triangleq \frac{1}{2}\mathrm{E}\Big\{x^{\mathrm{T}}(N,0)\,Q_{\mathrm{N}}\,x(N,0) + \sum_{m=0}^{N-1}\sum_{n=0}^{P-1}\begin{bmatrix}x(m,n)\\u(m,n)\end{bmatrix}^{\mathrm{T}}\begin{bmatrix}Q(n) & N(n)\\N^{\mathrm{T}}(n) & R(n)\end{bmatrix}\begin{bmatrix}x(m,n)\\u(m,n)\end{bmatrix}\Big\}, \tag{13}$$

where N is a positive, nonzero integer, Q_{N} is symmetric, positive semidefinite matrix, each $Q(n)$ is a symmetric, positive semidefinite matrix, and each $R(n)$ is a symmetric, positive definite matrix.

Except for the double indexing scheme for the independent variables, the finite-time optimal MR control law synthesis problem looks just like a finite-time optimal SR control law synthesis problem for a time-varying system. The equations for the optimal MR regulator and the MR Kalman estimator can consequently be determined by inspection of the well-known solution to this related problem. From Section 14.7 of Bryson and Ho (1975), by incorporating the double indexing scheme for the independent variables and making simple substitutions in notation only, we obtain the equations for the finite-time optimal MR regulator and the finite-time MR Kalman estimator:

$$u(m,n) = -C(m,n)\hat{x}(m,n)\,, \tag{14}$$

$$\hat{x}(m,n) = \bar{x}(m,n) + K(m,n)[y(m,n) - H(n)\bar{x}(m,n)]\,, \tag{15}$$

$$\bar{x}(m,n+1) = A(n)\hat{x}(m,n) + B(n)u(m,n)\,, \tag{16}$$

where

$$C(m,n) = [B^{\mathrm{T}}(n)\Lambda(m,n+1)B(n) + R(n)]^{-1} * [B^{\mathrm{T}}(n)\Lambda(m,n+1)A(n) + N^{\mathrm{T}}(n)]\,, \tag{17}$$

$$K(m,n) = \Omega(m,n)H^{\mathrm{T}}(n)[H(n)\Omega(m,n)H^{\mathrm{T}}(m,n) + V(n)]^{-1}\,, \tag{18}$$

and $\Lambda(m,n)$ satisfies

$$\Lambda(m,n) = A^{\mathrm{T}}(n)\Lambda(m,n+1)A(n) - C^{\mathrm{T}}(m,n)[R(n) + B^{\mathrm{T}}(n)\Lambda(m,n+1)B(n)]C(m,n) + Q(n)\,, \tag{19}$$

for $\Lambda(N,0) = Q_{\mathrm{N}}$; and $\Omega(m,n)$ satisfies

$$\Omega(m,n+1) = A(m,n)\{\Omega(m,n) - K(m,n)[H(n)\Omega(m,n)H^{\mathrm{T}}(m,n) + V(n)]K^{\mathrm{T}}(m,n)\}A^{\mathrm{T}}(m,n) + W(n)\,, \tag{20}$$

for $\Omega(0,0) = X_0$.

In fact, the discretization procedures of Chapter 2 are not quite compatible with (14) through (20). To make the dimensions of $u(m,n)$ and $y(m,n)$ the same for all n, the discretization procedures of Section 2.1 add, for some values of n, dummy control inputs to $u(m,n)$ and dummy measurements to $y(m,n)$. The $R(n)$ in (17) and the $V(n)$ in (18) are consequently singular for some values of n. The required fix is to delete the columns of zeros from each $B(n)$ and $N(n)$ and the rows and columns of zeros from each $R(n)$ that correspond to the dummy elements of $u(m,n)$, to delete the rows of zeros from each $H(n)$ and the rows and columns of zeros from each $V(n)$ that correspond to the dummy elements of $y(m,n)$, and to subsequently deal with control input and measurement vectors that have dimensions that vary with n. The resulting $Q(n)$ and $R(n)$ are guaranteed to be positive semidefinite and positive definite, respectively, if the corresponding matrices $\tilde{Q}$ and $\tilde{R}$ in the analog performance index are positive semidefinite and positive definite, respectively. The resulting $V(n)$ are guaranteed to be nonsingular if every physical measurement is subject to noise.

Infinite Time Case. The numerical values for $C(m,n)$ and $K(m,n)$ can be determined by propagating the matrix difference equation for $\Lambda(m,n)$ in (19)

backward and applying (17), and by propagating the matrix difference equation for $\Omega(m,n)$ in (20) forward and applying (18). Amit (1980) describes conditions involving the controllability and observability of the open-loop plant that guarantee that these difference equations settle to unique steady-state values for large N. Not surprisingly, these steady-state values are *not* constant in the usual sense, but are functions of n. It follows, from (17) and (18), that the steady-state regulator gain matrices and the steady-state Kalman estimator gain matrices are periodic in n as well; that is that

$$C(m,n) \to C(n) \qquad \text{and} \qquad K(m,n) \to K(n)$$

for large N. Substituting these steady-state gain matrices into (14) and (16), we obtain the equations for the steady-state optimal MR regulator and the steady-state MR Kalman estimator:

$$u(m,n) = -C(n)\hat{x}(m,n)\,, \tag{21}$$

$$\hat{x}(m,n) = \bar{x}(m,n) + K(n)[y(m,n) - H(n)\bar{x}(m,n)]\,, \tag{22}$$

$$\bar{x}(m,n+1) = A(n)\hat{x}(m,n) + B(n)u(m,n)\,. \tag{23}$$

Amit and Powell (1980, 81) developed a computer program to solve for $C(n)$ and $K(n)$ efficiently using eigenvector decomposition. In this approach, a discrete state model and performance index are formed that describe the BTP-to-BTP responses of the MR system. The BTP-to-BTP state model and the BTP-to-BTP performance index are time-invariant and SR. They are used to determine the steady-state values for $\Lambda(m,0)$ and $\Omega(m,0)$ directly, using an eigenvector decomposition algorithm designed for a time-invariant SR problem. The steady-state values for $\Lambda(m,n)$ and $\Omega(m,n)$, for $n = 1, 2, \ldots, P-1$, are then easily determined by propagating the matrix difference equations for $\Lambda(m,n)$ and $\Omega(m,n)$ backward and forward, respectively, for $P-1$ steps. The steady-state values for

the gain matrices $C(n)$ and $K(n)$, for $n=0, 1, \ldots, P-1$, are determined from the steady-state values for $\Lambda(m,n)$ and $\Omega(m,n)$ using (17) and (18).

Chapter 4

The Constrained Optimization Synthesis Method

This chapter describes a new method for MR synthesis. We shall call it the constrained optimization synthesis method. Section 4.1 discusses the motivation that led to the development of the method. Section 4.2 presents a formal statement of the constrained optimization problem. A numerical search algorithm for determining a solution is presented in Section 4.3. The search algorithm requires explicit calculations of the value of a performance index and of the gradient of this performance index with respect to the compensator parameters. Closed-form expressions for calculating this value and gradient are derived in Sections 4.4 and 4.5, respectively. Section 4.6 describes some features of the method that make it a powerful tool for synthesizing low-order compensators.

§4.1 Motivation. Amit and Powell (1980, 81) developed an efficient method for synthesizing optimal MR compensators. The constrained optimization synthesis method is an outgrowth of their work. An advantage of the optimal synthesis methods is that the control laws for all control loops are synthesized simultaneously, taking full advantage of all cross-coupling effects. A disadvantage of the optimal methods is that the resulting compensators are periodically time-varying. However,

in a study involving a simple mass-spring-mass system and fifty different steady-state optimal MR regulator designs, Amit and Powell (1980, 1981) found only a few cases where the performance of an optimal regulator was significantly better than that of its time-invariant averaged-gains approximation. This suggests that periodicity is often not a prerequisite for good performance in MR compensators.

The constrained optimization synthesis method was developed to bridge the gap between the optimal control law synthesis method and the successive loop closures synthesis method. Some advantages of the constrained optimization synthesis method are: (1) the control laws for all control loops are synthesized simultaneously, taking full advantage of all cross-coupling effects (which is the principal advantage of the optimal control law synthesis method); and (2) simple, low-order compensator structures are easily accommodated (which is the principal advantage of the successive loop closures synthesis method). The basic idea behind the constrained optimization synthesis method is to solve the steady-state optimal MR regulator problem, but with the solution constrained to be a linear, time-invariant, state feedback control law. In addition, linear constraints can be imposed on the elements of the feedback gain matrices. This is important because, by adding compensator states to the state vector and constraining certain feedback gain elements to fixed values, compensators of arbitrary structure and dynamic order can be synthesized.

§4.2 Statement of the Constrained Optimization Problem. An open-loop plant is assumed to be represented by the periodically time-varying discrete state equation

$$x(m,n+1) = A(n)\,x(m,n) + B(n)\,u(m,n) + w(m,n)\,, \tag{1}$$

for $m = 0,\ 1,\ \ldots$ and $n = 0,\ 1,\ \ldots,\ P-1$, where $x(m,n)$, $u(m,n)$, and $w(m,n)$ are the state, control input, and process noise input vectors, respectively, and P is

the number of STPs per BTP for the sampling policy. The initial state $x(0,0)$ is assumed to be zero. Let

$$\delta(i,j) \triangleq \begin{cases} 1 & \text{if } i = j; \\ 0 & \text{if } i \neq j. \end{cases} \tag{2}$$

The process noise is assumed to be a periodically stationary, zero-mean, gaussian, purely random sequence, with covariance $W(n)$, so that

$$\mathrm{E}\{w(k,l)\, w^{\mathrm{T}}(m,n)\} = W(n)\, \delta(kP+l, mP+n)\,, \tag{3}$$

where $\mathrm{E}\{\cdot\}$ is the expected value operator. The process noise and initial state are assumed to be uncorrelated.

The control input $u(m,n)$ is constrained to be a linear, periodically time-varying function of the state, so that

$$u(m,n) = -C(n)\, x(m,n)\,. \tag{4}$$

The $C(n)$ are further constrained to satisfy

$$C(n) = \sum_{r=0}^{M-1} \alpha_r(n) C_r\,, \tag{5}$$

where M is a positive, nonzero integer less than or equal to P, each C_r is a constant matrix, and the $\alpha_r(n)$ are scalar functions of n that satisfy

$$\alpha_p(n)\, \alpha_q(n) = \delta(p,q)\,. \tag{6}$$

The synthesis problem is to determine a set of feedback gains C_r, for $r = 0, 1, \ldots, M-1$, such that the performance index

$$J_{\mathrm{ss}} \triangleq \lim_{N\to\infty} \frac{1}{2N} \mathrm{E}\left\{ \sum_{m=0}^{N-1} \sum_{n=0}^{P-1} \begin{bmatrix} x(m,n) \\ u(m,n) \end{bmatrix}^{\mathrm{T}} \begin{bmatrix} Q(n) & N(n) \\ N^{\mathrm{T}}(n) & R(n) \end{bmatrix} \begin{bmatrix} x(m,n) \\ u(m,n) \end{bmatrix} \right\} \tag{7}$$

is minimized, where each $Q(n)$ and $R(n)$ is a symmetric, positive semidefinite matrix.

Remarks. Two points merit special attention:

1. In (5), M and the $\alpha_r(n)$ are design parameters. For example, if

$$M \triangleq P \qquad \text{and} \qquad \alpha_r(n) \triangleq \delta(r,n)\,, \tag{8}$$

then

$$u(m,n) = -C_n\, x(m,n)\,, \tag{9}$$

and the control law is periodically time-varying, in the same manner as the unconstrained optimal solution. On the other hand, if $M \triangleq 1$, then

$$u(m,n) = -C_0\, x(m,n)\,, \tag{10}$$

and the control law is time-invariant.

2. Although it appears that only full state feedback control laws are considered, in practice this is not the case. As shown in Section 4.6, additional linear constraints can be imposed on the elements of the C_r. This is important because, by including compensator states in the state vector and constraining certain feedback gain elements to fixed values, compensators of arbitrary structure and dynamic order can be synthesized.

§4.3 Solution Algorithm. The constrained optimization synthesis problem is difficult to solve. A closed-form solution for the feedback gains is not known. One approach is to invent an algorithm that conducts a numerical search for a set of feedback gains that satisfies the necessary conditions

$$\frac{\partial J_{SS}}{\partial C_r} = 0\,, \tag{11}$$

for $r = 0, 1, \ldots, M-1$, where $\partial J_{SS}/\partial C_r$ is the matrix whose (i,j)th element contains the gradient of J_{SS} with respect to the (i,j)th element of C_r.

Broussard and Halyo (1984) developed such an algorithm, for the case of a time-invariant (i.e., $M = 1$) output feedback control law. A problem with their approach is that it cannot handle control laws that fail to stabilize the stable closed-loop system. Consequently, the designer must determine a stabilizing guess for the control law before the numerical search can begin and special logic must be used to (hopefully) avoid destabilizing control laws during the search.

To avoid these difficulties, we chose a different approach. The key to this approach is the finite-time performance index

$$J(N) \triangleq \frac{1}{2N}\mathrm{E}\left\{\sum_{m=0}^{N-1}\sum_{n=0}^{P-1}\begin{bmatrix} x(m,n) \\ u(m,n) \end{bmatrix}^{\mathrm{T}}\begin{bmatrix} Q(n) & N(n) \\ N^{\mathrm{T}}(n) & R(n) \end{bmatrix}\begin{bmatrix} x(m,n) \\ u(m,n) \end{bmatrix}\right\}, \tag{12}$$

where the $Q(n)$, $R(n)$, and $N(n)$ are the same matrices as in (7). The performance index $J(N)$ is the finite-time analog of J_{SS}, in that

$$J_{\mathrm{SS}} = \lim_{N\to\infty} J(N)\,. \tag{13}$$

The advantage of working with $J(N)$ instead of J_{SS} is that the gradients $\partial J(N)/\partial C_r$, for $r = 0, 1, \ldots, M-1$, exist (and can be calculated) whether or not the closed-loop system is stable. The ultimate goal of every optimization is to determine a set of feedback gains C_r, for $r = 0, 1, \ldots, M-1$, such that (11) is satisfied. This is easily accomplished using $J(N)$ by setting N to a value that is large enough that NPT, which is the finite time for the performance index $J(N)$, is very large compared to the characteristic times of the closed-loop system.

The computer program that we developed for solving the constrained optimization problem is AMS (Algorithm for Multirate Synthesis). AMS reads the analog state model, the analog performance index, the sampling rates, the initial guess for the feedback gains, and the value of N from an input file. After forming the equivalent discrete state model and the equivalent discrete performance index, it conducts a numerical search to determine a set of feedback gains that minimizes

$J(N)$. The QNMDER algorithm is used for the numerical search. The QNMDER algorithm is a gradient-type search algorithm developed by Gill and Murray (1972, 81). It requires explicit evaluations of $J(N)$ and $\partial J(N)/\partial C_r$, for $r=0, 1, \ldots, M-1$, and uses these to determine an approximate Hessian matrix.

Once AMS has determined a set of feedback gains that minimizes $J(N)$, the gains are saved on a disk file and execution stops. The designer must then determine whether the gains represent a steady-state solution. If not, it is a simple matter to run AMS again, for a larger value of N, using the saved feedback gains from the previous run as the initial guess. This cycle is repeated for larger and larger values of N. A steady-state solution is obtained when NPT gets to be very large compared to the characteristic times of the closed-loop system.

At the early stages of an optimization, when the initial guess for the feedback gains is poor, N must be set to a small value to avoid numerical overflow. In each subsequent run, as the quality of the initial guess for the feedback gains improves, N can be increased by, say, a factor of 10. By re-optimizing for larger and larger values of N, a steady-state solution is usually obtained after 4 or 5 runs. See the User's Guide to AMS in Appendix C for further details.

The key to solving the constrained optimization problem by this method lies in an efficient means for evaluating $J(N)$ and $\partial J(N)/\partial C_r$. The expressions for $J(N)$ and $\partial J(N)/\partial C_r$ that we developed for AMS are derived in Sections 4.4 and 4.5. These are closed-form expressions with the special property that the number of machine operations per evaluation does not depend on N. For these expressions to be valid, the single restriction is that the closed-loop BTP state transition matrix must be diagonalizable (see Section 2.2 for a definition of the closed-loop BTP state transition matrix). This is not a serious limitation, however, because a non-diagonalizable closed-loop BTP state transition matrix rarely occurs.

§4.4 Closed-Form Expression for the Performance Index. The derivation in this section is modeled after similar developments for time-varying analog systems by Kleinman, Fortman, and Athans (1968), Johnson and Athans (1970), and Levine and Athans (1970). The key to the derivation is the following theorem, which treats the general case of a time-varying system, and includes provisions for a random initial state and a quadratic penalty on the terminal state. A proof of Theorem 1 is given in Appendix B.

Theorem 1. An open-loop plant is assumed to be represented by the time-varying discrete state equation

$$x(t+1) = A(t)\,x(t) + B(t)\,u(t) + w(t)\,, \tag{14}$$

for $t = t_0, t_0+1, \ldots, t_1-1$, where $x(t)$, $u(t)$, and $w(t)$ are the state, control input, and process noise input vectors, respectively. The initial state $x(t_0)$ is assumed to be a zero-mean, gaussian random vector, with covariance X_0. Let

$$\delta(i,j) \triangleq \begin{cases} 1 & \text{if } i = j\,; \\ 0 & \text{if } i \neq j\,. \end{cases} \tag{15}$$

The process noise $w(t)$ is assumed to be a zero-mean, gaussian, purely random sequence, with covariance $W(t)$, so that

$$\mathrm{E}\{w(t)\,w^{\mathrm{T}}(\tau)\} = W(t)\,\delta(t,\tau)\,, \tag{16}$$

where $\mathrm{E}\{\cdot\}$ is the expected value operator. The process noise and initial state are assumed to be uncorrelated.

The performance index is assumed to be

$$J \triangleq \frac{1}{2}\mathrm{E}\left\{x^{\mathrm{T}}(t_1)\,Q_1\,x(t_1) + \sum_{\tau=t_0}^{t_1-1} \begin{bmatrix} x(\tau) \\ u(\tau) \end{bmatrix}^{\mathrm{T}} \begin{bmatrix} Q(\tau) & N(\tau) \\ N^{\mathrm{T}}(\tau) & R(\tau) \end{bmatrix} \begin{bmatrix} x(\tau) \\ u(\tau) \end{bmatrix}\right\}, \tag{17}$$

where Q_1 is a symmetric, positive semidefinite matrix, and each $Q(\tau)$ and $R(\tau)$ is a symmetric, positive semidefinite matrix.

The control input is assumed to satisfy

$$u(t) = -C(t)\,x(t)\,. \tag{18}$$

Let

$$\Phi(\tau,t) \triangleq \Big[A(\tau-1)-B(\tau-1)\,C(\tau-1)\Big]\Big[A(\tau-2)-B(\tau-2)\,C(\tau-2)\Big] * \cdots * \Big[A(t)-B(t)\,C(t)\Big]\,, \tag{19}$$

for $t=t_0,\, t_0+1,\, \ldots,\, t_1-1$ and $\tau=t+1,\, t+2,\, \ldots,\, t_1$, and let

$$\Phi(t,t) \triangleq I_x\,, \tag{20}$$

where I_x an identity matrix with the same number of rows and columns as there are elements in $x(t)$. Let

$$Q_C(\mu) \triangleq \begin{bmatrix} I \\ -C(\mu) \end{bmatrix}^{\mathrm{T}} \begin{bmatrix} Q(\mu) & N(\mu) \\ N^{\mathrm{T}}(\mu) & R(\mu) \end{bmatrix} \begin{bmatrix} I \\ -C(\mu) \end{bmatrix}. \tag{21}$$

Let

$$\Psi(\tau) \triangleq \Phi^{\mathrm{T}}(t_1,\tau)\,Q_1\,\Phi(t_1,\tau) + \sum_{\substack{\mu=\tau \\ \tau\neq t_1}}^{t_1-1} \Phi^{\mathrm{T}}(\mu,\tau)\,Q_C(\mu)\,\Phi(\mu,\tau)\,. \tag{22}$$

Then: an equivalent expression for the performance index in (17) is

$$J = \frac{1}{2}\mathrm{E}\Big\{x^{\mathrm{T}}(t_0)\,\Psi(t_0)\,x(t_0) + \sum_{\tau=t_0}^{t_1-1} w^{\mathrm{T}}(\tau)\,\Psi(\tau+1)\,w(\tau)\Big\}\,. \tag{23}$$

Now we apply Theorem 1 to the constrained optimization problem of Section 4.2, where:

$$t_0 = 0\,, \tag{24}$$

$$t_1 = NP\,, \tag{25}$$

$$X_0 = 0\,, \tag{26}$$

$$Q_1 = 0\,, \tag{27}$$

$$A(mP+n) = A(n)\,, \tag{28}$$

$$B(mP+n) = B(n)\,, \tag{29}$$

$$W(mP+n) = W(n)\,, \tag{30}$$

$$Q(mP+n) = Q(n)\,, \tag{31}$$

$$N(mP+n) = N(n)\,, \tag{32}$$

$$R(mP+n) = R(n)\,, \tag{33}$$

$$C(mP+n) = C(n)\,, \tag{34}$$

for $m=0, 1, \ldots$ and $n=0, 1, \ldots, P-1$, where P is the number of STPs per BTP for the sampling policy.

From (17), using (27), (24), and (25), and substituting for the summation using

$$\sum_{r=0}^{NP-1} f(r) = \sum_{m=0}^{N-1} \sum_{n=0}^{P-1} f(mP+n)\,, \tag{35}$$

and using (31) through (33), we obtain

$$J = \frac{1}{2}\mathrm{E}\left\{\sum_{m=0}^{N-1} \sum_{n=0}^{P-1} \begin{bmatrix} x(mP+n) \\ u(mP+n) \end{bmatrix}^{\mathrm{T}} \begin{bmatrix} Q(n) & N(n) \\ N^{\mathrm{T}}(n) & R(n) \end{bmatrix} \begin{bmatrix} x(mP+n) \\ u(mP+n) \end{bmatrix}\right\}, \tag{36}$$

so that, comparing (12) with (36),

$$J(N) = \frac{1}{N}\, J\,. \tag{37}$$

From (19) and (20), using (28), (29), and (34), we obtain

$$\Phi(mP+n, mP+l) = \Phi(n, l)\,, \tag{38}$$

for $l=0, 1, \ldots, P$ and $n=l, l+1, \ldots, P$, and

$$\Phi(mP+n, kP+l) = \Phi(n, 0)\,[\Phi(P, 0)]^{m-k-1}\,\Phi(P, l)\,, \tag{39}$$

for $k=0, 1, \ldots, N-2$, $m=k+1, k+2, \ldots, N-1$, $l=0, 1, \ldots, P$, and $n=0, 1, \ldots, P$.

From (23), substituting for $\Psi(\tau+1)$ using (22), and using (24) through (27), (16), (37), and the properties of the expected value operator, we obtain

$$J(N) = \frac{1}{2N} \sum_{\tau=0}^{NP-1} \sum_{\substack{\mu=\tau+1 \\ \tau \neq NP-1}}^{NP-1} \Phi^{\mathrm{T}}(\mu, \tau+1)\, Q_C(\mu)\, \Phi(\mu, \tau+1)\, W(\tau)\,. \tag{40}$$

From (40), substituting for the double summation using

$$\begin{aligned} \sum_{\tau=0}^{NP-1} \sum_{\substack{\mu=\tau+1 \\ \tau \neq NP-1}}^{NP-1} f(\mu,\tau) &= \sum_{\substack{\tau=1 \\ NP \neq 1}}^{NP-1} \sum_{\mu=0}^{\tau-1} f(\tau,\mu) \\ &= \sum_{m=0}^{N-1} \sum_{\substack{n=1 \\ P \neq 1}}^{P-1} \sum_{l=1}^{n} f(mP+n, mP+l-1) \\ &\quad + \sum_{\substack{m=1 \\ N \neq 1}}^{N-1} \sum_{n=0}^{P-1} \sum_{k=0}^{m-1} \sum_{l=1}^{P} f(mP+n, kP+l-1)\,, \end{aligned} \tag{41}$$

we obtain

$$J(N) = \frac{1}{2N}(\mathcal{H}_1 + \mathcal{H}_2)\,, \tag{42}$$

where

$$\begin{aligned} \mathcal{H}_1 = \sum_{m=0}^{N-1} \sum_{\substack{n=1 \\ P \neq 1}}^{P-1} \sum_{l=1}^{n} &\Phi^{\mathrm{T}}(mP+n, mP+l) \\ &* Q_C(mP+n)\, \Phi(mP+n, mP+l)\, W(mP+l-1)\,, \end{aligned} \tag{43}$$

$$\begin{aligned} \mathcal{H}_2 = \sum_{\substack{m=1 \\ N \neq 1}}^{N-1} \sum_{n=0}^{P-1} \sum_{k=0}^{m-1} \sum_{l=1}^{P} &\Phi^{\mathrm{T}}(mP+n, kP+l) \\ &* Q_C(mP+n)\, \Phi(mP+n, kP+l)\, W(kP+l-1)\,. \end{aligned} \tag{44}$$

From (43), substituting for $\Phi(mP+n, mP+l)$ using (38), and using (21) and (30) through (34), we obtain

$$\mathcal{H}_1 = \sum_{m=0}^{N-1} \sum_{\substack{n=1 \\ P \neq 1}}^{P-1} \sum_{l=1}^{n} \Phi^{\mathrm{T}}(n, l)\, Q_C(n)\, \Phi(n, l)\, W(l-1)\,. \tag{45}$$

Let

$$\overline{Q}_C(l) \triangleq \sum_{n=l}^{P-1} \Phi^T(n,l)\, Q_C(n)\, \Phi(n,l)\,, \tag{46}$$

for $l=0, 1, \ldots, P-1$. From (45), substituting for the triple summation using

$$\sum_{m=0}^{N-1} \sum_{\substack{n=1 \\ P\neq 1}}^{P-1} \sum_{l=1}^{n} f(n,l) = N \sum_{\substack{l=1 \\ P\neq 1}}^{P-1} \sum_{n=l}^{P-1} f(n,l)\,, \tag{47}$$

and using (46), we obtain

$$\mathcal{H}_1 = N \sum_{\substack{l=1 \\ P\neq 1}}^{P-1} \overline{Q}_C(l)\, W(l-1)\,. \tag{48}$$

From (44), substituting for $\Phi(mP+n, kP+l)$ using (39), and using (21) and (30) through (34), we obtain

$$\mathcal{H}_2 = \sum_{\substack{m=1 \\ N\neq 1}}^{N-1} \sum_{n=0}^{P-1} \sum_{k=0}^{m-1} \sum_{l=1}^{P} \Phi^T(P,l)\, [\Phi^T(P,0)]^{m-k-1}\, \Phi^T(n,0)\, Q_C(n) \\ * \Phi(n,0)\, [\Phi(P,0)]^{m-k-1}\, \Phi(P,l)\, W(l-1)\,. \tag{49}$$

From (49), using (46), we obtain

$$\mathcal{H}_2 = \sum_{l=1}^{P} \Phi^T(P,l)\, \mathcal{H}_{21}\, \Phi(P,l)\, W(l-1)\,, \tag{50}$$

where

$$\mathcal{H}_{21} = \sum_{\substack{m=1 \\ N\neq 1}}^{N-1} \sum_{k=0}^{m-1} [\Phi^T(P,0)]^{m-k-1}\, \overline{Q}_C(0)\, [\Phi(P,0)]^{m-k-1}\,. \tag{51}$$

Now we assume that the closed-loop BTP state transition matrix $\Phi(P,0)$ is diagonalizable, so that $\Phi(P,0)$ can be written as

$$\Phi(P,0) = S\, \Lambda\, S^{-1}\,, \tag{52}$$

where S is an nonsingular matrix and Λ is a diagonal matrix. Let λ_i represent the ith diagonal element of Λ. Let $(\cdot)_{ij}$ represent the operator that returns the (i,j)th element of its matrix argument. From (51), using (52), we obtain

$$\mathcal{H}_{21} = S^{-T}\,\overline{\mathcal{H}}_{21}\,S^{-1}\,, \tag{53}$$

where

$$\left(\overline{\mathcal{H}}_{21}\right)_{ij} = \left(S^T\,\overline{Q}_C(0)\,S\right)_{ij} \sum_{\substack{m=0\\ N\neq 1}}^{N-2} \sum_{k=0}^{m} \lambda_i^{m-k}\,\lambda_j^{m-k}\,. \tag{54}$$

Together, (42), (48), (50), (53), (54), (46), (38), (39), and (52) represent a formulation for $J(N)$ that is ideally suited to the optimization algorithm of Section 4.3. In particular, the summation in (54), which is the only summation with limits that depend on N, can be evaluated in closed-form using formulas in Gradhteyn and Ryzhik (1980), so that the number of machine operations per performance index evaluation is independent of N.

§4.5 Closed-Form Expression for the Gradient. The derivation in this section is modeled after similar developments for time-varying analog systems by Kleinman, Fortman, and Athans (1968), Johnson and Athans (1970), and Levine and Athans (1970). The key to the derivation is the following theorem, which treats the general case of a time-varying system, and includes provisions for a random initial state and a quadratic penalty on the terminal state. A proof of Theorem 2 is given in Appendix B.

Theorem 2. An open-loop plant is assumed to be represented by the time-varying discrete state equation

$$x(t+1) = A(t)\,x(t) + B(t)\,u(t) + w(t)\,, \tag{55}$$

for $t = t_0, t_0+1, \ldots, t_1-1$, where $x(t)$, $u(t)$, and $w(t)$ are the state, control input, and process noise input vectors, respectively. The initial state $x(t_0)$ is assumed to be a zero-mean, gaussian random vector, with covariance X_0. Let

$$\delta(i,j) \triangleq \begin{cases} 1 & \text{if } i = j; \\ 0 & \text{if } i \neq j. \end{cases} \tag{56}$$

The process noise $w(t)$ is assumed to be a zero-mean, gaussian, purely random sequence, with covariance $W(t)$, so that

$$\mathrm{E}\{w(t)\, w^{\mathrm{T}}(\tau)\} = W(t)\, \delta(t,\tau)\,, \tag{57}$$

where $\mathrm{E}\{\cdot\}$ is the expected value operator. The process noise and initial state are assumed to be uncorrelated.

The performance index is assumed to be

$$J \triangleq \frac{1}{2}\mathrm{E}\left\{x^{\mathrm{T}}(t_1)\, Q_1\, x(t_1) + \sum_{\tau=t_0}^{t_1-1} \begin{bmatrix} x(\tau) \\ u(\tau) \end{bmatrix}^{\mathrm{T}} \begin{bmatrix} Q(\tau) & N(\tau) \\ N^{\mathrm{T}}(\tau) & R(\tau) \end{bmatrix} \begin{bmatrix} x(\tau) \\ u(\tau) \end{bmatrix}\right\}, \tag{58}$$

where Q_1 is a symmetric, positive semidefinite matrix, and each $Q(\tau)$ and $R(\tau)$ is a symmetric, positive semidefinite matrix.

The control input is assumed to satisfy

$$u(t) = -C(t)\, x(t)\,. \tag{59}$$

The $C(t)$ are further assumed to satisfy

$$C(t) = \sum_{\tau=0}^{M-1} \alpha_\tau(t) C_\tau\,, \tag{60}$$

where M is a positive, nonzero integer less than or equal to $t_1 - t_0$, each C_τ is a constant matrix, and the $\alpha_\tau(t)$ are scalar functions of t that satisfy

$$\alpha_p(t)\, \alpha_q(t) = \delta(p,q)\,. \tag{61}$$

Let

$$\Phi(\tau,t) \triangleq \Big[A(\tau-1)-B(\tau-1)\,C(\tau-1)\Big]\Big[A(\tau-2)-B(\tau-2)\,C(\tau-2)\Big] * \cdots * \Big[A(t)-B(t)\,C(t)\Big], \tag{62}$$

for $t=t_0, t_0+1, \ldots, t_1-1$ and $\tau=t+1, t+2, \ldots, t_1$, and let

$$\Phi(t,t) \triangleq I_x, \tag{63}$$

where I_x an identity matrix with the same number of rows and columns as there are elements in $x(t)$. Let

$$Q_C(\mu) \triangleq \begin{bmatrix} I \\ -C(\mu) \end{bmatrix}^{\mathrm{T}} \begin{bmatrix} Q(\mu) & N(\mu) \\ N^{\mathrm{T}}(\mu) & R(\mu) \end{bmatrix} \begin{bmatrix} I \\ -C(\mu) \end{bmatrix}. \tag{64}$$

Let

$$\Psi(\tau) \triangleq \Phi^{\mathrm{T}}(t_1,\tau)\,Q_1\,\Phi(t_1,\tau) + \sum_{\substack{\mu=\tau \\ \tau\neq t_1}}^{t_1-1} \Phi^{\mathrm{T}}(\mu,\tau)\,Q_C(\mu)\,\Phi(\mu,\tau). \tag{65}$$

Let

$$\overline{\Psi}(\tau) \triangleq -N^{\mathrm{T}}(\tau) + R(\tau)\,C(\tau) - B^{\mathrm{T}}(\tau)\,\Psi(\tau+1)\Big[A(\tau)-B(\tau)\,C(\tau)\Big]. \tag{66}$$

Then: if $\partial J/\partial C_r$ represents the matrix whose (i,j)th element contains the gradient of J with respect to the (i,j)th element of C_r,

$$\frac{\partial J}{\partial C_r} = \Big[\sum_{\tau=t_0}^{t_1-1} \alpha_r(\tau)\,\overline{\Psi}(\tau)\,\Phi(\tau,t_0)\,X_0\,\Phi^{\mathrm{T}}(\tau,t_0)\Big] + \Big[\sum_{\substack{\tau=t_0+1 \\ t_0\neq t_1-1}}^{t_1-1} \sum_{\mu=t_0}^{\tau-1} \alpha_r(\tau)\,\overline{\Psi}(\tau)\,\Phi(\tau,\mu+1)\,W(\mu)\,\Phi^{\mathrm{T}}(\tau,\mu+1)\Big], \tag{67}$$

for $r=0, 1, \ldots, M-1$.

Now we apply Theorem 2 to the constrained optimization problem of Section 4.3, where:

$$t_0 = 0, \tag{68}$$

$$t_1 = NP\,, \tag{69}$$

$$X_0 = 0\,, \tag{70}$$

$$Q_1 = 0\,, \tag{71}$$

$$A(mP+n) = A(n)\,, \tag{72}$$

$$B(mP+n) = B(n)\,, \tag{73}$$

$$W(mP+n) = W(n)\,, \tag{74}$$

$$Q(mP+n) = Q(n)\,, \tag{75}$$

$$N(mP+n) = N(n)\,, \tag{76}$$

$$R(mP+n) = R(n)\,, \tag{77}$$

$$\alpha_r(mP+n) = \alpha_r(n)\,, \tag{78}$$

$$C(mP+n) = C(n)\,, \tag{79}$$

for $m=0, 1, \ldots$ and $n=0, 1, \ldots, P-1$, where P is the number of STPs per BTP for the sampling policy.

From (61), using (71), (68), and (69), and substituting for the summation using

$$\sum_{\tau=0}^{NP-1} f(\tau) = \sum_{m=0}^{N-1}\sum_{n=0}^{P-1} f(mP+n)\,, \tag{80}$$

and using (75) through (77), we obtain

$$J = \frac{1}{2}\mathrm{E}\Big\{\sum_{m=0}^{N-1}\sum_{n=0}^{P-1}\begin{bmatrix} x(mP+n) \\ u(mP+n)\end{bmatrix}^{\mathrm{T}}\begin{bmatrix} Q(n) & N(n) \\ N^{\mathrm{T}}(n) & R(n)\end{bmatrix}\begin{bmatrix} x(mP+n) \\ u(mP+n)\end{bmatrix}\Big\}\,, \tag{81}$$

so that, comparing (12) with (81),

$$J(N) = \frac{1}{N}J\,. \tag{82}$$

From (62) and (63), using (72), (73), and (79), we obtain

$$\Phi(mP+n, mP+l) = \Phi(n,l)\,, \tag{83}$$

for $l=0, 1, \ldots, P$ and $n=l, l+1, \ldots, P$, and

$$\Phi(mP+n,kP+l) = \Phi(n,0)\,[\Phi(P,0)]^{m-k-1}\,\Phi(P,l)\,, \tag{84}$$

for $k=0, 1, \ldots, N-2$, $m=k+1, k+2, \ldots, N-1$, $l=0, 1, \ldots, P$, and $n=0, 1, \ldots, P$.

Let

$$C(\tau,\mu) \triangleq \alpha_\tau(\tau)\left[-N^{\mathrm{T}}(\tau) + R(\tau)C(\tau)\right]\Phi(\tau,\mu+1)\,W(\mu)\,\Phi^{\mathrm{T}}(\tau,\mu+1)\,, \tag{85}$$

and let

$$D(\tau,\mu) \triangleq \alpha_\tau(\tau)\left\{-B^{\mathrm{T}}(\tau)\,\Psi(\tau+1)\left[A(\tau)-B(\tau)\,C(\tau)\right]\right\} * \Phi(\tau,\mu+1)\,W(\mu)\,\Phi^{\mathrm{T}}(\tau,\mu+1)\,. \tag{86}$$

From (67), substutuuting for $\overline{\Psi}(\tau)$ using (66), and using (70), (68), (69), (82), (85), and (86), we obtain

$$\frac{\partial J(N)}{\partial C_\tau} = \frac{1}{N}\Big[\sum_{\substack{\tau=1\\ NP\neq 1}}^{NP-1}\sum_{\mu=0}^{\tau-1} C(\tau,\mu) + D(\tau,\mu)\Big]\,. \tag{87}$$

To simplify the notation, we assume that $P \geq 2$. From (87), substituting for the double sum over $C(\tau,\mu)$ using

$$\sum_{\tau=1}^{NP-1}\sum_{\mu=0}^{\tau-1} f(\tau,\mu) = \sum_{m=0}^{N-1}\sum_{n=1}^{P-1}\sum_{l=0}^{n-1} f(mP+n,mP+l) + \sum_{\substack{m=1\\ N\neq 1}}^{N-1}\sum_{n=0}^{P-1}\sum_{k=0}^{m-1}\sum_{l=0}^{P-1} f(mP+n,kP+l)\,, \tag{88}$$

and for the double sum over $D(\tau,\mu)$ using

$$\begin{aligned}\sum_{\tau=1}^{NP-1}\sum_{\mu=0}^{\tau-1} f(\tau,\mu) &= \sum_{l=0}^{P-2} f((N-1)P+P-1,(N-1)P+l)\\ &+ \sum_{\substack{n=1\\ P\neq 2}}^{P-2}\sum_{l=0}^{n-1} f((N-1)P+n,(N-1)P+l) + \sum_{\substack{m=1\\ N\neq 1}}^{N-1}\sum_{l=0}^{P-2} f((m-1)P+P-1,(m-1)P+l)\\ &+ \sum_{\substack{m=0\\ N\neq 1}}^{N-2}\sum_{\substack{n=1\\ P\neq 2}}^{P-2}\sum_{l=0}^{n-1} f(mP+n,mP+l) + \sum_{\substack{k=0\\ N\neq 1}}^{N-2}\sum_{l=0}^{P-1} f((N-1)P+P-1,kP+l)\end{aligned}$$

$$+\sum_{n=0}^{P-2}\sum_{\substack{k=0\\N\neq 1}}^{N-2}\sum_{l=0}^{P-1} f((N-1)P+n,kP+l)+\sum_{\substack{m=2\\N\neq 1\\N\neq 2}}^{N-1}\sum_{k=0}^{m-2}\sum_{l=0}^{P-1} f((m-1)P+P-1,kP+l)$$

$$+\sum_{\substack{m=1\\N\neq 1\\N\neq 2}}^{N-2}\sum_{n=0}^{P-2}\sum_{k=0}^{m-1}\sum_{l=0}^{P-1} f(mP+n,kP+l)\,, \tag{89}$$

we obtain

$$\frac{\partial J(N)}{\partial C_r}=\frac{1}{N}\Big(C_1+C_2+D_1+D_2+D_3+D_4+D_5+D_6+D_7+D_8\Big)\,, \tag{90}$$

where

$$C_1=\sum_{m=0}^{N-1}\sum_{n=1}^{P-1}\sum_{l=0}^{n-1} C(mP+n,mP+l)\,, \tag{91}$$

$$C_2=\sum_{\substack{m=1\\N\neq 1}}^{N-1}\sum_{n=0}^{P-1}\sum_{k=0}^{m-1}\sum_{l=0}^{P-1} C(mP+n,kP+l)\,, \tag{92}$$

$$D_1=\sum_{l=0}^{P-2} D((N-1)P+P-1,(N-1)P+l)\,, \tag{93}$$

$$D_2=\sum_{\substack{n=1\\P\neq 2}}^{P-2}\sum_{l=0}^{n-1} D((N-1)P+n,(N-1)P+l)\,, \tag{94}$$

$$D_3=\sum_{\substack{m=1\\N\neq 1}}^{N-1}\sum_{l=0}^{P-2} D((m-1)P+P-1,(m-1)P+l)\,, \tag{95}$$

$$D_4=\sum_{\substack{m=0\\N\neq 1}}^{N-2}\sum_{\substack{n=1\\P\neq 2}}^{P-2}\sum_{l=0}^{n-1} D(mP+n,mP+l)\,, \tag{96}$$

$$D_5=\sum_{\substack{k=0\\N\neq 1}}^{N-2}\sum_{l=0}^{P-1} D((N-1)P+P-1,kP+l)\,, \tag{97}$$

$$D_6=\sum_{n=0}^{P-2}\sum_{\substack{k=0\\N\neq 1}}^{N-2}\sum_{l=0}^{P-1} D((N-1)P+n,kP+l)\,, \tag{98}$$

$$\mathcal{D}_7 = \sum_{\substack{m=2 \\ N\neq 1 \\ N\neq 2}}^{N-1} \sum_{k=0}^{m-2} \sum_{l=0}^{P-1} \mathcal{D}((m-1)P+P-1, kP+l)\,, \tag{99}$$

$$\mathcal{D}_8 = \sum_{\substack{m=1 \\ N\neq 1 \\ N\neq 2}}^{N-2} \sum_{n=0}^{P-2} \sum_{k=0}^{m-1} \sum_{l=0}^{P-1} \mathcal{D}(mP+n, kP+l)\,. \tag{100}$$

From (91), substituting for $C(mP+n, mP+l)$ using (85) and for $\Phi(mP+n, mP+l+1)$ using (83), and using (74) through (79), we obtain

$$C_1 = \sum_{m=0}^{N-1} \sum_{n=1}^{P-1} \sum_{l=0}^{n-1} \alpha_r(n) \left(-N^{\mathrm{T}}(n)+R(n)C(n)\right) * \Phi(n, l+1)\, W(l)\, \Phi^{\mathrm{T}}(n, l+1)\,. \tag{101}$$

Let

$$\overline{W}(n) \triangleq \sum_{l=0}^{n-1} \Phi(n, l+1)\, W(l)\, \Phi^{\mathrm{T}}(n, l+1)\,, \tag{102}$$

for $n=1, 2, \ldots, P$. From (101), using (102), we obtain

$$C_1 = N \sum_{n=1}^{P-1} \alpha_r(n) \left(-N^{\mathrm{T}}(n)+R(n)C(n)\right) \overline{W}(n)\,. \tag{103}$$

And (103) and (102) represent an ideal formulation for C_1 in that all summation limits are independent of N.

The corresponding development for C_2 is only slightly more complicated. From (92), substituting for $C(mP+n, kP+l)$ using (85), and for $\Phi(mP+n, kP+l+1)$ using (84), and using (74) through (79), we obtain

$$C_2 = \sum_{\substack{m=1 \\ N\neq 1}}^{N-1} \sum_{n=0}^{P-1} \sum_{k=0}^{m-1} \sum_{l=0}^{P-1} \alpha_r(n) \left(-N^{\mathrm{T}}(n)+R(n)C(n)\right) * \Phi(n, 0)\, [\Phi(P, 0)]^{m-k-1}\, \Phi(P, l+1)\, W(l) * \Phi^{\mathrm{T}}(P, l+1)\, [\Phi^{\mathrm{T}}(P, 0)]^{m-k-1}\, \Phi^{\mathrm{T}}(n, 0)\,. \tag{104}$$

From (104), using (102), we obtain

$$C_2 = \sum_{n=0}^{P-1} \alpha_r(n) \left(-N^{\mathrm{T}}(n) + R(n)C(n)\right) \Phi(n,0)\, C_{21}\, \Phi^{\mathrm{T}}(n,0)\,, \tag{105}$$

where

$$C_{21} = \sum_{\substack{m=1 \\ N\neq 1}}^{N-1} \sum_{k=0}^{m-1} [\Phi(P,0)]^{m-k-1}\, \overline{W}(P)\, [\Phi^{\mathrm{T}}(P,0)]^{m-k-1}\,. \tag{106}$$

Now we assume that the closed-loop BTP state transition matrix $\Phi(P,0)$ is diagonalizable, so that $\Phi(P,0)$ can be written as

$$\Phi(P,0) = S\,\Lambda\,S^{-1}\,, \tag{107}$$

where S is a nonsingular matrix and Λ is a diagonal matrix. Let λ_i represent the ith diagonal element of Λ. Let $(\cdot)_{ij}$ represent the operator that returns the (i,j)th element of its matrix argument. From (106), using (107), we obtain

$$C_{21} = S\,\overline{C}_{21}\,S^{\mathrm{T}}\,, \tag{108}$$

where

$$\left(\overline{C}_{21}\right)_{ij} = \left(S^{-1}\,\overline{W}(P)\,S^{-\mathrm{T}}\right)_{ij} \sum_{\substack{m=0 \\ N\neq 1}}^{N-2} \sum_{k=0}^{m} \lambda_i^{m-k}\lambda_j^{m-k}\,. \tag{109}$$

And (105), (108), (109), and (102) represent an ideal formulation for C_2 in that: (1) the summation limits in (105) and (102) are independent of N; and (2) the nested sum in (109) is a finite series that can be evaluated in closed-form using formulas in Gradhteyn and Ryzhik (1980).

The corresponding developments for D_1 through D_8 follow the same design. From (65), using (71) and (69), and substituting for the summation using

$$\sum_{\mu=mP+n}^{NP-1} f(\mu, mP+n) = \left[\sum_{q=n}^{P-1} f(mP+q, mP+n)\right] + \left[\sum_{\substack{p=m+1 \\ m\neq N-1}}^{N-1} \sum_{q=0}^{P-1} f(pP+q, mP+n)\right], \tag{110}$$

for $m=0, 1, \ldots, N-1$ and $n=0, 1, \ldots, P-1$, and using (64), (75) through (77), and (79) we obtain

$$\Psi(mP+n) = \Big[\sum_{q=n}^{P-1} \Phi(mP+q, mP+n)\, Q_C(q)\, \Phi^{\mathrm{T}}(mP+q, mP+n)\Big] + \Big[\sum_{\substack{p=m+1 \\ m\neq N-1}}^{N-1} \sum_{q=0}^{P-1} \Phi(pP+q, mP+n)\, Q_C(q)\, \Phi^{\mathrm{T}}(pP+q, mP+n)\Big] \quad (111)$$

for $m=0, 1, \ldots, N-1$ and $n=0, 1, \ldots, P-1$, and

$$\Psi(NP) = 0\,. \quad (112)$$

From (93), substituting for $\mathcal{D}((N-1)P+P-1, (N-1)P+l)$ using (86), and for $\Psi(NP)$ using (112), we obtain

$$\mathcal{D}_1 = 0\,. \quad (113)$$

Let

$$\overline{Q}_C(n) \triangleq \sum_{q=n}^{P-1} \Phi^{\mathrm{T}}(q, n)\, Q_C(q)\, \Phi(q, n)\,, \quad (114)$$

for $n=0, 1, \ldots, P-1$. From (94), substituting for $\mathcal{D}((N-1)P+n, (N-1)P+l)$ using (86), for $\Psi((N-1)P+n+1)$ using (111), and for $\Phi((N-1)P+n, (N-1)P+l+1)$ using (83), and using (72) through (74), (78), (79), (102), and (114), we obtain

$$\mathcal{D}_2 = -\sum_{\substack{n=1 \\ P\neq 2}}^{P-2} \alpha_r(n)\, B^{\mathrm{T}}(n)\, \overline{Q}_C(n+1)\, \Phi(n+1, n)\, \overline{W}(n)\,. \quad (115)$$

From (95), substituting for $\mathcal{D}((m-1)P+P-1, (m-1)P+l)$ using (86), for $\Psi(mP)$ using (111), and for $\Phi((m-1)P+P-1, (m-1)P+l+1)$ using (83), and using (72) through (74), (78), (79), (102), and (114), we obtain

$$\mathcal{D}_3 = -\alpha_r(P-1)\, B^{\mathrm{T}}(P-1)\, \mathcal{D}_{31}\, \Phi(P, P-1)\overline{W}(P-1)\,, \quad (116)$$

where

$$\mathcal{D}_{31} = \sum_{\substack{m=1 \\ N\neq 1}}^{N-1} \sum_{p=m}^{N-1} [\Phi^{\mathrm{T}}(P, 0)]^{p-m}\, \overline{Q}_C(0)\, [\Phi(P, 0)]^{p-m}\,. \quad (117)$$

From (117), substituting for $\Phi(P,0)$ using (107), we obtain

$$\mathcal{D}_{31} = S^{-T}\,\overline{\mathcal{D}}_{31}\,S^{-1}, \tag{118}$$

where

$$\left(\overline{\mathcal{D}}_{31}\right)_{ij} = \left(S^T\,\overline{Q}_C(0)\,S\right)_{ij} \sum_{\substack{m=0\\N\neq 1}}^{N-2}\sum_{p=m}^{N-2} \lambda_i^{p-m}\,\lambda_j^{p-m}. \tag{119}$$

From (96), substituting for $\mathcal{D}(mP+n, mP+l)$ using (86), for $\Psi(mP+n+1)$ using (111), and for $\Phi(mP+n, mP+l+1)$ using (83), and using (72) through (74), (78), (79), (102), and (114), we obtain

$$\mathcal{D}_4 = -\sum_{\substack{n=1\\P\neq 2}}^{P-2} \alpha_r(n)\,B^T(n)\Big\{(N-1)\overline{Q}_C(n+1) + \Phi^T(P,n+1)\,\mathcal{D}_{41}\,\Phi(P,n+1)\Big\}$$
$$* \,\Phi(n+1,n)\,\overline{W}(n), \tag{120}$$

where

$$\mathcal{D}_{41} = \sum_{\substack{m=0\\N\neq 1}}^{N-2}\sum_{p=m+1}^{N-1} [\Phi^T(P,0)]^{p-m-1}\,\overline{Q}_C(0)\,[\Phi(P,0)]^{p-m-1}. \tag{121}$$

From (121), substituting for $\Phi(P,0)$ using (107), we obtain

$$\mathcal{D}_{41} = S^{-T}\,\overline{\mathcal{D}}_{41}\,S^{-1}, \tag{122}$$

where

$$\left(\overline{\mathcal{D}}_{41}\right)_{ij} = \left(S^T\,\overline{Q}_C(0)\,S\right)_{ij} \sum_{\substack{m=0\\N\neq 1}}^{N-2}\sum_{p=m}^{N-2} \lambda_i^{p-m}\,\lambda_j^{p-m}. \tag{123}$$

From (97), substituting for $\mathcal{D}((N-1)P+P-1, kP+l)$ using (86), and for $\Psi(NP)$ using (112), we obtain

$$\mathcal{D}_5 = 0. \tag{124}$$

From (98), substituting for $\mathcal{D}((N-1)P+n, kP+l)$ using (86), for $\Psi((N-1)P+n+1)$ using (111), and for $\Phi((N-1)P+n, kP+l+1)$ using (84), and using (72) through (74), (78), (79), (102), and (114), we obtain

$$\mathcal{D}_6 = -\sum_{n=0}^{P-2} \alpha_r(n)\,B^T(n)\,\overline{Q}_C(n+1)\,\Phi(n+1,0)\,\mathcal{D}_{61}\,\Phi^T(n,0), \tag{125}$$

where

$$\mathcal{D}_{61} = \sum_{\substack{k=1 \\ N\neq 1}}^{N-1} [\Phi(P,0)]^{N-1-k}\, \overline{W}(P)\, [\Phi^{\mathrm{T}}(P,0)]^{N-1-k}. \tag{126}$$

From (126), substituting for $\Phi(P,0)$ using (107), we obtain

$$\mathcal{D}_{61} = S\, \overline{\mathcal{D}}_{61} S^{\mathrm{T}}, \tag{127}$$

where

$$\left(\overline{\mathcal{D}}_{61}\right)_{ij} = \left(S^{-1}\, \overline{W}(P)\, S^{-\mathrm{T}}\right)_{ij} \sum_{\substack{k=0 \\ N\neq 1}}^{N-2} \lambda_i^{N-2-k}\, \lambda_j^{N-2-k}. \tag{128}$$

From (99), substituting for $\mathcal{D}((m-1)P+P-1, kP+l)$ using (86), for $\Psi(mP)$ using (111), and for $\Phi((m-1)P+P-1, kP+l+1)$ using (84), and using (72) through (74), (78), (79), (102), and (114), we obtain

$$\mathcal{D}_7 = -\alpha_r(P-1)\, B^{\mathrm{T}}(P-1)\, \mathcal{D}_{71}\, \Phi^{\mathrm{T}}(P-1,0), \tag{129}$$

where

$$\mathcal{D}_{71} = \sum_{\substack{m=2 \\ N\neq 1 \\ N\neq 2}}^{N-1} \sum_{k=1}^{m-1} \sum_{p=m}^{N-1} [\Phi^{\mathrm{T}}(P,0)]^{p-m}\, \overline{Q}_C(0) [\Phi(P,0)]^{p-k} * \overline{W}(P)\, [\Phi^{\mathrm{T}}(P,0)]^{m-1-k}. \tag{130}$$

From (130), substituting for $\Phi(P,0)$ using (107), and letting $\underline{x}$ denote the number of elements in $x(m,n)$, we obtain

$$\mathcal{D}_{71} = S^{-\mathrm{T}}\, \overline{\mathcal{D}}_{71}\, S^{\mathrm{T}}, \tag{131}$$

where

$$\left(\overline{\mathcal{D}}_{71}\right)_{ij} = \sum_{\beta=1}^{\underline{x}} \left(S^{\mathrm{T}}\, \overline{Q}_C(0)\, S\right)_{i\beta} \left(S^{-1}\, \overline{W}(P)\, S^{-\mathrm{T}}\right)_{\beta j} * \sum_{\substack{m=0 \\ N\neq 1 \\ N\neq 2}}^{N-3} \sum_{k=0}^{m} \sum_{p=m}^{N-3} \lambda_i^{p-m}\, \lambda_\beta^{p+1-k}\, \lambda_j^{m-k}. \tag{132}$$

From (100), substituting for $\mathcal{D}(mP+n, kP+l)$ using (86), for $\Psi(mP+n+1)$ using (111), and for $\Phi(mP+n, kP+l+1)$ using (84), and using (72) through (74), (78), (79), (102), and (114), we obtain

$$\mathcal{D}_8 = -\sum_{n=0}^{P-2} \alpha_r(n)\, B^{\mathrm{T}}(n) \Big\{ \overline{Q}_C(n+1)\, \Phi(n+1,0)\, \mathcal{D}_{81} * \Phi^{\mathrm{T}}(P, n+1)\, \mathcal{D}_{82} \Big\} \Phi^{\mathrm{T}}(n,0)\,, \tag{133}$$

where

$$\mathcal{D}_{81} = \sum_{\substack{m=1 \\ N\neq 1 \\ N\neq 2}}^{N-2} \sum_{k=1}^{m} [\Phi(P,0)]^{m-k}\, \overline{W}(P)\, [\Phi^{\mathrm{T}}(P,0)]^{m-k}\,, \tag{134}$$

$$\mathcal{D}_{82} = \sum_{\substack{m=1 \\ N\neq 1 \\ N\neq 2}}^{N-2} \sum_{k=1}^{m} \sum_{p=m+1}^{N-1} [\Phi^{\mathrm{T}}(P,0)]^{p-m-1}\, \overline{Q}_C(0)\, [\Phi(P,0)]^{p-k} * \overline{W}(P)\, [\Phi^{\mathrm{T}}(P,0)]^{m-k}\,. \tag{135}$$

From (134), substituting for $\Phi(P,0)$ using (86), we obtain

$$\mathcal{D}_{81} = S\, \overline{\mathcal{D}}_{82}\, S^{\mathrm{T}}\,, \tag{136}$$

where

$$\left(\overline{\mathcal{D}}_{81}\right)_{ij} = \left(S^{-1}\, \overline{W}(P)\, S^{-\mathrm{T}}\right)_{ij} \sum_{\substack{m=0 \\ N\neq 1 \\ N\neq 2}}^{N-3} \sum_{k=0}^{m} \lambda_i^{m-k}\, \lambda_j^{m-k}\,. \tag{137}$$

From (135), substituting for $\Phi(P,0)$ using (86), we obtain

$$\mathcal{D}_{82} = S^{-\mathrm{T}}\, \overline{\mathcal{D}}_{82}\, S^{\mathrm{T}}\,, \tag{138}$$

where

$$\left(\overline{\mathcal{D}}_{82}\right)_{ij} = \sum_{\beta=1}^{\underline{z}} \left(S^{\mathrm{T}}\, \overline{Q}_C(0)\, S\right)_{i\beta} \left(S^{-1}\, \overline{W}(P)\, S^{-\mathrm{T}}\right)_{\beta j} * \sum_{\substack{m=0 \\ N\neq 1 \\ N\neq 2}}^{N-3} \sum_{k=0}^{m} \sum_{p=m}^{N-3} \lambda_i^{p-m}\, \lambda_\beta^{p+1-k}\, \lambda_j^{m-k}\,. \tag{139}$$

Together, (90), (103), (105), (108), (109), (113),(115), (116), (118), (119), (120), (122), (123), (124), (125), (127), (128), (129), (131), (132), (133), (136), (138), (137), (139), (102), (114), (83), (84), and (107) represent a formulation for $\partial J(N)/\partial C_r$ that is ideally suited to the optimization algorithm of Section 4.3. In particular, all summations with limits that depend on N can be evaluated in closed-form using formulas in Gradhteyn and Ryzhik (1980), so that the number of machine operations per gradient evaluation is independent of N.

§4.6 Linear Constraints on the Feedback Gains. An advantage of the solution algorithm of Section 4.3 is that additional linear constraints can be imposed on the elements of the feedback gain matrices. Let $\underline{x}$ and $\underline{u}$ represent the number of elements in $x(m,n)$ and $u(m,n)$, respectively. If the elements of the C_r are constrained to satisfy

$$\left(C_r\right)_{ij} = \left[\sum_{m=0}^{M-1}\sum_{p=1}^{\underline{u}}\sum_{q=1}^{\underline{x}} k_{rijmpq}\left(C_m\right)_{pq}\right] + l_{rij}\,, \tag{140}$$

for $r=0, 1, \ldots, M-1$, $i=1, 2, \ldots, \underline{u}$, and $j=1, 2, \ldots, \underline{x}$, where each k_{rijmpq} and l_{rij} is a constant, then, from elementary calculus,

$$\left(\frac{\partial J(N)}{\partial (C_r)_{ij}}\right)^* = \sum_{m=0}^{M-1}\sum_{p=1}^{\underline{u}}\sum_{q=1}^{\underline{x}} k_{mpqrij}\,\frac{\partial J(N)}{\partial (C_m)_{pq}}\,, \tag{141}$$

where $\partial J(N)/\partial (C_m)_{pq}$ on the right-hand side is the gradient ignoring the constraints, and $(\partial J(N)/\partial (C_r)_{ij})^*$ on the left-hand side is the gradient with the constraints in effect. In particular, if $(C_r)_{ij}$ is to be constrained to be fixed, so that

$$\left(C_r\right)_{ij} = l_{rij}\,, \tag{142}$$

then, from (140) and (141),

$$\left(\frac{\partial J(N)}{\partial (C_r)_{ij}}\right)^* = 0\,, \tag{143}$$

and we see that constraining a feedback gain element to be fixed is as simple as zeroing the corresponding gradient element.

As indicated in Appendix C, AMS offers the designer the option to constrain any feedback gain element to be fixed. This is important because, by adding compensator states to the state vector and constraining certain feedback gain elements to be fixed, compensators of arbitrary structure and dynamic order can be synthesized.

Chapter 5

Mass-Spring-Mass Design Example

In this chapter we deal with an example design problem involving a simple mass-spring-mass (MKM) system. The open-loop system is described in Section 5.1. The compensator design work is described in Section 5.2. A method for determining the steady-state state and control covariance responses to a prescribed process noise is developed in Section 5.3. Performance comparisons for the different compensators are presented in Section 5.4. Section 5.5 presents a summary and discussion of the important results.

§5.1 Open-Loop System Description. The open-loop MKM system is shown in Figure 5.1. Rigid bodies A and B have masses M and m, respectively, and are connected by a linear spring with spring constant k. Generalized coordinate x_1 is the displacement of A with respect to a fixed point. Generalized coordinate x_2 is the displacement of B with respect to A. The control inputs $\bar{u}$ and $\tilde{u}$ are forces acting on A and B, respectively. The process noise w_c is modeled as a force acting on B that satisfies the state equation

$$\dot{w}_c(t) = -a\, w_c(t) + \sqrt{2a}\, w(t)\,, \tag{1}$$

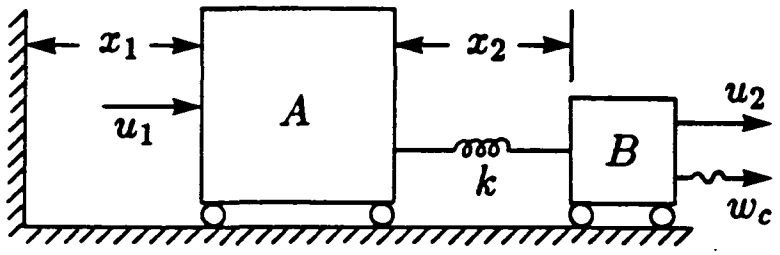

Figure 5.1 Open-Loop MKM System.

with $w_c(0) = 0$, where $w(t)$ is stationary, zero-mean, gaussian white noise of unit intensity, so that

$$\mathrm{E}\{w(t)\} = 0\,, \tag{2}$$

$$\mathrm{E}\{w(t+\tau)w(t)\} = \delta(\tau)\,, \tag{3}$$

where $\delta(\cdot)$ is the Dirac delta function. From (1) through (3), we obtain

$$\mathrm{E}\{w_c(t)\} = 0\,, \tag{4}$$

$$\lim_{t\to\infty} \mathrm{E}\{w_c(t+\tau)w_c(t)\} = \mathrm{e}^{-a|\tau|}\,, \tag{5}$$

so that, in the steady-state, $w_c(t)$ is a stationary, zero-mean, gaussian random process of unit variance, with correlation time $1/a$.

The dynamics of the plant plus the process noise are represented by the analog state equation

$$\dot{x}(t) = F\,x(t) + \bar{G}\,\bar{u}(t) + \tilde{G}\,\tilde{u}(t) + G_w\,w(t)\,, \tag{6}$$

where

$$x(t) \triangleq [\,x_1(t) \quad \dot{x}_1(t) \quad x_2(t) \quad \dot{x}_2(t) \quad w_c(t)\,]^{\mathrm{T}}\,, \tag{7}$$

$$F \triangleq \begin{bmatrix} 0 & 1 & 0 & 0 & 0 \\ 0 & 0 & \frac{k}{M} & 0 & 0 \\ 0 & 0 & 0 & 1 & 0 \\ 0 & 0 & -(\frac{k}{M}+\frac{k}{m}) & 0 & \frac{1}{m} \\ 0 & 0 & 0 & 0 & -a \end{bmatrix}\,, \tag{8}$$

$$\bar{G} \triangleq [\,0 \quad \tfrac{1}{M} \quad 0 \quad -\tfrac{1}{M} \quad 0\,]^{\mathrm{T}}\,, \tag{9}$$

$$\tilde{G} \triangleq [0 \quad 0 \quad 0 \quad \tfrac{1}{m} \quad 0]^{\mathrm{T}}, \tag{10}$$

$$G_w \triangleq [0 \quad 0 \quad 0 \quad 0 \quad \sqrt{2a}]^{\mathrm{T}}. \tag{11}$$

§5.2 Compensator Designs. The section describes the compensator design work. The coverage is in 5 subsections, although, in practice, the design process is not so conveniently separable. The subsections describe the performance objectives, the compensator structure, the sampling policies, and the synthesis of the different compensators.

Performance Objectives. The performance objective was to minimize the system's responses to the process noise $w_c(t)$. This was to be accomplished using reasonable levels of control, and the real-time computation load was to be as low as possible.

Compensator Structure. The compensator was constrained to be a constant gain control law, with $\bar{u}$ feeding back x_1 and $\dot{x}_1$, and $\tilde{u}$ feeding back x_2 and $\dot{x}_2$.

Sampling Rates Selection. For sampling rates selection, we first expressed the performance objectives in terms of the desired locations for the closed-loop poles in the s-plane. We dealt with cases where $M \gg m$ and the spring is soft—soft enough that the open-loop vibration frequency is substantially less than the characteristic frequency of the high frequency closed-loop poles. Under these conditions, the $x_1/\dot{x}_1$-to-$\bar{u}$ and $x_2/\dot{x}_2$-to-$\tilde{u}$ control loops are primarily coupled to the low frequency and high frequency closed-loop poles, respectively.

The following subsection describes the specific design cases that we considered. One MR compensator and one SR compensator were designed for each design case. Let S_{SR} represent the sampling rate for a SR compensator. Let S_{MR1} and S_{MR2} represent the sampling rates for the $x_1/\dot{x}_1$-to-$\bar{u}$ and $x_2/\dot{x}_2$-to-$\tilde{u}$ control

loops, respectively, for a MR compensator. For real-time operation of either compensator, the number of multiplications per $\bar{u}$ update is the same as the number of multiplications per $\tilde{u}$ update. Consequently, the computation loads for real-time operation of the two compensators will be the same if S_{MR1}, S_{MR2}, and S_{SR} satisfy

$$S_{MR1} + S_{MR2} = 2\,S_{SR}\,. \tag{12}$$

For each design case, we picked S_{SR} such that

$$S_{SR} = k_{SR}\,f_{CL2}\,, \tag{13}$$

where f_{CL2} represents the characteristic frequency in hertz of the high-frequency desired s-plane closed-loop poles, and k_{SR} was either 5 (for a slow-sampling-rates case) or 20 (for a fast-sampling-rates case). For the same design case, we picked S_{MR1} and S_{MR2} using

$$S_{MR1} = k_{MR}\,f_{CL1} \qquad \text{and} \qquad S_{MR2} = k_{MR}\,f_{CL2}\,, \tag{14}$$

where k_{MR} is a constant, and f_{CL1} and f_{CL2} represent the characteristic frequencies in hertz of the low-frequency and high-frequency desired s-plane closed-loop poles, respectively. To ensure that the computation loads for real-time operation of the two compensators are the same, we picked k_{MR} (and thus S_{MR1} and S_{MR2}) such that (12) is satisfied.

Specific Design Cases. Tables 5.1 and 5.2 describe in detail the specific design cases that we considered. There are three cases in all. One MR and one SR compensator were designed for each design case. Table 5.1 lists the values of all fixed parameters. The case-dependent parameters are in Table 5.2. The mass ratio M/m is fixed at 10. The break frequency a for the process noise shaping filter is fixed at a large value compared to the characteristic frequencies of the

desired s-plane closed-loop poles, so that the process noise is effectively white. The symbols f and ς denote a natural frequency and a damping ratio, respectively, with the subscripts OL or CL indicating open-loop or closed-loop, respectively, and the trailing 1 or 2 indicating association with the low frequency or high frequency poles, respectively. The parameter S_{SR} represents the sampling rate for a SR compensator. The parameters S_{MR1} and S_{MR2} represent the sampling rates for the $x_1/\dot{x}_1$-to-$\bar{u}$ and $x_2/\dot{x}_2$-to-$\tilde{u}$ control loops, respectively, for a MR compensator.

Table 5.1 Fixed MKM Parameters.

PARAMETER	VALUE
M	1 kg
m	0.1 kg
a	1000π sec^{-1}
f_{OL1}	0 hertz
ς_{OL1}	0
ς_{OL2}	0
f_{CL1}	1 hertz
ς_{CL1}	$1/\sqrt{2}$
ς_{CL2}	$1/\sqrt{2}$

Table 5.2 Variable MKM Parameters.

PARAMETER	UNITS	NUMERIC VALUE		
		Case 1	Case 2	Case 3
f_{OL2}	hertz	4	2	4
f_{CL2}/f_{CL1}	—	8	4	8
S_{MR2}/S_{MR1}	—	8	4	8
S_{SR}/f_{CL2}	samples/cycle	5	5	20
S_{MR2}/S_{SR}	—	1.78	1.6	1.78

For Design Case 1, the desired s-plane closed-loop poles are critically damped and have characterisic frequencies of 1 and 8 hertz. Taking 8 hertz as the desired

closed-loop bandwidth for the $x_2/\dot{x}_2$-to-$\tilde{u}$ control loop, we picked $S_{\rm SR}$ using (13) at 40 samples/second, or 5 times this desired control bandwidth. For the MR compensator, taking 1 and 8 hertz as the desired control bandwidths for the $x_1/\dot{x}_1$-to-$\bar{u}$ and $x_2/\dot{x}_2$-to-$\tilde{u}$ control loops, respectively, we picked $S_{\rm MR1}$ and $S_{\rm MR2}$ using (12) and (14) at 8.89 and 71.1 samples/second, respectively, or 8.89 times the associated desired control bandwidths.

Design Case 2 is the same as Case 1, except that the characteristic frequency of the high frequency desired s-plane closed-loop poles is 4 hertz. Taking 4 hertz as the desired closed-loop bandwidth for the $x_2/\dot{x}_2$-to-$\tilde{u}$ control loop, we picked $S_{\rm SR}$ using (13) at 20 samples/second, or 5 times this desired control bandwidth. For the MR compensator, taking 1 and 4 hertz as the desired control bandwidths for the $x_1/\dot{x}_1$-to-$\bar{u}$ and $x_2/\dot{x}_2$-to-$\tilde{u}$ control loops, respectively, we picked $S_{\rm MR1}$ and $S_{\rm MR2}$ using (12) and (14) at 8 and 32 samples/second, respectively, or 8 times the associated desired control bandwidths.

Design Case 3 is the same as Case 1, except that all sampling rates are increased by a factor of 4. For the SR compensator, we picked $S_{\rm SR}$ using (13) at 160 samples/second, or 20 times the desired control bandwidth for the $x_2/\dot{x}_2$-to-$\tilde{u}$ control loop. For the MR compensator, we picked $S_{\rm MR1}$ and $S_{\rm MR2}$ using (12) and (14) at 35.6 and 284 samples/second, respectively, or 35.6 times the associated desired control bandwidths.

Synthesis. All compensators were synthesized using the successive loop closures synthesis method of Section 3.1. For each MR compensator, we synthesized the control law for the $x_2/\dot{x}_2$-to-$\tilde{u}$ control loop first, then re-discretized the model at the slower sampling rate with the $x_2/\dot{x}_2$-to-$\tilde{u}$ loop closed and synthesized the $x_1/\dot{x}_1$-to-$\bar{u}$ control loop. The same procedure was used for each SR compensator except that the same sampling rate was used for both control loops. With only one position

feedback gain and one rate feedback gain in each control loop, the feedback gains were easily determined by trial and error using interactive computer displays of the closed-loop poles.

Figure 5.2 is a z-plane plot of the $x_2/\dot{x}_2$-to-$\tilde{u}$ control loop design for the Case 1 MR compensator. The sampling rate is 71.1 samples/second. The os are the open-loop poles. The □s are the high frequency desired closed-loop poles. The ×s are the actual closed-loop poles. The x_2-to-$\tilde{u}$ and $\dot{x}_2$-to-$\tilde{u}$ feedback gains are 91.8 N/m/sec and 5.24 N/m/sec, respectively.

Figure 5.3 is a z-plane plot of the subsequent $x_1/\dot{x}_1$-to-$\bar{u}$ control loop design for the Case 1 MR compensator. The sampling rate is 8.89 samples/second. The os are the low frequency (i.e., rigid body) open-loop poles. The □s near the origin are the high frequency desired closed-loop poles. The other □ pair are the low-frequency desired closed-loop poles. The ×s are the actual closed-loop poles (the final closed-loop poles with the Case 1 MR compensator), obtained for x_1-to-$\bar{u}$ and $\dot{x}_1$-to-$\bar{u}$ feedback gains of 25.4 N/m and 7.30 N/m/sec, respectively. In Figure 5.3, the small movements of the high frequency closed-loop poles away from their desired locations are due to the closure of the $x_1/\dot{x}_1$-to-$\bar{u}$ control loop. These movements are one consequence of the approximations inherent the application of the successive loop closures synthesis method.

Figure 5.4 is a z-plane plot of the Case 1 SR compensator design. The sampling rate is 40 samples/second. The os are the open-loop poles, the □s are the desired closed-loop poles, and the ×s are the final actual closed-loop poles. The small movements of the high frequency closed-loop poles away from their desired locations are again due to the closure of the $x_1/\dot{x}_1$-to-$\bar{u}$ control loop.

For completeness, the z-plane plots of the desired and final actual closed-loop poles for the Case 2 and 3 compensators are included in Figures 5.5 through 5.8.

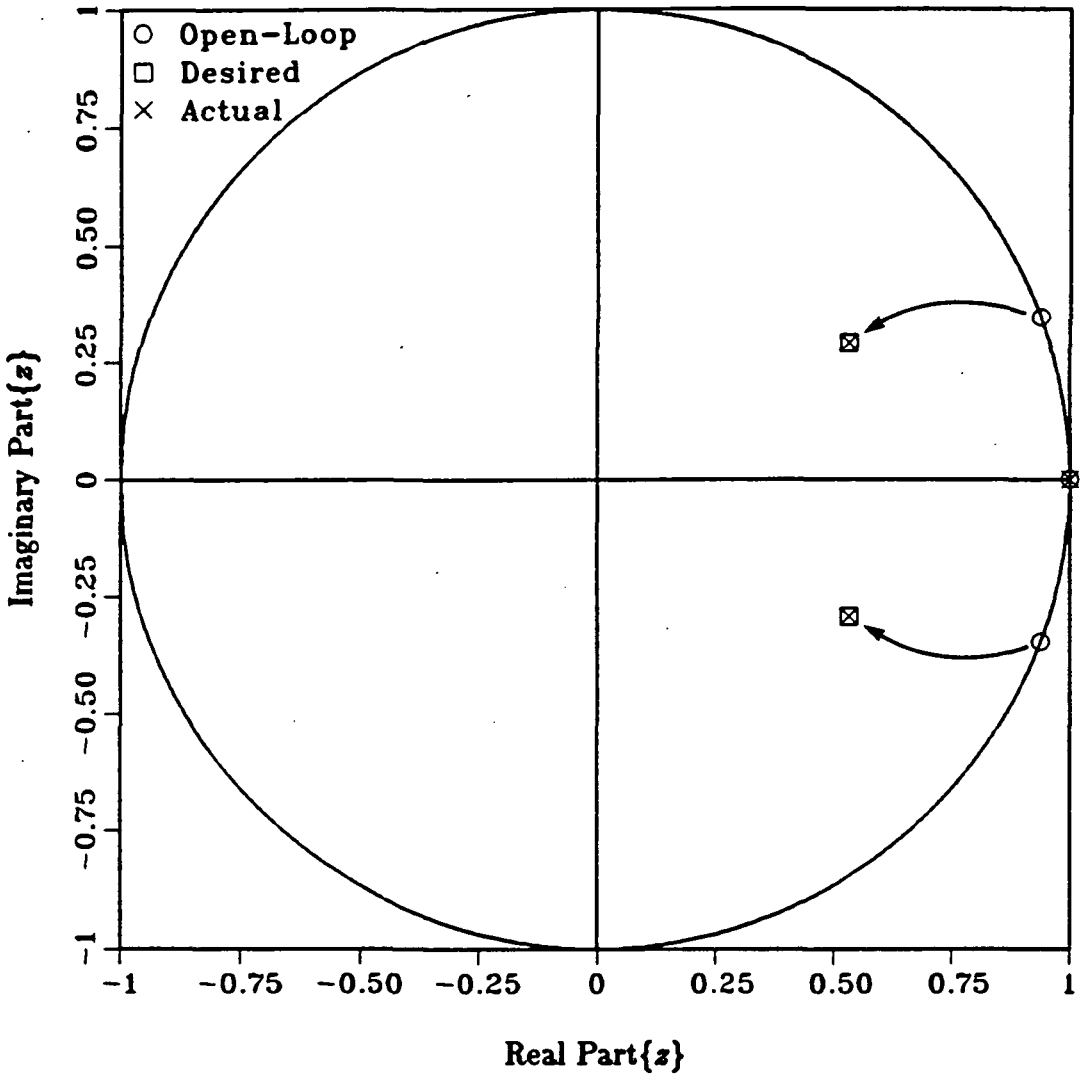

Figure 5.2 Case 1 MR Compensator $x_2/\dot{x}_2$-to-$\tilde{u}$ Loop Design.

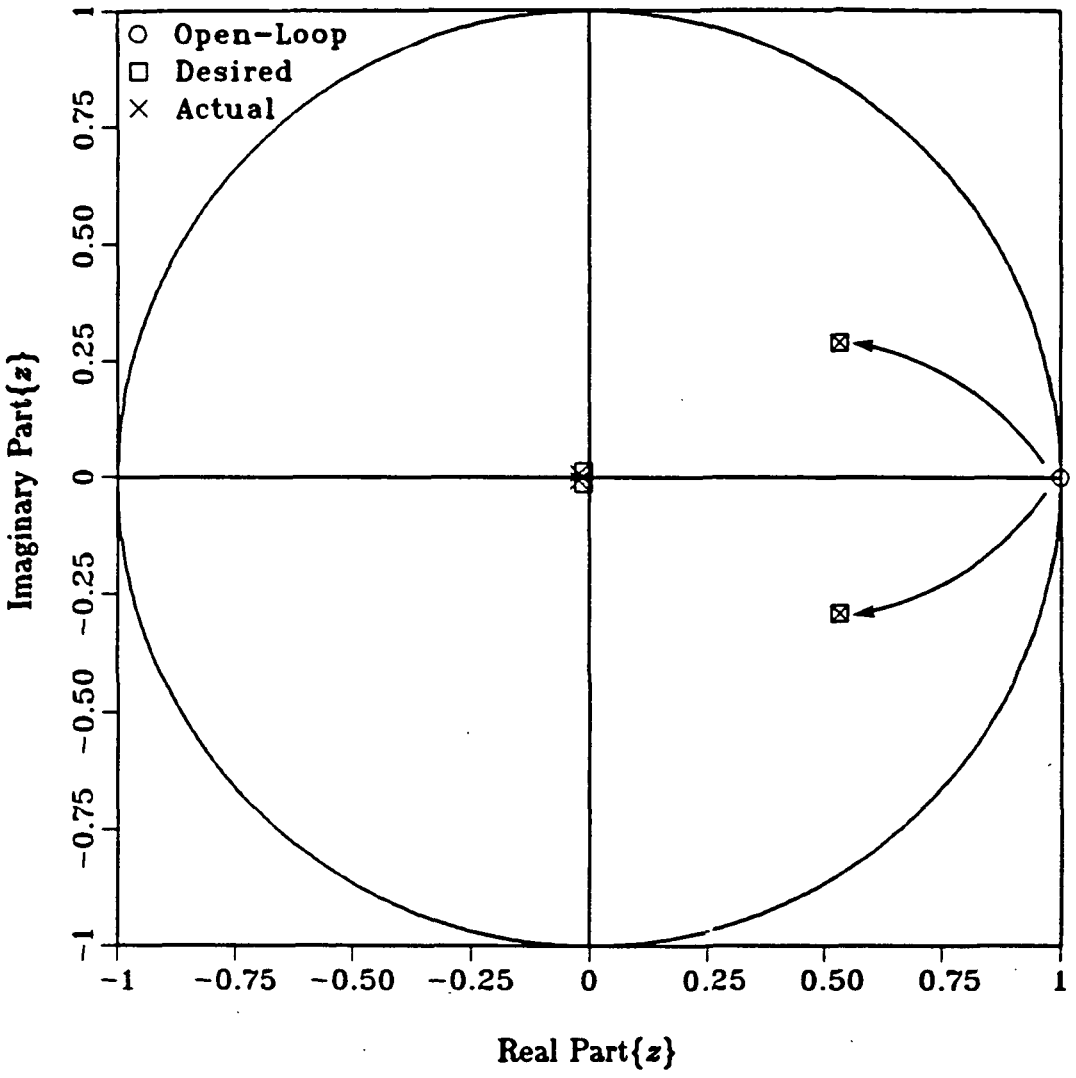

Figure 5.3 Case 1 MR Compensator $x_1/\dot{x}_1$-to-$\bar{u}$ Loop Design.

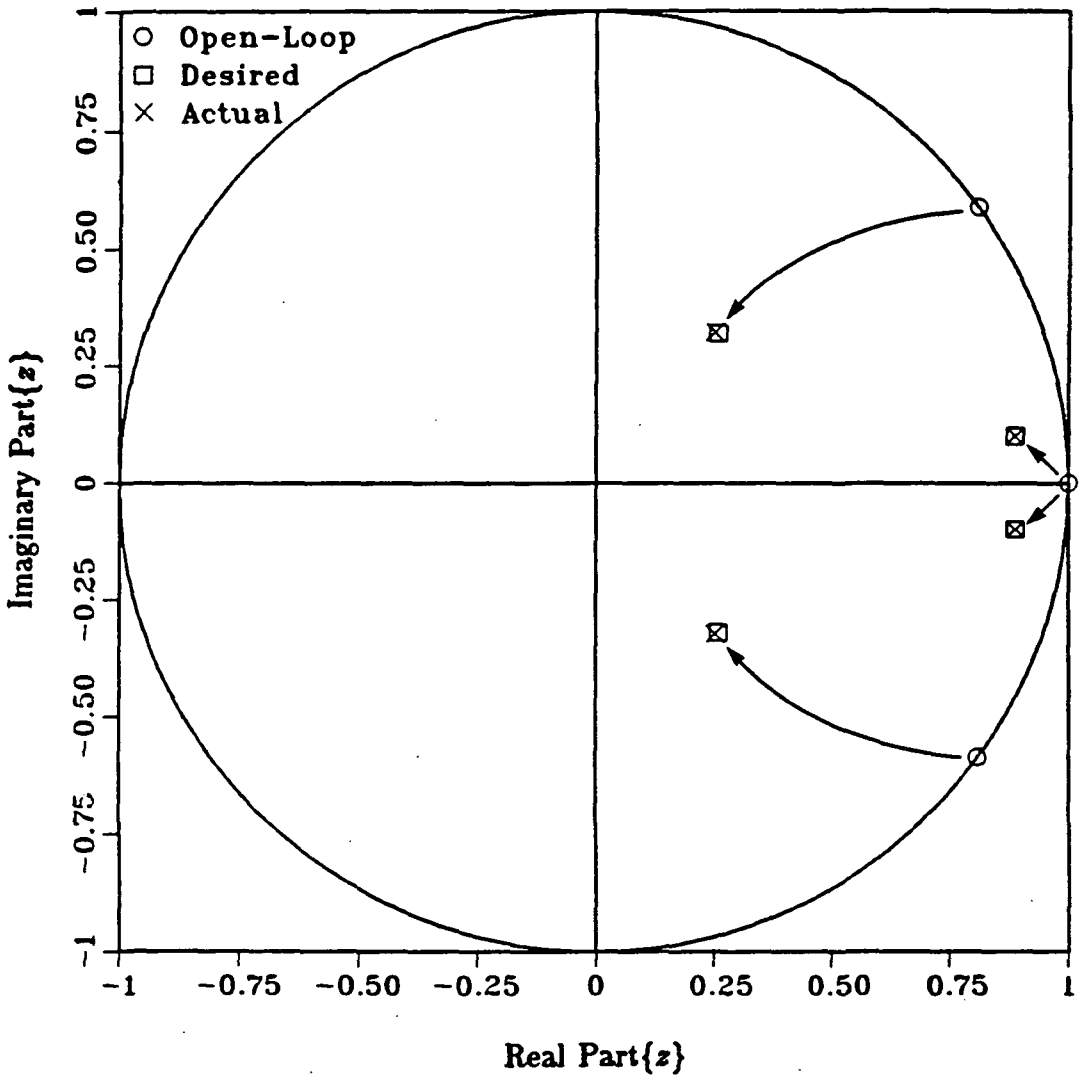

Figure 5.4 Case 1 SR Compensator Design.

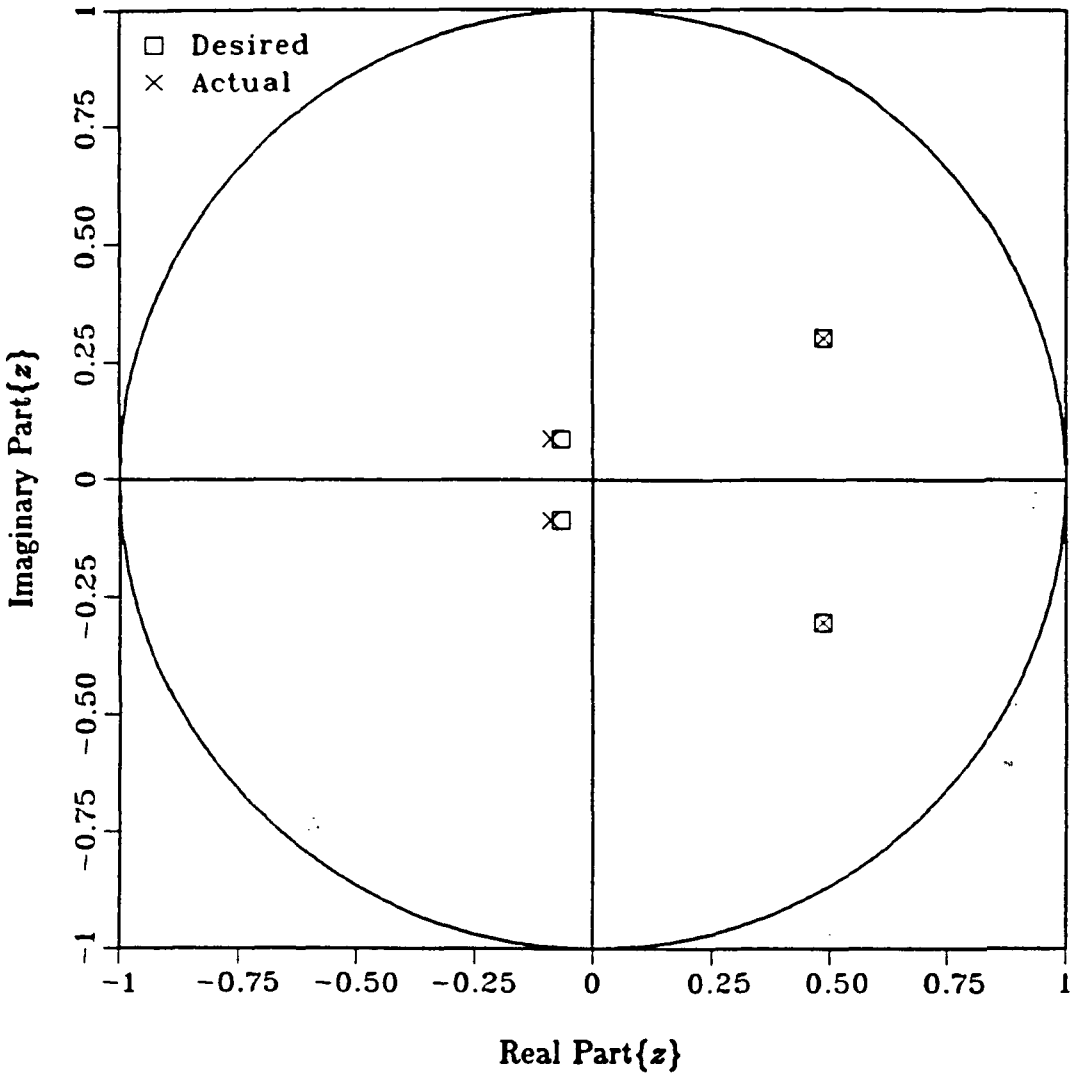

Figure 5.5 Closed-Loop Poles with Case 2 MR Compensator.

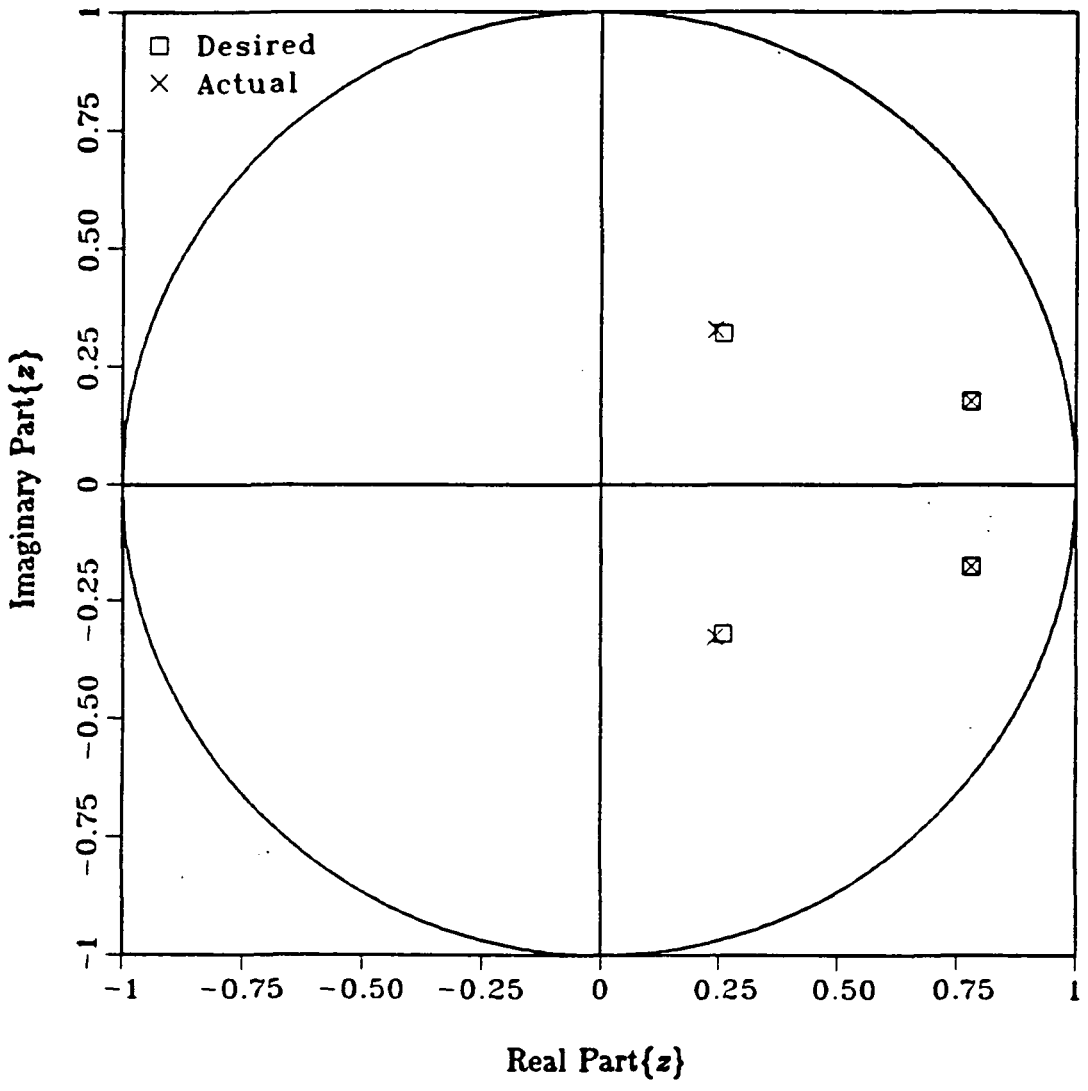

Figure 5.6 Closed-Loop Poles with Case 2 SR Compensator.

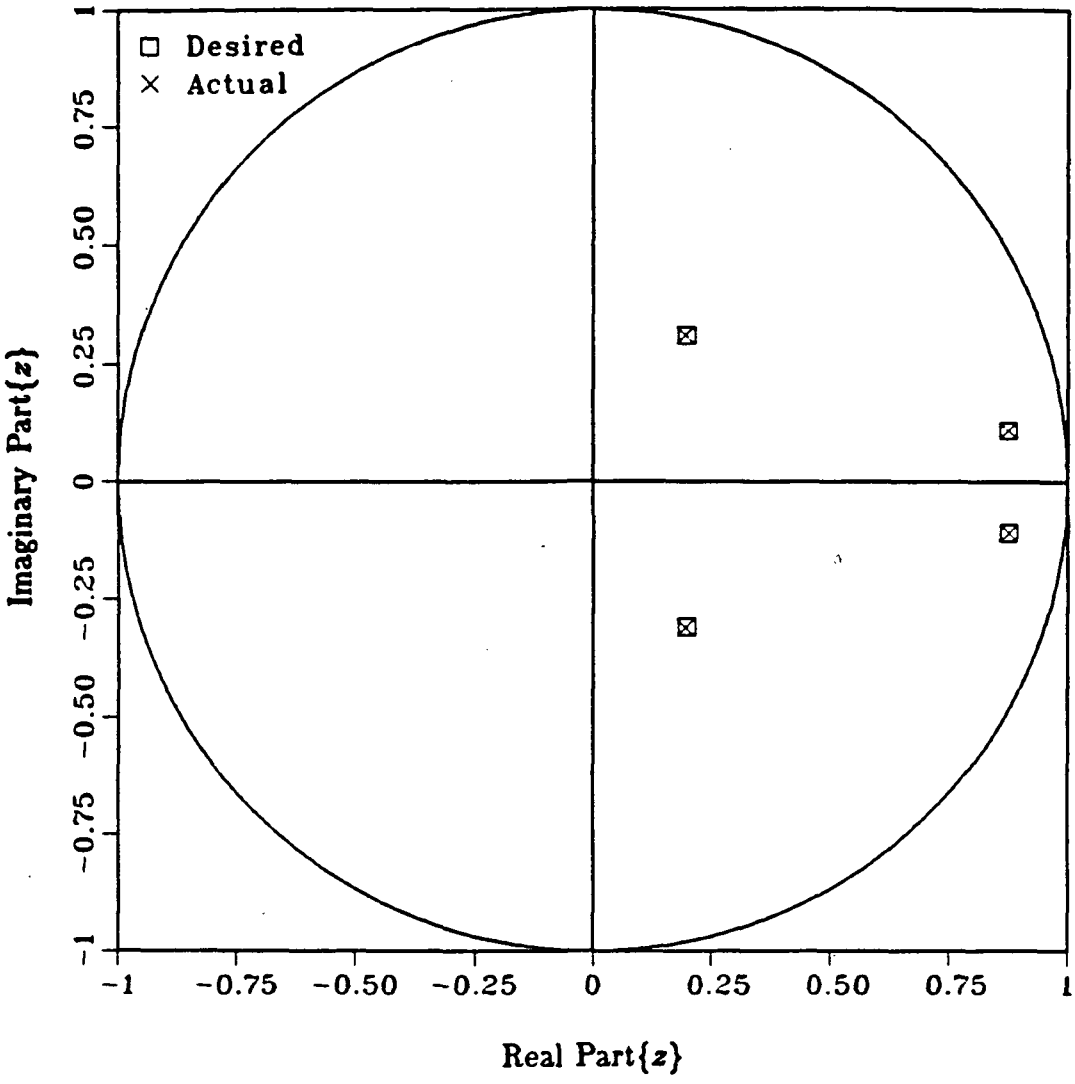

Figure 5.7 Closed-Loop Poles with Case 3 MR Compensator.

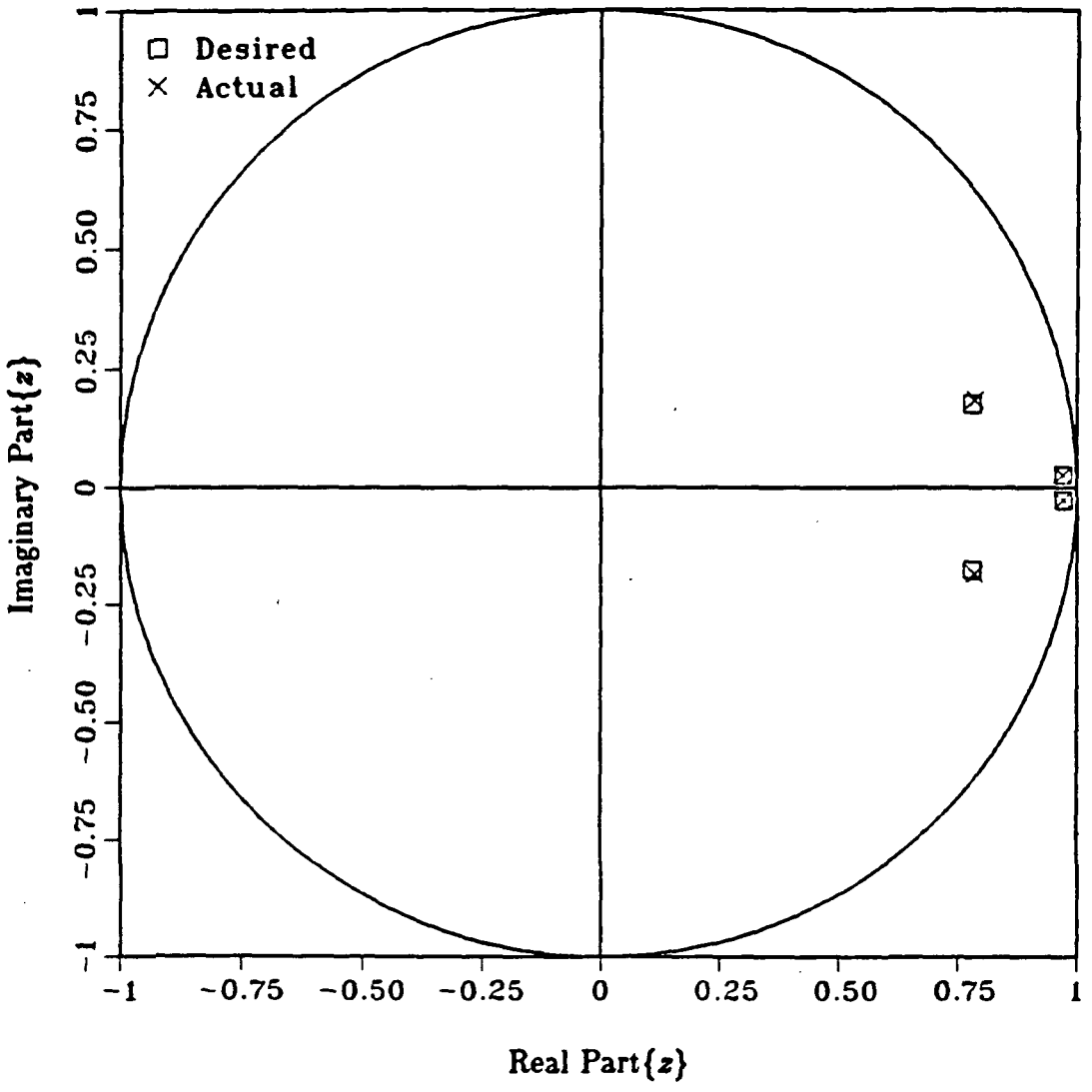

Figure 5.8 Closed-Loop Poles with Case 3 SR Compensator.

The feedback gains for the MR and SR compensators for all three design cases are in Table 5.3.

Table 5.3 MKM Compensator Feedback Gains.

DESIGN	FEEDBACK GAINS			
	x_1-to-u_1 (N/m)	$\dot{x}_1$-to-u_1 (N/m/sec)	x_2-to-u_2 (N/m)	$\dot{x}_2$-to-u_2 (N/m/sec)
Case 1 MR	25.4	7.30	91.8	5.24
Case 1 SR	38.0	8.96	44.5	4.13
Case 2 MR	24.6	7.19	20.9	2.53
Case 2 SR	34.9	8.58	11.1	2.06
Case 3 MR	36.0	8.60	160.	6.58
Case 3 SR	39.7	9.07	140.	6.20

§5.3 Steady-State Response to Process Noise. We shall use the steady-state root-mean-square (RMS) closed-loop state and control responses to the process noise $w_c(t)$ to compare the performance of the different compensators. For a MR or SR compensator, let T represent the sampling period for the $x_2/\dot{x}_2$-to-$\tilde{u}$ control loop. Let P represent the number of STPs per BTP for the sampling policy, so that PT is the sampling period for the $x_1/\dot{x}_1$-to-$\bar{u}$ control loop. Let

$$A \triangleq \mathrm{e}^{FT}, \tag{15}$$

$$\bar{B} \triangleq \int_0^T \mathrm{e}^{Ft}\, dt\, \bar{G}, \tag{16}$$

$$\tilde{B} \triangleq \int_0^T \mathrm{e}^{Ft}\, dt\, \tilde{G}. \tag{17}$$

For the system in (6), let $x(m,n)$ represent the analog state vector $x(t)$ at the $(mP+n)$th sampling instant. Let $\bar{u}(m,n)$ and $\tilde{u}(m,n)$ represent the analog control inputs $\bar{u}(t)$ and $\tilde{u}(t)$, respectively at the $(mP+n)$th sampling instant. Let $w(m,n)$ represent the effect of the analog white noise $w(t)$ that occurs between the $(mP+n)$th

and $(mP+n+1)$th sampling instants on $x(t)$ at the $(mP+n+1)$th sampling instant; that is, let

$$w(m,n) \triangleq \int_{(mP+n)T}^{(mP+n+1)T} e^{F((mP+n+1)T-t)}\, G_w\, w(t)\, dt\,. \tag{18}$$

The closed-loop state responses to the analog white noise $w(t)$ then satisfy

$$x(m,n+1) = A\,x(m,n) + \bar{B}\,\bar{u}(m,n) + \tilde{B}\,\tilde{u}(m,n) + w(m,n)\,, \tag{19}$$

for $m=0, 1, \ldots$ and $n=0, 1, \ldots, P-1$.

The control inputs $\bar{u}(m,n)$ and $\tilde{u}(m,n)$ are assumed to satisfy

$$\bar{u}(m,n) = -\bar{C}\,x(m,0)\,, \tag{20}$$

$$\tilde{u}(m,n) = -\tilde{C}(n)\,x(m,n) - \tilde{c}(n)\,\bar{u}(m,n)\,. \tag{21}$$

Let I represent an identity matrix with the same number of rows and columns as there are elements in $x(m,n)$. Let

$$\begin{aligned}
\Phi(0) &\triangleq I\,,\\
\Phi(1) &\triangleq [A - \tilde{B}\,\tilde{C}(0)]\,\Phi(0) - \bar{B}\,\bar{C} + \tilde{B}\,\tilde{c}(0)\,\bar{C}\,,\\
\Phi(2) &\triangleq [A - \tilde{B}\,\tilde{C}(1)]\,\Phi(1) - \bar{B}\,\bar{C} + \tilde{B}\,\tilde{c}(1)\,\bar{C}\,,\\
&\;\;\vdots \qquad\qquad \vdots \qquad\qquad \vdots\\
\Phi(P) &\triangleq [A - \tilde{B}\,\tilde{C}(P-1)]\,\Phi(P-1) - \bar{B}\,\bar{C} + \tilde{B}\,\tilde{c}(P-1)\,\bar{C}\,.
\end{aligned} \tag{22}$$

Let

$$\begin{aligned}
\Gamma(1) &\triangleq I\,,\\
\Gamma(2) &\triangleq [\,(A - \tilde{B}\,\tilde{C}(1))\,\Gamma(1) \quad I\,]\,,\\
\Gamma(3) &\triangleq [\,(A - \tilde{B}\,\tilde{C}(2))\,\Gamma(2) \quad I\,]\,,\\
&\;\;\vdots \qquad\qquad \vdots\\
\Gamma(P) &\triangleq [\,(A - \tilde{B}\,\tilde{C}(P-1))\,\Gamma(P-1) \quad I\,]\,.
\end{aligned} \tag{23}$$

Let

$$\begin{aligned}
\bar{w}(m,0) &\triangleq w(m,0)\,,\\
\bar{w}(m,1) &\triangleq \begin{bmatrix} w(m,0)\\ w(m,1)\end{bmatrix},\\
&\vdots \qquad\quad \vdots\\
\bar{w}(m,P-1) &\triangleq \begin{bmatrix} w(m,0)\\ w(m,1)\\ \vdots\\ w(m,P-1)\end{bmatrix}.
\end{aligned} \tag{24}$$

From (19), substituting for $\bar{u}(m,n)$ using (20), and for $\tilde{u}(m,n)$ using (21), and using (22), (23), and (24), we obtain

$$\begin{aligned}
x(m,1) &= \Phi(1)\,x(m,0) + \Gamma(1)\,\bar{w}(m,0)\,,\\
x(m,2) &= \Phi(2)\,x(m,0) + \Gamma(2)\,\bar{w}(m,1)\,,\\
&\vdots \qquad\quad \vdots \qquad\qquad \vdots\\
x(m+1,0) &= \Phi(P)\,x(m,0) + \Gamma(P)\,\bar{w}(m,P-1)\,.
\end{aligned} \tag{25}$$

From the last equation in (25), using

$$\mathrm{E}\{x(m,0)\,\bar{w}^{\mathrm{T}}(m,P-1)\} = 0\,, \tag{26}$$

we obtain

$$\begin{aligned}
\mathrm{E}\{x(m+1,0)\,x^{\mathrm{T}}(m+1,0)\} &= \Phi(P)\,\mathrm{E}\{x(m,0)\,x^{\mathrm{T}}(m,0)\}\,\Phi^{\mathrm{T}}(P)\\
&\quad + \Gamma(P)\,\mathrm{E}\{\bar{w}(m,P-1)\,\bar{w}^{\mathrm{T}}(m,P-1)\}\,\Gamma^{\mathrm{T}}(P)\,.
\end{aligned} \tag{27}$$

Let

$$X(m,n) \triangleq \mathrm{E}\{x(m,n)\,x^{\mathrm{T}}(m,n)\}\,, \tag{28}$$

$$\bar{W}(n) \triangleq \mathrm{E}\{\bar{w}(m,n)\,\bar{w}^{\mathrm{T}}(m,n)\}\,. \tag{29}$$

From (27), using (28) and (29), we obtain

$$X(m+1,0) = \Phi(P)\,X(m,0)\,\Phi^{\mathrm{T}}(P) + \Gamma(P)\,\bar{W}(P-1)\,\Gamma^{\mathrm{T}}(P)\,. \tag{30}$$

Assuming that the closed-loop system is stable, the unique steady-state solution to (30) is easily determined by setting $X(m+1,0)=X(m,0)$ and solving the resulting set of simultaneous linear equations for the elements of $X(m,0)$. Let $X(0)$ represent this solution. The matrix $X(0)$ is the steady-state closed-loop state covariance in response to the analog white noise $w(t)$ at the first sampling instant in a BTP. Let $X(1), X(2), \ldots, X(P-1)$ represent the corresponding steady-state state covariances at the other $P-1$ sampling instants in a BTP. From (25), using (28), (29), and (31), we obtain

$$\begin{aligned} X(1) &= \Phi(1)\,X(0)\,\Phi^{\mathrm{T}}(1) + \Gamma(1)\,\bar{W}(0)\,\Gamma^{\mathrm{T}}(1), \\ X(2) &= \Phi(2)\,X(0)\,\Phi^{\mathrm{T}}(2) + \Gamma(2)\,\bar{W}(1)\,\Gamma^{\mathrm{T}}(2), \\ &\vdots \qquad\qquad \vdots \qquad\qquad \vdots \\ X(P-1) &= \Phi(P-1)\,X(0)\,\Phi^{\mathrm{T}}(P-1) + \Gamma(P-1)\,\bar{W}(P-2)\,\Gamma^{\mathrm{T}}(P-1). \end{aligned} \tag{31}$$

The first 4 diagonal elements of $X(n)$ are the steady-state variances of the analog states $x_1(t)$, $\dot{x}_1(t)$, $x_2(t)$, and $\dot{x}_2(t)$, respectively, in response to the analog process noise $w_c(t)$, at the nth sampling instant in a BTP. From (20), the corresponding steady-state variance of the control input $\tilde{u}(t)$ is

$$\lim_{m\to\infty} \mathrm{E}\{\tilde{u}^2(m,n)\} = \tilde{C}\,X(0)\,\tilde{C}^{\mathrm{T}}. \tag{32}$$

From (21), using (25), (30), and (31), the corresponding steady-state variance of the control input $\tilde{u}(t)$ at the nth sampling instant in a BTP is

$$\begin{aligned} \lim_{m\to\infty} \mathrm{E}\{\tilde{u}^2(m,n)\} &= \tilde{C}(n)\,X(n)\,\tilde{C}^{\mathrm{T}}(n) - \tilde{C}(n)\,\Phi(n)\,X(0)\,\tilde{C}^{\mathrm{T}}\,\tilde{c}(n) \\ &\quad - (\tilde{C}(n)\,\Phi(n)\,X(0)\,\tilde{C}^{\mathrm{T}}\,\tilde{c}(n))^{\mathrm{T}} + \tilde{c}(n)\,\tilde{C}\,X(0)\,\tilde{C}^{\mathrm{T}}\,\tilde{c}(n). \end{aligned} \tag{33}$$

§5.4 Performance Comparisons. The performance of the Case 1 MR compensator is compared with that of the Case 1 SR compensator in Figure 5.9. The numerator and denominator values above each bar are the steady-state RMS

closed-loop responses to the process noise $w_c(t)$ with the MR and SR compensators, respectively, in units of meters for x_1 and x_2, meters/second for $\dot{x}_1$ and $\dot{x}_2$, and newtons for u_1 and u_2*. Each bar in the figure has a height equal to the value of the ratio above it.

The performance of the Case 1 MR compensator is markedly better than that of the Case 1 SR compensator. The steady-state RMS $x_1(m,n)$ and $\dot{x}_1(m,n)$ responses are about the same with the two compensators, while the steady-state RMS $x_2(m,n)$ and $\dot{x}_2(m,n)$ responses with the MR compensator are markedly reduced. Furthermore, the steady-state RMS control activities are less with the MR compensator.

The same results for the Case 2 MR and SR compensators are plotted in the same manner in Figure 5.10. Comparing the Case 2 responses with the Case 1 responses, we see markedly similar patterns in the steady-state RMS response ratios. Evidently, for this system, under these conditions, the performance benefits of MR compensation over SR compensation are markedly insensitive to the spectral separation of the closed-loop poles.

The same results for the Case 3 MR and SR compensators are plotted in the same manner in Figure 5.11. Comparing the Case 3 responses with the Case 1 responses, we see markedly different patterns in the steady-state RMS response ratios. Evidently, for this system, under these conditions, the performance benefits of MR compensation over SR compensation decrease with increasing sampling rates. This is not surprising, however, since the corresponding steady-state RMS responses

* For a SR compensator, we define the steady-state RMS response to be the square root of the steady-state variance at the sampling instants. For a MR compensator, we define the steady-state RMS response to be the square root of the mean of the steady-state variances at the P sampling instants in a BTP.

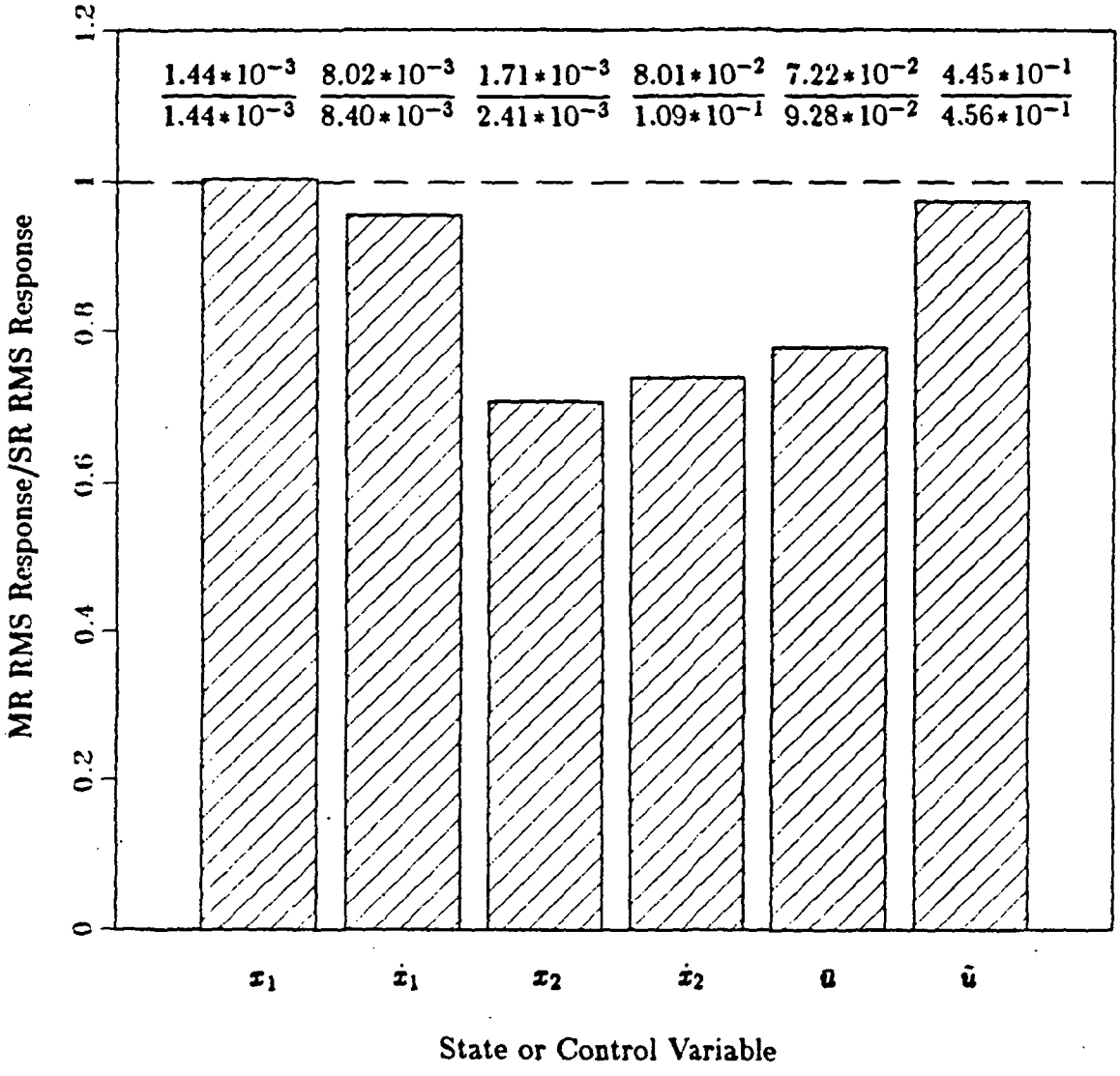

Figure 5.9 Ratios of Steady-State RMS Responses to Process Noise with Case 1 Compensators.

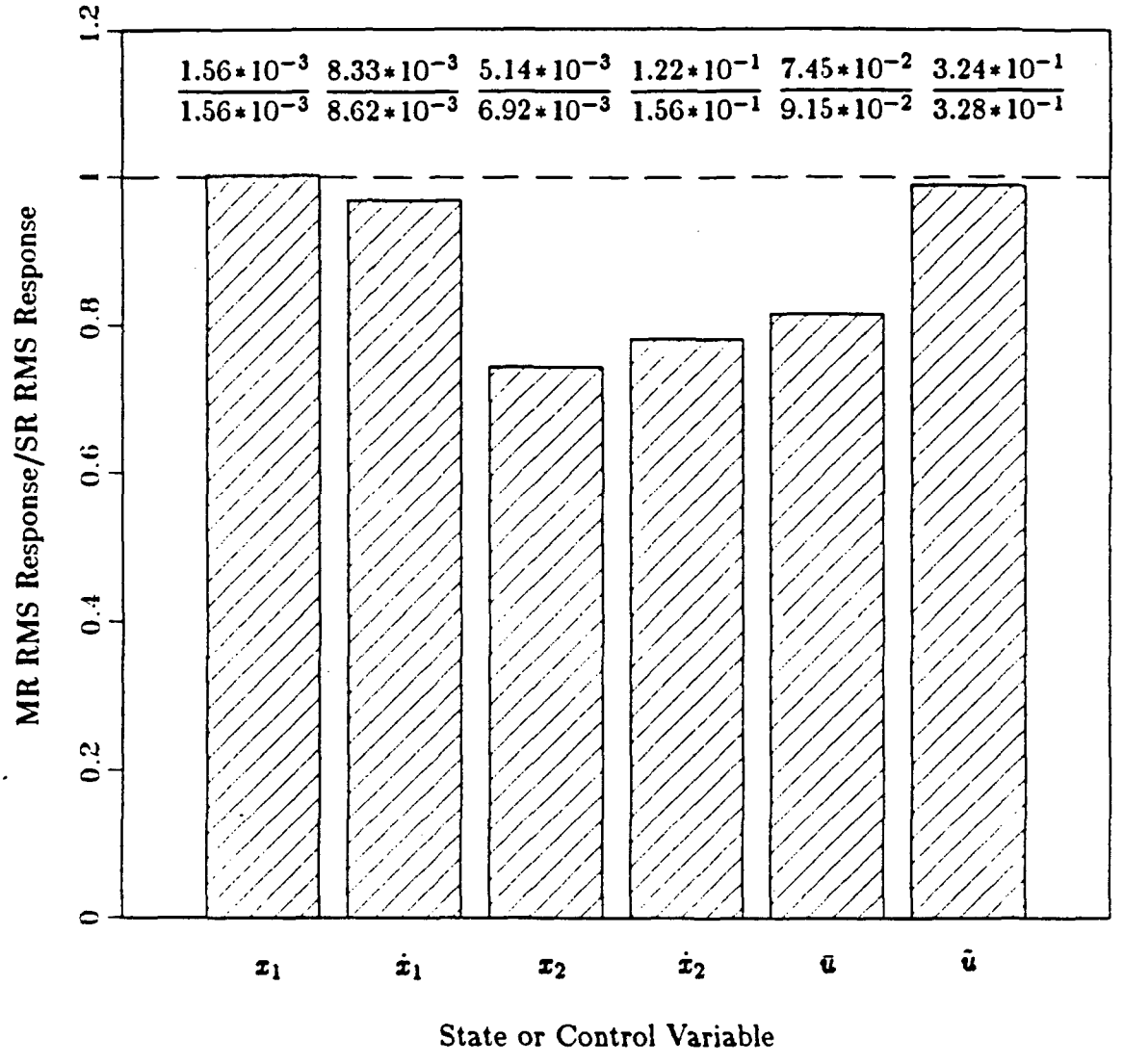

Figure 5.10 Ratios of Steady-State RMS Responses to Process Noise with Case 2 Compensators.

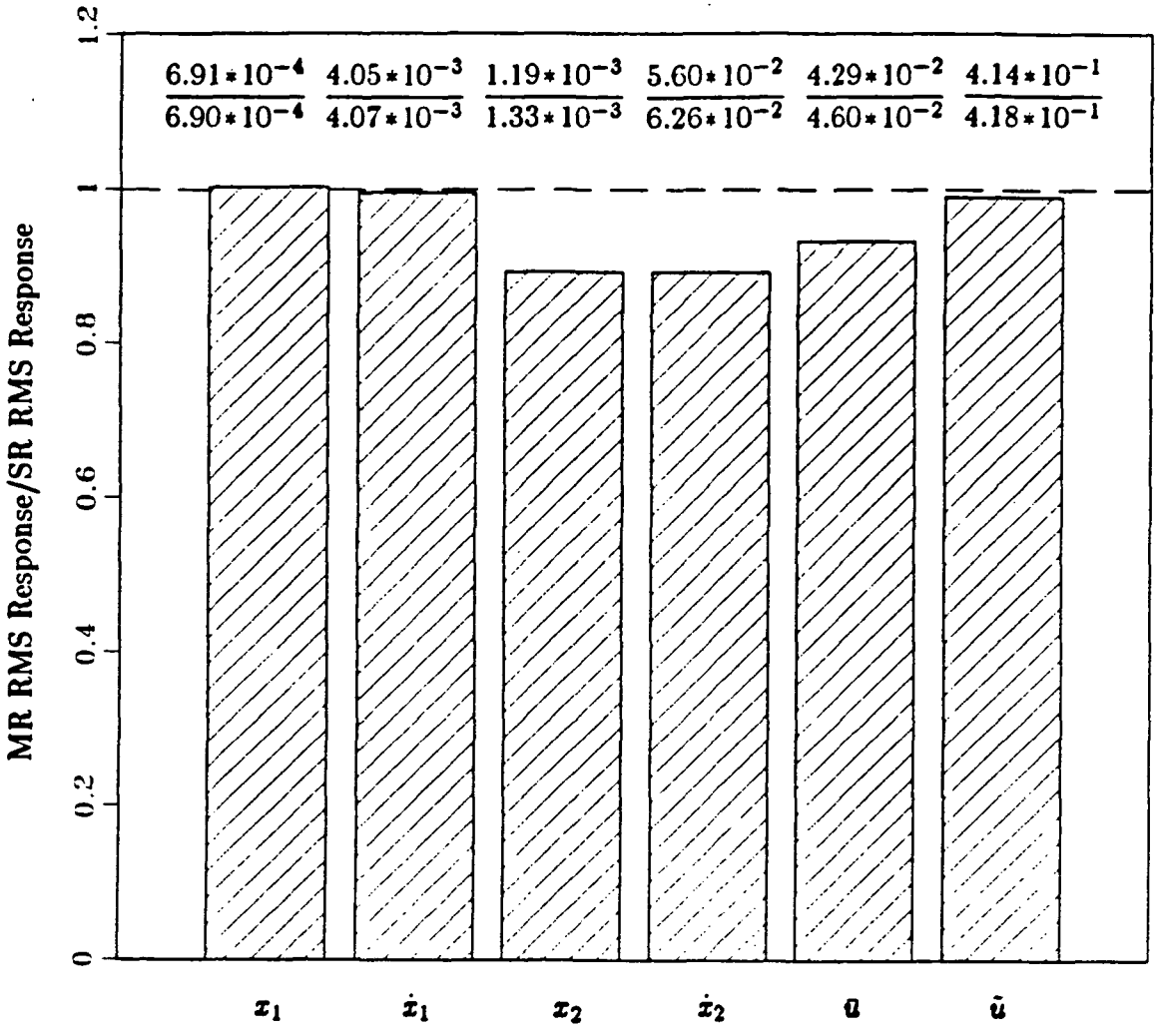

Figure 5.11 Ratios of Steady State RMS Responses to Process Noise with Case 3 Compensators.

will be identical with MR and SR compensators designed in this way with very fast sampling rates.

§5.5 Summary and Discussion. This section contains two subsections. The first presents the basic results of the MKM design studies. In the second, we take a second look at the use of other synthesis methods.

Basic Results. We dealt with the simple MKM system in Figure 5.1. With the attenuation of the system's responses to the process noise $w_c(t)$ as the performance objective, we experimented with different design conditions to determine circumstances under which a MR compensator outperforms a comparable SR compensator.

Three design cases were considered. The successive loop closures synthesis method was used to synthesize one MR compensator and one SR compensator for each design case. For each SR compensator, the sampling rate was picked to be a multiple of the characteristic frequency of the fastest desired s-plane closed-loop poles. For each MR compensator, the sampling rate for each control loop was picked to be a multiple of the characteristic frequency of the desired s-plane closed-loop poles most coupled to that specific loop. Furthermore, for each design case, the sampling rates were picked such that the computation load for real-time operation of the MR compensator is the same as that for real-time operation of the SR compensator.

The process noise $w_c(t)$ was modeled as a stationary, zero-mean, gaussian random process of unit variance, with a short correlation time compared to the characteristic times of all closed-loop poles. The steady-state RMS state and control responses to $w_c(t)$ were determined with the different compensators.

For the MKM system, under these conditions, we conclude that:

1) For slow sampling (characterized by SR sampling at 5 times the characteristic frequency in hertz of the fastest desired s-plane closed-loop poles), MR compensation is superior to SR compensation, for ratios of the characteristic frequencies of the desired s-plane closed-loop poles as low as 4-to-1.
2) The performance benefits of MR compensation over SR compensation are sampling-rate dependent. At the fast sampling rates (characterized by SR sampling at 20 times the characteristic frequency in hertz of the fastest desired s-plane closed-loop poles), the relative reductions in the steady-state RMS state and control responses with MR as compared to SR compensation were only about 1/3 of those obtained at the slow sampling rates.

The insensitivity of the performance benefits of MR compensation over SR compensation to the spectral separation of the closed-loop poles suggests that faster sampling of the $x_2/\dot{x}_2$-to-$\tilde{u}$ control loop at the expense of slower sampling of the $x_1/\dot{x}_1$-to-$\bar{u}$ control loop is desirable purely because the $x_2/\dot{x}_2$-to-$\tilde{u}$ control loop is more directly coupled to the process noise $w_c(t)$. Figure 5.12 presents further evidence to this effect. The steady-state RMS state and control responses in Figure 5.12 were obtained with the Case 1 MR and SR compensators, by the same procedure that was used to generate Figure 5.9, except that the process noise $w_c(t)$ was modeled as a force acting on body A instead of body B. Under these conditions, the steady-state RMS x_1 and x_2 responses are 52% more and only 17% less, respectively, with the MR compensator.

Use of Other Synthesis Methods. Could further improvements in performance be obtained if the optimal control law synthesis method or the constrained optimization synthesis method were used? The results in Figure 5.13 indicate that the answer is no. The denominator values in Figure 5.13 are the steady-state RMS state and control responses to $w_c(t)$ acting on body B with the Case 2

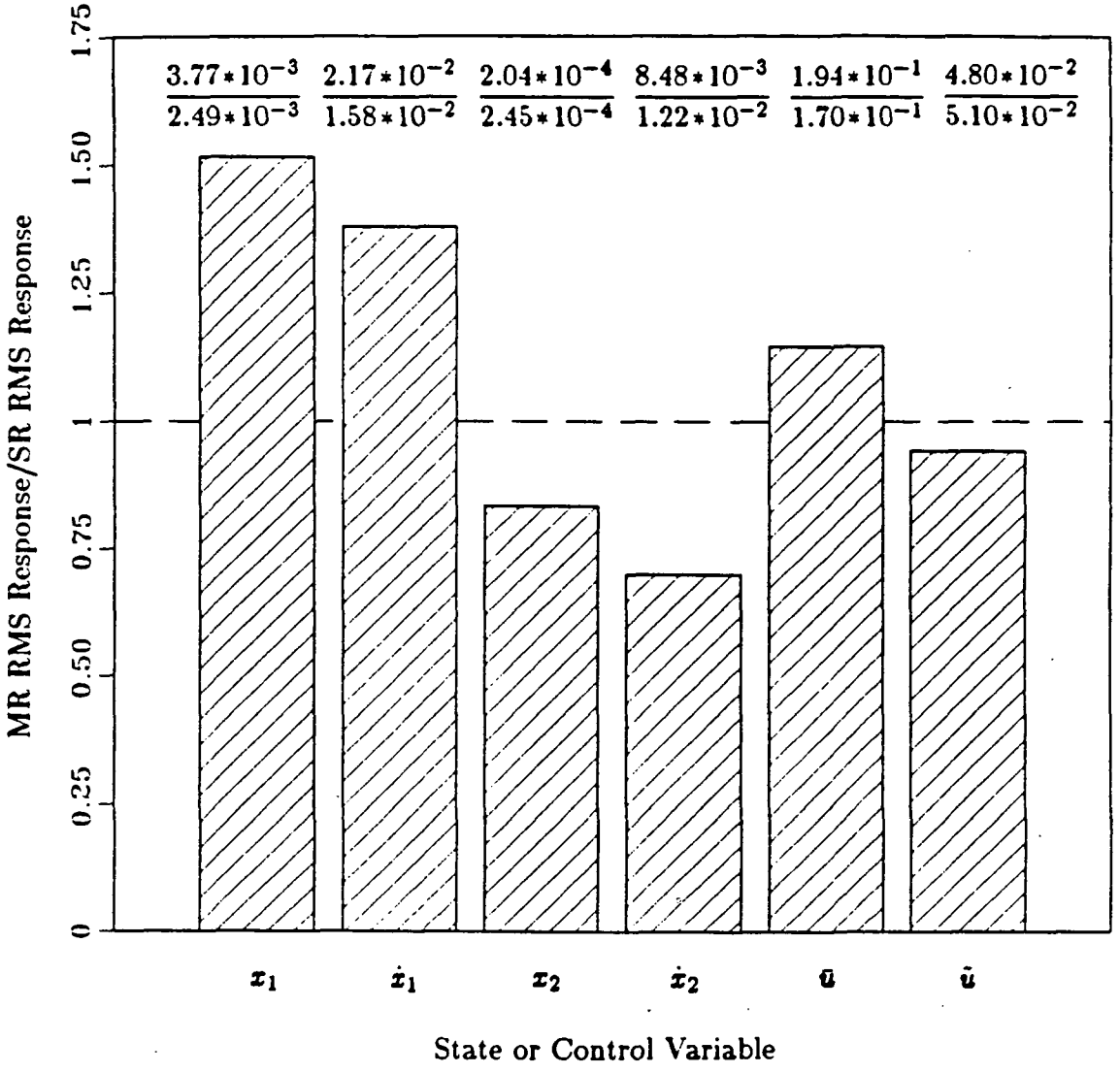

Figure 5.12 Ratios of Steady-State RMS Responses to Process Noise Acting on Body A with Case 1 Compensators.

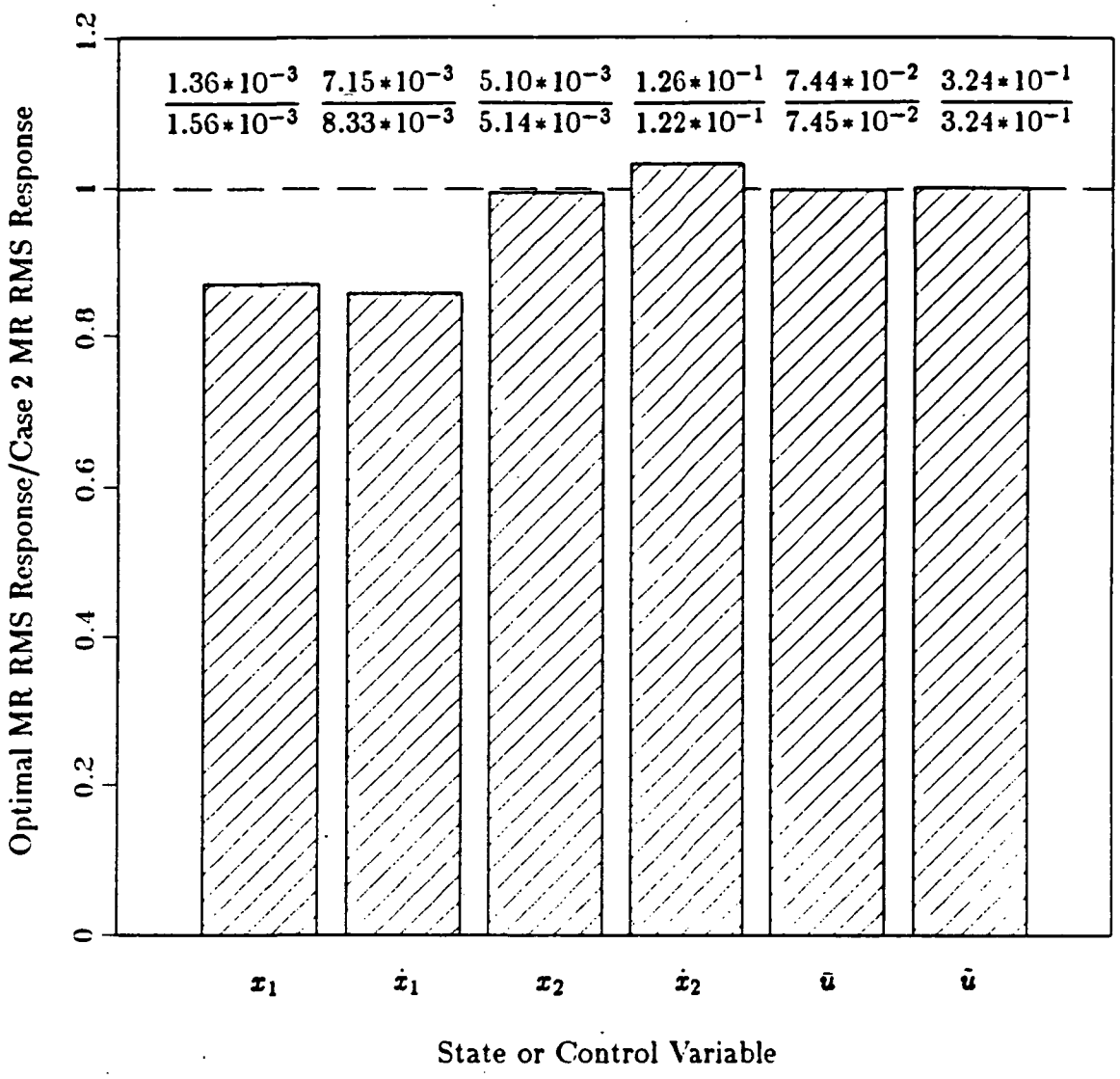

Figure 5.13 Ratios of Steady-State RMS Response to Process Noise with Optimal MR and Case 2 MR Compensators.

MR compensator. The numerator values are the corresponding steady-state RMS state and control responses with a MR compensator synthesized using the optimal control law synthesis method of Section 3.2. The sampling rates for the optimal compensator were 8 samples/second for the $x_1/\dot{x}_1/x_2/\dot{x}_2$-to-$\bar{u}$ control loop, and 32 samples/second for the $x_1/\dot{x}_1/x_2/\dot{x}_2/\bar{u}$-to-$\tilde{u}$ control loop. These are the same sampling rates that were used in the Case 2 MR compensator, except that the optimal MR compensator uses a full state feedback control law for each control loop.

For the optimal compensator performance index, we chose

$$J = \int_0^\infty q_{11}\, x_1^2(t) + q_{22}\, x_2^2(t) + r_{11}\, \bar{u}^2(t) + r_{22}\, \tilde{u}^2(t)\, dt\,. \tag{34}$$

We varied q_{11}, q_{22}, r_{11}, and r_{22} to obtain steady-state RMS closed-loop state responses to $w_c(t)$ that were less than those obtained with the Case 2 MR compensator, for the same steady-state RMS closed-loop control activities. The best results were obtained with

$$J = \int_0^\infty 10\, x_1^2(t) + 400\, x_2^2(t) + 0.014\, \bar{u}^2(t) + 0.1\, \tilde{u}^2(t)\, dt\,. \tag{35}$$

The corresponding optimal MR control laws are

$$\bar{u}(m,n) = -\bar{C}\, x(m,0)\,, \tag{36}$$

$$\tilde{u}(m,n) = -\tilde{C}(n)\, x(m,n) - \tilde{c}(n)\, \bar{u}(m,n)\,, \tag{37}$$

for $m = 0, 1, \ldots$ and $n = 0, 1, \ldots, 3$, where

$$\bar{C} = [\,16.6 \quad 5.75 \quad 4.94 \quad -0.126\,]\,, \tag{38}$$

$$\begin{aligned}
\tilde{C}(0) &= [\,1.92 \quad 0.641 \quad 24.9 \quad 2.41\,]\,,\\
\tilde{C}(1) &= [\,0.335 \quad 0.0881 \quad 24.3 \quad 2.42\,]\,,\\
\tilde{C}(2) &= [\,0.390 \quad 0.121 \quad 24.3 \quad 2.41\,]\,,\\
\tilde{C}(3) &= [\,0.890 \quad 0.309 \quad 24.6 \quad 2.42\,]\,,
\end{aligned} \tag{39}$$

$$\begin{aligned} \tilde{c}(0) &= 0\,, \\ \tilde{c}(1) &= -0.0965\,, \\ \tilde{c}(2) &= -0.0877\,, \\ \tilde{c}(3) &= -0.0529\,. \end{aligned} \tag{40}$$

The presence of the $x_1/\dot{x}_1/\bar{u}$-to-$\tilde{u}$ and $x_2/\dot{x}_2$-to-$\bar{u}$ cross-feed terms in the optimal MR control laws implies that the computation load for real-time operation of the optimal MR compensator is more than twice that for real-time operation of the Case 2 MR compensator. In the light of this, the 13 and 14% reductions in the steady-state RMS x_1 and $\dot{x}_1$ responses in Figure 5.12 do not represent a significant improvement in performance.

Finally, given the small reductions in the x_1 and $\dot{x}_1$ responses in Figure 5.12, it would be pointless to apply the constrained optimization synthesis method of Chapter 4 to this problem, because the reductions in the steady-state RMS x_1, $\dot{x}_1$, x_2, and $\dot{x}_2$ responses with a compensator synthesized using the constrained optimization synthesis method will be less (for the same steady-state RMS control activities) than those obtained with the optimal MR compensator.

Chapter 6

Two Link Robot Arm Design Example

In this chapter we deal with an example design problem involving a two link robot arm (TLA). The open-loop system is described in Section 6.1. The compensator design work is described in Section 6.2. Performance comparisons for the different compensators are presented in Section 6.3. Section 6.4 presents a summary and discussion of the important results.

§6.1 Open-Loop System Description. The open-loop system is shown in Figure 6.1. It is a simplified model of an experimental arm studied by Chiang (1986). Point O is fixed and the two links are rigid. The axes of the rotational joints located at the root and wrist are parallel, and are oriented so that all motions are in a horizontal plane. Reference line R is fixed in the plane of motion and passes through point O. Generalized coordinate θ is the angle of rotation of the first link with respect to R. Generalized coordinate δ is the distance from the tip of the manipulator to R. The wrist angle ϕ is a redundant coordinate. The root angle θ and the tip position δ are measured, and the measurements are assumed to be noise-free. Control inputs u_1 and u_2 are motor torques acting at the root and wrist,

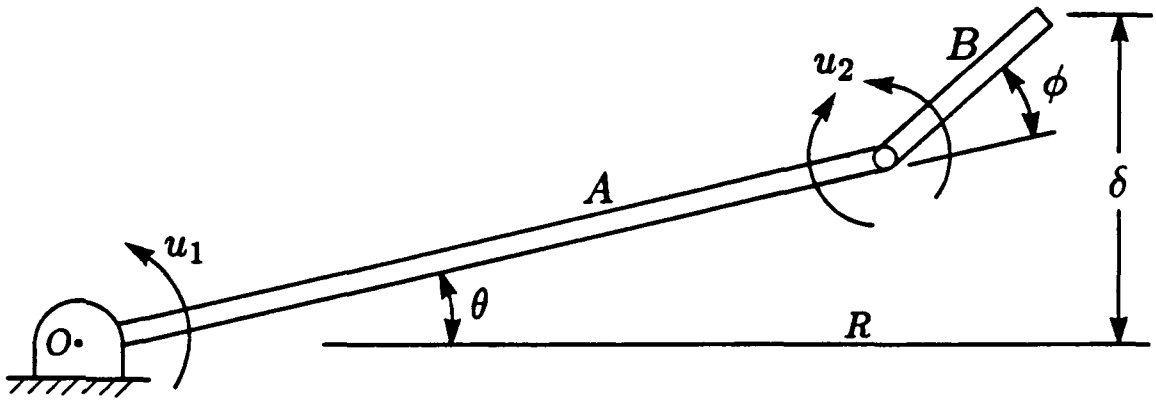

Figure 6.1 Open-Loop TLA System.

respectively.

A linear state equation that describes the motions of this system for small θ and small δ is derived in Appendix A. Let M and L represent the mass per unit length and the length, respectively, of the first link. Let m and l represent the corresponding quantities for the second link. The analog state equation is

$$\dot{p}(t) = F\,p(t) + G\,u(t)\,, \tag{1}$$

where

$$p(t) \triangleq [\,\theta(t) \quad \dot{\theta}(t) \quad \delta(t) \quad \dot{\delta}(t)\,]^{\mathrm{T}}\,, \tag{2}$$

$$u(t) \triangleq [\,u_1(t) \quad u_2(t)\,]^{\mathrm{T}}\,, \tag{3}$$

$$F \triangleq \begin{bmatrix} 0 & 1 & 0 & 0 \\ 0 & 0 & 0 & 0 \\ 0 & 0 & 0 & 1 \\ 0 & 0 & 0 & 0 \end{bmatrix}, \tag{4}$$

$$G \triangleq \frac{1}{e}\begin{bmatrix} 0 & 0 \\ a & -b \\ 0 & 0 \\ -c & d \end{bmatrix}, \tag{5}$$

$$a \triangleq \frac{1}{3}ml^3\,, \tag{6}$$

$$b \triangleq \frac{1}{6}ml^2(2l + 3L)\,, \tag{7}$$

$$c \triangleq \frac{1}{6}mLl^3\,, \tag{8}$$

$$d \triangleq \frac{1}{6}ml^2(3L^2 + Ll) + \frac{1}{3}ML^3l\,, \tag{9}$$

$$e \triangleq \frac{1}{9}MmL^3l^3 + \frac{1}{12}m^2L^2l^4\,. \tag{10}$$

Table 6.1 TLA System Parameters.

PARAMETER	VALUE
M	1.28 kg/m
L	0.965 m
m	0.977 kg/m
l	0.167 m
$\|u_1\|_{MAX}$	1.42 N·m
$\|u_2\|_{MAX}$	0.170 N·m

The values for M, L, m, and l, and for $|u_1|_{MAX}$ and $|u_2|_{MAX}$, the maximum motor torques at the root and wrist, respectively, are in Table 6.1. These are the values for the experimental arm reported by Chiang (1986).

§6.2 Compensator Designs. This section describes the compensator design work. The coverage is is in 5 subsections, although, in practice, the design process is not so conveniently separable. The subsections describe the performance objectives, the compensator structure, the sampling policies, the specific design cases, and the synthesis of the different compensators.

Performance Objectives. The performance objective was to obtain the fastest possible responses to tip positioning commands. This was to be accomplished using reasonable levels of control, and the real-time computation load was to be as low as possible.

Compensator Structure. The compensator structure that we chose is shown in Figure 6.2. It is a double lead network with cross-feed terms. The symbol z^{-1} represents a one-sample delay. The symbol ZOH represents represents a zero-order

hold. The sampling period for δ and u_2 is T. The sampling period for θ and u_1 is PT, where P is a positive, nonzero integer. The synthesis problem is to choose the compensator parameters α_i, β_{ij}, and γ_{ij}, for $i,j=1,2$.

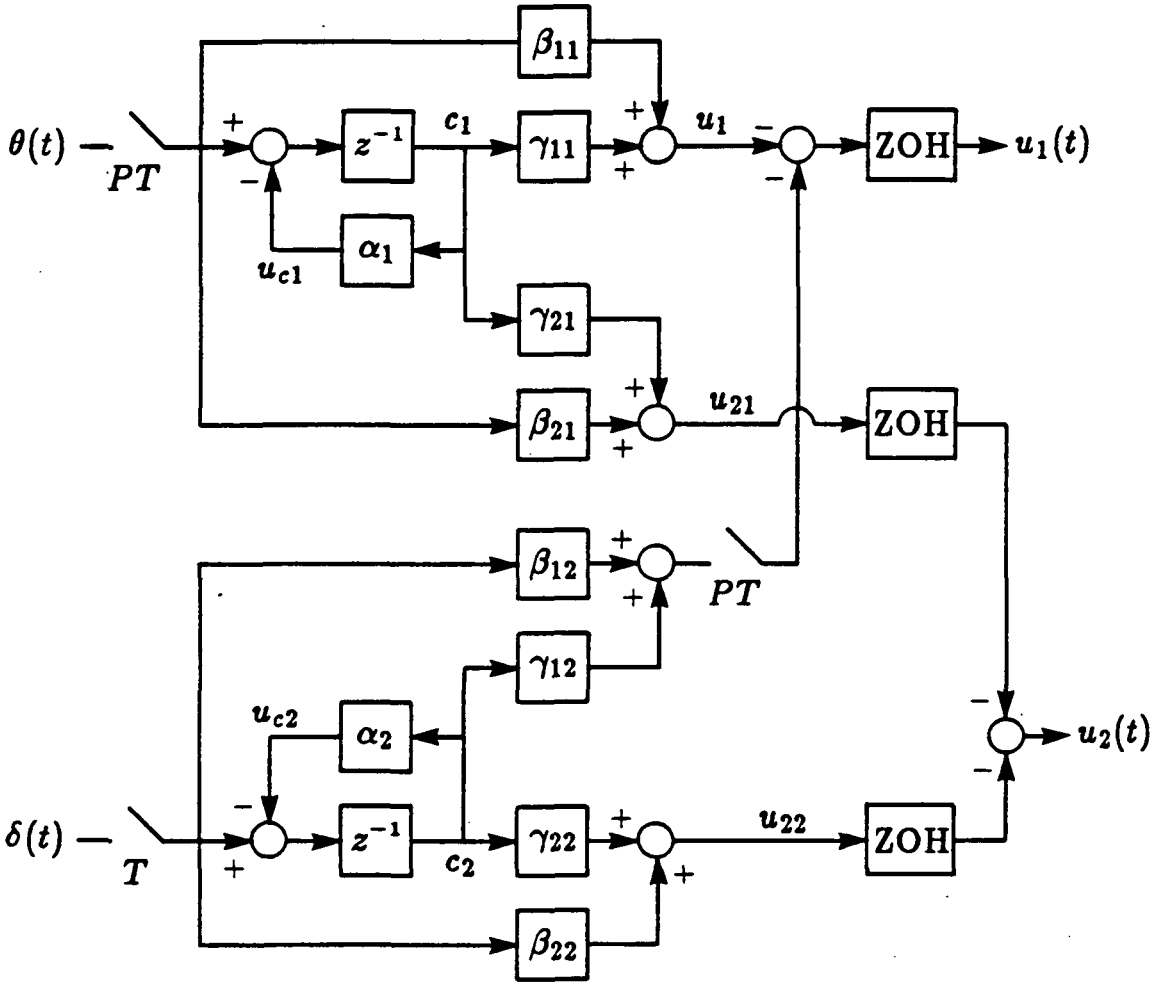

Figure 6.2 TLA Compensator Structure.

Sampling Policies. For sampling rates selection, we first expressed the performance objectives in terms of the desired locations for the closed-loop poles in the s-plane. We picked the sampling rates for θ, u_1, δ and u_2 based on assumptions regarding the coupling of the closed-loop θ, u_1, δ, and u_2 responses to the closed-loop poles. The purpose of the wrist member (i.e., the combination of the wrist

motor and the second link) is to compensate for the low-bandwidth control at the root with relatively high-bandwidth control at the wrist (Chiang, 1986). Thus, the θ and u_1 responses will be primarily coupled to the low frequency closed-loop poles, and the δ and u_2 responses will be primarily coupled to the high frequency closed-loop poles.

The following subsection describes the specific design cases that we considered. One MR compensator and one SR compensator were designed for each design case. Let S_{SR} represent the sampling rate for a SR compensator. Let S_{MR1} represent the sampling rate for θ and u_1 for a MR compensator. Let S_{MR2} represent the sampling rate for δ and u_2 for the same MR compensator. For real-time operation of either compensator, the number of multiplications per u_1 update is the same as the number of multiplications per u_2 update. Consequently, the MR compensator will require the same average number of machine operations per unit time as the SR compensator if S_{MR1}, S_{MR2}, and S_{SR} satisfy

$$S_{MR1} + S_{MR2} = 2\, S_{SR}\,. \tag{11}$$

For each design case, we picked S_{SR} such that

$$S_{SR} = k_{SR}\, f_{CL2}\,, \tag{12}$$

where f_{CL2} represents the characteristic frequency in hertz of the high-frequency desired s-plane closed-loop poles, and k_{SR} was either 5 (for a slow-sampling-rates case) or 20 (for a fast-sampling-rates case). For the same design case, we picked S_{MR1} and S_{MR2} using

$$S_{MR1} = k_{MR}\, f_{CL1} \qquad \text{and} \qquad S_{MR2} = k_{MR}\, f_{CL2}\,, \tag{13}$$

where k_{MR} is a constant, and f_{CL1} and f_{CL2} represent the characteristic frequencies in hertz of the low-frequency and high-frequency desired s-plane closed-loop poles,

respectively. To ensure that the computation loads for real-time operation of the two compensators are the same, we picked k_{MR} (and thus S_{MR1} and S_{MR2}) such the (11) is satisfied.

Design Cases. Tables 6.2 and 6.3 describe in detail the specific design cases that we considered. There are three cases in all. One MR and one SR compensator were designed for each design case. Table 6.2 lists the values of all fixed parameters. The case dependent parameters are in Table 6.3. The symbols f and ς denote a natural frequency and a damping ratio, respectively, with the subscripts OL or CL indicating open-loop or closed-loop, respectively, and the trailing 1 or 2 indicating association with low frequency or high frequency poles, respectively. The parameter S_{SR} is the sampling rate for a SR compensator. The parameter S_{MR1} is the sampling rate for θ and u_1 for a MR compensator. The parameter S_{MR2} is the sampling rate for δ and u_2 for a MR compensator.

Table 6.2 Fixed TLA Design Parameters.

PARAMETER	VALUE
f_{OL1}	0 hertz
ς_{OL1}	0
ς_{OL2}	0
f_{CL1}	0.5 hertz
ς_{CL1}	$1/\sqrt{2}$
ς_{CL2}	$1/\sqrt{2}$

For Design Case 1, the desired s-plane closed-loop poles are critically damped and have characteristic frequencies of 0.5 and 4 hertz. For the SR compensator, we picked S_{SR} using (12) at 20 samples/second, or 5 times the characteristic frequency of the high frequency desired s-plane closed-loop poles. For the MR compensator, we picked S_{MR1} and S_{MR2} using (11) and (13) at 4.45 and 35.6 samples/second, respectively, or 8.89 times the characteristic frequencies of the low frequency and

Table 6.3 Variable TLA Design Parameters.

PARAMETER	UNITS	NUMERIC VALUE		
		Case 1	Case 2	Case 3
f_{CL2}/f_{CL1}	—	8	4	8
S_{MR2}/S_{MR1}	—	8	4	8
S_{SR}/f_{CL2}	samples/cycle	5	5	20
S_{MR2}/S_{SR}	—	1.78	1.6	1.78

high frequency desired s-plane closed-loop poles, respectively.

Design Case 2 is the same as Case 1, except that the characteristic frequency of the high frequency desired s-plane closed-loop poles is 2 hertz. For the SR compensator, we picked S_{SR} using (12) at 10 samples/second, or 5 times the characteristic frequency of the high frequency desired s-plane closed-loop poles. For the MR compensator, we picked S_{MR1} and S_{MR2} using (11) and (13) at 4 and 16 samples/second, respectively, or 8 times the characteristic frequencies of the low frequency and high frequency desired s-plane closed-loop poles, respectively.

Design Case 3 is the same as Case 1, except that all sampling rates are increased by a factor of 4. For the SR compensator, we picked S_{SR} using (12) at 80 samples/second, or 20 times the characteristic frequency of the high frequency desired s-plane closed-loop poles. For the MR compensator, we picked S_{MR1} and S_{MR2} using (11) and (13) at 17.8 and 142 samples/second, respectively, or 35.6 times the characteristic frequencies of the low frequency and high frequency desired s-plane closed-loop poles, respectively.

Synthesis. With ten compensator parameters to determine, including four cross-feed terms, the compensator structure in Figure 6.2 is complicated enough that it is difficult to apply the successive loop closures synthesis method of Section 3.1. Furthermore, because the compensator structure in Figure 6.2 has a reduced

dynamic order (i.e., a dynamic order that is less than that of the plant), the optimal control law synthesis method of Section 3.2 cannot be applied. For synthesis, we used the constrained optimization synthesis method of Chapter 4 because it easily handles the compensator structure in Figure 6.2.

The constrained optimization synthesis method determines a feedback control law that minimizes a performance index that is a quadratic sum of the state and control responses to a prescribed process noise. It is the user's responsibility to determine a suitable model for this noise; the method requires only that it takes the form of a periodically stationary, zero-mean, gaussian, purely random input sequence. Following Schmidt's suggestion (1985), from his work on a one-link version of the Chiang arm, we used disturbance torques acting at the root and wrist actuators to model the process noise. Let

$$w(t) \triangleq [\, w_1(t) \quad w_2(t) \,] \,, \tag{14}$$

where $w_1(t)$ and $w_2(t)$ are the disturbance torques acting at the root and wrist actuators, respectively. The torques $w_1(t)$ and $w_2(t)$ are assumed to be mutually uncorrelated, stationary, zero-mean, gaussian white noise processes of intensities $\tilde{W}_1$ and $\tilde{W}_2$, respectively, so that

$$\mathrm{E}\{w(t)\, w^{\mathrm{T}}(\tau)\} = \tilde{W}\, \delta(t-\tau) \,, \tag{15}$$

where $\delta(\cdot)$ is the Dirac delta function, and

$$\tilde{W} = \begin{bmatrix} \tilde{W}_1 & 0 \\ 0 & \tilde{W}_2 \end{bmatrix} . \tag{16}$$

Adding the process noise $w(t)$ to the state model of the analog plant in (1), we obtain

$$\dot{p}(t) = F\, p(t) + G\, u(t) + G\, w(t) \,. \tag{17}$$

Let $p(m,n)$ represent the state of the analog plant $p(t)$ in (17) at the $(mP+n)$th sampling instant. Let $c_1(m,n)$, $c_2(m,n)$, $u_1(m,n)$, $u_{21}(m,n)$, $u_{22}(m,n)$, $u_{c1}(m,n)$, and $u_{c2}(m,n)$ represent the signals so labeled in Figure 6.2 at the $(mP+n)$th sampling instant. Let $h_1(m,n)$ and $h_2(m,n)$ represent the states of the zero-order holds for $u_1(m,n)$ and $u_{21}(m,n)$, respectively, in Figure 6.2, at the $(mP+n)$th sampling instant. Let $w(m,n)$ represent the effect on $p(t)$ at the $(mP+n+1)$th sampling instant of the process noise that occurs between the $(mP+n)$th and $(mP+n+1)$th sampling instants; that is let

$$w(m,n) \triangleq \int_{(mP+n)T}^{(mP+n+1)T} e^{F((mP+n+1)T-t)} G\, w(t)\, dt\,. \tag{18}$$

Let

$$A \triangleq e^{FT}\,, \tag{19}$$

$$B \triangleq \int_0^T e^{Ft} dt\, G\,, \tag{20}$$

and let B_1 and B_2 represent the first and second columns, respectively, of B. Let I_p represent an identity matix with the same number of rows and columns as there are elements in $p(t)$. Then, for the closed-loop system made up of the analog plant in (17) plus the compensator in Figure 6.2, the responses to $w(t)$ satisfy

$$x(m,n+1) = A(n)\, x(m,n) + B(n)\, u(m,n) + B_w\, w(m,n)\,, \tag{21}$$

with

$$u(m,n) = -C\, x(m,n)\,, \tag{22}$$

for $m=0, 1, \ldots$ and $n=0, 1, \ldots, P-1$, where

$$x(m,n) \triangleq [\,p^{\mathrm{T}}(m,n) \quad h_1(m,n) \quad h_2(m,n) \quad c_1(m,n) \quad c_2(m,n)\,]^{\mathrm{T}}\,, \tag{23}$$

$$u(m,n) \triangleq [\,u_1(m,n) \quad u_{21}(m,n) \quad u_{22}(m,n) \quad u_{c1}(m,n) \quad u_{c2}(m,n)\,]^{\mathrm{T}}\,, \tag{24}$$

C-2

$$A(0) \triangleq \begin{bmatrix} & & & & 0 & 0 & 0 & 0 \\ & & & & 0 & 0 & 0 & 0 \\ & A & & & 0 & 0 & 0 & 0 \\ & & & & 0 & 0 & 0 & 0 \\ 0 & 0 & 0 & 0 & 0 & 0 & 0 & 0 \\ 0 & 0 & 0 & 0 & 0 & 0 & 0 & 0 \\ 1 & 0 & 0 & 0 & 0 & 0 & 0 & 0 \\ 0 & 0 & 1 & 0 & 0 & 0 & 0 & 0 \end{bmatrix}, \tag{25}$$

$$A(1) \triangleq A(2) \triangleq \cdots \triangleq A(P-1) \triangleq \begin{bmatrix} & & A & & B_1 & B_2 & 0 & 0 \\ & & & & & & 0 & 0 \\ & & & & & & 0 & 0 \\ & & & & & & 0 & 0 \\ 0 & 0 & 0 & 0 & 1 & 0 & 0 & 0 \\ 0 & 0 & 0 & 0 & 0 & 1 & 0 & 0 \\ 0 & 0 & 0 & 0 & 0 & 0 & 1 & 0 \\ 0 & 0 & 1 & 0 & 0 & 0 & 0 & 0 \end{bmatrix}, \tag{26}$$

$$B(0) \triangleq \begin{bmatrix} & & & 0 & 0 & 0 \\ & & & 0 & 0 & 0 \\ B_1 & B_2 & B_2 & 0 & 0 & 0 \\ & & & 0 & 0 & 0 \\ 1 & 0 & 0 & 0 & 0 & 0 \\ 0 & 1 & 0 & 0 & 0 & 0 \\ 0 & 0 & 0 & 0 & 1 & 0 \\ 0 & 0 & 0 & 0 & 0 & 1 \end{bmatrix}, \tag{27}$$

$$B(1) \triangleq B(2) \triangleq \cdots \triangleq B(P-1) \triangleq \begin{bmatrix} 0 & 0 & & 0 & 0 & 0 \\ 0 & 0 & & 0 & 0 & 0 \\ 0 & 0 & B_2 & 0 & 0 & 0 \\ 0 & 0 & & 0 & 0 & 0 \\ 0 & 0 & 0 & 0 & 0 & 0 \\ 0 & 0 & 0 & 0 & 0 & 0 \\ 0 & 0 & 0 & 0 & 0 & 0 \\ 0 & 0 & 0 & 0 & 0 & 1 \end{bmatrix}, \tag{28}$$

$$B_w \triangleq \begin{bmatrix} & & & \\ & I_p & & \\ & & & \\ 0 & 0 & 0 & 0 \\ 0 & 0 & 0 & 0 \\ 0 & 0 & 0 & 0 \\ 0 & 0 & 0 & 0 \end{bmatrix}, \tag{29}$$

$$C \triangleq \begin{bmatrix} \beta_{11} & 0 & \beta_{12} & 0 & 0 & 0 & \gamma_{11} & \gamma_{12} \\ \beta_{21} & 0 & 0 & 0 & 0 & 0 & \gamma_{21} & 0 \\ 0 & 0 & \beta_{22} & 0 & 0 & 0 & 0 & \gamma_{22} \\ 0 & 0 & 0 & 0 & 0 & 0 & \alpha_1 & 0 \\ 0 & 0 & 0 & 0 & 0 & 0 & 0 & \alpha_2 \end{bmatrix} . \tag{30}$$

If $P=1$ the compensator in Figure 6.2 is SR. In this case, the formulation in (21) through (30) simplifies to

$$x(m+1,0) = A(0)\,x(m,0) + B(0)\,u(m,0) + B_w\,w(m,0)\,, \tag{31}$$

with

$$u(m,0) = -C\,x(m,0)\,, \tag{32}$$

for $m=0, 1, \ldots,$ where

$$x(m,0) \triangleq [\,p^{\mathrm{T}}(m,0) \quad c_1(m,0) \quad c_2(m,0)\,]^{\mathrm{T}}\,, \tag{33}$$

$$u(m,0) \triangleq [\,u_1(m,0) \quad u_{22}(m,0) \quad u_{c1}(m,0) \quad u_{c2}(m,0)\,]^{\mathrm{T}}\,, \tag{34}$$

$$A(0) \triangleq \begin{bmatrix} & & & & 0 & 0 \\ & & A & & 0 & 0 \\ & & & & 0 & 0 \\ & & & & 0 & 0 \\ 1 & 0 & 0 & 0 & 0 & 0 \\ 0 & 0 & 1 & 0 & 0 & 0 \end{bmatrix}, \tag{35}$$

$$B(0) \triangleq \begin{bmatrix} & & 0 & 0 \\ & B & 0 & 0 \\ & & 0 & 0 \\ & & 0 & 0 \\ 0 & 0 & 1 & 0 \\ 0 & 0 & 0 & 1 \end{bmatrix}, \tag{36}$$

$$B_w \triangleq \begin{bmatrix} & & & \\ & I_p & & \\ & & & \\ 0 & 0 & 0 & 0 \\ 0 & 0 & 0 & 0 \end{bmatrix}, \tag{37}$$

$$C \triangleq \begin{bmatrix} \beta_{11} & 0 & \beta_{12} & 0 & \gamma_{11} & \gamma_{12} \\ \beta_{21} & 0 & \beta_{22} & 0 & \gamma_{21} & \gamma_{22} \\ 0 & 0 & 0 & 0 & \alpha_1 & 0 \\ 0 & 0 & 0 & 0 & 0 & \alpha_2 \end{bmatrix} . \tag{38}$$

The key point in each of these formulations is that the compensator parameters appear exclusively as elements of the state feedback gain matrix C. The constrained optimization synthesis method of Chapter 4 can consequently be used. We used the constrained optimization synthesis method and applied the AMS computer program to determine values for the compensator parameters α_i, β_{ij}, and γ_{ij}, for $i,j=1,2$, that minimized a performance index of the form

$$\tilde{J}_{\rm SS} \triangleq \lim_{N\to\infty} \tilde{J}(N)\,, \tag{39}$$

where

$$\tilde{J}(N) \triangleq \mathrm{E}\Big\{\frac{1}{2NPT}\int_0^{NPT} \begin{bmatrix} p(t) \\ u(t) \end{bmatrix}^{\mathrm{T}} \begin{bmatrix} \tilde{Q} & 0 \\ 0 & \tilde{R} \end{bmatrix} \begin{bmatrix} p(t) \\ u(t) \end{bmatrix} dt\Big\}\,. \tag{40}$$

The discretization procedures of Sections 2.1 and 2.2 are part of the AMS package. For each optimization, the discretization procedures were called first to solve for the discrete state model of the plant, the covariance of the stationary, zero-mean, gaussian, purely random input sequence $w(m,n)$, and the discrete equivalent to the analog performance index, given the sampling rates, the analog state model of the plant, the compensator structure, and the synthesis parmeters $\tilde{W}_1$, $\tilde{W}_2$, $\tilde{Q}$, and $\tilde{R}$.

Because each optimization requires a gradient search to determine the compensator parameters, a considerable effort went into determining reasonable values for $\tilde{W}_1$, $\tilde{W}_2$, $\tilde{Q}$, and $\tilde{R}$ prior to the first optimization for each design case. For the process noise levels $\tilde{W}_1$ and $\tilde{W}_2$, we picked values such that

$$\frac{\tilde{W}_1}{\tilde{W}_2} = \frac{|u_1|^2_{\rm MAX}}{|u_2|^2_{\rm MAX}}\,, \tag{41}$$

where the values for $|u_1|_{\rm MAX}$ and $|u_2|_{\rm MAX}$ were obtained from Table 6.1. For $\tilde{Q}$ and $\tilde{R}$, we used an approach suggested by Parsons (1982) and substituted values from analog linear quadratic regulator designs that obtained analog closed-loop poles that

matched the appropriate set of desired s-plane closed-loop poles from Tables 6.2 and 6.3.

For the analog regulator designs, we used a performance index identical to $\tilde{J}_{ss}$ in (39). We constrained the performance index weighting matrices $\tilde{Q}$ and $\tilde{R}$ to be diagonal. We constrained the $\dot{\theta}^2$ and $\dot{\delta}^2$ elements of $\tilde{Q}$ to be zero. Let $\tilde{R}_1$ and $\tilde{R}_2$ represent the $u_1^2(t)$ and $u_2^2(t)$ elements, respectively, of $\tilde{R}$. Let $\tilde{Q}_\theta$ and $\tilde{Q}_\delta$ represent the θ^2 and δ^2 elements, respectively, of $\tilde{Q}$. For $\tilde{R}_1$ and $\tilde{R}_2$, we picked values such that

$$\frac{\tilde{R}_1}{\tilde{R}_2} = \frac{1/|u_1|^2_{MAX}}{1/|u_2|^2_{MAX}}, \tag{42}$$

where the values for $|u_1|_{MAX}$ and $|u_2|_{MAX}$ were obtained from Table 6.1. For $\tilde{Q}_\theta$ and $\tilde{Q}_\delta$, we used trial-and-error to determine values for each design case such that the closed-loop analog regulator poles matched appropriate set of desired s-plane closed-loop poles from Tables 6.2 and 6.3.

Table 6.4 TLA Synthesis Parameters.

		NUMERIC VALUE		
PARAMETER	UNITS	Case 1	Case 2	Case 3
$\tilde{W}_1$	$(\text{N}\cdot\text{m})^2$	69.4	69.4	69.4
$\tilde{W}_2$	$(\text{N}\cdot\text{m})^2$	1.	1.	1.
Q_θ	—	21.	21.3	21.
Q_δ	m^{-2}	1850.	115.	1850.
R_1	$(\text{N}\cdot\text{m})^{-2}$	1.	1.	1.
R_2	$(\text{N}\cdot\text{m})^{-2}$	69.4	69.4	69.4

The final values for the synthesis parameters for the three design cases are in Table 6.4. For the MR compensators, the performance index weighting on $u_2(t)$ was handled in a special way. From Figure 6.2, if $P \neq 1$ the analog control $u_2(t)$ is the sum of a slow-rate component $u_{21}(t)$ and a fast-rate component $u_{22}(t)$. In this

case, it is convenient to separate $u_2(t)$ into these components at the analog-model level. The equivalent $\tilde{R}$ element is then a 2-by-2 block, with $\tilde{R}_2$ at every position, since

$$u_2(t) = u_{21}(t) + u_{22}(t)$$
$$\Rightarrow u_2(t)\,\tilde{R}_2\,u_2(t) = \begin{bmatrix} u_{21}(t) \\ u_{22}(t) \end{bmatrix}^T \begin{bmatrix} \tilde{R}_2 & \tilde{R}_2 \\ \tilde{R}_2 & \tilde{R}_2 \end{bmatrix} \begin{bmatrix} u_{21}(t) \\ u_{22}(t) \end{bmatrix}.$$

The corresponding solutions for the compensator parameters are in Tables 6.5 through 6.7. The peformance characteristics of these compensators are compared in the following section.

Table 6.5 TLA Compensator Parameters for Case 1.

PARAMETER	UNITS	NUMERIC VALUE	
		MR	SR
α_1	—	0.485	0.618
β_{11}	N·m	11.3	60.7
β_{12}	N	0.393	7.81
γ_{11}	N·m	−13.5	−91.7
γ_{12}	N	1.07	−13.3
α_2	—	0.553	0.687
β_{21}	N·m	0.0976	0.559
β_{22}	N	13.4	7.04
γ_{21}	N·m	−0.121	−0.849
γ_{22}	N	−16.9	−9.13

Figure 6.3 is a z-plane plot of the closed-loop BTP poles (see Section 2.2 for the deffinition of a closed-loop BTP pole) with the Case 1 MR compensator. The □s are the e^{sPT} transformations of the desired s-plane closed-loop poles. The ×s are the actual closed-loop BTP poles. The two real ×s are the compensator poles.

Table 6.6 TLA Compensator Parameters for Case 2.

PARAMETER	UNITS	NUMERIC VALUE	
		MR	SR
α_1	—	0.332	0.625
β_{11}	N·m	8.75	29.3
β_{12}	N	0.970	4.78
γ_{11}	N·m	−9.13	−42.1
γ_{12}	N	−0.192	−7.22
α_2	—	0.577	0.684
β_{21}	N·m	0.0527	0.234
β_{22}	N	3.03	1.78
γ_{21}	N·m	−0.0695	−0.348
γ_{22}	N	−3.83	−2.30

Table 6.7 TLA Compensator Parameters for Case 3.

PARAMETER	UNITS	NUMERIC VALUE	
		MR	SR
α_1	—	0.0705	0.373
β_{11}	N·m	37.2	213.
β_{12}	N	8.05	23.6
γ_{11}	N·m	−36.0	−287.
γ_{12}	N	−8.05	−35.5
α_2	—	0.354	0.412
β_{21}	N·m	0.327	1.94
β_{22}	N	54.0	30.7
γ_{21}	N·m	−0.323	−2.63
γ_{22}	N	−67.4	−38.2

Since pole assignment is not the objective of the constrained optimization synthesis method, an exact match of the desired and actual closed-loop poles is not expected. It is encouraging, however, that the low frequency complex-conjugate closed-loop BTP poles in Figure 6.3 are close to their desired locations.

But the BTP poles in Figure 6.3 are a poor indicator of the system's high frequency behavior because the BTP is large compared to the characteristic times of the high frequency closed-loop poles. Figure 6.4 provides some indication of this high frequency behavior. The sampling rate for Figure 6.4 is the fast $1/T$ sampling rate for the Case 1 MR compensator. The □s are the e^{sT} transformations of the high frequency desired s-plane closed-loop poles for Case 1. The ×s are the actual closed-loop poles with just the δ-to-u_2 tip controller portion of the Case 1 MR compensator (i.e., with the Case 1 MR compensator, but with α_1, β_{11}, β_{12}, β_{21}, γ_{11}, γ_{12}, and γ_{21} set to zero). The real × in the left half plane is the pole associated with the tip controller portion of the Case 1 MR compensator.

Figure 6.5 is the corresponding z-plane plot of the closed-loop poles for the Case 1 SR compensator. The □s are the e^{sT} transformations of the desired s-plane closed-loop poles. The ×s are the actual closed-loop poles. The two real ×s are the compensator poles.

For completeness, the z-plane plots of the closed-loop poles for the Case 2 and 3 compensators are shown in Figures 6.6 through 6.11.

§6.3 Performance Comparisons. The performance comparisons in this section are based on the closed-loop responses to a reference tip positioning command. The servo configuration that we chose is in Figure 6.12. The command input is $\delta_c(t)$, in meters. The feed-forward operator $1/(L+l)$ generates a θ command that yields a (nearly) zero steady-state wrist angle, for any steady-state δ_c value that is small compared to $L+l$.

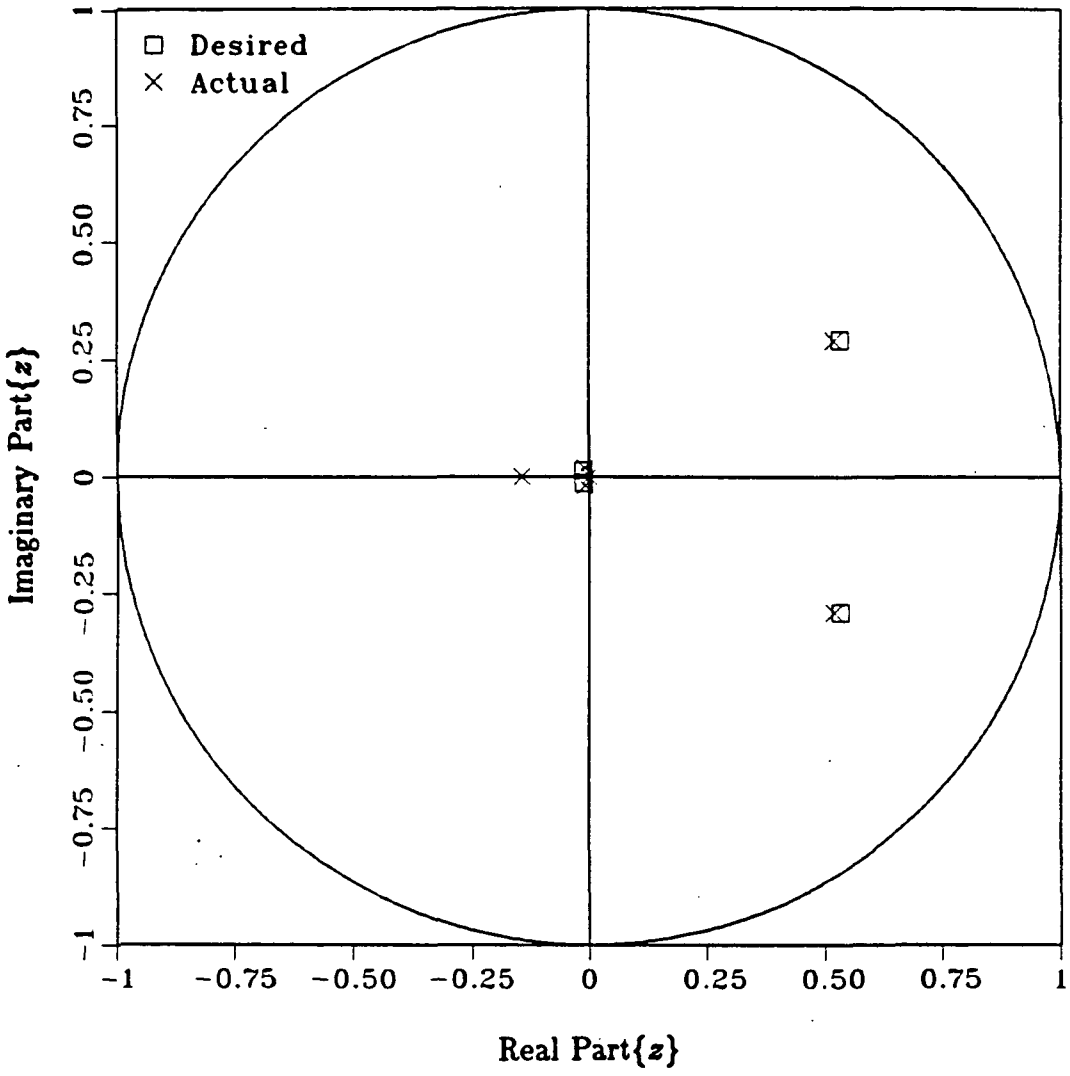

Figure 6.3 Closed-Loop BTP Poles with Case 1 MR Compensator. (Sampling Rate = 4.45 Samples/Second.)

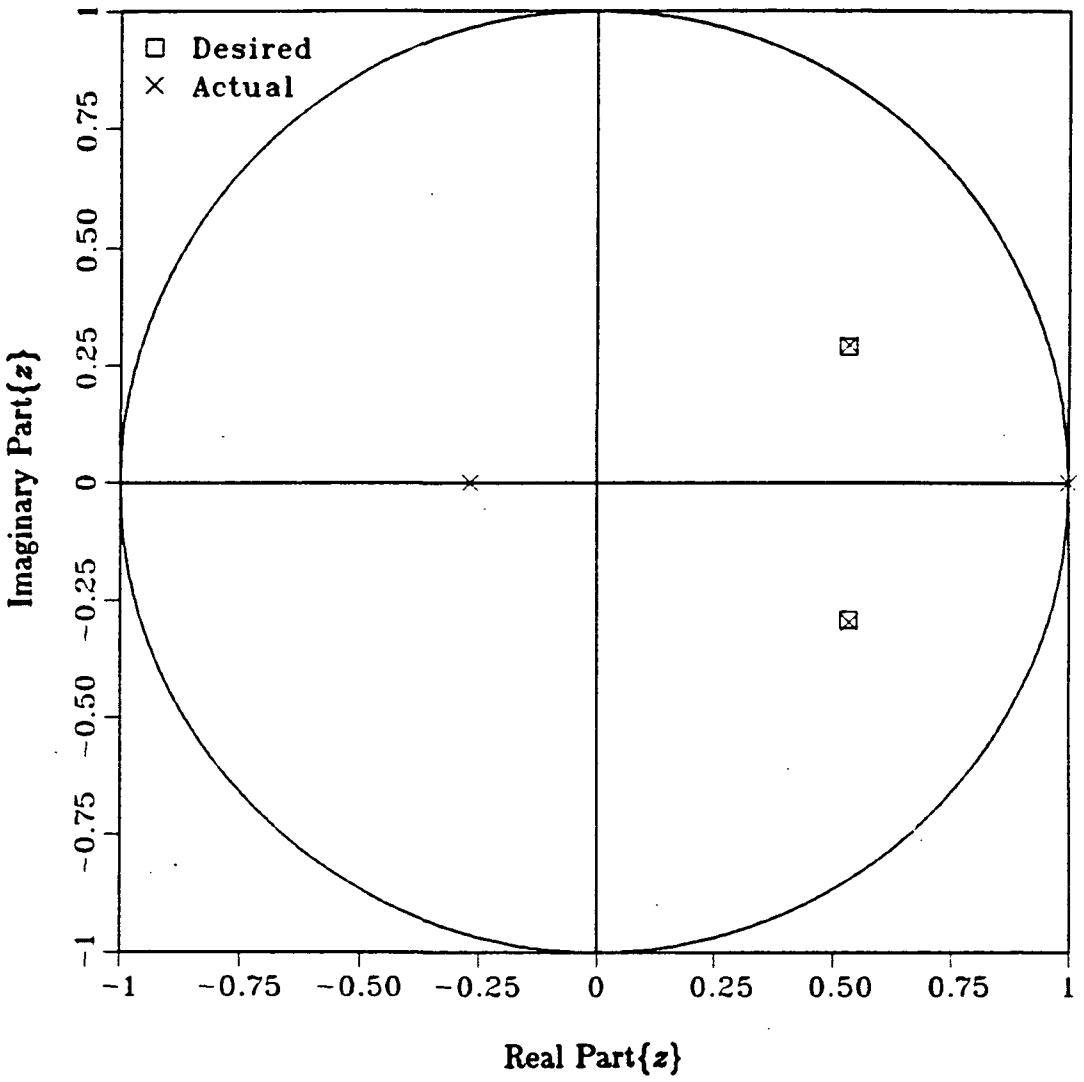

Figure 6.4 Closed-Loop Poles with Tip Controller Portion of Case 1 MR Compensator. (Sampling Rate = 35.56 Samples/Second.)

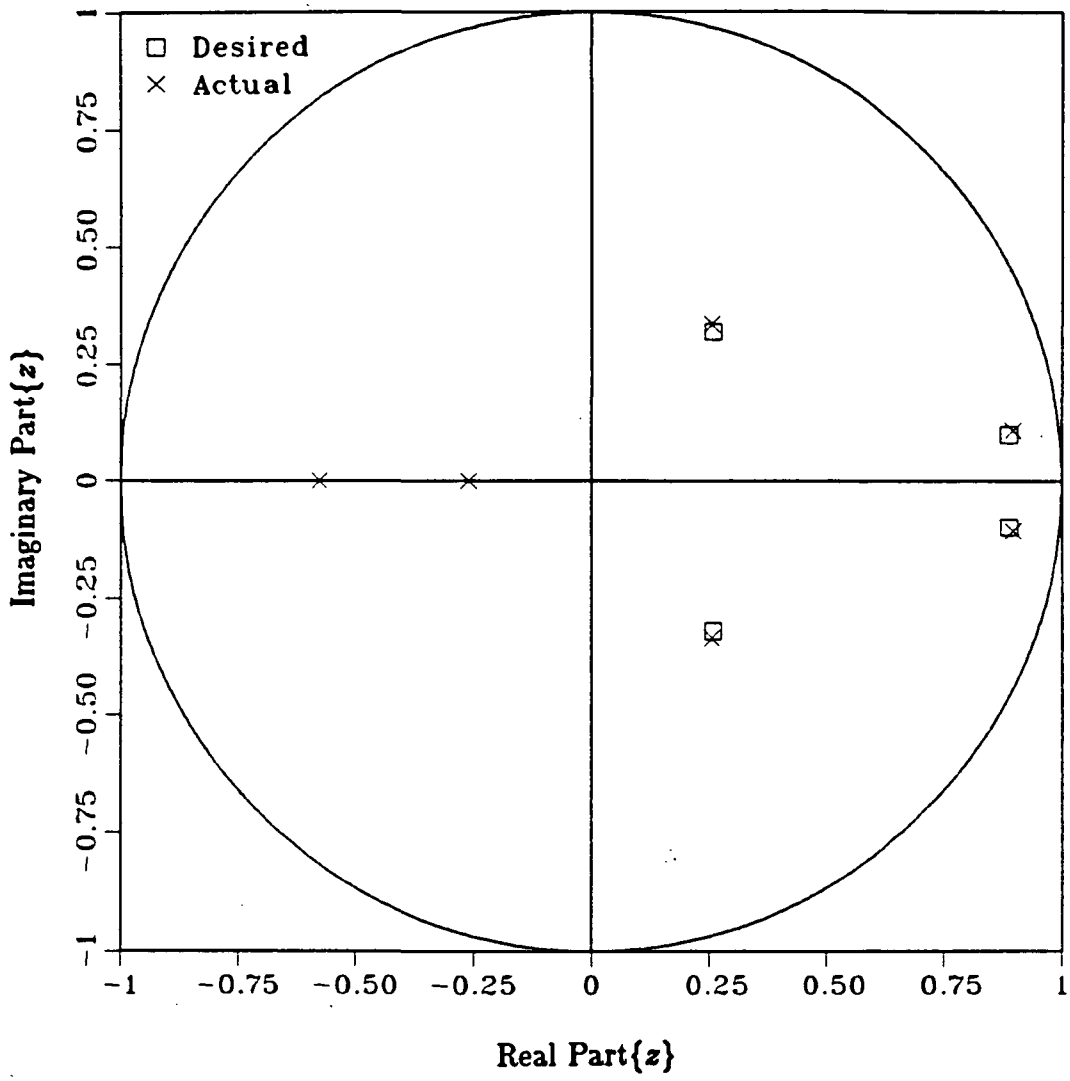

Figure 6.5 Closed-Loop Poles with Case 1 SR Compensator. (Sampling Rate = 20 Samples/Second.)

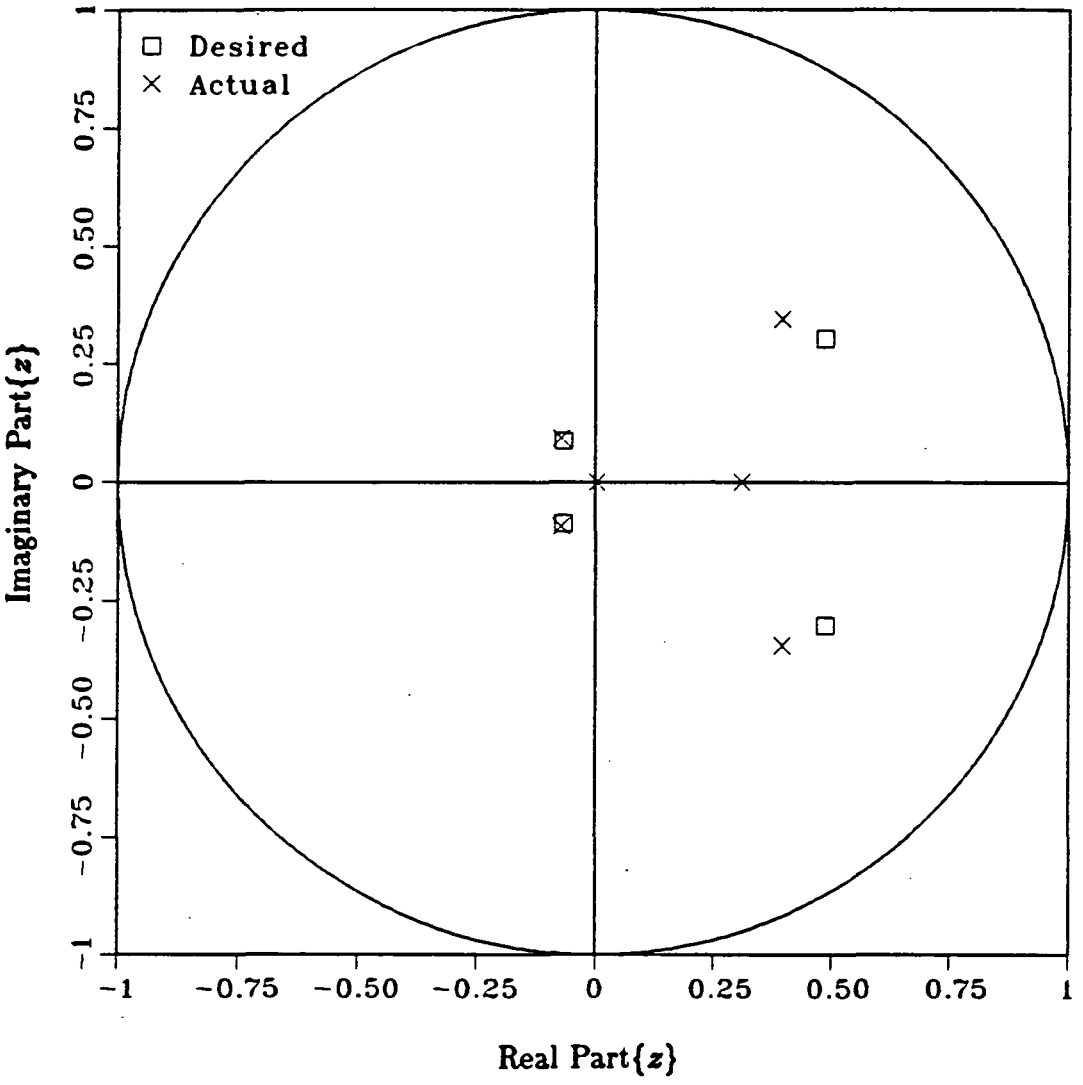

Figure 6.6 Closed-Loop BTP Poles with Case 2 MR Compensator. (Sampling Rate = 4 Samples/Second.)

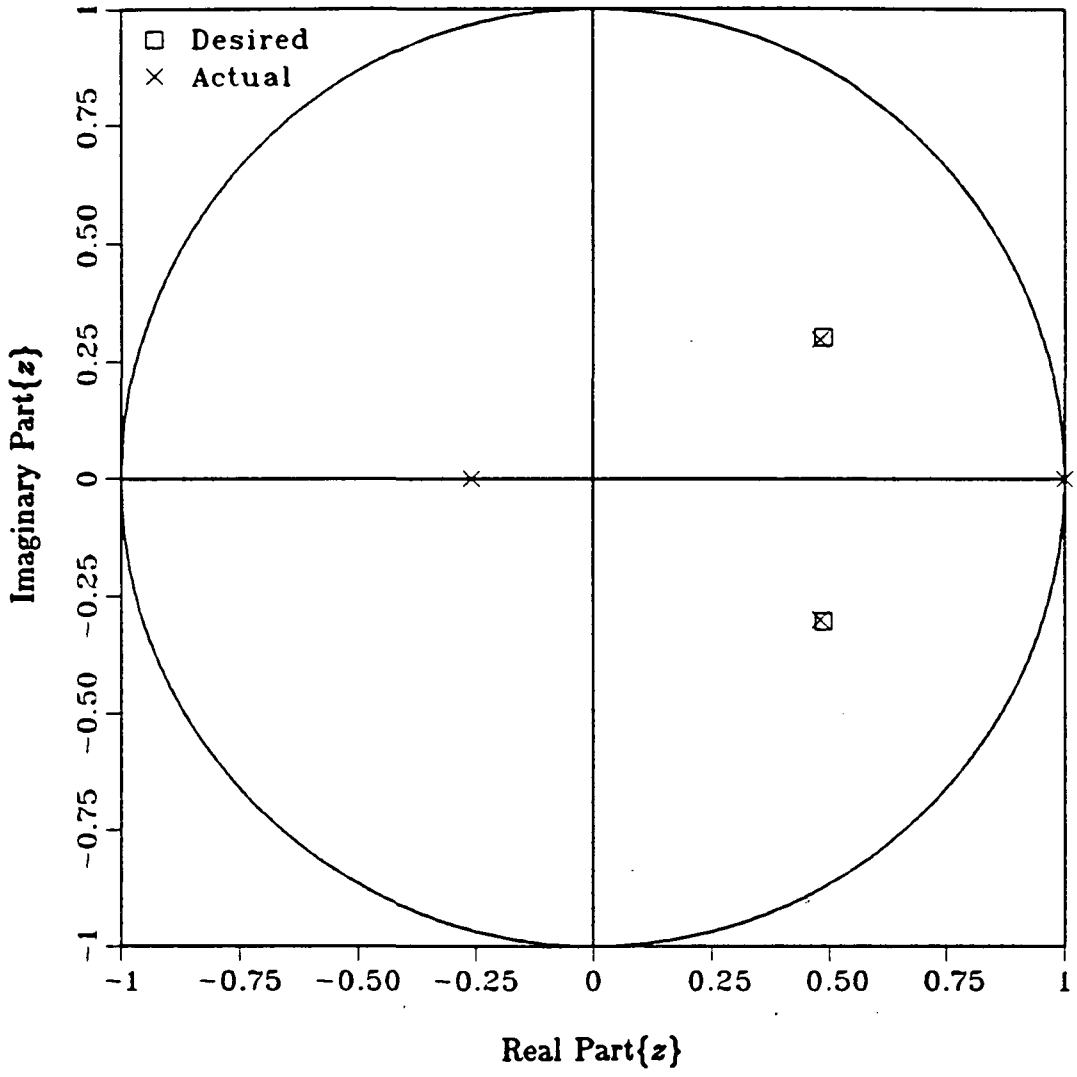

Figure 6.7 Closed-Loop Poles with Tip Controller Portion of Case 2 MR Compensator. (Sampling Rate = 16 Samples/Second.)

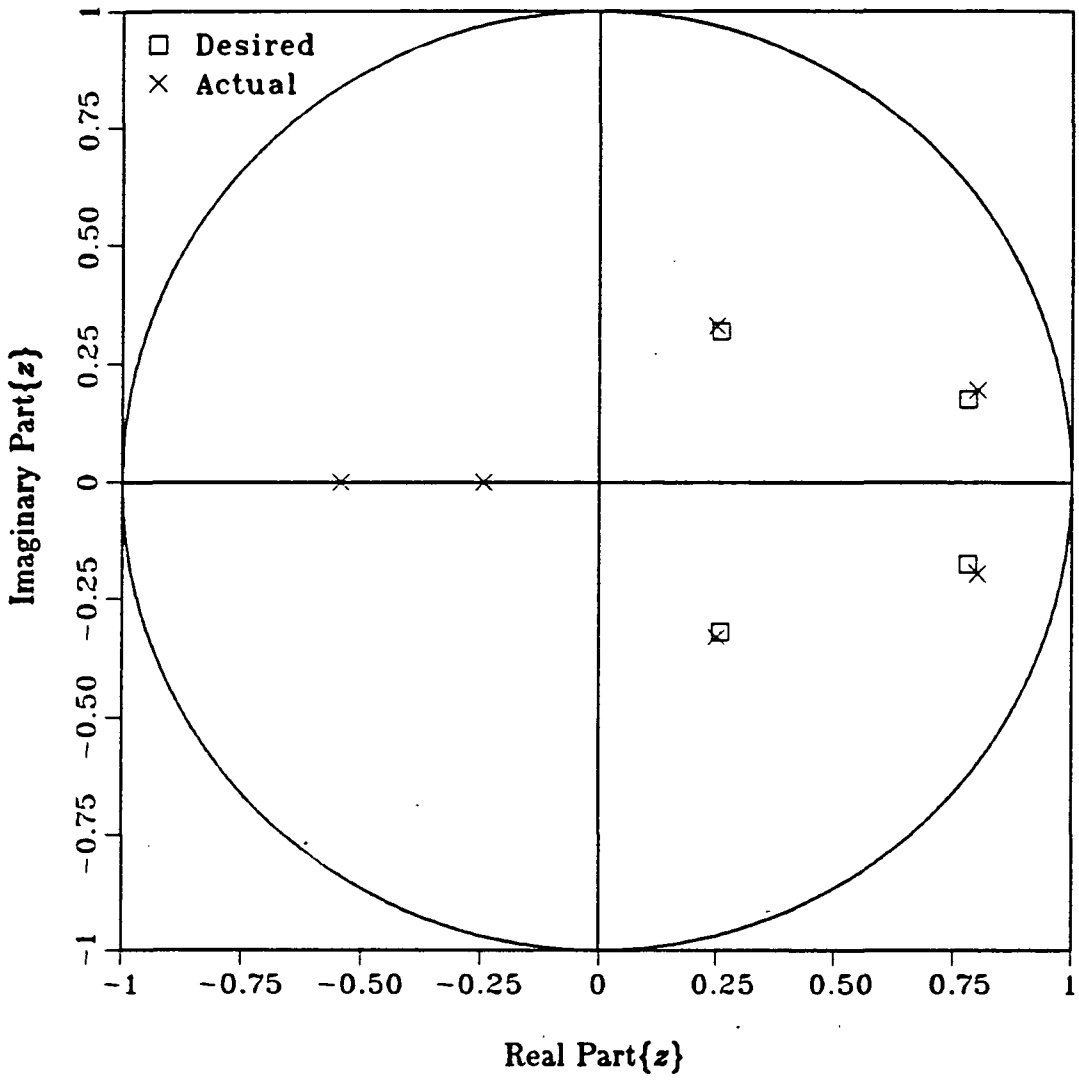

Figure 6.8 Closed-Loop Poles with Case 2 SR Compensator. (Sampling Rate = 10 Samples/Second.)

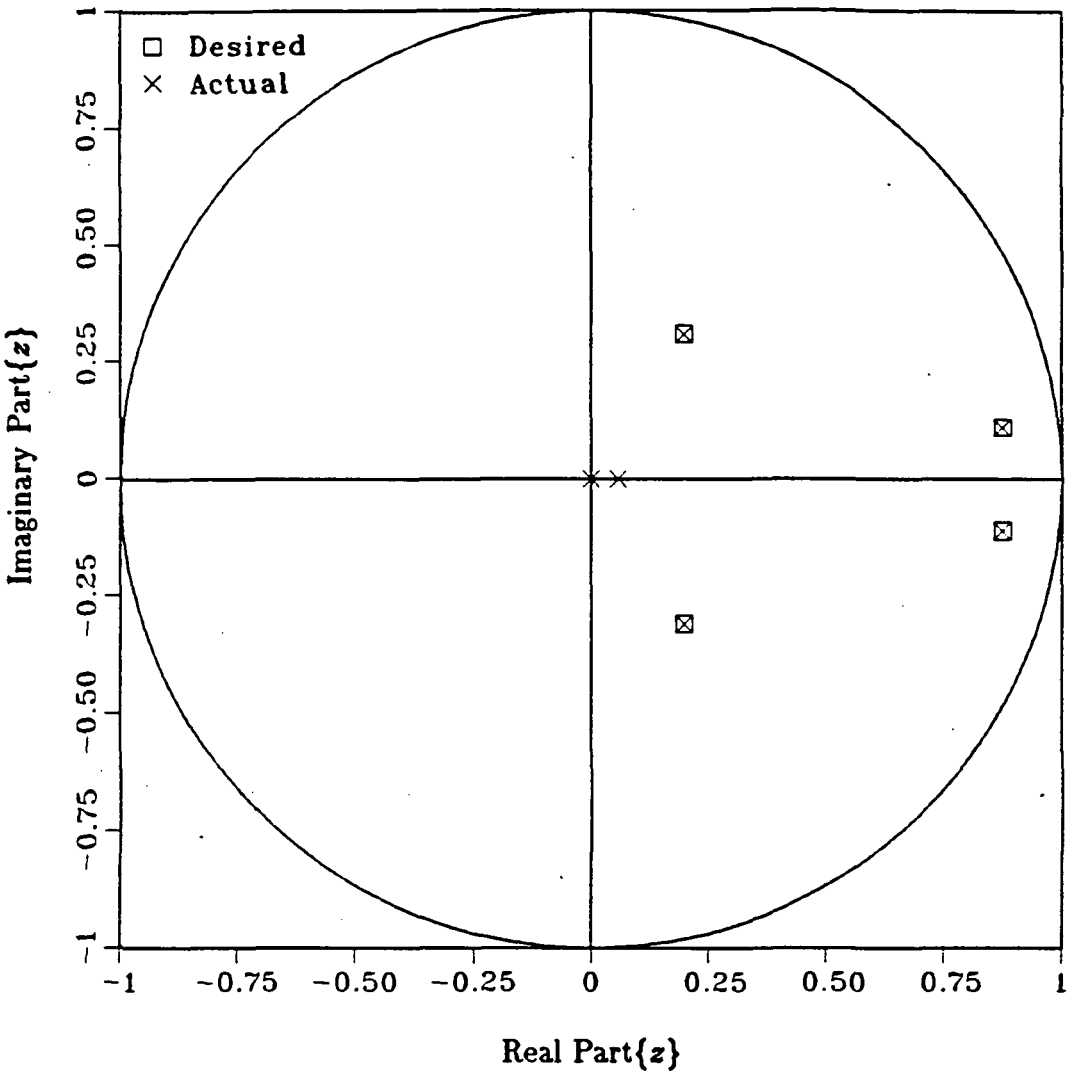

Figure 6.9 Closed-Loop BTP Poles with Case 3 MR Compensator. (Sampling Rate = 17.8 Samples/Second.)

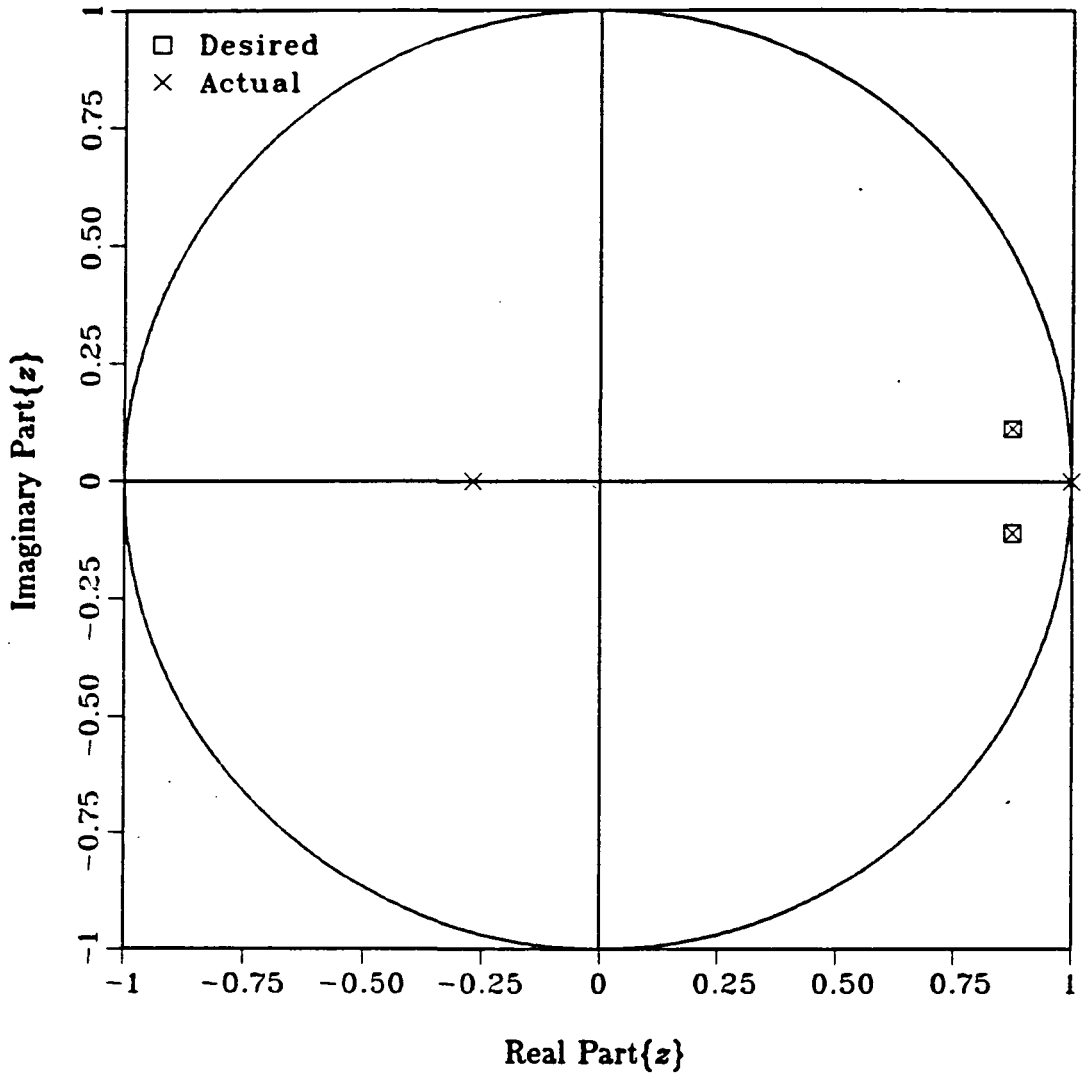

Figure 6.10 Closed-Loop Poles with Tip Controller Portion of Case 3 MR Compensator. (Sampling Rate = 142 Samples/Second.)

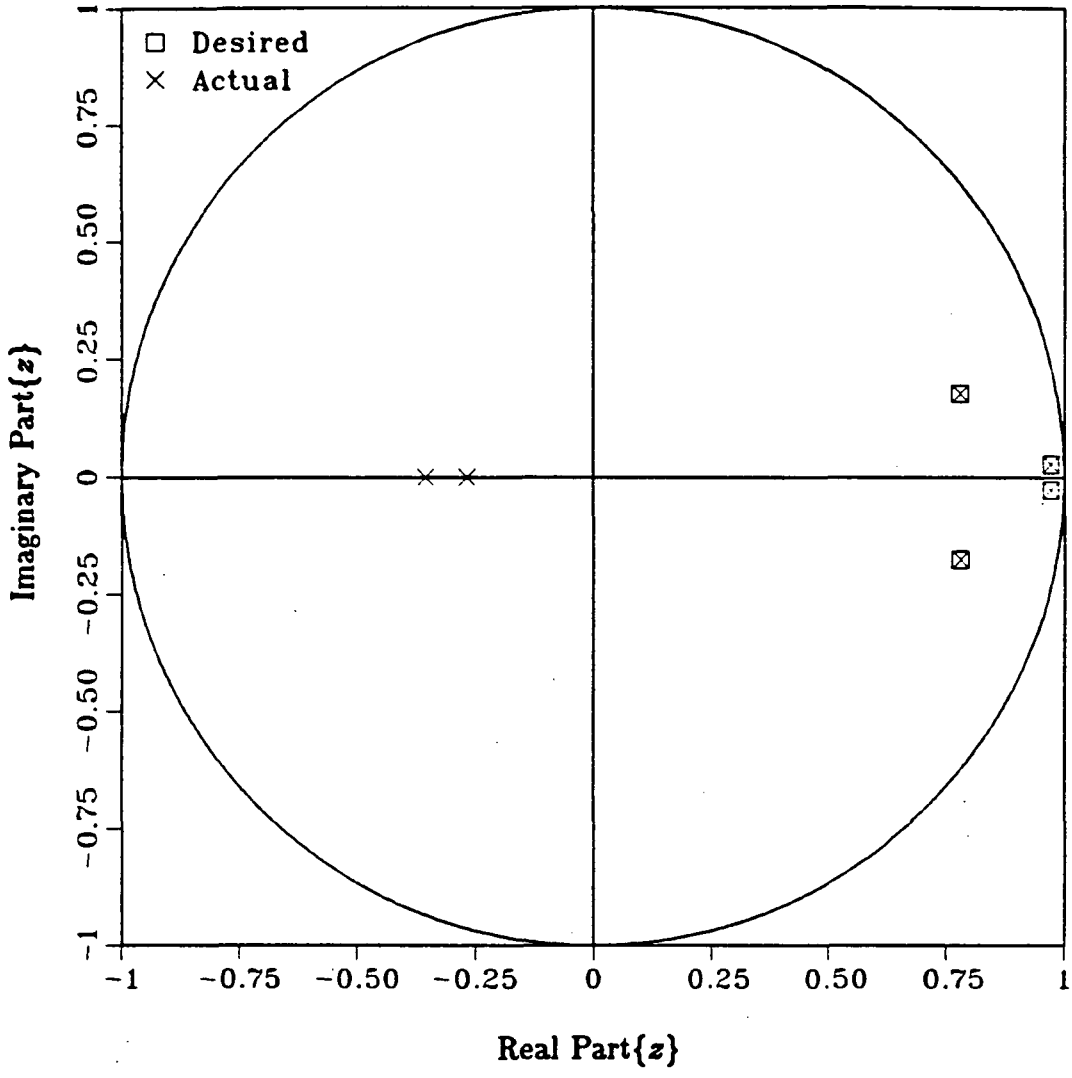

Figure 6.11 Closed-Loop Poles with Case 3 SR Compensator. (Sampling Rate = 80 Samples/Second.)

The reference tip positioning command is

$$\delta_c(t) \triangleq \begin{cases} 0.\ \text{m} & \text{if } t \le 0; \\ 0.01(1-\cos 2\pi f t)\ \text{m} & \text{if } 0 \le t \le 1/2f; \\ 0.01\ \text{m} & \text{if } 1/2f \le t. \end{cases} \tag{43}$$

It is a 0.01 meter step command, but with the transition defined as one half of a cosine wave. The smooth transition avoids the impulsive control responses that would otherwise occur with lead compensation. For each design case, we set the frequency f of the cosine wave to the characteristic frequency of the high frequency desired s-plane closed-loop poles for that case from Table 6.3. The resulting tip positioning commands are shown in Figure 6.13.

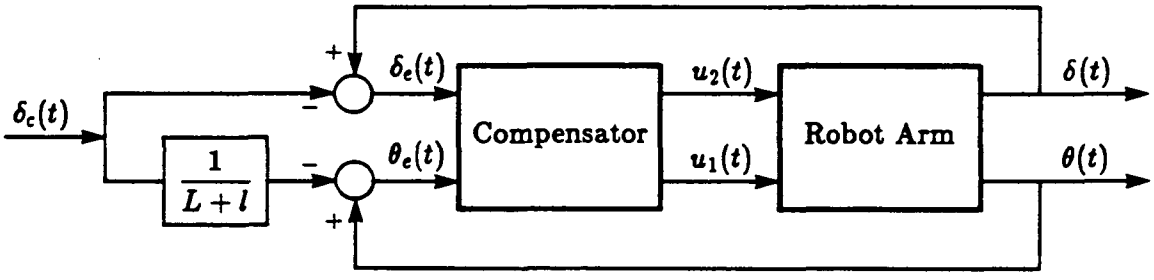

Figure 6.12 TLA Servo Configuration.

The closed-loop responses to the Case 1 tip positioning command with the Case 1 MR and SR compensators are shown in Figures 6.14 through 6.18. These responses were obtained by simulating the nonlinear equations of motion for the TLA system that are derived in Appendix A. The dot-dashed curves are the responses with the MR compensator. The dashed curves are the responses with the SR compensator. The solid curves are the responses with an equivalent fast-sampling-rate SR compensator. The fast-sampling-rate compensator has the same structure as the Case 1 MR and SR compensators and was synthesized using AMS for the same process noise levels and performance index. Its 500 samples/second sampling rate is so fast compared to the characteristic frequencies of the closed-loop

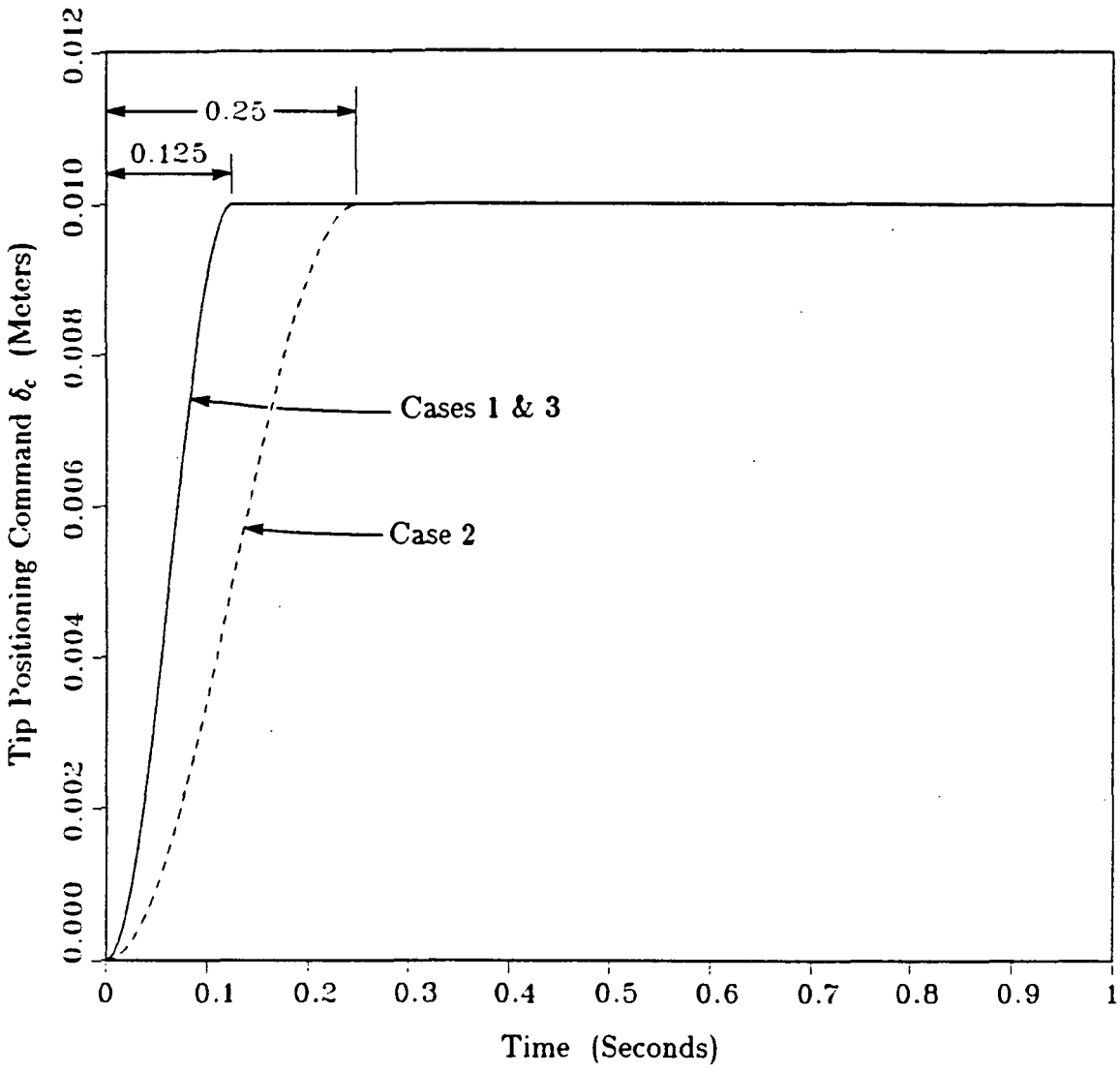

Figure 6.13 TLA Tip Positioning Commands.

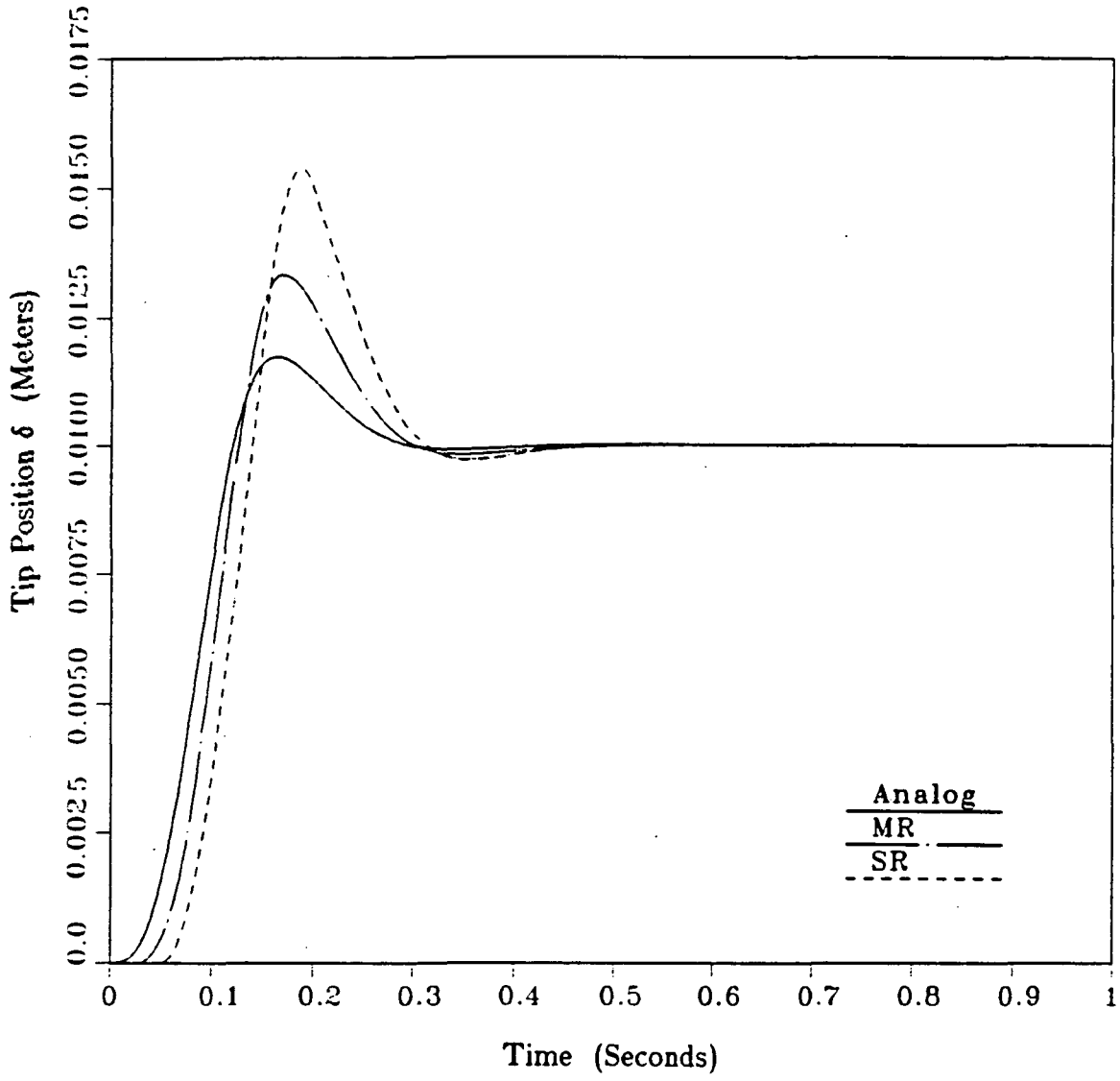

Figure 6.14 Tip Position Responses to Case 1 Tip Positioning Command with Case 1 Compensators.

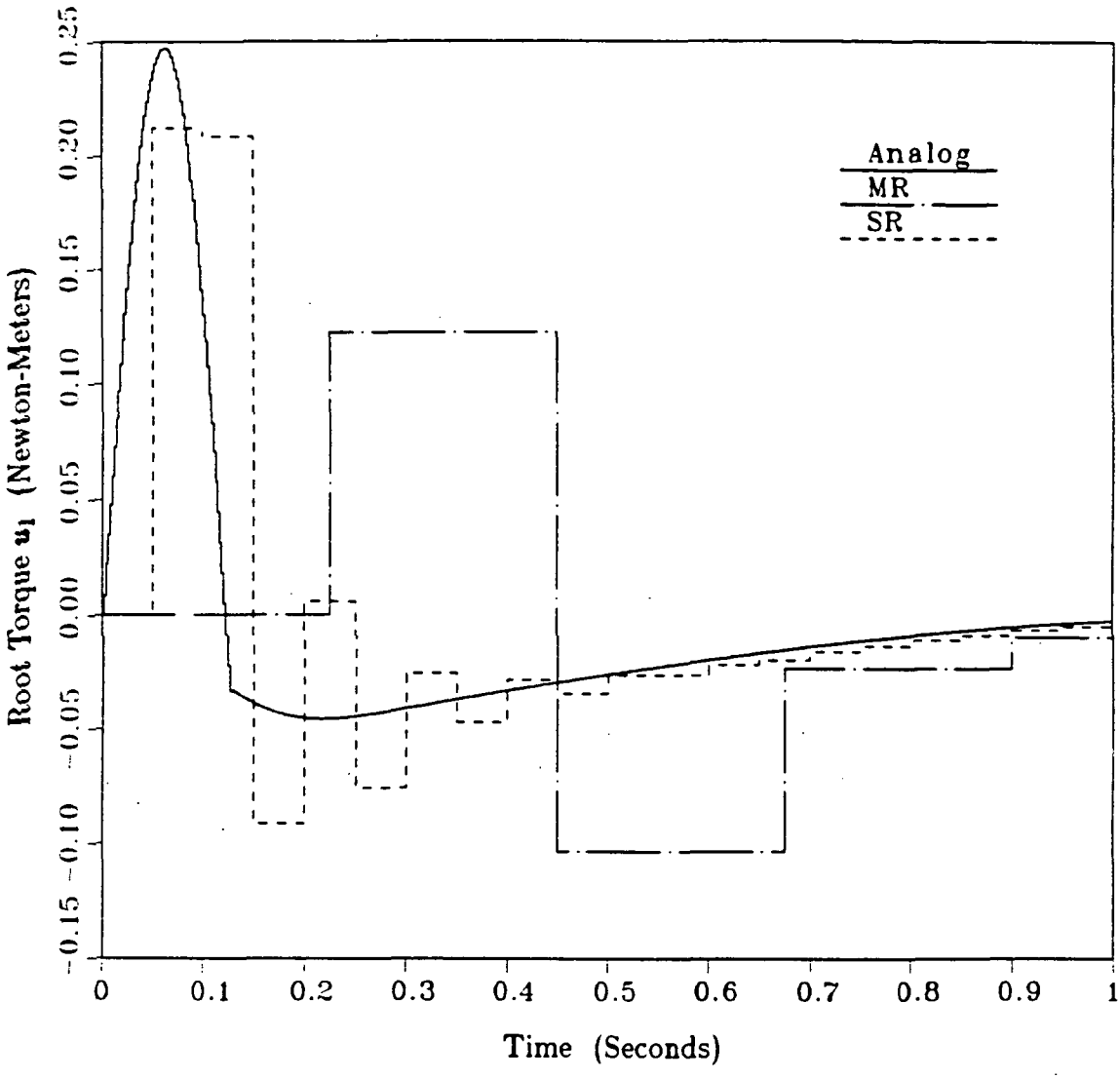

Figure 6.15 Root Torque Responses to Case 1 Tip Positioning Command with Case 1 Compensators.

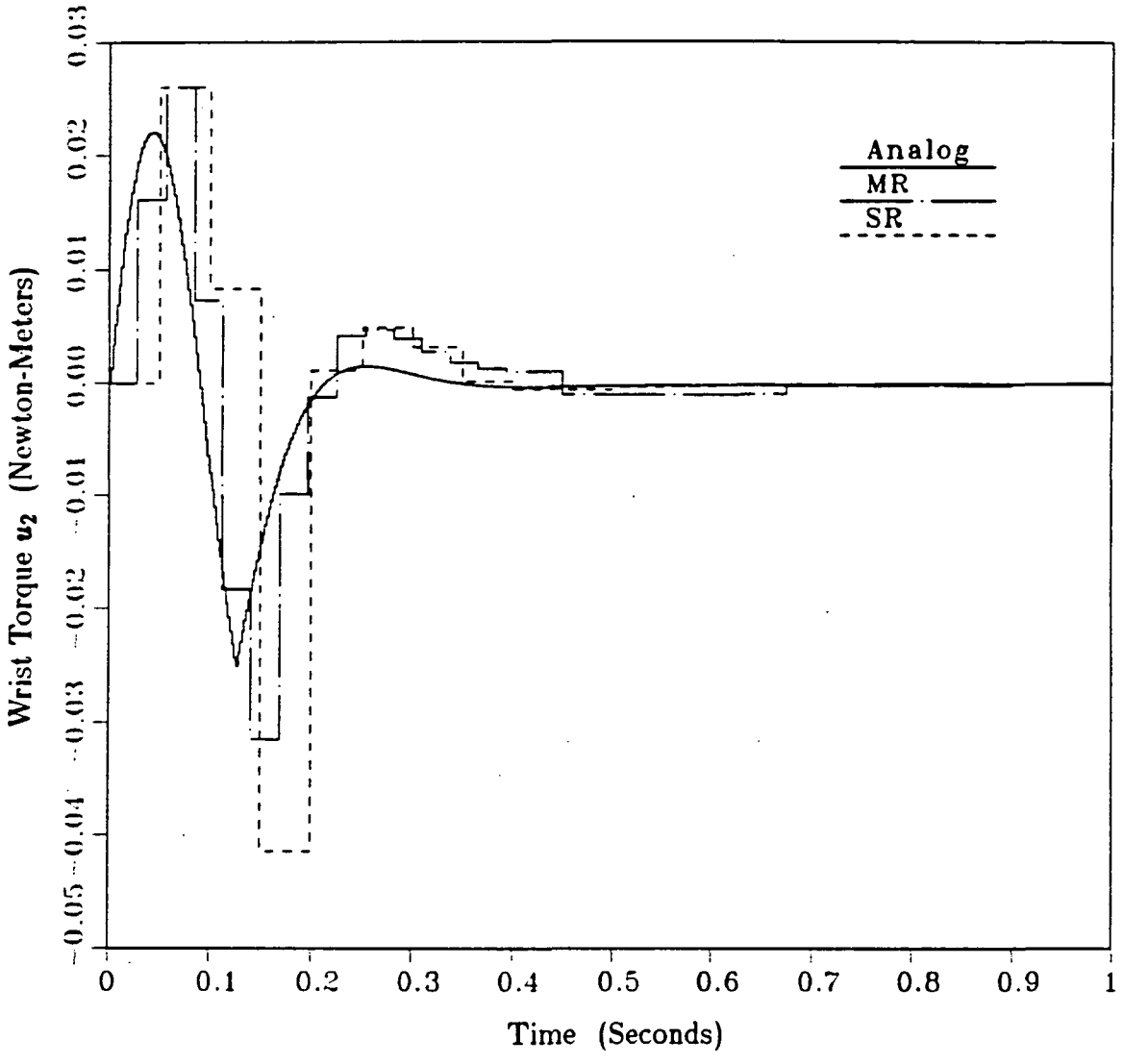

Figure 6.16 Wrist Torque Responses to Case 1 Tip Positioning Command with Case 1 Compensators.

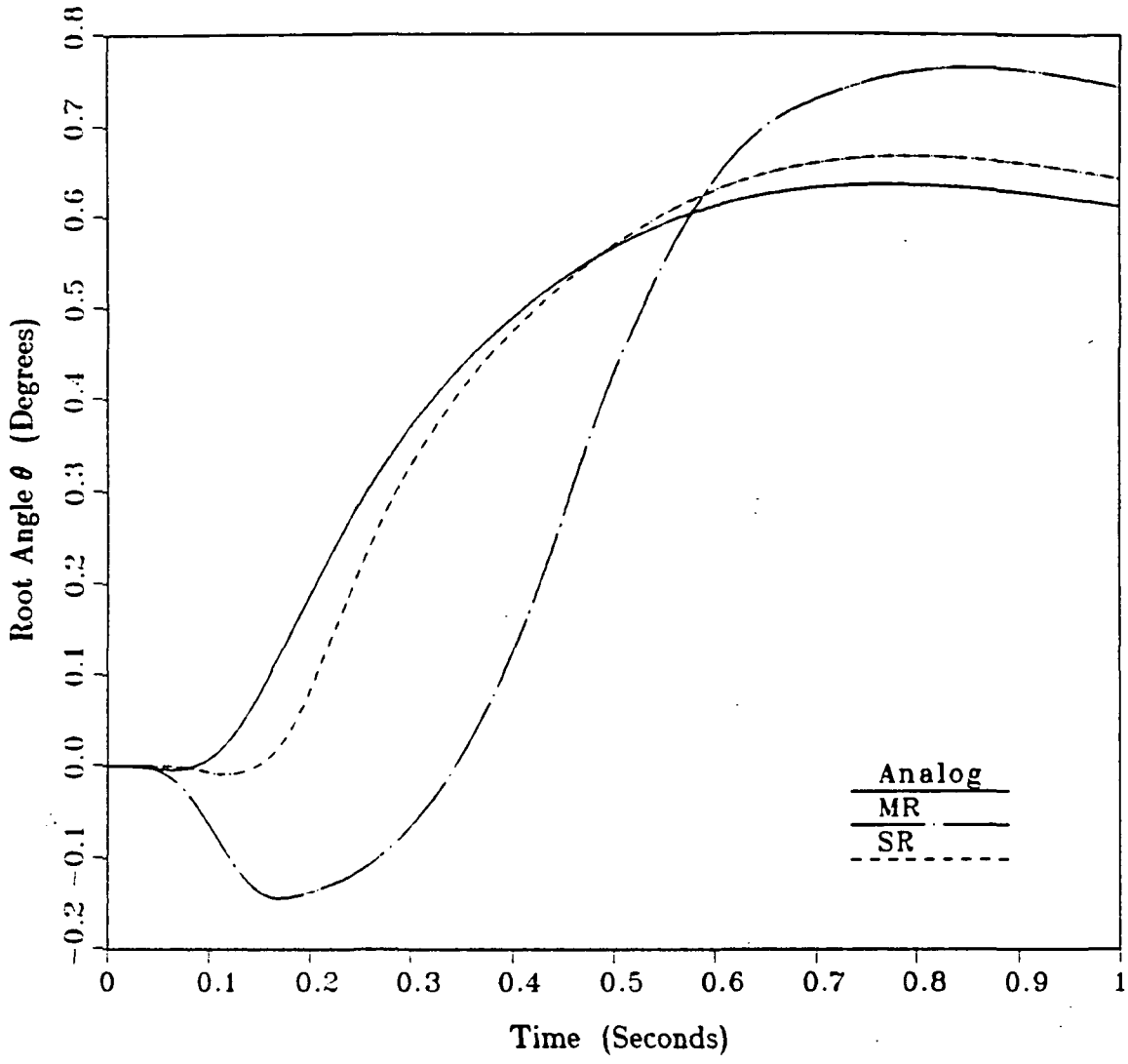

Figure 6.17 Root Angle Responses to Case 1 Tip Positioning Command with Case 1 Compensators.

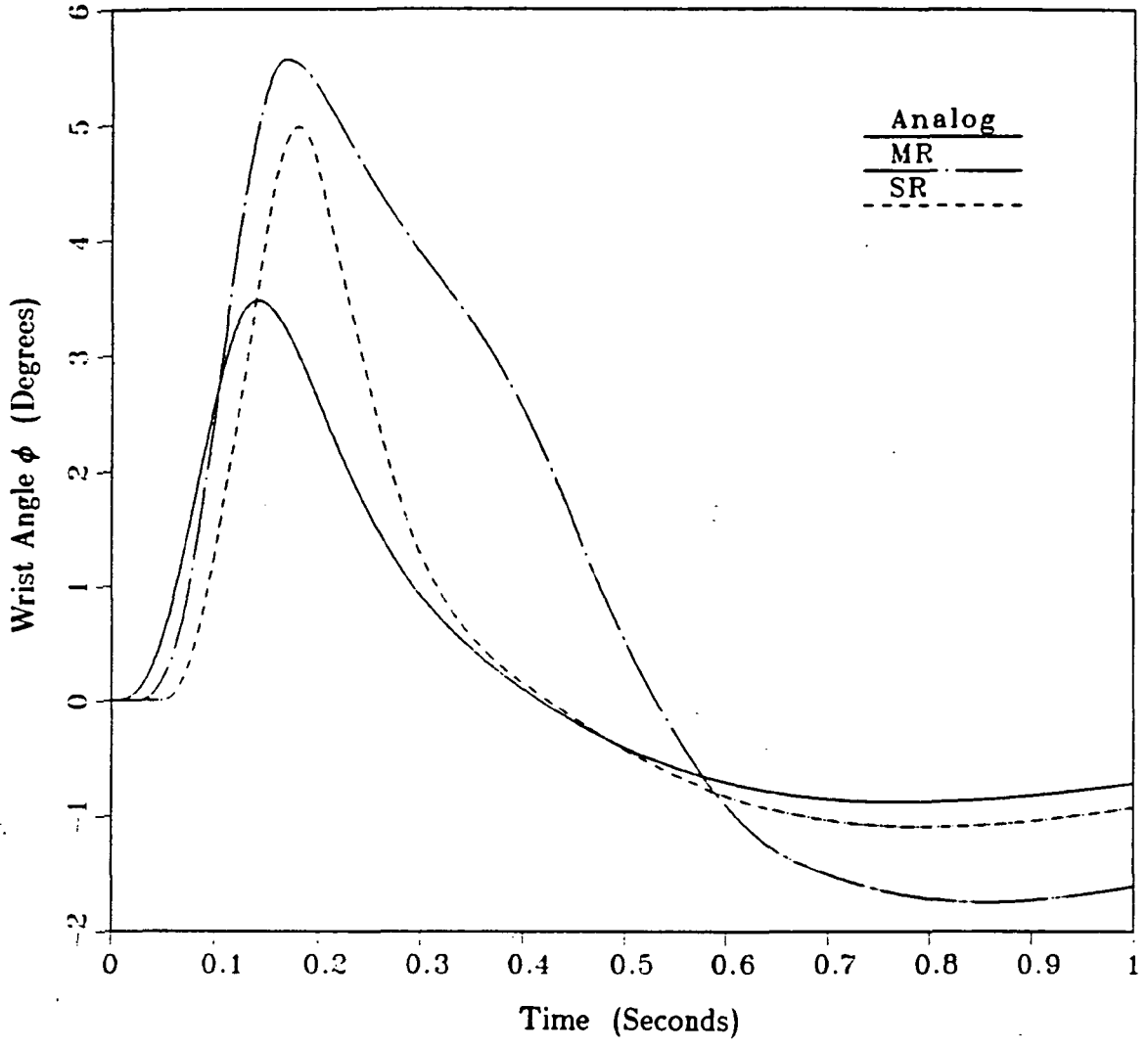

Figure 6.18 Wrist Angle Responses to Case 1 Tip Positioning Command with Case 1 Compensators.

poles that the solid curves represent, in effect, the responses with the analog equivalent to the Case 1 MR and SR compensators.

The performance of the Case 1 MR compensator is markedly better than that of the Case 1 SR compensator. In Figure 6.14, the peak overshoot of the steady-state δ value is 21% less with the MR compensator than with the SR compensator. In Figure 6.16, the delay time for the initial control response to the command input is 44% less with the MR compensator than with the SR compensator. If the responses with the analog compensator are ideal, then the increase in the peak overshoot of the steady-state δ value in Figure 6.14 is 56% less with the MR compensator than with the SR compensator. As indicated by the MR and SR control responses in Figures 6.15 and 6.16, the performance benefits with the MR compensator as compared to the SR compensator were obtained at virtually no additional cost in terms of the control effort required.

The corresponding $\delta(t)$, $u_1(t)$, and $u_2(t)$ closed-loop responses to the Case 2 tip positioning command with the Case 2 MR and SR compensators are shown in Figure 6.19 throuh 6.21. The solid curves in these figures are the responses with a 250 samples/second SR compensator that has the same compensator structure as the Case 2 MR and SR compensators and was synthesized for the same process noise levels and performance index, so that these curves represent, in effect, the responses with the analog equivalent to the Case 2 MR and SR compensators.

Figures 6.19 through 6.22 show the the (slight) effects of a factor-of-two reduction (compared to Case 1) in the spectral separation of the closed-loop poles. In Figure 6.19, the peak overshoot of the steady-state δ value is 25% less with the MR compensator than with the SR compensator. In Figure 6.21, the delay time for the initial control response to the command input is 38% less with the MR compensator than with the SR compensator. If the responses with the analog

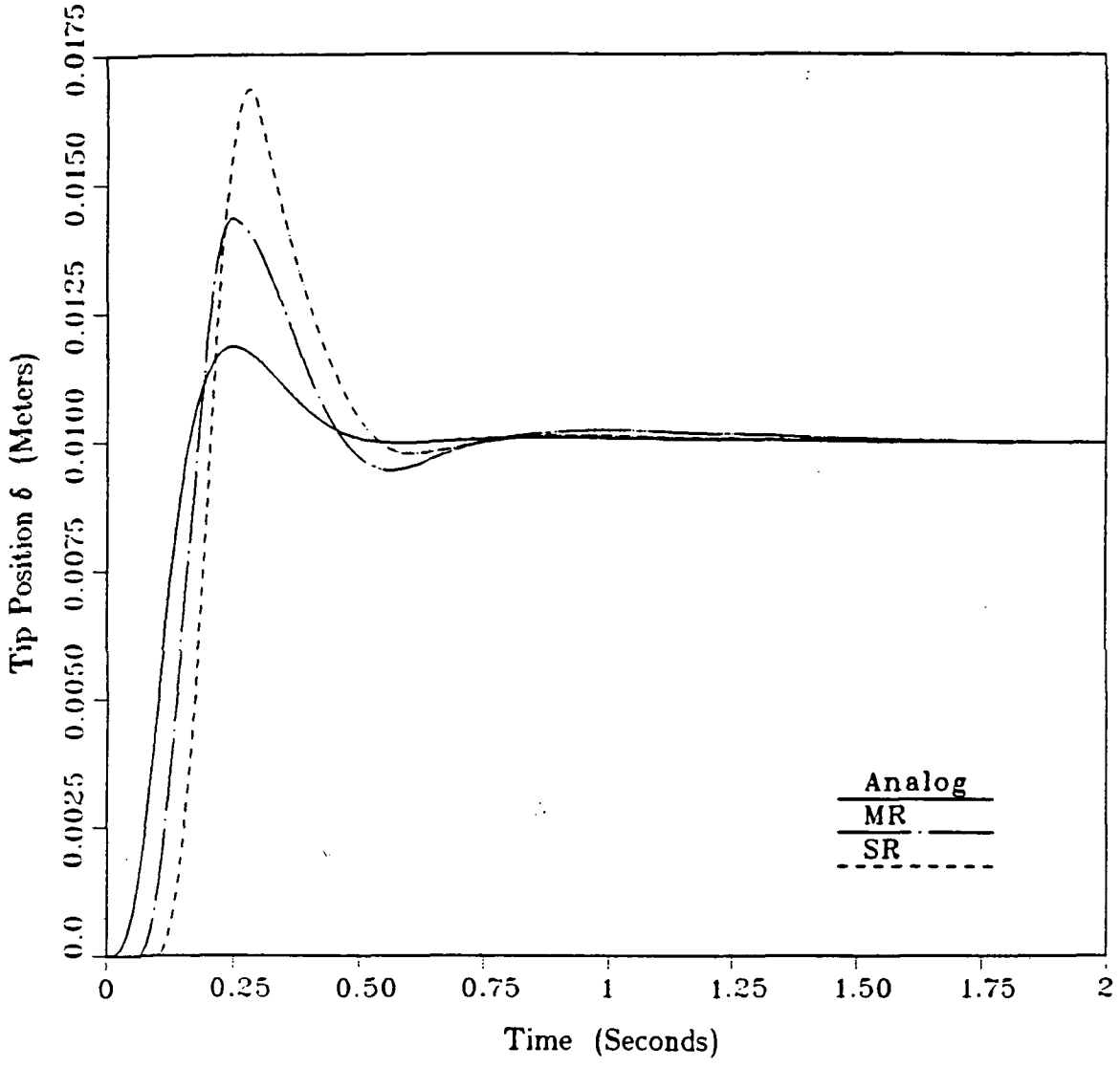

Figure 6.19 Tip Position Responses to Case 2 Tip Positioning Command with Case 2 Compensators.

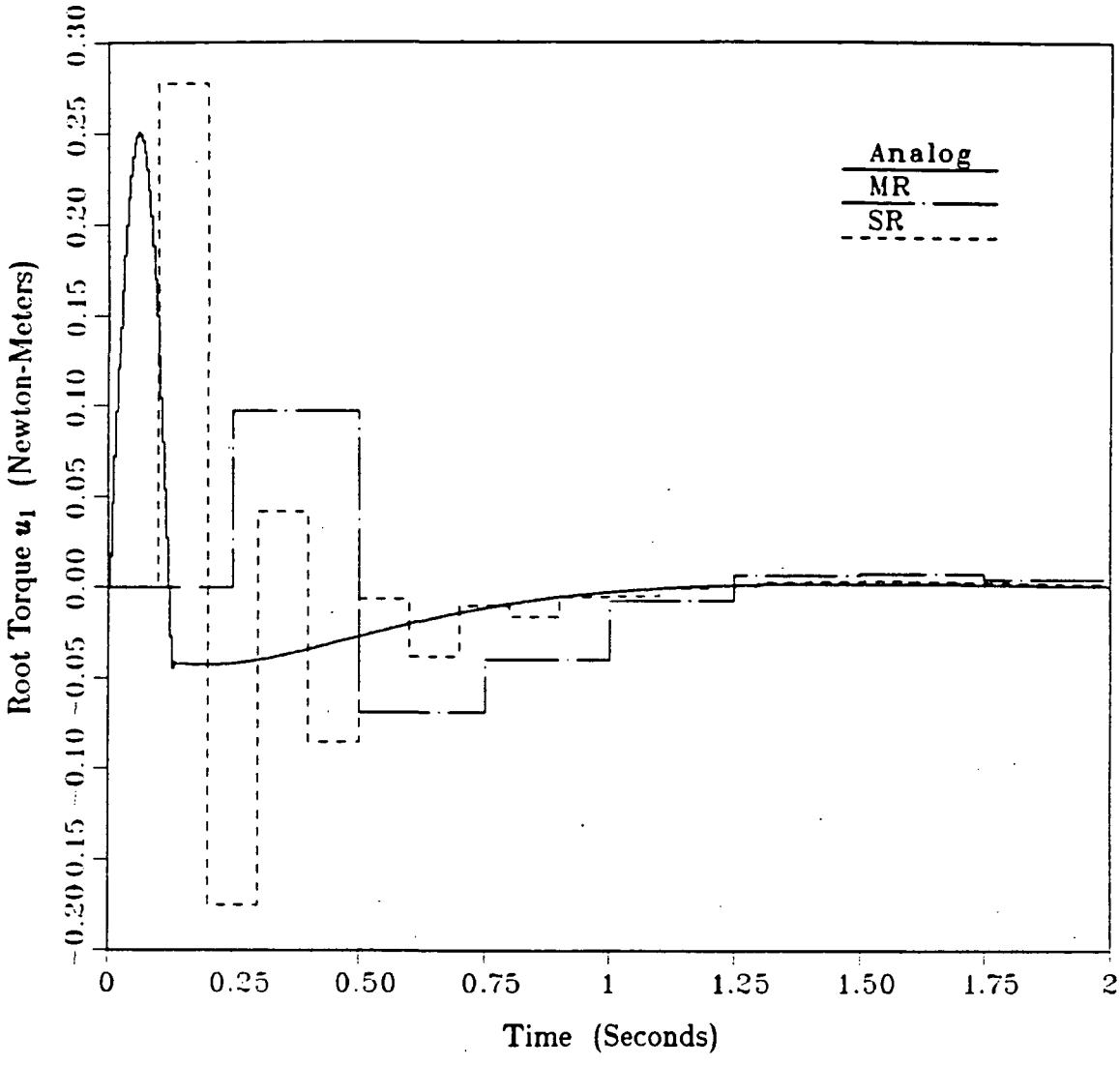

Figure 6.20 Root Torque Responses to Case 2 Tip Positioning Command with Case 2 Compensators.

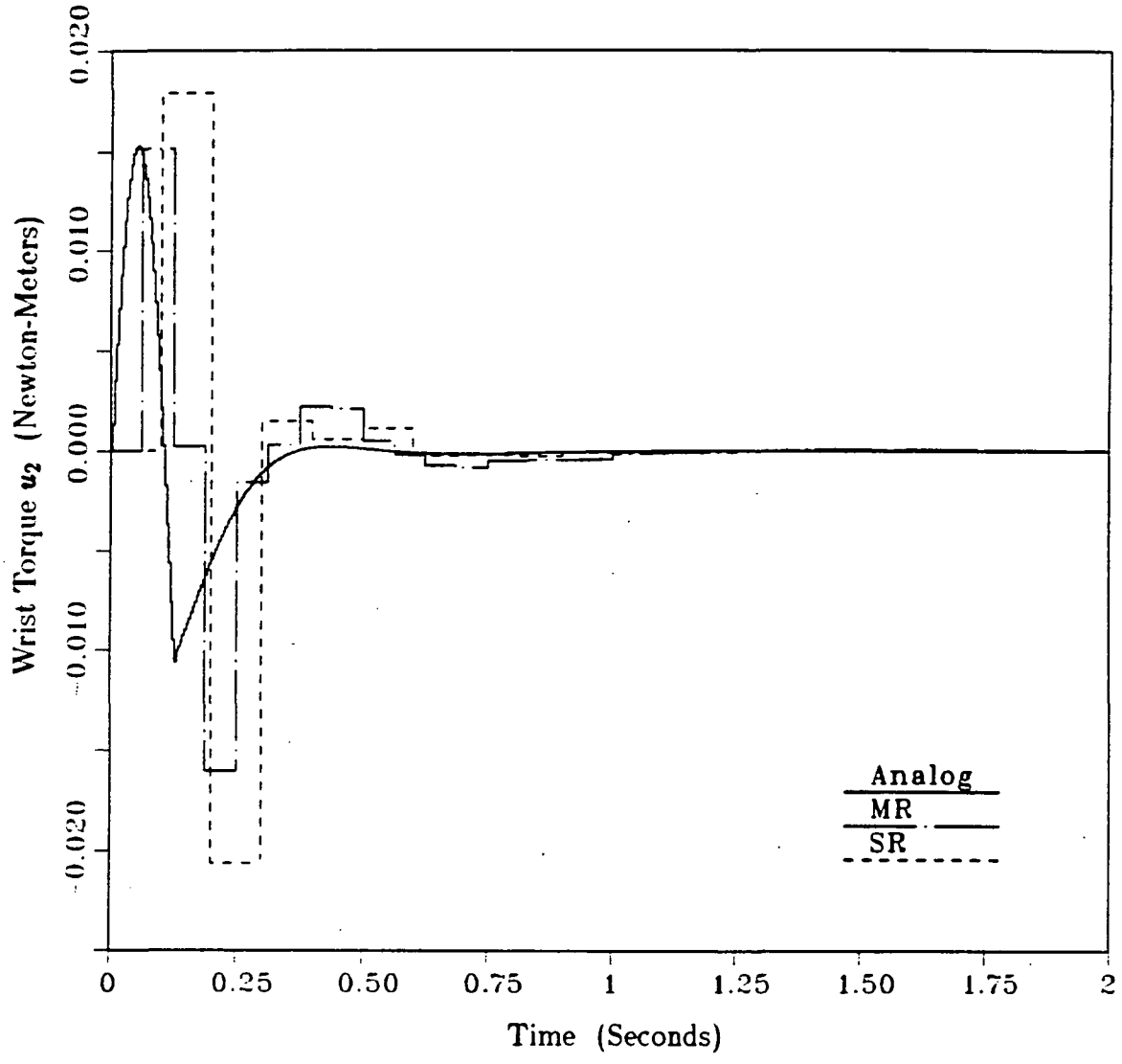

Figure 6.21 Wrist Torque Responses to Case 2 Tip Positioning Command with Case 2 Compensators.

compensator are ideal, then the increase in the peak overshoot of the steady-state δ value in Figure 6.19 is 50% less with the MR compensator than with the SR compensator. As indicated by the MR and SR control responses in Figures 6.20 and 6.21, the performance benefits with the MR compensator as compared to the SR compensator were obtained at virtually no additional cost in terms of the control effort required.

The corresponding $\delta(t)$, $u_1(t)$, and $u_2(t)$ closed-loop responses to the Case 3 tip positioning command for the Case 3 MR and SR compensators are shown in Figures 6.22 through 6.24. The solid curves in these figures are the responses with a 500 samples/second SR compensator that has the same structure as the Case 3 MR and SR compensators and was synthesized for the same process noise levels and performance index, so that these curves represent, in effect, the responses with the analog equivalent to the Case 3 MR and SR compensators.

Figures 6.22 through 6.24 show the effects of a factor-of-four increase (compared to Case 1) in all sampling rates. In Figure 6.22, the peak overshoot of the steady-state δ value is only 3% less with the MR compensator than with the SR compensator. In Figure 6.24, the delay time for the initial control response to the command input is 44% less with the MR compensator than with the SR compensator. If the responses with the analog compensator are ideal, then the increase in the peak overshoot of the steady-state δ value in Figure 6.22 is 56% less with the MR compensator than with the SR compensator. As indicated by the MR and SR control responses in Figures 6.23 and 6.24, the performance benefits with the MR compensator as compared to the SR compensator were obtained at virtually no additional cost in terms of the control effort required. But the absolute reductions in the delay time and the peak overshoot are so small that the performance of the MR compensator is, for practical purposes, the same as that of the SR compensator.

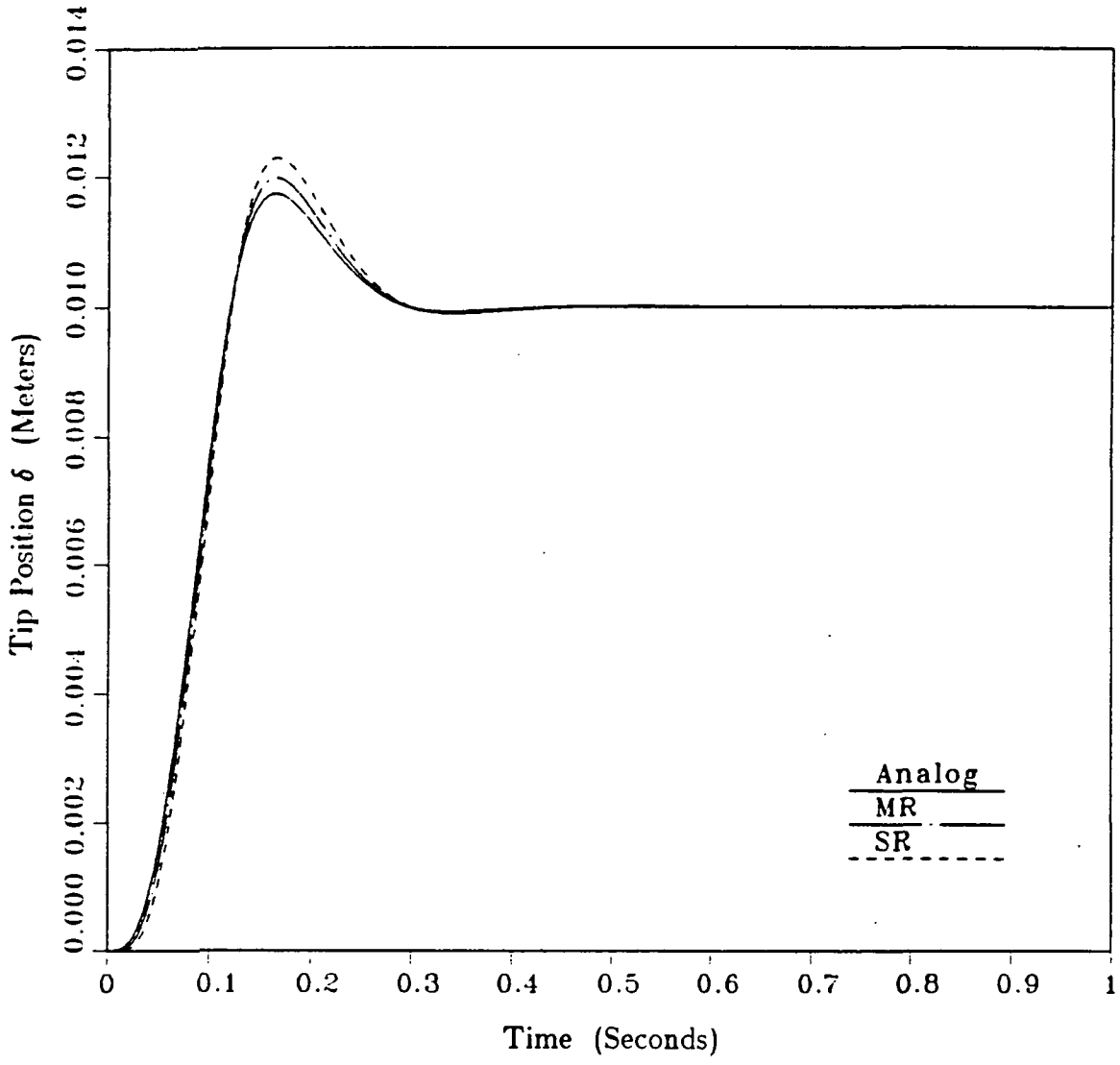

Figure 6.22 Tip Position Responses to Case 3 Tip Positioning Command with Case 3 Compensators.

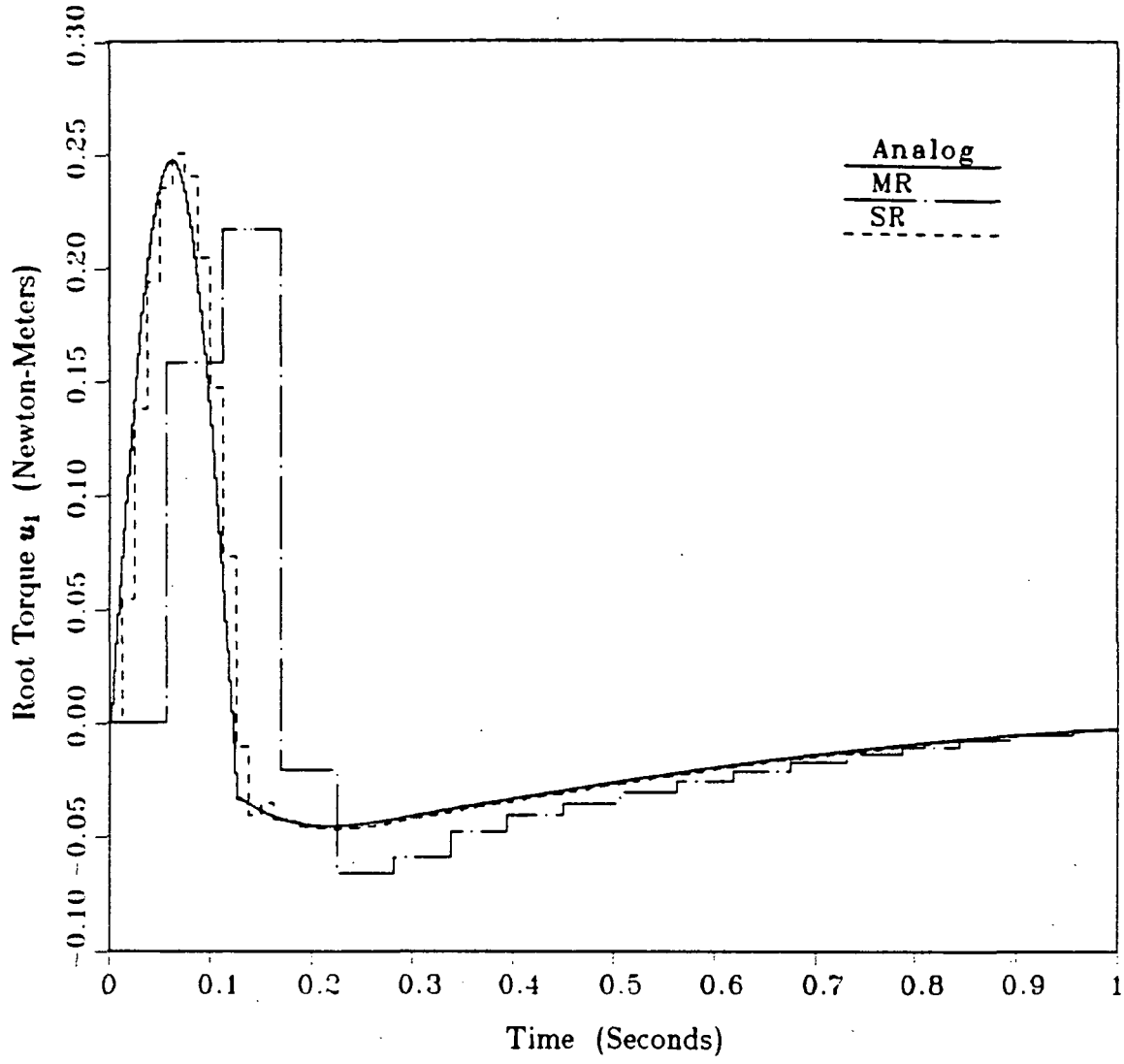

Figure 6.23 Root Torque Responses to Case 3 Tip Positioning Ccommand with Case 3 Compensators.

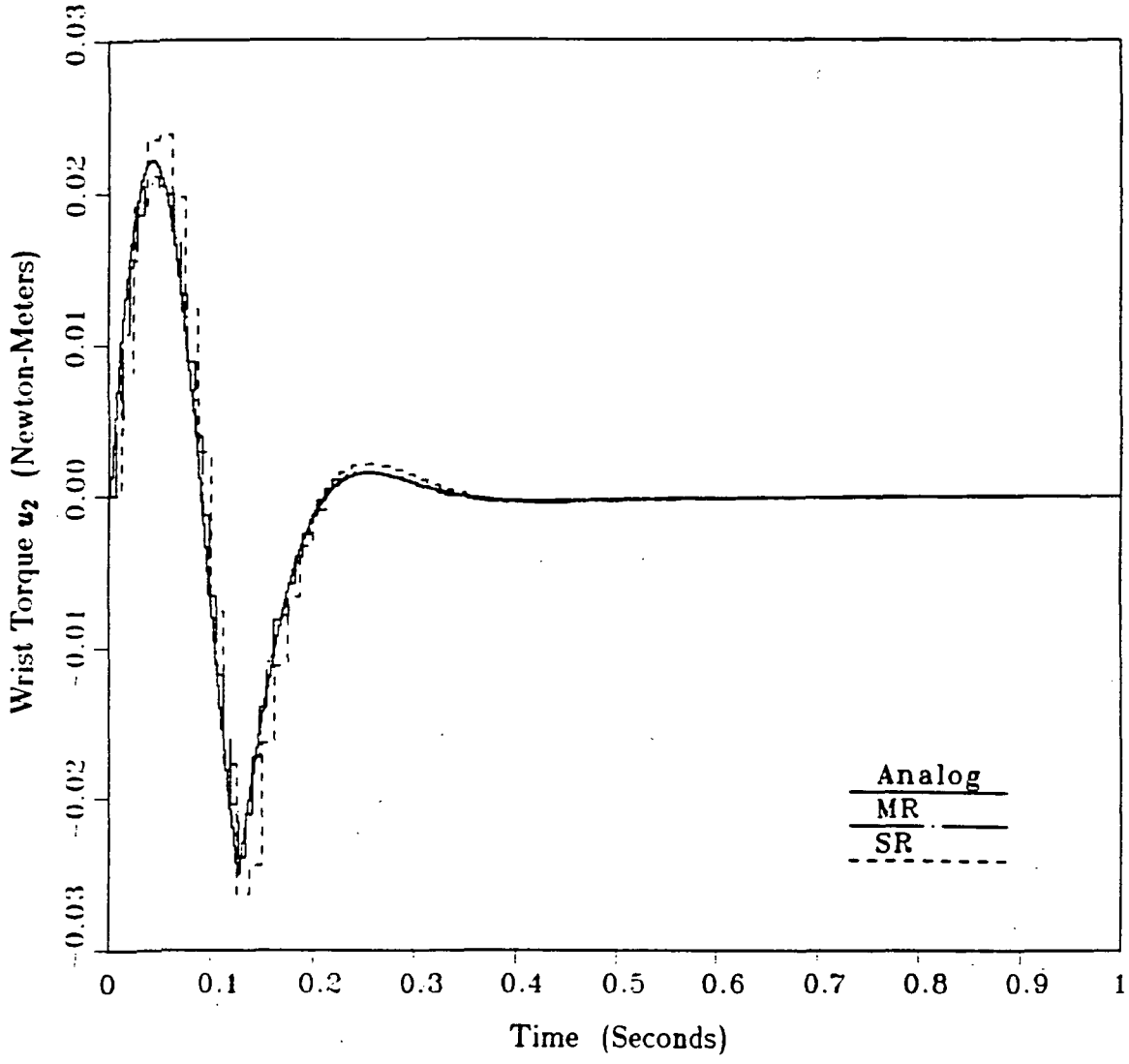

Figure 6.24 Wrist Torque Responses to Case 3 Tip Positioning Command with Case 3 Compensators.

§6.4 Summary and Discussion. This section contains 3 subsections. The first presents a summary of the important results from Sections 6.1 through 6.3. The second and third take a second look at the use of the successive loop closures and optimal control law synthesis methods, in the light of the results from Sections 6.1 through 6.3.

Basic Results. We dealt with the TLA system in Figure 6.1, and the compensator structure in Figure 6.2. The performance objective was to obtain the fastest possible response to tip positioning commands. We experimented with different design conditions to determine circumstances under which a MR compensator out performs a comparable SR compensator.

Three design cases were considered. The constrained optimization synthesis method was used to synthesize one MR compensator and one SR compensator for each design case. For each SR compensator, the sampling rate was picked at either 5 or 20 times the characteristic frequency in hertz of the fastest desired s-plane closed-loop poles. For each MR compensator, the sampling rate for each measurement or control variable was picked to be a multiple of the characteristic frequency of the desired s-plane closed-loop poles most coupled to that specific variable. Furthermore, for each design case, the sampling rates were picked such that the computation load for real-time operation of the MR compensator is the same as that for real-time operation of the SR compensator.

Performance comparisons were conducted for the different compensators. The comparisons were based on the closed-loop responses to a reference tip positioning command.

For the TLA system, under these conditions, we conclude that:

1) For slow sampling (characterized by SR sampling at 5 times the characteristic frequency in hertz of the fastest desired s-plane closed-loop poles), MR

compensation is superior to SR compensation, for ratios of the characteristic frequencies of the desired s-plane closed-loop poles as low as 4-to-1.

2) The performance benefits of MR compensation over SR compensation are sampling-rate dependent. At the fast sampling rates (characterized by SR sampling at 20 times the characteristic frequency in hertz of the fastest desired s-plane closed-loop poles), the performance of the MR compensator was, for practical purposes, the same as that of the SR compensator.

Use of the Successive Loop Closures Synthesis Method. We stated in Section 6.2 that the compensator structure in Figure 6.2 is complicated enough that it would be difficult to apply the successive loop closures synthesis method. It would be easy to apply the successive loop closures synthesis method if the compensator cross feed terms β_{12}, β_{21}, γ_{12}, and γ_{21} could be neglected. The simulation results in Figures 6.25 through 6.27 indicate, however, that the cross-feed terms (or some of them) are essential for good closed-loop performance. The solid curves in these figures are the closed-loop responses to the Case 1 tip positioning command with the Case 1 MR compensator. The dashed curves are the corresponding responses with a MR compensator that uses the same sampling rates and was synthesized using AMS for the same process noise levels and performance index, but with the compensator cross-feed terms set to zero.

The values for the compensator parameters for the NXF MR compensator are in Table 6.8. The z-plane plots for the NXF MR compensator that correspond to those for the Case 1 MR compensator in Figures 6.3 and 6.4 are in Figures 6.28 and 6.29.

The responses in Figures 6.25 through 6.27 clearly indicate that the compensator cross-feed terms are important for good compensator performance. Furthermore, for determining values for the cross-feed terms, the z-plane plots in

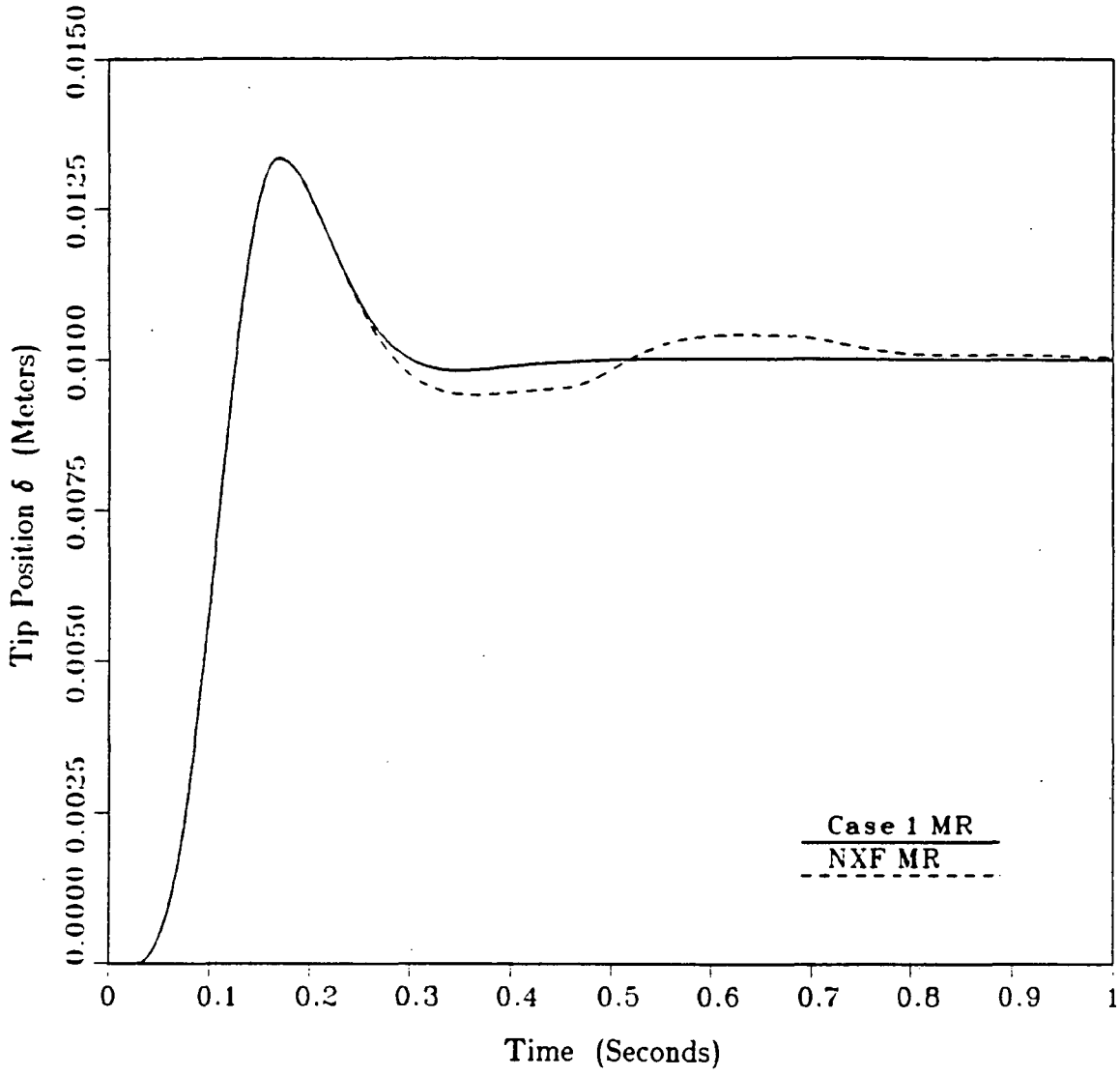

Figure 6.25 Tip Position Responses to Case 1 Tip Positioning Command with Case 1 MR and NXF MR Compensator.

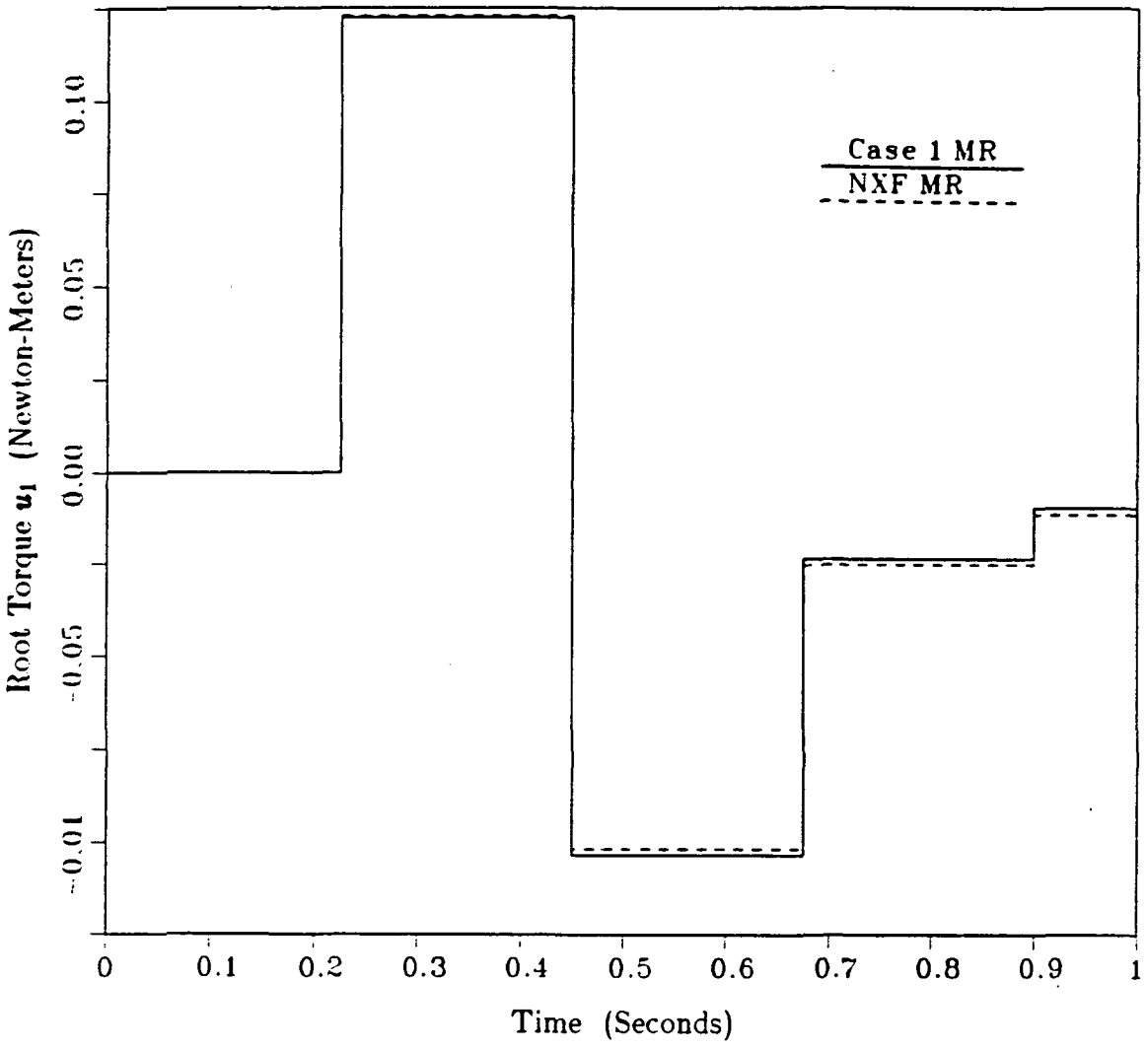

Figure 6.26 Root Torque Responses to Case 1 Tip Positioning Command with Case 1 MR and NXF MR Compensators.

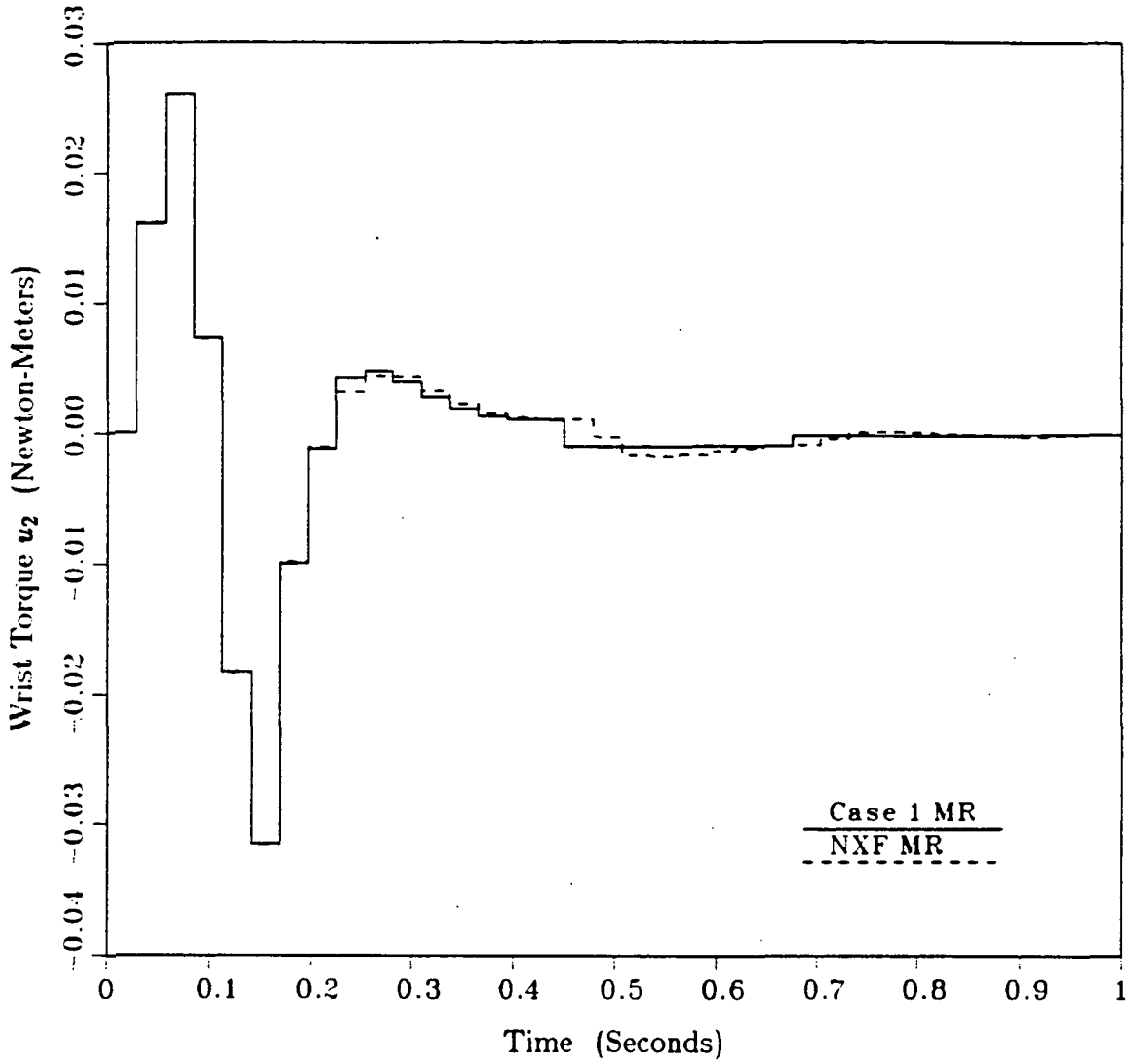

Figure 6.27 Wrist Torque Responses to Case 1 Tip Positioning Command with Case 1 MR and NXF MR Compensators.

Figures 6.28 and 6.29 are of no use whatsoever. This is because the cross-feed terms are primarily associated with the zeros of the closed-loop δ_c-to-δ transfer function. Unfortunately, a means for determining the locations that correspond to the intuitive notion of these zeros is not known, because the closed-loop system is time-varying.

Table 6.8 TLA NXF MR Compensator Parameters.

PARAMETER	UNITS	NUMERIC VALUE
α_1	—	0.471
β_{11}	N·m	11.1
β_{12}	N	0.
γ_{11}	N·m	−13.2
γ_{12}	N	0.
α_2	—	0.552
β_{21}	N·m	0.
β_{22}	N	13.5
γ_{21}	N·m	0.
γ_{22}	N	−16.9

It would be difficult to apply the successive loop closures synthesis method to the compensator structure of Figure 6.2 directly. It may be possible to reformulate the design problem such that a MR compensator with acceptable cross-feed terms can be determined using a slightly different approach suggested by Bryson (1986). For the analog state equation in (1), if we let

$$\bar{u}(t) = G\,u(t)\,, \tag{44}$$

we obtain

$$\dot{p}(t) = F\,p(t) + \bar{u}(t)\,. \tag{45}$$

And the $\tilde{\theta}(t)$ and $\tilde{\delta}(t)$ state equations are

$$\tilde{\theta}(t) = \bar{u}_1(t)\,, \tag{46}$$

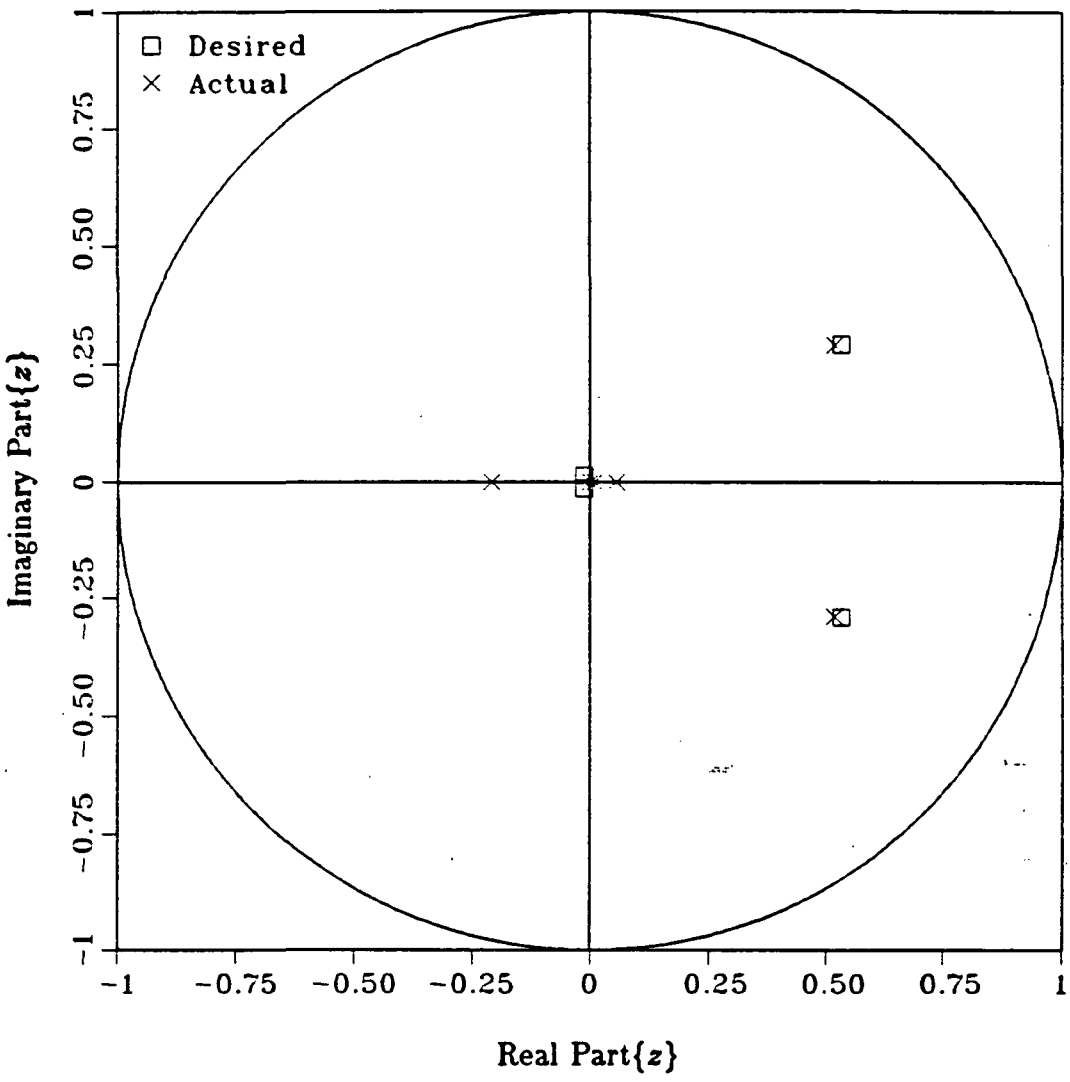

Figure 6.28 Closed-Loop BTP Poles with NXF MR Compensators. (Sampling Rate = 4.45 Samples/Second.)

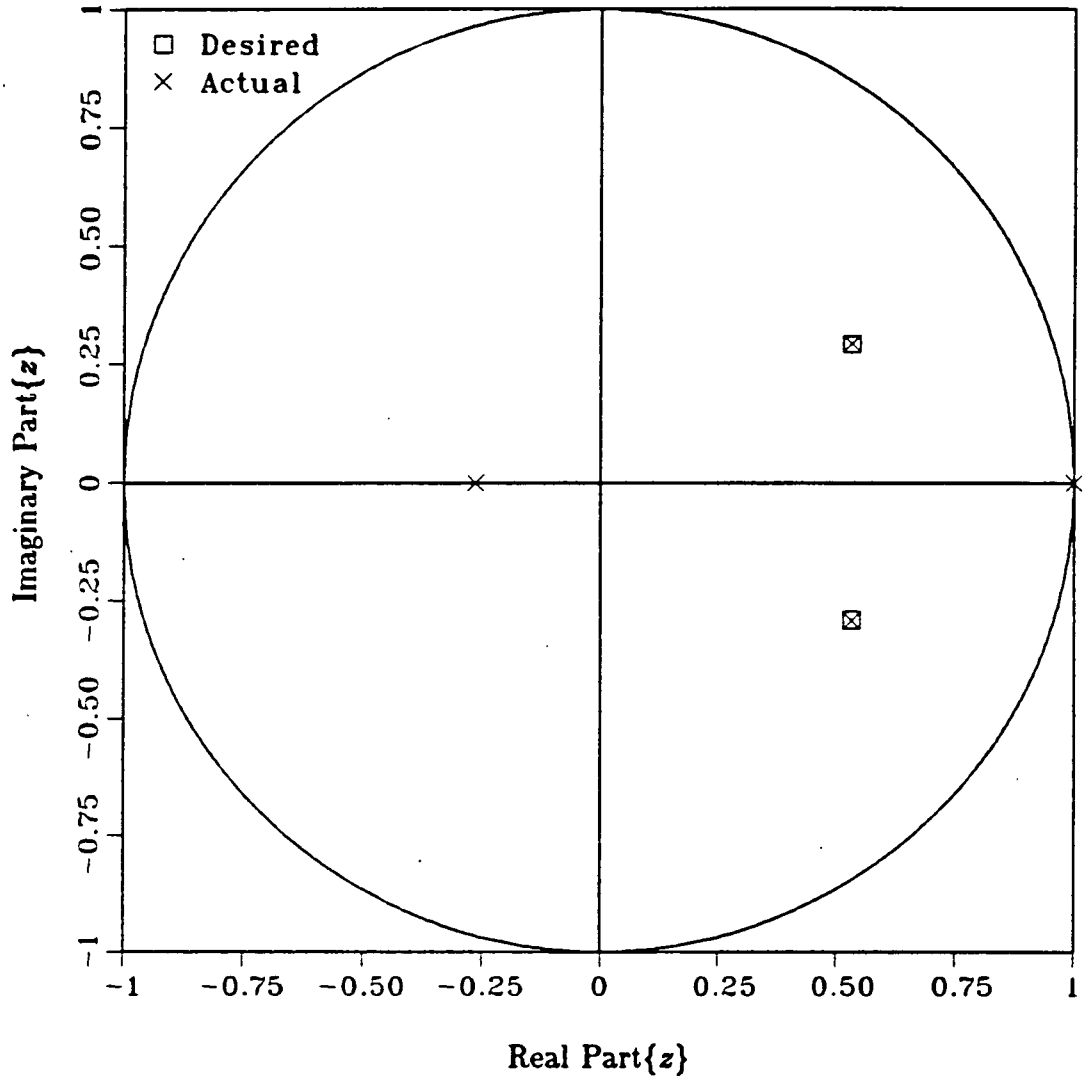

Figure 6.29 Closed-Loop Poles with Tip Controller Portion of NXF MR Compensator. (Sampling Rate = 35.56 Samples/Second.)

$$\bar{\delta}(t) = \bar{u}_2(t)\,, \tag{47}$$

where $\bar{u}_1(t)$ and $\bar{u}_2(t)$ are the first and second elements, respectively, of $\bar{u}(t)$.

The successive loop closures synthesis method could easily be used to determine a MR compensator for the $\bar{u}_1(t)$ and $\bar{u}_2(t)$ system in (46) and (47). We speculate that, with some simplifying assumptions, a MR compensator for the $u_1(t)$ and $u_2(t)$ system with adequate cross-feed could be determined from the MR compensator for the $\bar{u}_1(t)$ and $\bar{u}_2(t)$ system. This is a matter for further research.

Use of the Optimal Control Law Synthesis Method. Another interesting topic is the consistent overshoot of the steady-state δ value, in the responses in Figures 6.14, 6.19, and 6.22. For a SR system with 2 critically damped poles and 1 zero, Franklin and Powell (Section 2.4, 1980) discuss the effect of zero location on peak overshoot in response to a step command. For any real zero location between -1 and $+1$, it is shown that an overshoot always occurs and that its magnitude decreases with increasing sampling rate. This is entirely consistent with the responses in Figures 6.14, 6.19, and 6.22. The sampling rate for δ and u_2 is consistently higher in the MR compensators than in the SR compensators. Thus, the peak overshoot of the steady-state δ value should be consistently lower with the MR compensators than with the SR compensators.

What other compensator structure could be used to reduce this overshoot? One possibility is to add rate sensors that measure $\dot{\theta}$ and $\dot{\delta}$. This yields a full state feedback compensator structure, to which optimal control law synthesis method of Section 3.2 can be applied. We used the optimal control law synthesis method of Section 3.2 to synthesize optimal compensators comparable to the Case 1 MR and SR compensators of Section 6.2. For the optimal SR compensator, we picked the same sampling rate that was used in the Case 1 SR compensator. For θ, $\dot{\theta}$, δ, $\dot{\delta}$, and u_2 sampling in the optimal MR compensator, we picked the same sampling rate that

was used for δ and u_2 sampling in the Case 1 MR compensator. For u_1 sampling in the optimal MR compensator, we picked the same sampling rate that was used for θ and u_1 sampling in the Case 1 MR compensator. Finally, we synthesized the optimal MR and SR compensators using the same performance index that was used to synthesize the Case 1 MR and SR compensators.

Let P represent the ratio of the fast sampling rate to the slow sampling rate in the optimal MR compensator. The optimal MR control laws are

$$u_1(m,n) = -\bar{C}\,p(m,0)\,, \tag{48}$$

$$u_{21}(m,n) = 0\,, \tag{49}$$

$$u_{22}(m,n) = -\tilde{C}(n)\,p(m,n) - \tilde{c}(n)\,u_1(m,n)\,, \tag{50}$$

for $m=0, 1, \ldots$ and $n=0, 1, \ldots, P-1$, where $u_1(m,n)$, $u_{21}(m,n)$, $u_{22}(m,n)$, and $p(m,n)$ have the same meanings as in (21) through (30), and

$$\bar{C} = [\,2.79 \quad 1.61 \quad 0.535 \quad 0.295\,]\,, \tag{51}$$

$$\tilde{C}(0) = [\,0.0196 \quad 0.0147 \quad 3.15 \quad 0.230\,]\,, \tag{52}$$

$$\tilde{C}(1) = [\,-0.00734 \quad -0.000952 \quad 3.15 \quad 0.227\,]\,, \tag{53}$$

$$\tilde{C}(2) = [\,-0.00819 \quad -0.00157 \quad 3.15 \quad 0.227\,]\,, \tag{54}$$

$$\tilde{C}(3) = [\,-0.00930 \quad -0.00232 \quad 3.15 \quad 0.227\,]\,, \tag{55}$$

$$\tilde{C}(4) = [\,-0.0102 \quad -0.00295 \quad 3.15 \quad 0.227\,]\,, \tag{56}$$

$$\tilde{C}(5) = [\,-0.00978 \quad -0.00247 \quad 3.15 \quad 0.227\,]\,, \tag{57}$$

$$\tilde{C}(6) = [\,-0.00620 \quad -0.000109 \quad 3.15 \quad 0.228\,]\,, \tag{58}$$

$$\tilde{C}(7) = [\,0.00294 \quad 0.00540 \quad 3.15 \quad 0.229\,]\,, \tag{59}$$

$$\tilde{c}(0) = 0.\,, \tag{60}$$

$$\tilde{c}(1) = -0.00982\,, \tag{61}$$

$$\tilde{c}(2) = -0.0103\,, \tag{62}$$

$$\tilde{c}(3) = -0.0108\,, \tag{63}$$

$$\tilde{c}(4) = -0.0112\,, \tag{64}$$

$$\tilde{c}(5) = -0.0108\,, \tag{65}$$

$$\tilde{c}(6) = -0.00915\,, \tag{66}$$

$$\tilde{c}(7) = -0.00557\,. \tag{67}$$

The elements of $\tilde{C}(n)$ are plotted versus n in Figure 6.30 through 6.33. The $\tilde{c}(n)$ are plotted versus n in Figure 6.34.

The corresponding optimal SR control laws are

$$u_1(m,0) = -\bar{C}\,p(m,0)\,, \tag{68}$$

$$u_{21}(m,n) = 0\,, \tag{69}$$

$$u_{22}(m,0) = -\tilde{C}(0)\,p(m,0)\,, \tag{70}$$

for $m=0, 1, \ldots,$ where

$$\bar{C} = [\,4.09 \quad 1.95 \quad -0.599 \quad 0.267\,]\,, \tag{71}$$

$$\tilde{C}(0) = [\,0.0337 \quad 0.0180 \quad 2.17 \quad 0.192\,]\,. \tag{72}$$

The closed-loop responses to the Case 1 tip positioning command with the optimal MR and optimal SR compensators are shown in Figures 6.35 through 6.37. These responses were obtained by the same simulation procedures as were used to obtain Figures 6.14 through 6.24. In Figures 6.35 through 6.37, the solid curves are the responses with the optimal MR compensator. The dashed curves are the responses with the optimal SR compensator. The dot-dashed curves are the responses with a *constant gains* approximation to the optimal MR compensator. The sampling rates for the constant gains compensator are the same as in the optimal MR compensator, except that the sampling rate for θ and $\dot{\theta}$ is the same slow $1/PT$ sampling rate that is used to sample only u_1 in the optimal MR compensator.

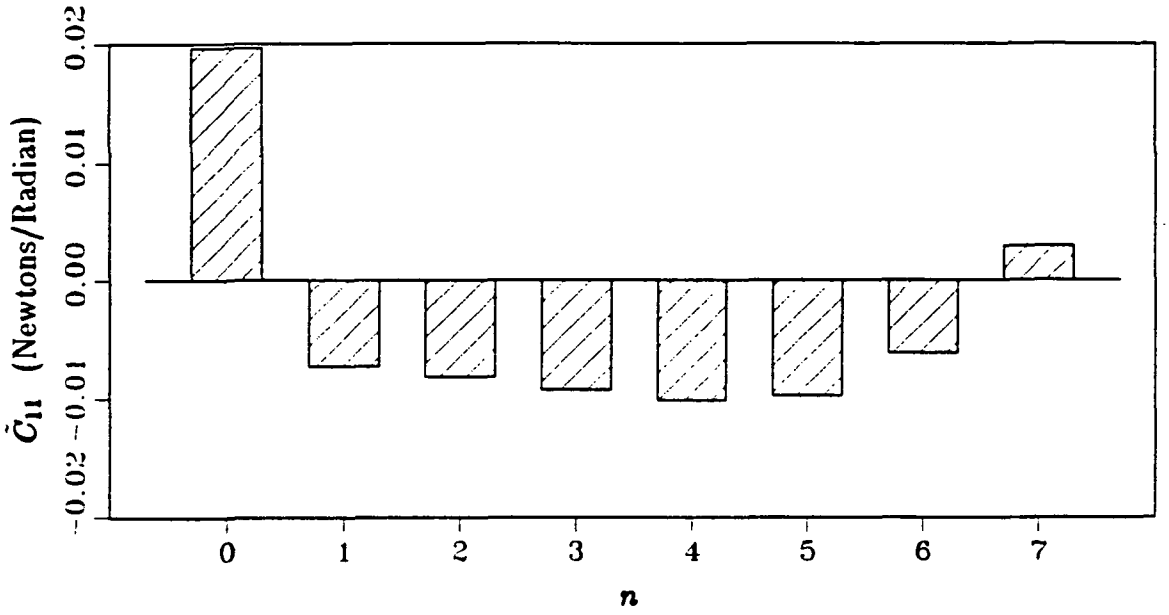

Figure 6.30 Optimal Feedback Gain $\tilde{C}_{11}(n)$ versus n.

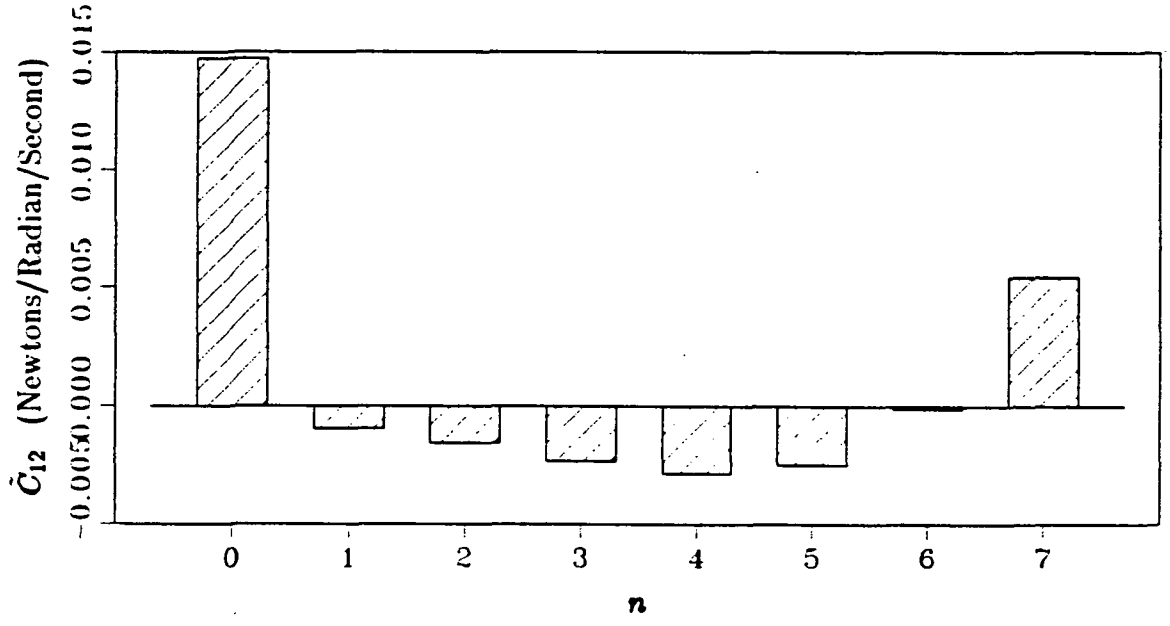

Figure 6.31 Optimal Feedback Gain $\tilde{C}_{12}(n)$ versus n.

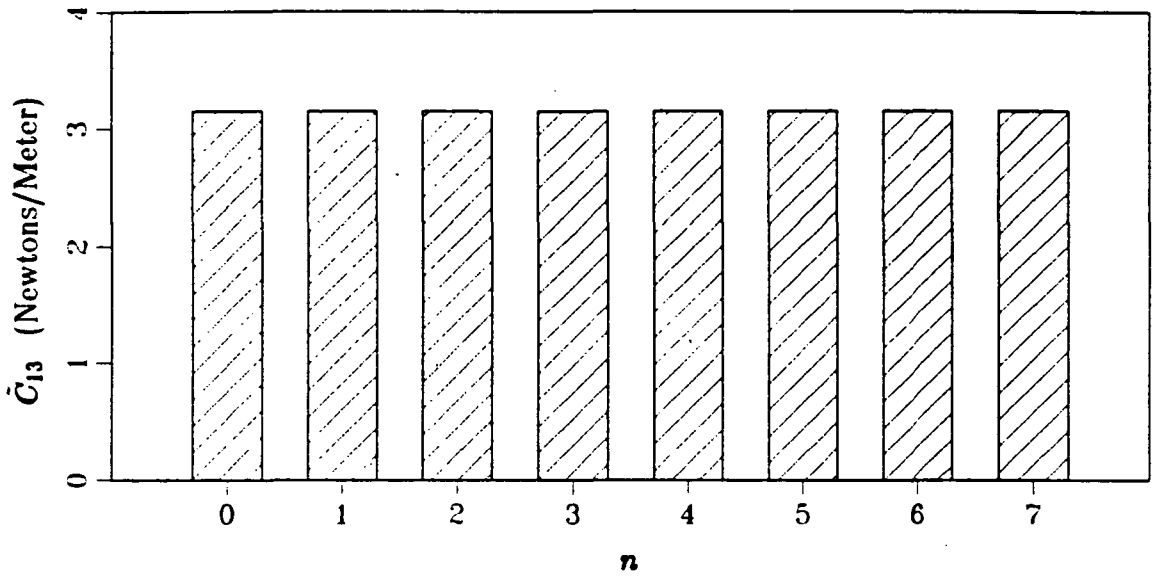

Figure 6.32 Optimal Feedback Gain $\tilde{C}_{13}(n)$ versus n.

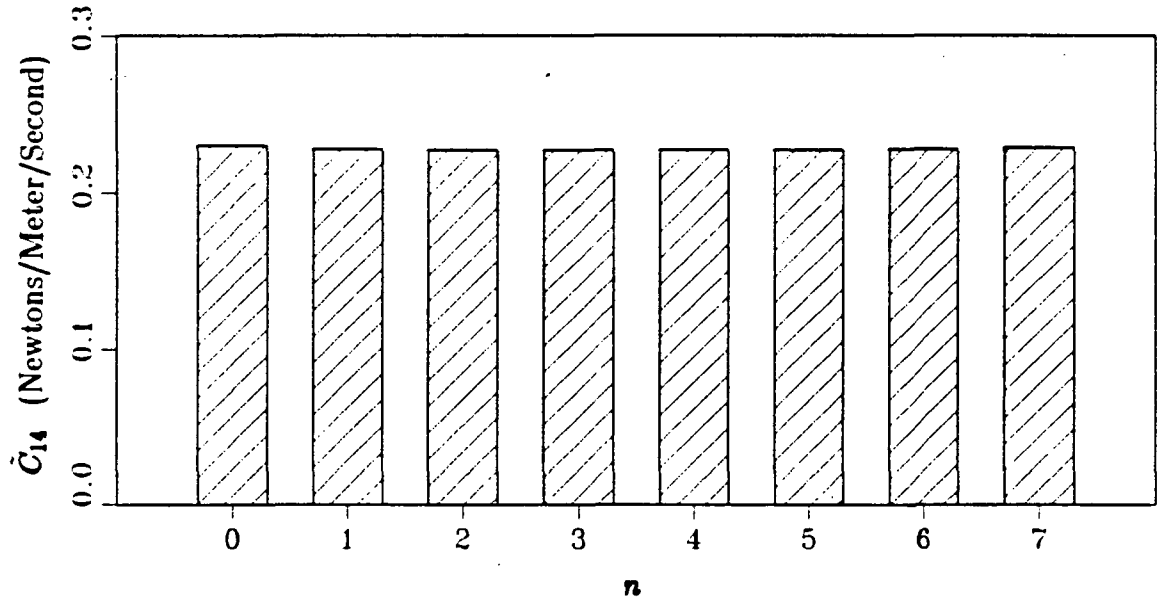

Figure 6.33 Optimal Feedback Gain $\tilde{C}_{14}(n)$ versus n.

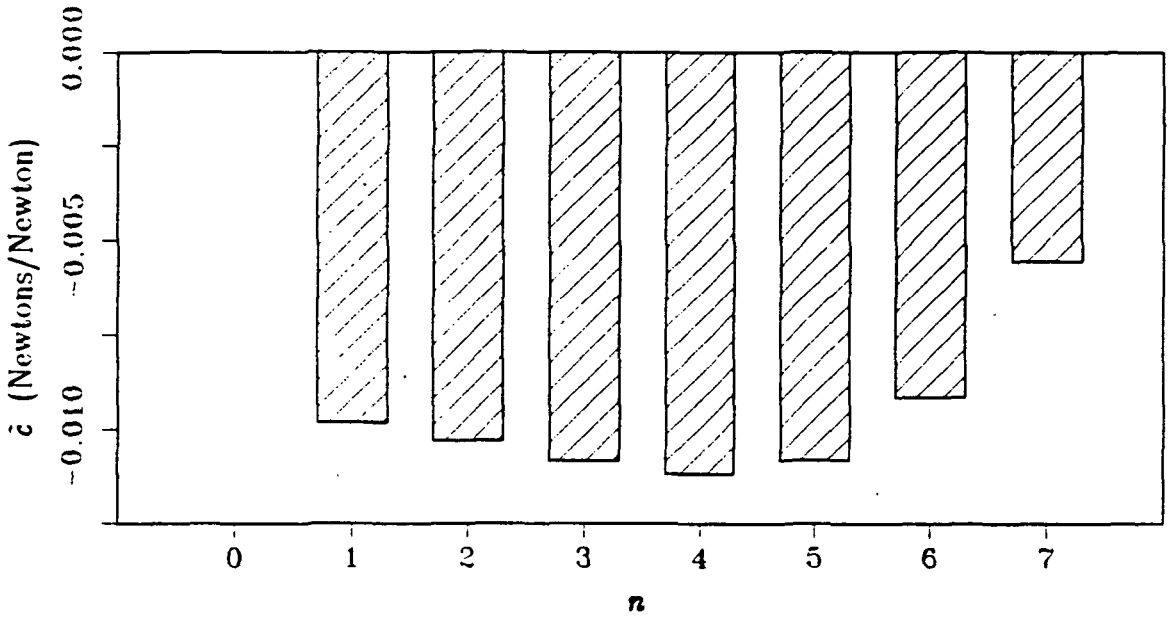

Figure 6.34 Optimal Feedback Gain $\tilde{c}(n)$ versus n.

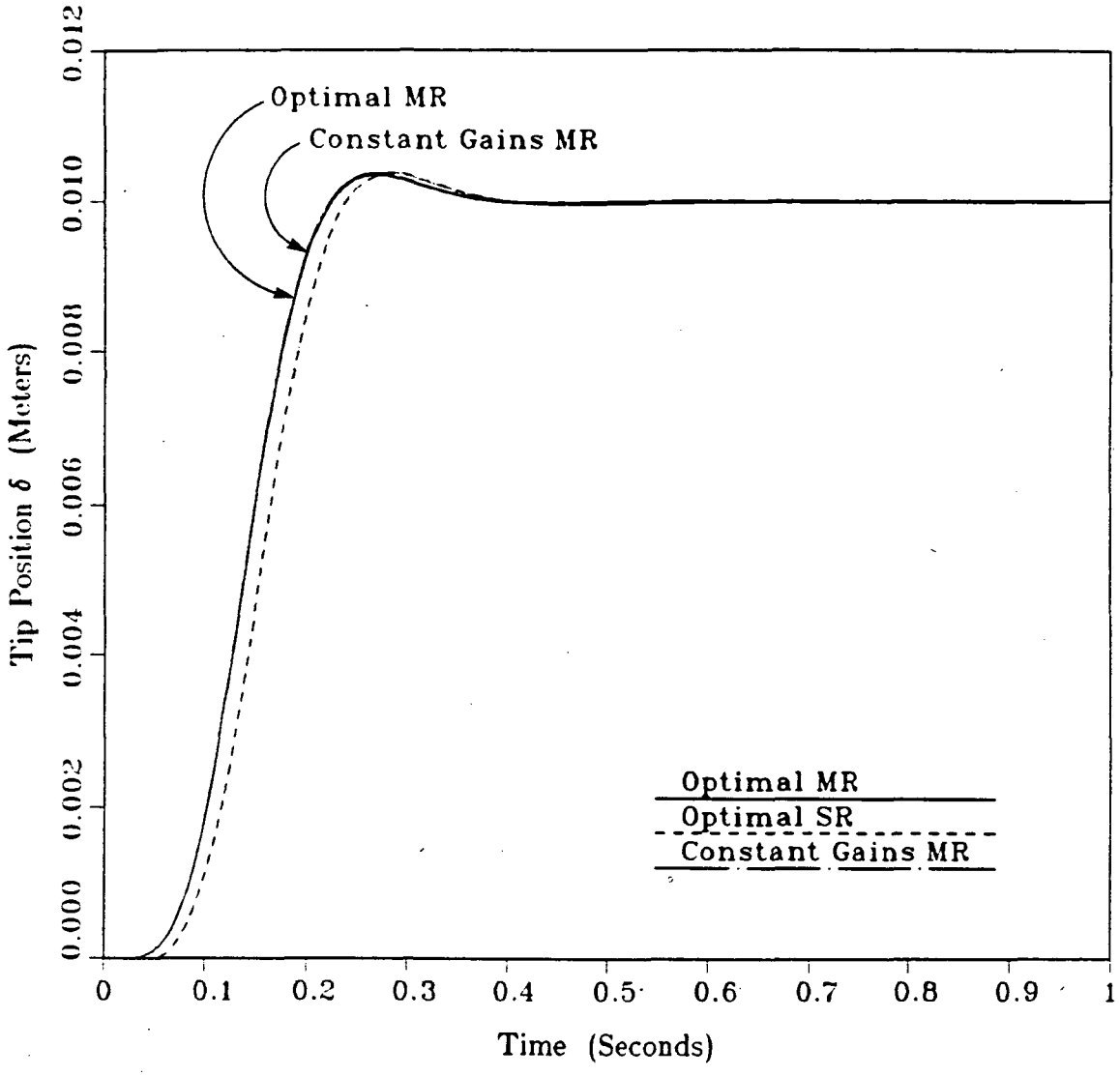

Figure 6.35 Tip Position Responses to Case 1 Tip Positioning Command with Optimal MR, Optimal SR, and Constant Gains MR Compensators.

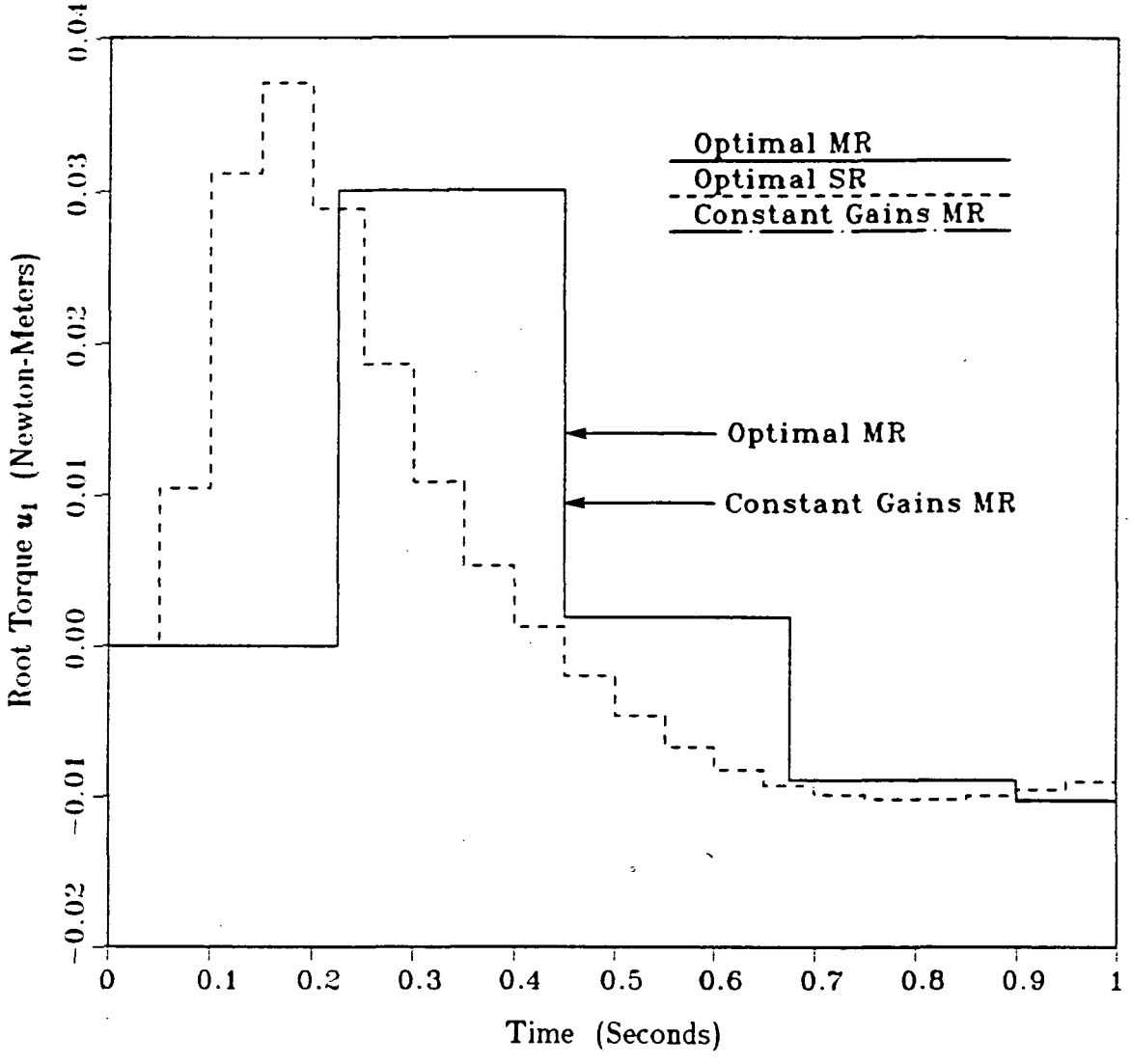

Figure 6.36 Root Torque Responses to Case 1 Tip Positioning Command with Optimal MR, Optimal SR, and Constant Gains MR Compensators.

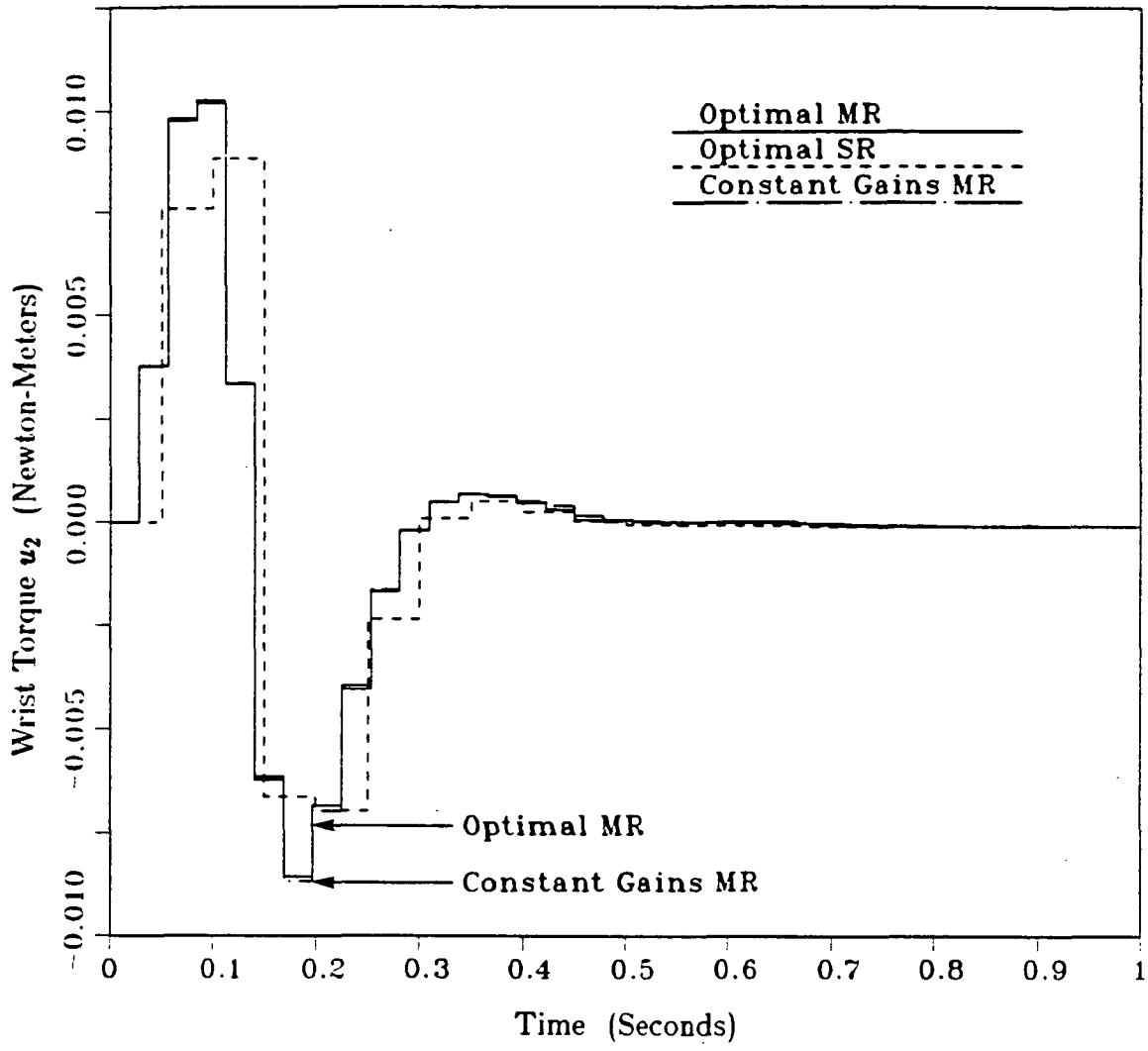

Figure 6.37 Wrist Torque Responses to Case 1 Tip Positioning Command with Optimal MR, Optimal SR, and Constant Gains MR Compensators.

The constant gains compensator has the same full state feedback compensator structure as the optimal compensators, and it was synthesized using AMS for the same process noise levels and performance index. The constant gains MR control laws are

$$u_1(m,n) = -\bar{C}\, p(m,0)\,, \tag{73}$$

$$u_{21}(m,n) = -\tilde{C}_1\, p(m,0)\,, \tag{74}$$

$$u_{22}(m,n) = -\tilde{C}_2\, p(m,n)\,, \tag{75}$$

for $m=0, 1, \ldots$ and $n=0, 1, \ldots, P-1$, where

$$\bar{C} = [\,2.79 \quad 1.61 \quad 0.535 \quad 0.293\,]\,, \tag{76}$$

$$\tilde{C}_1 = [\,0.0201 \quad 0.0121 \quad 0. \quad 0.\,]\,, \tag{77}$$

$$\tilde{C}_2 = [\,0. \quad 0. \quad 3.16 \quad 0.228\,]\,. \tag{78}$$

From the responses in Figures 6.35 through 6.37, we conclude that:

1) The peak overshoot of the steady-state δ value is markedly less with the optimal MR compensator than with the Case 1 MR compensator. The same can be said for the optimal SR compensator as compared to the Case 1 SR compensator.
2) The performance of the constant gains MR compensator is, for practical purposes, the same as that of the optimal MR compensator. That a constant gains MR compensator could be synthesized that is capable of performance so close to that of the optimal MR compensator is presumably a consequence of the fact that the optimal MR feedback gains $\tilde{C}_{13}(n)$ and $\tilde{C}_{14}(n)$ (in Figures 6.32 and 6.33) are virtually independent of n.

Chapter 7
Concluding Remarks

The conclusions of this research and the recommendations for further research are the subjects of Sections 7.1 and 7.2, respectively.

§7.1 Conclusions. This section contains three subsections. The first deals with the constrained optimization synthesis method of Chapter 4. The second and third present the conclusions of the mass-spring-mass design study of Chapter 5 and the two link robot arm design study of Chapters 5 and 6.

The Constrained Optimization Synthesis Method. The constrained optimization synthesis method was shown to be a powerful tool for synthesizing MR or SR digital compensators. The advantages of this method are: (1) the control laws for all control loops are synthesized simultaneously, taking full advantage of all cross-coupling effects; and (2) the compensator structure is arbitrary, and simple, low-order compensator structures are easily accomodated. The method requires a gradient search to determine a control law that minimizes a quadratic performance index. The gradients are calculated exactly, using a closed-form expression, and a finite-time performance index is used so that a stabilizing initial guess for the control laws is not required.

MR or SR Compensation? The performance characteristics of MR and SR compensators were compared in the context of the mass-spring-mass and two link robot arm example design problems. The comparisons were objective in that they involved MR and SR compensators that were designed to satisfy the same performance objectives and required the same average number of machine operations per unit time for real-time operation. We conclude that:

1. For the slow sampling rates (characterized by SR sampling at 5 times the characteristic frequency in hertz of the fastest desired closed-loop poles), the MR compensators markedly and consistently out-performed their SR counterparts, for ratios of the characteristic frequencies of the desired closed-loop poles as low as 4-to-1.
2. For the fast sampling rates (characterized by SR sampling at 20 times the characteristic frequency in hertz of the fastest desired closed-loop poles), the MR compensators out-performed their SR counterparts, but the performance benefits were much less than in the slow-sampling-rates cases.

Which Method for MR Synthesis? We compared the successive loop closures synthesis method of Section 3.1, the optimal control law synthesis method of Section 3.2, and the constrained optimization synthesis method of Chapter 4 in the context of the mass-spring-mass and two link robot arm example design problems. We conclude that:

1. For the mass-spring-mass system, autonomous operation of each control effector is adequate to obtain good closed-loop performance and the successive loop closures synthesis method is ideal.
2. For the two link robot arm system, the control effectors must *cooperate* to obtain good closed-loop performance and it is difficult to apply the successive loop closures synthesis method.

3. For the two link robot arm system, the best closed-loop responses to tip positioning commands were obtained with an optimal MR compensator. A problem with this compensator is that it is periodically time-varying. Such periodicity is *not* a prerequisite for good closed-loop performance. A time-invariant MR compensator with performance characteristics virtually identical to those of the optimal MR compensator was synthesized using the constrained optimization synthesis method.
4. The advantages of the constrained optimization synthesis method were clearly demonstrated in that:
   1) For the two link robot arm system, the constrained optimization synthesis method was shown to be a good method for synthesizing a second-order compensator to control the tip position.
   2) For the two link robot arm system, the constrained optimization synthesis method was shown to be the only method suitable for synthesizing a time-invariant compensator with performance characteristics comparable to the best optimal MR compensator.

§7.2 Recommendations for Further Research. The following subsections present topics for further research in 4 areas.

Sampling Rates Selection. We chose compensator sampling rates based on the characteristic frequencies of the desired closed-loop poles. A better approach would take the performance objectives into account more directly. The need for this was clearly demonstrated when it was shown that, for the mass-spring-mass system, fast sampling of the $x_2/\dot{x}_2$-to-u_2 control loop at the expense of slow sampling of the $x_1/\dot{x}_1$-to-u_1 control loop is desirable purely because the $x_2/\dot{x}_2$-to-u_2 loop is more directly coupled to the disturbance source.

In short, MR synthesis offers the designer the flexibility to choose more than

one sampling rate, but the task is also greater, and more research is needed in this area.

High Frequency Characteristics of MR Systems. As pointed out in Section 6.2, the closed-loop BTP poles of a MR system are generally a poor indicator of its high frequency behavior. This is because the BTP is generally large compared to the characteristic times of the high frequency closed-loop poles.

The idea of Thompson, Stein, and Athans (1983) is to treat the combination of the control law, the analog-to-digital converter, and the digital-to-analog converter as an analog device, and then assess stability of the closed-loop system in the analog sense. This is a promising approach, but many details remain to be worked out.

MR Discrete Approximations to Analog Compensators. For SR sampling there are numerous schemes for determining a discrete approximation to a single-input, single-output analog compensator. For MR sampling, an algorithm for determining a discrete approximation to a multi-input, multi-output analog compensator would be useful. More research is needed in this area.

Improved Optimization Schemes. A more computationally efficient algorithm for solving the constrained optimization problem would utilize a simpler performance index for the early stages of an optimization. See Ly's discussion (1982) of the optimization algorithm for the SANDY program and Sun's discussion (1985) of an improved optimization algorithm for the SANDY program for additional ideas for research in this area.

Appendix A

Two Link Robot Arm Dynamical Equations

The open-loop system is shown in Figure A.1. It is a simplified model of an experimental arm studied by Chiang (1986). Point O is fixed and links A and B are rigid. Body C is a point mass at the tip of the manipulator. The axes of rotational joints located at the root and wrist are parallel, and are oriented so that all motions are in a horizontal plane. Reference line R is fixed in the plane of motion and passes through point O. Generalized coordinate θ is the angle of rotation of A with respect to R. Generalized coordinate ϕ is the angle of rotation of B with respect to the A. The tip position δ is a redundant coordinate. Control inputs u_1 and u_2 are torques acting at the root and wrist, respectively.

The full nonlinear dynamical equations for this system were determined via a straightforward application of Kane's (1972) method. Let M and L represent the mass per unit length and the length, respectively, of A. Let m and l represent the mass per unit length and the length, respectively, of B. Let T represent the mass of C. The dynamical equations are:

$$\ddot{\theta}[\frac{1}{3}ML^3 + ml(L^2 + \frac{1}{3}l^2) + T(L^2 + l^2) + (ml + 2T)Ll\cos\theta]$$
$$+ \ddot{\phi}[\frac{1}{3}ml^3 + Tl^2 + (\frac{1}{2}ml + T)Ll\cos\phi]$$

$$-\dot{\phi}^2[(\frac{1}{2}ml+T)Ll\sin\phi]-\dot{\theta}\dot{\phi}[(ml+2T)Ll\sin\phi]=u_1\,, \tag{1}$$

$$\ddot{\theta}[\frac{1}{3}ml^3+Tl^2+(\frac{1}{2}ml+T)Ll\cos\phi]+\ddot{\phi}[\frac{1}{3}ml^3+Tl^2]$$
$$+\dot{\theta}^2[(\frac{1}{2}ml+T)Ll\sin\phi]=u_2\,. \tag{2}$$

Now we assume that θ and ϕ are small enough that $\cos\theta=1$, $\sin\theta=\theta$, $\cos\phi=1$, and $\sin\phi=\phi$, and that $\dot{\theta}$ and $\dot{\phi}$ are small enough that terms in products of $\dot{\theta}$ and $\dot{\phi}$ in (1) and (2) are negligible compared to terms in $\ddot{\theta}$ and $\ddot{\phi}$. From (1) and (2), we obtain

$$\begin{bmatrix}\dot{\theta}\\ \ddot{\theta}\\ \dot{\phi}\\ \ddot{\phi}\end{bmatrix}=\begin{bmatrix}0&1&0&0\\0&0&0&0\\0&0&0&1\\0&0&0&0\end{bmatrix}\begin{bmatrix}\theta\\ \dot{\theta}\\ \phi\\ \dot{\phi}\end{bmatrix}+\left(\frac{1}{ad-bc}\right)\begin{bmatrix}0&0\\d&-b\\0&0\\-c&a\end{bmatrix}\begin{bmatrix}u_1\\u_2\end{bmatrix}, \tag{3}$$

where

$$a\triangleq\frac{1}{3}ML^3+ml(L^2+Ll+\frac{1}{3}l^2)+T(L+l)^2\,, \tag{4}$$

$$b\triangleq\frac{1}{3}ml^3+Tl^2+(\frac{1}{2}ml+T)Ll\,, \tag{5}$$

$$c\triangleq b\,, \tag{6}$$

$$d\triangleq\frac{1}{3}ml^3+Tl^2\,. \tag{7}$$

From (3), transforming to θ and δ coordinates using

$$\begin{bmatrix}\theta\\ \dot{\theta}\\ \delta\\ \dot{\delta}\end{bmatrix}=\begin{bmatrix}1&0&0&0\\0&1&0&0\\L+l&0&l&0\\0&L+l&0&l\end{bmatrix}\begin{bmatrix}\theta\\ \dot{\theta}\\ \phi\\ \dot{\phi}\end{bmatrix},$$

we obtain

$$\dot{p}(t)=F\,p(t)+G\,u(t)\,, \tag{8}$$

where

$$p(t)\triangleq[\,\theta(t)\quad\dot{\theta}(t)\quad\delta(t)\quad\dot{\delta}(t)\,]^{\mathrm{T}}\,, \tag{9}$$

$$u(t)\triangleq[\,u_1(t)\quad u_2(t)\,]^{\mathrm{T}}\,, \tag{10}$$

$$F \triangleq \begin{bmatrix} 0 & 1 & 0 & 0 \\ 0 & 0 & 0 & 0 \\ 0 & 0 & 0 & 1 \\ 0 & 0 & 0 & 0 \end{bmatrix}, \tag{11}$$

$$G \triangleq \left(\frac{1}{ad-bc}\right) \begin{bmatrix} 0 & 0 \\ d & -b \\ 0 & 0 \\ (L+l)d - lc & -(L+l)b + la \end{bmatrix}. \tag{12}$$

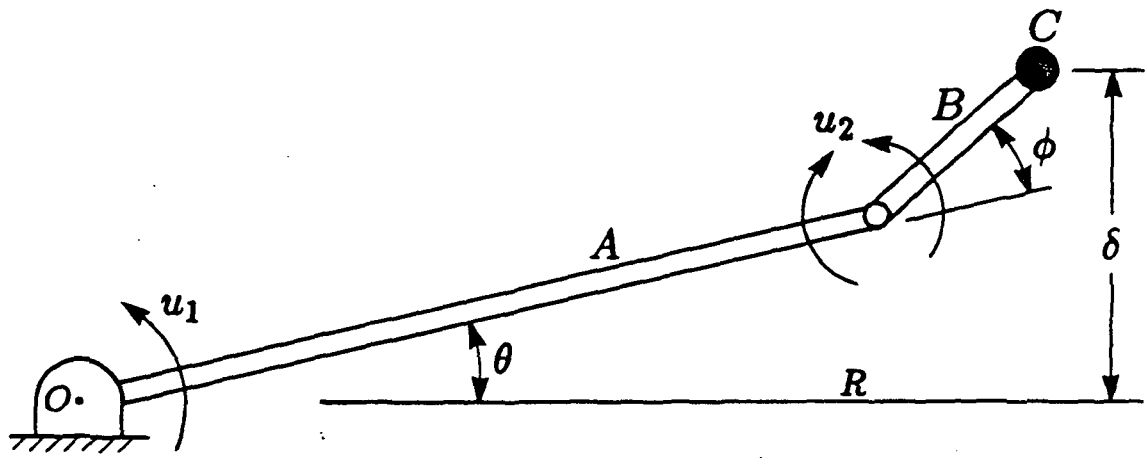

Figure A.1 Open-Loop TLA System with Tip Mass

Appendix B

Proofs for Theorems 1 and 2

An open-loop plant is assumed to be represented by the time-varying discrete state equation

$$x(t+1) = A(t)\,x(t) + B(t)\,u(t) + w(t)\,, \tag{1}$$

for $t = t_0,\ t_0+1,\ \ldots,\ t_1-1$, where $x(t)$, $u(t)$, and $w(t)$ are the state, control input, and process noise input vectors, respectively. The initial state $x(t_0)$ is assumed to be a zero-mean, gaussian random vector, with covariance X_0. Let

$$\delta(i,j) \triangleq \begin{cases} 1 & \text{if } i = j; \\ 0 & \text{if } i \neq j. \end{cases} \tag{2}$$

The process noise is assumed to be a zero-mean, gaussian, purely random sequence, with covariance $W(t)$, so that

$$\mathrm{E}\{w(t)\,w^{\mathrm{T}}(\tau)\} = W(t)\,\delta(t,\tau)\,, \tag{3}$$

where $\mathrm{E}\{\cdot\}$ is the expected value operator. The process noise and initial state are assumed to be uncorrelated.

The performance index is assumed to be

$$J(t;u(\cdot)) \triangleq \frac{1}{2}\mathrm{E}\Big\{x^{\mathrm{T}}(t_1)\,Q_1\,x(t_1) + \sum_{\substack{\tau=t \\ t\neq t_1}}^{t_1-1} \begin{bmatrix} x(\tau) \\ u(\tau) \end{bmatrix}^{\mathrm{T}} \begin{bmatrix} Q(\tau) & N(\tau) \\ N^{\mathrm{T}}(\tau) & R(\tau) \end{bmatrix} \begin{bmatrix} x(\tau) \\ u(\tau) \end{bmatrix}\Big\}, \tag{4}$$

where Q_1 is a symmetric, positive semidefinite matrix, and each $Q(\tau)$ and $R(\tau)$ is a symmetric, positive semidefinite matrix.

The control input is assumed to satisfy

$$u(t) = -C(t)\,x(t)\,. \tag{5}$$

Let I_x represent an identity matrix with the same number of rows and columns as there are elements in $x(t)$. Let

$$\Phi(\tau,t) \triangleq \Big(A(\tau-1)-B(\tau-1)\,C(\tau-1)\Big)\Big(A(\tau-2)-B(\tau-2)\,C(\tau-2)\Big)* \\ \cdots * \Big(A(t)-B(t)\,C(t)\Big)\,, \tag{6}$$

for $t=t_0,\, t_0+1,\, \ldots,\, t_1-1$ and $\tau=t+1,\, t+2,\, \ldots,\, t_1$, and let

$$\Phi(t,t) \triangleq I_x\,, \tag{7}$$

so that the $\Phi(\tau,t)$ satisfy

$$\Phi(\tau+1,t) = \Big(A(\tau)-B(\tau)\,C(\tau)\Big)\Phi(\tau,t)\,. \tag{8}$$

Let

$$Q_C(t) \triangleq \begin{bmatrix} I \\ -C(t) \end{bmatrix}^{\mathrm{T}} \begin{bmatrix} Q(t) & N(t) \\ N^{\mathrm{T}}(t) & R(t) \end{bmatrix} \begin{bmatrix} I \\ -C(t) \end{bmatrix}\,. \tag{9}$$

Let

$$\Psi(t) \triangleq \Phi^{\mathrm{T}}(t_1,t)\,Q_1\,\Phi(t_1,t) + \sum_{\substack{\tau=t \\ t\neq t_1}}^{t_1-1} \Phi^{\mathrm{T}}(\tau,t)\,Q_C(\tau)\,\Phi(\tau,t)\,, \tag{10}$$

for $t=t_0,\, t_0+1,\, \ldots,\, t_1$, so that the $\Psi(t)$ satisfy

$$\Psi(t) = \Big(A(t)-B(t)\,C(t)\Big)^{\mathrm{T}}\Psi(t+1)\Big(A(t)-B(t)\,C(t)\Big) + Q_C(t)\,, \tag{11}$$

for $\Psi(t_1) = Q_1$.

Theorem 1. An equivalent expression for the performance index in (4) is

$$J(t;u(\cdot)) = \frac{1}{2}\mathrm{E}\Big\{x^{\mathrm{T}}(t)\,\Psi(t)\,x(t) + \sum_{\substack{\tau=t \\ t\neq t_1}}^{t_1-1} w^{\mathrm{T}}(\tau)\,\Psi(\tau+1)\,w(\tau)\Big\}\,, \tag{12}$$

for $t=t_0, t_0+1, \ldots, t_1$.

Proof. From (4), using (5) and (9), we obtain

$$J(t;u(\cdot)) = \frac{1}{2}\mathrm{E}\Big\{x^{\mathrm{T}}(t_1)\,Q_1\,x(t_1) + \sum_{\substack{\tau=t\\ t\neq t_1}}^{t_1-1} x^{\mathrm{T}}(\tau)\,Q_C(\tau)\,x(\tau)\Big\}, \tag{13}$$

for $t=t_0, t_0+1, \ldots, t_1$. From (1), using (5), (8), and (7), we obtain

$$x(\tau) = \Phi(\tau,t)\,x(t) + \sum_{\substack{\mu=t\\ t\neq\tau}}^{\tau-1} \Phi(\tau,\mu+1)\,w(\mu)\,, \tag{14}$$

for $t=t_0, t_0+1, \ldots, t_1$ and $\tau=t, t+1, \ldots, t_1$. From (13), substituting for $x(t_1)$ and $x(\tau)$ using (14), we obtain

$$\begin{aligned} J(t;u(\cdot)) = \frac{1}{2}\mathrm{E}\Big\{ &\Big[\Phi(t_1,t)\,x(t) + \sum_{\substack{\mu=t\\ t\neq t_1}}^{t_1-1} \Phi(t_1,\mu+1)\,w(\mu)\Big]^{\mathrm{T}} Q_1 \\ &* \Big[\Phi(t_1,t)\,x(t) + \sum_{\substack{\mu=t\\ t\neq t_1}}^{t_1-1} \Phi(t_1,\mu+1)\,w(\mu)\Big] \\ &+ \sum_{\substack{\tau=t\\ t\neq t_1}}^{t_1-1} \Big[\Phi(\tau,t)\,x(t) + \sum_{\substack{\mu=t\\ t\neq\tau}}^{\tau-1} \Phi(\tau,\mu+1)\,w(\mu)\Big]^{\mathrm{T}} Q_C(\tau) \\ &* \Big[\Phi(\tau,t)\,x(t) + \sum_{\substack{\mu=t\\ t\neq\tau}}^{\tau-1} \Phi(\tau,\mu+1)\,w(\mu)\Big]\Big\}, \end{aligned} \tag{15}$$

for $t=t_0, t_0+1, \ldots, t_1$. Most of the product terms in (15) are zero, and we obtain

$$\begin{aligned} J(t;u(\cdot)) = \frac{1}{2}\mathrm{E}\Big\{ &x^{\mathrm{T}}(t)\,\Phi^{\mathrm{T}}(t_1,t)\,Q_1\,\Phi(t_1,t)\,x(t) \\ &+ \Big[\sum_{\substack{\mu=t\\ t\neq t_1}}^{t_1-1} w^{\mathrm{T}}(\mu)\,\Phi^{\mathrm{T}}(t_1,\mu+1)\,Q_1\,\Phi(t_1,\mu+1)\,w(\mu)\Big] \\ &+ \Big[\sum_{\substack{\tau=t\\ t\neq t_1}}^{t_1-1} x^{\mathrm{T}}(t)\,\Phi^{\mathrm{T}}(\tau,t)\,Q_C(\tau)\,\Phi(\tau,t)\,x(t)\Big] \\ &+ \Big[\sum_{\substack{\tau=t\\ t\neq t_1}}^{t_1-1}\sum_{\substack{\mu=t\\ t\neq\tau}}^{\tau-1} w^{\mathrm{T}}(\mu)\,\Phi^{\mathrm{T}}(\tau,\mu+1)\,Q_C(\tau)\,\Phi(\tau,\mu+1)\,w(\mu)\Big]\Big\}, \end{aligned} \tag{16}$$

for $t=t_0, t_0+1, \ldots, t_1$.

From (16), substituting for the double summation using

$$\sum_{\substack{\tau=t \\ t\neq t_1}}^{t_1-1} \sum_{\substack{\mu=t \\ t\neq\tau}}^{\tau-1} f(\tau,\mu) = \sum_{\substack{\mu=t \\ t\neq t_1}}^{t_1-1} \sum_{\substack{\tau=\mu+1 \\ \mu\neq t_1-1}}^{t_1-1} f(\tau,\mu), \tag{17}$$

we obtain

$$\begin{aligned} J(t;u(\cdot)) = \frac{1}{2}\mathrm{E}\Big\{ x^{\mathrm{T}}(t)\Big[\Phi^{\mathrm{T}}(t_1,t)\,Q_1\,\Phi(t_1,t) + \sum_{\substack{\tau=t \\ t\neq t_1}}^{t_1-1} \Phi^{\mathrm{T}}(\tau,t)\,Q_C(\tau)\,\Phi(\tau,t)\Big] x(t) \\ + \sum_{\substack{\mu=t \\ t\neq t_1}}^{t_1-1} w^{\mathrm{T}}(\mu)\Big[\Phi^{\mathrm{T}}(t_1,\mu+1)\,Q_1\,\Phi(t_1,\mu+1) \\ + \sum_{\substack{\tau=\mu+1 \\ \mu\neq t_1-1}}^{t_1-1} \Phi^{\mathrm{T}}(\tau,\mu+1)\,Q_C(\tau)\,\Phi(\tau,\mu+1)\Big] w(\mu)\Big\}, \end{aligned} \tag{18}$$

for $t=t_0, t_0+1, \ldots, t_1$. And from (18), using (10), we obtain

$$J(t;u(\cdot)) = \frac{1}{2}\mathrm{E}\Big\{ x^{\mathrm{T}}(t)\,\Psi(t)\,x(t) + \sum_{\substack{\mu=t \\ t\neq t_1}}^{t_1-1} w^{\mathrm{T}}(\mu)\,\Psi(\mu+1)\,w(\mu)\Big\}, \tag{19}$$

for $t=t_0, t_0+1, \ldots, t_1$.

Now let $u_1(t) = -C_1(t)\,x(t)$ and $u_2(t) = -C_2(t)\,x(t)$ be two different control laws. Let

$$\begin{aligned} \Phi_i(\tau,t) \triangleq \Big(A(\tau-1)-B(\tau-1)\,C_i(\tau-1)\Big)\Big(A(\tau-2)-B(\tau-2)\,C_i(\tau-2)\Big)* \\ \cdots * \Big(A(t)-B(t)\,C_i(t)\Big), \end{aligned} \tag{20}$$

for $t=t_0, t_0+1, \ldots, t_1-1$ and $\tau=t+1, t+2, \ldots, t_1$, and let

$$\Phi_i(t,t) \triangleq I_x. \tag{21}$$

Let

$$Q_{C_i}(t) \triangleq \begin{bmatrix} I \\ -C_i(t) \end{bmatrix}^{\mathrm{T}} \begin{bmatrix} Q(t) & N(t) \\ N^{\mathrm{T}}(t) & R(t) \end{bmatrix} \begin{bmatrix} I \\ -C_i(t) \end{bmatrix}. \tag{22}$$

Let

$$\Psi_i(t) \triangleq \Phi_i^{\mathrm{T}}(t_1,t)\,Q_1\,\Phi_i(t_1,t) + \sum_{\substack{\tau=t\\ t\neq t_1}}^{t_1-1} \Phi_i^{\mathrm{T}}(\tau,t)\,Q_{C_i}(\tau)\,\Phi_i(\tau,t)\,, \tag{23}$$

for $t=t_0, t_0+1, \ldots, t_1$, so that the $\Psi_i(t)$ satisfy

$$\Psi_i(t) = \Big(A(t)-B(t)\,C_i(t)\Big)^{\mathrm{T}}\Psi_i(t+1)\Big(A(t)-B(t)\,C_i(t)\Big) + Q_{C_i}(t)\,, \tag{24}$$

for $\Psi_i(t_1) = Q_1$.

From Theorem 1 and the properties of the expected value operator, the difference in the performance index if $u_2(t)$ is applied instead of $u_1(t)$ is

$$\begin{aligned} J(t;u_2(\cdot)) - J(t;u_1(\cdot)) = \frac{1}{2}\mathrm{E}\Big\{ & x^{\mathrm{T}}(t)\Big(\Psi_2(t)-\Psi_1(t)\Big)x(t) \\ & + \sum_{\substack{\tau=t\\ t\neq t_1}}^{t_1-1} w^{\mathrm{T}}(\tau)\Big(\Psi_2(\tau+1)-\Psi_1(\tau+1)\Big)w(\tau)\Big\}\,, \end{aligned} \tag{25}$$

for $t=t_0, t_0+1, \ldots, t_1$.

Lemma 1. The $\Psi_2(t)-\Psi_1(t)$ in (25) satisfy

$$\begin{aligned} \Psi_2(t)-\Psi_1(t) = \sum_{\substack{\tau=t\\ t\neq t_1}}^{t_1-1} \Phi_2^{\mathrm{T}}(\tau,t)\Big\{ & \Big(C_2(\tau)-C_1(\tau)\Big)^{\mathrm{T}} \\ & * \Big[-N^{\mathrm{T}}(\tau)+R(\tau)C_1(\tau)-B^{\mathrm{T}}(\tau)\Psi_1(\tau+1)\Big(A(\tau)-B(\tau)C_2(\tau)\Big)\Big] \\ & + \Big[-N^{\mathrm{T}}(\tau)+R(\tau)C_1(\tau)-B^{\mathrm{T}}(\tau)\Psi_1(\tau+1)\Big(A(\tau)-B(\tau)C_2(\tau)\Big)\Big]^{\mathrm{T}} \\ & * \Big(C_2(\tau)-C_1(\tau)\Big) + \Big(C_2(\tau)-C_1(\tau)\Big)^{\mathrm{T}}\Big[R(\tau)-B^{\mathrm{T}}(\tau)\Psi_1(\tau+1)B(\tau)\Big] \\ & * \Big(C_2(\tau)-C_1(\tau)\Big)\Big\}\Phi_2(\tau,t)\,, \end{aligned} \tag{26}$$

for $t=t_0, t_0+1, \ldots, t_1$.

Proof. From (24) and (22), the $\Psi_1(\tau)$ in (25) satisfy

$$\begin{aligned} \Psi_1(\tau) = & \Big(A(\tau)-B(\tau)C_1(\tau)\Big)^{\mathrm{T}}\Psi_1(\tau+1)\Big(A(\tau)-B(\tau)C_1(\tau)\Big) \\ & + Q(\tau) - C_1^{\mathrm{T}}(\tau)N^{\mathrm{T}}(\tau) - N(\tau)C_1(\tau) + C_1^{\mathrm{T}}(\tau)R(\tau)C_1(\tau)\,, \end{aligned} \tag{27}$$

for $\tau = t, t+1, \ldots, t_1-1$. From (27), substituting for $A(\tau)-B(\tau)C_1(\tau)$ using

$$A(\tau) - B(\tau)C_1(\tau) = A(\tau) - B(\tau)C_2(\tau) + B(\tau)\Big(C_2(\tau) - C_1(\tau)\Big)\,, \tag{28}$$

we obtain

$$\begin{aligned}
\Psi_1(\tau) = {} & \Big(A(\tau)-B(\tau)\,C_2(\tau)\Big)^{\mathrm{T}}\Psi_1(\tau+1)\Big(A(\tau)-B(\tau)\,C_2(\tau)\Big) \\
& + \Big(A(\tau)-B(\tau)\,C_2(\tau)\Big)^{\mathrm{T}}\Psi_1(\tau+1)B(\tau)\Big(C_2(\tau)-C_1(\tau)\Big) \\
& + \Big[B(\tau)\Big(C_2(\tau)-C_1(\tau)\Big)\Big]^{\mathrm{T}}\Psi_1(\tau+1)\Big(A(\tau)-B(\tau)\,C_2(\tau)\Big) \\
& + \Big[B(\tau)\Big(C_2(\tau)-C_1(\tau)\Big)\Big]^{\mathrm{T}}\Psi_1(\tau+1)B(\tau)\Big(C_2(\tau)-C_1(\tau)\Big) \\
& + Q(\tau) - C_1^{\mathrm{T}}(\tau)N^{\mathrm{T}}(\tau) - N(\tau)C_1(\tau) + C_1^{\mathrm{T}}(\tau)R(\tau)C_1(\tau)\,.
\end{aligned} \tag{29}$$

But, on the other hand, the $\Psi_2(\tau)$ in (25) satisfy

$$\begin{aligned}
\Psi_2(\tau) = {} & \Big(A(\tau)-B(\tau)\,C_2(\tau)\Big)^{\mathrm{T}}\Psi_2(\tau+1)\Big(A(\tau)-B(\tau)\,C_2(\tau)\Big) \\
& + Q(\tau) - C_2^{\mathrm{T}}(\tau)N^{\mathrm{T}}(\tau) - N(\tau)C_2(\tau) + C_2^{\mathrm{T}}(\tau)R(\tau)C_2(\tau)\,,
\end{aligned} \tag{30}$$

for $\tau = t, t+1, \ldots, t_1-1$. Subtracting (30) from (29), and using

$$\begin{aligned}
C_2^{\mathrm{T}}(\tau)R(\tau)C_2(\tau) - C_1^{\mathrm{T}}(\tau)R(\tau)C_1(\tau) = {} & \Big(C_2(\tau)-C_1(\tau)\Big)^{\mathrm{T}}R(\tau)\Big(C_2(\tau)-C_1(\tau)\Big) \\
& + \Big(C_2(\tau)-C_1(\tau)\Big)^{\mathrm{T}}R(\tau)C_1(\tau) + C_1^{\mathrm{T}}(\tau)R(\tau)\Big(C_2(\tau)-C_1(\tau)\Big)\,,
\end{aligned} \tag{31}$$

we obtain

$$\begin{aligned}
\Psi_2(\tau)-\Psi_1(\tau) = {} & \Big(A(\tau)-B(\tau)\,C_2(\tau)\Big)^{\mathrm{T}}\Big(\Psi_2(\tau+1)-\Psi_1(\tau+1)\Big)\Big(A(\tau)-B(\tau)\,C_2(\tau)\Big) \\
& + \Big(C_2(\tau)-C_1(\tau)\Big)^{\mathrm{T}}\Big[-N^{\mathrm{T}}(\tau)+R(\tau)C_1(\tau)-B^{\mathrm{T}}(\tau)\Psi_1(\tau+1)\Big(A(\tau)-B(\tau)C_2(\tau)\Big)\Big] \\
& + \Big[-N^{\mathrm{T}}(\tau)+R(\tau)C_1(\tau)-B^{\mathrm{T}}(\tau)\Psi_1(\tau+1)\Big(A(\tau)-B(\tau)C_2(\tau)\Big)\Big]^{\mathrm{T}}\Big(C_2(\tau)-C_1(\tau)\Big) \\
& + \Big(C_2(\tau)-C_1(\tau)\Big)^{\mathrm{T}}\Big[R(\tau)-B^{\mathrm{T}}(\tau)\Psi_1(\tau+1)B(\tau)\Big]\Big(C_2(\tau)-C_1(\tau)\Big)\,.
\end{aligned} \tag{32}$$

And (26) is the solution to (32) that satisfies the boundry condition $\Psi_2(t_1)-\Psi_1(t_1)=0$.

Now assume that the $C(t)$ in (5) satisfy

$$C(t) = \sum_{r=0}^{M-1} \alpha_r(t) C_r , \tag{33}$$

where M is a positive, nonzero integer less than or equal to $t_1 - t_0$, each C_r is a constant matrix, and the $\alpha_r(t)$ are scalar functions of t that satisfy

$$\alpha_p(n)\, \alpha_q(n) = \delta(p, q) . \tag{34}$$

Let

$$\overline{\Psi}(\tau) \triangleq -N^{\mathrm{T}}(\tau) + R(\tau)\, C(\tau) - B^{\mathrm{T}}(\tau)\, \Psi(\tau+1) \Big(A(\tau) - B(\tau)\, C(\tau) \Big) . \tag{35}$$

Theorem 2. If $\partial J(t_0; u(\cdot))/\partial C_r$ represents the matrix whose $(i,j)^{\text{th}}$ element contains the gradient of $J(t_0; u(\cdot))$ with respect to the $(i,j)^{\text{th}}$ element of C_r, then

$$\frac{\partial J(t_0; u(\cdot))}{\partial C_r} = \Big[\sum_{\tau=t_0}^{t_1-1} \alpha_r(\tau)\, \overline{\Psi}(\tau)\, \Phi(\tau, t_0)\, X_0\, \Phi^{\mathrm{T}}(\tau, t_0) \Big] + \Big[\sum_{\substack{\tau=t_0+1 \\ t_0 \neq t_1-1}}^{t_1-1} \sum_{\mu=t_0}^{\tau-1} \alpha_r(\tau)\, \overline{\Psi}(\tau)\, \Phi(\tau, \mu+1)\, W(\mu)\, \Phi^{\mathrm{T}}(\tau, \mu+1) \Big] , \tag{36}$$

for $r = 0, 1, \ldots, M-1$.

Proof. Let

$$C_1(t) \triangleq \sum_{i=0}^{M-1} \alpha_i(t)\, C_i \tag{37}$$

$$C_2(t) \triangleq C_1(t) + \alpha_r(t)\, \epsilon\, \Delta_r \tag{38}$$

where M, the C_i, and the $\alpha_i(t)$, are in accordance with (33) and (34), $0 \leq r \leq M-1$, ϵ is a scalar, and Δ_r is an arbitrary matrix with the dimensions of C_r.

From Theorem 1 and the properties of the expected value operator, the difference in the performance index if $u_2(t)$ is applied instead of $u_1(t)$ is

$$J(t_0; u_2(\cdot)) - J(t_0; u_1(\cdot)) = \frac{1}{2} \mathrm{tr} \Big\{ X_0 \Big(\Psi_2(t_0) - \Psi_1(t_0) \Big) + \sum_{\tau=t_0}^{t_1-1} W(\tau) \Big(\Psi_2(\tau+1) - \Psi_1(\tau+1) \Big) \Big\} , \tag{39}$$

where $\mathrm{tr}\{\cdot\}$ is the trace operator. From Lemma 1, the $\Psi_2(t)-\Psi_1(t)$ in (39) satisfy

$$\begin{aligned}\Psi_2(t)-\Psi_1(t) = \sum_{\substack{\tau=t\\ t\neq t_1}}^{t_1-1} \Phi_2^{\mathrm{T}}(\tau,t)\Big\{\Big(C_2(\tau)-C_1(\tau)\Big)^{\mathrm{T}} \\ * \Big[-N^{\mathrm{T}}(\tau)+R(\tau)C_1(\tau)-B^{\mathrm{T}}(\tau)\Psi_1(\tau+1)\Big(A(\tau)-B(\tau)C_2(\tau)\Big)\Big] \\ + \Big[-N^{\mathrm{T}}(\tau)+R(\tau)C_1(\tau)-B^{\mathrm{T}}(\tau)\Psi_1(\tau+1)\Big(A(\tau)-B(\tau)C_2(\tau)\Big)\Big]^{\mathrm{T}} \\ * \Big(C_2(\tau)-C_1(\tau)\Big) + \Big(C_2(\tau)-C_1(\tau)\Big)^{\mathrm{T}}\Big[R(\tau)-B^{\mathrm{T}}(\tau)\Psi_1(\tau+1)B(\tau)\Big] \\ * \Big(C_2(\tau)-C_1(\tau)\Big)\Big\}\Phi_2(\tau,t)\,, \qquad (40)\end{aligned}$$

for $t=t_0, t_0+1, \ldots, t_1$.

Let $(\cdot)_{ij}$ represent the operator that returns the $(i,j)^{\mathrm{th}}$ element of its matrix argument. From (20) and (21), using (37) and (38), we obtain

$$\Phi_2(\tau,t) = \Phi_1(\tau,t) - \epsilon\Big(\sum_{\substack{i=t\\ t\neq\tau}}^{\tau-1} \Phi_1(\tau,i+1)B(i)\alpha_\tau(i)\,\Delta_\tau\,\Phi_1(i,t)\Big) + \Re(\epsilon,\tau,t)\,, \qquad (41)$$

for $t=t_0, t_0+1, \ldots, t_1$ and $\tau=t, t+1, \ldots, t_1$, where $\Re(\epsilon,\tau,t)$ is a matrix all of whose elements satisfy

$$\lim_{\epsilon\to 0}\frac{(\Re(\epsilon,\tau,t))_{ij}}{\epsilon} = 0\,. \qquad (42)$$

From (40), substituting for $C_2(\tau)$ using (38) and for $\Phi_2(\tau,t)$ using (41), we obtain

$$\begin{aligned}\Psi_2(t)-\Psi_1(t) = \sum_{\substack{\tau=t\\ t\neq t_1}}^{t_1-1}\Big[\Phi_1(\tau,t) - \epsilon\Big(\sum_{\substack{i=t\\ t\neq\tau}}^{\tau-1}\Phi_1(\tau,i+1)B(i)\alpha_\tau(i)\,\Delta_\tau\,\Phi_1(i,t)\Big) \\ + \Re(\epsilon,\tau,t)\Big]^{\mathrm{T}}\Big\{\Big(\alpha_\tau(\tau)\epsilon\,\Delta_\tau\Big)^{\mathrm{T}}\Big[-N^{\mathrm{T}}(\tau)+R(\tau)C_1(\tau)-B^{\mathrm{T}}(\tau)\Psi_1(\tau+1) \\ * \Big(A(\tau)-B(\tau)(C_1(\tau)+\alpha_\tau(\tau)\epsilon\,\Delta_\tau\Big)\Big] + \Big[-N^{\mathrm{T}}(\tau)+R(\tau)C_1(\tau) \\ - B^{\mathrm{T}}(\tau)\Psi_1(\tau+1)\Big(A(\tau)-B(\tau)(C_1(\tau)+\alpha_\tau(\tau)\epsilon\,\Delta_\tau\Big)\Big]^{\mathrm{T}}\Big(\alpha_\tau(\tau)\epsilon\,\Delta_\tau\Big) \\ + \Big(\alpha_\tau(\tau)\epsilon\,\Delta_\tau\Big)^{\mathrm{T}}\Big[R(\tau)-B^{\mathrm{T}}(\tau)\Psi_1(\tau+1)B(\tau)\Big]\Big(\alpha_\tau(\tau)\epsilon\,\Delta_\tau\Big)\Big\} \\ + \Big[\Phi_1(\tau,t) - \epsilon\Big(\sum_{\substack{i=t\\ t\neq\tau}}^{\tau-1}\Phi_1(\tau,i+1)B(i)\alpha_\tau(i)\,\Delta_\tau\,\Phi_1(i,t)\Big) + \Re(\epsilon,\tau,t)\Big]\,, \qquad (43)\end{aligned}$$

for $t=t_0, t_0+1, \ldots, t_1$. From (43), combining terms of second and higher order in ϵ, we obtain

$$\begin{aligned}\Psi_2(t)-\Psi_1(t) = \Big[\sum_{\substack{\tau=t\\ t\neq t_1}}^{t_1-1} \Phi_1^{\mathrm{T}}(\tau,t)\Big\{\Big(\alpha_r(\tau)\epsilon\,\Delta_r\Big)^{\mathrm{T}} \\ * \Big[-N^{\mathrm{T}}(\tau)+R(\tau)C_1(\tau)-B^{\mathrm{T}}(\tau)\Psi_1(\tau+1)\Big(A(\tau)-B(\tau)\,C_1(\tau)\Big) \\ + \Big[-N^{\mathrm{T}}(\tau)+R(\tau)C_1(\tau)-B^{\mathrm{T}}(\tau)\Psi_1(\tau+1)\Big(A(\tau)-B(\tau)\,C_1(\tau)\Big)^{\mathrm{T}} \\ * \Big(\alpha_r(\tau)\epsilon\,\Delta_r\Big)\Big\}\Phi_1(\tau,t)\Big] + \Re(\epsilon,t)\,, \end{aligned} \tag{44}$$

for $t=t_0, t_0+1, \ldots, t_1$, where $\Re(\epsilon,t)$ is a matrix all of whose elements satisfy

$$\lim_{\epsilon\to 0}\frac{(\Re(\epsilon,t))_{ij}}{\epsilon}=0\,. \tag{45}$$

Letting

$$\overline{\Psi}_1(\tau)\triangleq -N^{\mathrm{T}}(\tau)+R(\tau)C_1(\tau)-B^{\mathrm{T}}(\tau)\Psi_1(\tau+1)\Big(A(\tau)-B(\tau)C_1(\tau)\Big)\,, \tag{46}$$

(44) can be written

$$\begin{aligned}\Psi_2(t)-\Psi_1(t) = \epsilon\Big[\sum_{\substack{\tau=t\\ t\neq t_1}}^{t_1-1}\alpha_r(\tau)\Phi_1^{\mathrm{T}}(\tau,t)\Big\{\Delta_r^{\mathrm{T}}\,\overline{\Psi}_1(\tau)+\overline{\Psi}_1^{\mathrm{T}}(\tau)\,\Delta_r\Big\}\Phi_1(\tau,t)\Big] \\ +\Re(\epsilon,t)\,,\end{aligned} \tag{47}$$

for $t=t_0, t_0+1, \ldots, t_1$.

From (39), substituting for $\Psi_2(t_0)-\Psi_1(t_0)$ and $\Psi_2(\tau+1)-\Psi_1(\tau+1)$ using (23), we obtain

$$\begin{aligned}J(t_0;u_2(\cdot))-J(t_0;u_1(\cdot)) = \frac{1}{2}\mathrm{tr}\Big\{\mathrm{X}_0\Big(\epsilon\Big[\sum_{\tau=t_0}^{t_1-1}\alpha_r(\tau)\Phi_1^{\mathrm{T}}(\tau,t_0) \\ * \Big\{\Delta_r^{\mathrm{T}}\,\overline{\Psi}_1(\tau)+\overline{\Psi}_1^{\mathrm{T}}(\tau)\,\Delta_r\Big\}\Phi_1(\tau,t_0)\Big]+\Re(\epsilon,t_0)\Big) \\ +\sum_{\mu=t_0}^{t_1-1}W(\mu)\Big(\epsilon\Big[\sum_{\substack{\tau=\mu+1\\ \mu\neq t_1-1}}^{t_1-1}\alpha_r(\tau)\Phi_1^{\mathrm{T}}(\tau,\mu+1) \\ * \Big\{\Delta_r^{\mathrm{T}}\,\overline{\Psi}_1(\tau)+\overline{\Psi}_1^{\mathrm{T}}(\tau)\,\Delta_r\Big\}\Phi_1(\tau,\mu+1)\Big]+\Re(\epsilon,\mu+1)\Big)\Big\}\,.\end{aligned} \tag{48}$$

From (48), substituting for the double summation using

$$\sum_{\mu=t_0}^{t_1-1}\sum_{\substack{\tau=\mu+1\\ \mu\neq t_1-1}}^{t_1-1} f(\tau,\mu) = \sum_{\substack{\tau=t_0+1\\ t_0\neq t_1-1}}^{t_1-1}\sum_{\mu=t_0}^{\tau-1} f(\tau,\mu)\,, \tag{49}$$

and using the properties of the trace operator, and combining terms of second and higher order in ϵ, we obtain

$$J(t_0;u_2(\cdot))-J(t_0;u_1(\cdot)) = \mathrm{tr}\Big\{\epsilon\Big(\Big[\sum_{\tau=t_0}^{t_1-1}\alpha_r(\tau)\Phi_1(\tau,t_0)X_0\Phi_1^{\mathrm{T}}(\tau,t_0)\overline{\Psi}_1^{\mathrm{T}}(\tau)\Big]$$
$$+\Big[\sum_{\substack{\tau=t_0+1\\ t_0\neq t_1-1}}^{t_1-1}\sum_{\mu=t_0}^{\tau-1}\alpha_r(\tau)\Phi_1(\tau,\mu+1)W(\mu)\Phi_1^{\mathrm{T}}(\tau,\mu+1)\overline{\Psi}_1^{\mathrm{T}}(\tau)\Big]\Big)\Delta_r+\Re(\epsilon)\Big\}, \tag{50}$$

where $\Re(\epsilon)$ is a matrix all of whose elements satisfy

$$\lim_{\epsilon\to 0}\frac{(\Re(\epsilon))_{ij}}{\epsilon}=0\,. \tag{51}$$

Equation (50) is of the form

$$J(t_0;u_2(\cdot))-J(t_0;u_1(\cdot)) = \mathrm{tr}\Big\{\epsilon\,\mathrm{K}\,\Delta_r+\Re(\epsilon)\Big\}\,, \tag{52}$$

where

$$K \triangleq \Big(\sum_{\tau=t_0}^{t_1-1}\alpha_r(\tau)\Phi_1(\tau,t_0)X_0\Phi_1^{\mathrm{T}}(\tau,t_0)\overline{\Psi}_1^{\mathrm{T}}(\tau)\Big)$$
$$+\Big(\sum_{\substack{\tau=t_0+1\\ t_0\neq t_1-1}}^{t_1-1}\sum_{\mu=t_0}^{\tau-1}\alpha_r(\tau)\Phi_1(\tau,\mu+1)W(\mu)\Phi_1^{\mathrm{T}}(\tau,\mu+1)\overline{\Psi}_1^{\mathrm{T}}(\tau)\Big)\,, \tag{53}$$

and it is easy to show (let Δ_r be a matrix of zeros except for a one at position i-j, then take the limit in (52) as $\epsilon\to 0$) that

$$\frac{\partial J(t_0;u_1(\cdot))}{\partial C_r} = K^{\mathrm{T}}$$
$$=\Big(\sum_{\tau=t_0}^{t_1-1}\alpha_r(\tau)\overline{\Psi}_1(\tau)\Phi_1(\tau,t_0)X_0\Phi_1^{\mathrm{T}}(\tau,t_0)\Big)$$
$$+\Big(\sum_{\substack{\tau=t_0+1\\ t_0\neq t_1}}^{t_1-1}\sum_{\mu=t_0}^{\tau-1}\alpha_r(\tau)\overline{\Psi}_1(\tau)\Phi_1(\tau,\mu+1)W(\mu)\Phi_1^{\mathrm{T}}(\tau,\mu+1)\Big)\,, \tag{54}$$

for $r=0,\,1,\,\ldots,\,M-1$.

Appendix C

User's Guide to AMS

The three phases of AMS execution are: (1) input, (2) optimization, and (3) output. A summary of the three phases and a description of all input and output data formats are presented in the following sections. For further information, a listing of the AMS Fortran program will be furnished upon request.

§C.1 Optimization Phase of Execution. The optimization phase of AMS execution consists of a series of iterations to determine a set of feedback gains that minimizes the discrete performance index. An iteration consists of a linear search and a subsequent step in the linear search direction. For each iteration, the linear search direction is determined based on the value of the performance index, the gradient of the performance index with respect to the feedback gains, and the approximate Hessian matrix (which contains second derivative information). The linear search determines a step length that yields a set of feedback gains that approximately minimizes the performance index. The step is executed and the values for the feedback gains, performance index, gradient, and approximate Hessian matrix are updated to complete the iteration.

The iterations continue until the normalized gradient with respect to every

feedback gain element is less that or equal to the specified tolerance *TOL*. Specifically, if $J(NN)$ represents the performance index and $FGM(r)_{ij}$ represents a feedback gain element, then convergence is assumed when

$$\frac{\partial J(NN)/J(NN)}{\partial (FGM(r))_{ij}/(FGM(r))_{ij}} \leq TOL\,, \tag{1}$$

for every feedback gain element $(FGM(r))_{ij}$.

The parameters for the optimization phase fall into five catagories: (1) the parameters that regulate the numerical search; (2) the state model description of the plant; (3) the constraints on and the initial guess for the state feedback gains; (4) the finite time for and the weighting matrices for the performance index; (5) the parameters associated with the initial guess for the approximate Hessian matrix.

The parameters that regulate the numerical search are:

NITRMX: The upper bound for the number of iterations.

TOL: The tolerance parameter in (1).

COST: The estimated lower bound for the value of the performance index.

STEPMX: The upper bound for the step length for any linear search step.

The state model description of the plant is

$$x(m,n+1) = ASM(n)\,x(m,n) + BSM(n)\,u(m,n) + w(m,n)\,, \tag{2}$$

for $m=0,\ 1,\ \ldots$ and $n=1,\ 2,\ \ldots,\ TT$, where $x(m,n)$ is the IX-by-1 state vector, $u(m,n)$ is the IU-by-1 control input vector, $w(m,n)$ is the IX-by-1 process noise input vector, and each $ASM(n)$ and $BSM(n)$ is a constant matrix. To simplify the programming, we avoided the $TT=1$ case so that TT must be at least 2*.

* The $TT = 1$ case represents SR sampling. A SR sampling policy is easily accommodated, however, by setting $TT=2$ and stipulating that all control inputs are sampled at every STP.

The state feedback control law is

$$u(m,n) = -C(n)\,x(m,n)\,, \tag{3}$$

where each $C(n)$ is a constant matrix. Each $C(n)$ is constrained to satisfy

$$C(n) = \sum_{r=1}^{MM} \Big(ALPHA\Big)_{nr} * FGM(r)\,, \tag{4}$$

where MM is a positive, nonzero integer less than or equal to TT, $(ALPHA)_{ij}$ is the (i,j)th element of the matrix $ALPHA$ all the elements of which are either 1 or 0, and each $FGM(r)$ is a constant matrix.

The elements of the $FGM(r)$ are the independent variables for the optimization. The (i,j)th element of $FGM(r)$ is unconstrained or constrained to be fixed depending upon whether the (i,j)th element of the matrix $NOGRDF(r)$ is 1 or 0, respectively.

The process noise vector $w(m,n)$ is assumed to be a periodically stationary, zero-mean, gaussian, purely random sequence with covariance $GWG(n)$, so that

$$\mathrm{E}\{w(m,n)\,w^{\mathrm{T}}(k,l)\} = GWG(n) * \delta(mTT+n, kTT+l)\,, \tag{5}$$

where

$$\delta(i,j) \triangleq \begin{cases} 1 & \text{if } i = j\,; \\ 0 & \text{if } i \neq j\,. \end{cases} \tag{6}$$

The performance index is

$$J(NN) \triangleq \sum_{m=0}^{NN-1} \sum_{n=1}^{TT} \begin{bmatrix} x(m,n) \\ u(m,n) \end{bmatrix}^{\mathrm{T}} \begin{bmatrix} QCST(n) & NCST(n) \\ NCST^{\mathrm{T}}(n) & RCST(n) \end{bmatrix} \begin{bmatrix} x(m,n) \\ u(m,n) \end{bmatrix}. \tag{7}$$

where NN is a positive, nonzero integer, and each $QCST(n)$, $NCST(n)$, and $RCST(n)$ is a constant matrix. To simplify the programming, we avoided the $NN = 1$ case so that NN must be at least 2.

The approximate Hessian matrix is stored in a factored form in the two vectors *HESS* and *HESFAC*. At the end of every run, *HESS* and *HESFAC* are saved on a

disk file so that they can be used as the initial guess for the approximate Hessian matrix in a subsequent run. The parameters for the optimization phase that are associated with the approximate Hessian matrix are:

HESFLG: The logical parameter that indicates whether an initial guess for the approximate Hessian matrix is available. If *HESFLG* is true, *HESS* and *HESFAC* are used as the approximate Hessian matrix for the first iteration. If *HESFLG* is false, an identity matrix is used as the approximate Hessian matrix (i.e., a steepest decent search algorithm is used) for the first iteration.

HESS: The lower triangular factor of the cholesky factorization of the approximate Hessian matrix, stored as an $(N*(N-1)/2)$-by-1 vector, where $N \triangleq IU*IX*MM$.

HESFAC: The diagonal elements of the diagonal factor of the cholesky factorization of the approximate Hessian matrix, stored as an N-by-1 vector, where $N \triangleq IU*IX*MM$.

On the AMS Output File, the first section of printout from the optimization phase of execution is a simple echo of the parameters for the optimization phase. This is followed by the printout from the numerical search. The printout from each iteration gives the status of the numerical search immediately *before* the linear search step for that iteration is taken. This status is indicated by the values of the following variables:

FGM(r): The rth feedback gain matrix, for $r=1, 2, \ldots, MM$.

GRDF(r): The gradient of the performance index $J(NN)$ with respect to *FGM*(r), for $r=1, 2, \ldots, MM$.

GNORM(r): The normalized gradient of the performance index $J(NN)$ with respect to *FGM*(r), for $r=1, 2, \ldots, MM$. The (i,j)th element of *GNORM*(r) contains the quantity on the left hand side of (1).

CONVERGENCE PARAMETER: The absolute value of the largest (in an absolute value sense) single element of $GNORM(r)$, for $r = 1, 2, \ldots, MM$. This value is compared with the value of *TOL* after each iteration to determine whether convergence as defined in (1) has occurred.

NUMBER OF COST EVALUATIONS: The number of performance index evaluations for the iteration.

NUMBER OF GRADIENT EVALUATIONS: The number of gradient evaluations for the iteration.

LINEAR SEARCH STEP SIZE: The step size for the linear search step for the iteration.

PERCENT COST REDUCTION: The percent reduction in the value of the performance index for the iteration.

The last section of the printout from the optimization phase shows the final statistics for the optimization. This includes a table of the final closed-loop BTP poles.

Example AMS Input, Output, and Save Files are included at the end of this appendix. These files are from a final AMS run for the Case 1 MR compensator of Chapter 6. The printout from the optimization phase of execution begins on page 7 of the example output file.

§C.2 Input Phase of Execution. The sole purpose of the input phase of execution is to establish the values for the parameters for the optimization phase. The parameters that regulate the numerical search, the constraints on and the initial guess for the state feedback control law, the finite time for the performance index, and the parameters associated with the approximate Hessian matrix are read directly from the AMS Input File. The discrete state model description of the plant and the weighting matrices for the discrete performance index are generated

by discretizing the analog state model description of the plant and the analog performance index.

The analog state model description of the plant is

$$\dot{p}(t) = F\,p(t) + GU\,u(t) + GW\,w(t)\,, \tag{8}$$

where $p(t)$ is the *IXA*-by-1 state vector, $u(t)$ is the *IUA*-by-1 control input vector, $w(t)$ is the *IWA*-by-1 process noise input vector, and F, GU, and GW are constant matrices. The initial state $p(0)$ is assumed to be zero.

The process noise vector $w(t)$ is assumed to be stationary, zero-mean, gaussian, white noise of intensity *WA*, so that

$$\mathrm{E}\{w(t)\,w^{\mathrm{T}}(\tau)\} = WA * \delta(t-\tau)\,, \tag{9}$$

where $\delta(t)$ is the Dirac delta function.

The STP (shortest time period) for the sampling policy is *TSEC*, in seconds, and *TT* is the integer number of STPs per BTP (basic time period) for the sampling policy. To simplify the programming, we avoided the $TT = 1$ case so that *TT* must be at least 2*.

The analog control input vector $u(t)$ is assumed to be partitioned so that

$$u(t) = \begin{bmatrix} u_1(t) \\ u_2(t) \end{bmatrix}, \tag{10}$$

where $u_1(t)$ is the *IU*1-by-1 vector that includes all control inputs that are not sampled at every STP, and $u_2(t)$ it the *IU*2-by-1 vector that includes all control inputs that are sampled at every STP. The sampling schedules for the elements of $u_1(t)$ are defined by the *TT*-by-*IU*1 switching matrix *STBL*. The (i,j)th element of

* The $TT = 1$ case represents SR sampling. A SR sampling policy is easily accommodated, however, by setting $TT = 2$ and stipulating that all control inputs are sampled at every STP.

STBL is 1 or 0 depending upon whether the jth element of $u_1(t)$ is sampled and held or just held, respectively, at the start of the ith STP in a BTP.

The analog performance index is

$$\tilde{J}(NN) = \mathrm{E}\left\{\int_0^{NN*TT*TSEC} \begin{bmatrix} p(t) \\ u(t) \end{bmatrix}^{\mathrm{T}} \begin{bmatrix} QA & 0 \\ 0 & RA \end{bmatrix} \begin{bmatrix} p(t) \\ u(t) \end{bmatrix} dt\right\}, \tag{11}$$

where *NN* is a nonzero, positive integer, and *QA* and *RA* are constant matrices. To simplify the programming, we avoided the $NN = 1$ case so that *NN* must be at least 2.

In addition to accommodating standard discretizations of an analog plant and an analog performance index, the AMS program is designed so that partitions can be added to the coefficient matrices for the discrete state model, the covariance matrices for the discrete process noise, and the weighting matrices for the discrete performance index. Such partitions can be used to model the interactions between the analog plant and a dynamic compensator, so that compensators of arbitrary structure and dynamic order can be synthesized.

For the input phase of execution, the state vector $x(m,n)$ for the discrete state model in (2) is partitioned so that

$$x(m,n) = \begin{bmatrix} p(m,n) \\ h(m,n) \\ c(m,n) \end{bmatrix}, \tag{12}$$

where $p(m,n)$ is an *IXA*-by-1 vector, $h(m,n)$ is an *IU*1-by-1 vector, and $c(m,n)$ is an *IXC*-by-1 vector. Similarly, the control input input vector $u(m,n)$ for the discrete state model is partitioned so that

$$u(m,n) = \begin{bmatrix} u_1(m,n) \\ u_2(m,n) \\ u_c(m,n) \end{bmatrix}, \tag{13}$$

where $u_1(m,n)$ is an *IU*1-by-1 vector, $u_2(m,n)$ is an *IU*2-by-1 vector, and $u_c(m,n)$ is an *IUC*-by-1 vector.

In (12), the vector $p(m,n)$ represents the state vector $p(t)$ of the analog plant in (8) at the $(mTT+n)$th sampling instant. The vector $h(m,n)$ is the state vector of zero-order hold states for the $u_1(m,n)$ controls in (13), so that $h(m,n)$ represents the analog control input vector $u_1(t)$ in (10) at the $(mTT+n)$th sampling instant. The vector $c(m,n)$ is the state vector for the dynamic compensator at the $(mTT+n)$th sampling instant.

In (13), the vector $u_1(m,n)$ is the discrete control input vector that effects the state vector $h(m,n)$ in (12). The vector $u_2(m,n)$ represents the analog control input vector $u_2(t)$ in (10) at the $(mTT+n)$th sampling instant. The vector $u_c(m,n)$ is the discrete control input vector that effects the state vector $c(m,n)$ in (12).

Let $IU \triangleq IU1+IU2+IUC$. Let $IX \triangleq IXA+IU1+IXC$. For the input phase of execution, each coefficient matrix $ASM(n)$ for the discrete state model in (2) is partitioned so that

$$ASM(n) = \begin{bmatrix} ASMP(n) \\ ASMH(n) \\ ASMC(n) \end{bmatrix}, \tag{14}$$

where $ASMP(n)$ is an IXA-by-IX constant matrix, $ASMH(n)$ is an IXH-by-IX constant matrix, and $ASMC(n)$ is an IXC-by-IX constant matrix. Similarly, each coefficient matrix $BSM(n)$ for the discrete state model is partitioned so that

$$BSM(n) = \begin{bmatrix} BSMP(n) & 0 \\ BSMH(n) & 0 \\ 0 & BSMC(n) \end{bmatrix}, \tag{15}$$

where $BSMP(n)$ is an IXA-by-IUA constant matrix, $BSMH(n)$ is an IXH-by-IUA constant matrix, and $BSMC(n)$ is an IXC-by-IUC constant matrix.

The $ASMC(n)$ partition of each $ASM(n)$ and the $BSMC(n)$ partition of each $BSM(n)$ are read directly from the AMS Input File. The $ASMP(n)$ and $ASMH(n)$ partitions of each $ASM(n)$ and the $BSMP(n)$ and $BSMH(n)$ partitions of each $BSM(n)$ are generated automatically, given the coefficient matrices for the analog

state model, and the sampling policy as defined by the parameters *TSEC*, *TT*, and *STBL*.

The weighting matrices $QCST(n)$, $NCST(n)$, and $RCST(n)$, for $n=1,2,\ldots,TT$, for the discrete performance index are generated automatically, with all partitions involving $c(m,n)$ and $u_c(m,n)$ set to zero, given the coefficient matrices for the analog state model, the weighting matrices for the analog performance index, and the sampling policy.

Finally, each covariance matrix $GWG(n)$ for the discrete process noise is generated automatically, with all partitions involving $c(m,n)$ set to zero, given the coefficient matrices for the analog state model, the intensity matrix for the analog process noise, and the sampling policy.

Table C.1 Format for the AMS Input File.

Parameter	Type	Range	Format
NN	Integer	≥ 2	(2I13,3D13.5,L13)
NITRMX	Integer	≥ 0	
TOL	Real	≥ 0	
COST	Real	≥ 0	
STEPMX	Real	> 0	
HESFLG	Logical	—	
IXA	Integer	≥ 1	(8I3)
IXC	Integer	≥ 0	
IU1	Integer	≥ 0	
IU2	Integer	≥ 0	
IUC	Integer	≥ 0	
IWA	Integer	≥ 1	
TT	Integer	≥ 2	
MM	Integer	≥ 1	
TSEC	Real	> 0	(D13.5)

The format for the AMS Input File is given in Tables A.1 and A.2. The parameters in these tables are read in the given order, using the indicated Fortran

formats. All matrices are read by rows, with each row starting on a new line. The elements of each of the vectors *HESFAC* and *HESS* are read consecutively, six elements per line.

Table C.2 Format for the AMS Input File Continued.

Parameter	Type	Dimensions	Format
F	Real	*IXA*-by-*IXA*	(6D13.5)
GU	Real	*IXA*-by-*IUA*	(6D13.5)
GW	Real	*IXA*-by-*IWA*	(6D13.5)
WA	Real	*IWA*-by-*IWA*	(6D13.5)
QA	Real	*IXA*-by-*IXA*	(6D13.5)
RA	Real	*IUA*-by-*IUA*	(6D13.5)
ASMC(1)	Real	*IXC*-by-*IX*	(6D13.5)
⋮	⋮	⋮	⋮
ASMC(*TT*)	Real	*IXC*-by-*IX*	(6D13.5)
BSMC(1)	Real	*IXC*-by-*IUC*	(6D13.5)
⋮	⋮	⋮	⋮
BSMC(*TT*)	Real	*IXC*-by-*IUC*	(6D13.5)
STBL	Integer	*TT*-by-*IU*1	(50I2)
ALPHA	Integer	*TT*-by-*MM*	(50I2)
FGM(1)	Real	*IU*-by-*IX*	(6D13.5)
⋮	⋮	⋮	⋮
FGM(*TT*)	Real	*IU*-by-*IX*	(6D13.5)
NOGRDF(1)	Integer	*IU*-by-*IX*	(50I2)
⋮	⋮	⋮	⋮
NOGRDF(*TT*)	Integer	*IU*-by-*IX*	(50I2)
HESFAC	Real	N*-by-1	(6D13.5)
HESS	Real	$(N*(N-1))$-by-1*	(6D13.5)

Column 3 of Table A.1 lists the restrictions on the dimension parameters. The

* $N \triangleq IU*IX*MM$.

AMS Main Program uses these dimensions to automatically allocate storage space for all parameters and work space for all calculations in a single vector Z. The vector Z is currently dimensioned at 20000 elements. This dimension of will have to be increased to accommodate problems with dimensions substantially larger than those of the example design problems of Chapters 5 and 6.

The printout from the input phase of execution consists of a simple echo of most of the data read from the AMS Input File. On the AMS Output File at the end of this appendix, this printout starts on page 1.

§C.3 Output Phase of Execution. The sole purpose of the output phase of execution is to save the final values for the feedback gains and the approximate Hessian matrix so that they can be used as the initial guess for these variables in a subsequent run. During the output phase, the final values for $FGM(r)$, for $r = 1, 2, \ldots, MM$, and for *HESFAC* and *HESS* are written to the AMS Save File. The format for this file is given in Table A.3. All matrices are written by rows, with each row starting on a new line. The elements of each of the vectors *HESFAC* and *HESS* are written consecutively, six elements per line.

Table C.3 Format for the AMS Save File.

Parameter	Type	Dimensions	Format
$FGM(1)$	Real	IU-by-IX	(1P6D13.5)
⋮	⋮	⋮	⋮
$FGM(TT)$	Real	IU-by-IX	(1P6D13.5)
HESFAC	Real	N*-by-1	(1P6D13.5)
HESS	Real	$(N*(N-1))$-by-1*	(1P6D13.5)

A copy of the AMS Save File from the example AMS run discussed above is included at the end of this appendix.

* $N \triangleq IU*IX*MM$.

Page 1 of Example AMS Input File

```
        10000           10  1.00000D-05  0.00000D+00  1.00000D+01            F
 4  2  2  1  2  2  8  1
 2.81250D-02
 0.00000D+00  1.00000D+00  0.00000D+00  0.00000D+00
 0.00000D+00  0.00000D+00  0.00000D+00  0.00000D+00
 0.00000D+00  0.00000D+00  0.00000D+00  1.00000D+00
 0.00000D+00  0.00000D+00  0.00000D+00  0.00000D+00
 0.00000D+00  0.00000D+00  0.00000D+00
 2.36841D+00 -2.29340D+01 -2.29340D+01
 0.00000D+00  0.00000D+00  0.00000D+00
-1.14276D+00  1.21587D+02  1.21587D+02
 0.00000D+00  0.00000D+00
 2.36841D+00 -2.29340D+01
 0.00000D+00  0.00000D+00
-1.14276D+00  1.21587D+02
 6.94440D-01  0.00000D+00
 0.00000D+00  1.00000D-02
 2.10000D-01  0.00000D+00  0.00000D+00  0.00000D+00
 0.00000D+00  0.00000D+00  0.00000D+00  0.00000D+00
 0.00000D+00  0.00000D+00  1.85000D+01  0.00000D+00
 0.00000D+00  0.00000D+00  0.00000D+00  0.00000D+00
 1.00000D-02  0.00000D+00  0.00000D+00
 0.00000D+00  6.94440D-01  6.94440D-01
 0.00000D+00  6.94440D-01  6.94440D-01
 1.00000D+00  0.00000D+00  0.00000D+00  0.00000D+00  0.00000D+00  0.00000D+00
 0.00000D+00  0.00000D+00
 0.00000D+00  0.00000D+00  1.00000D+00  0.00000D+00  0.00000D+00  0.00000D+00
 0.00000D+00  0.00000D+00
 0.00000D+00  0.00000D+00  0.00000D+00  0.00000D+00  0.00000D+00  0.00000D+00
 1.00000D+00  0.00000D+00
 0.00000D+00  0.00000D+00  1.00000D+00  0.00000D+00  0.00000D+00  0.00000D+00
 0.00000D+00  0.00000D+00
 0.00000D+00  0.00000D+00  0.00000D+00  0.00000D+00  0.00000D+00  0.00000D+00
 1.00000D+00  0.00000D+00
 0.00000D+00  0.00000D+00  1.00000D+00  0.00000D+00  0.00000D+00  0.00000D+00
 0.00000D+00  0.00000D+00
 0.00000D+00  0.00000D+00  0.00000D+00  0.00000D+00  0.00000D+00  0.00000D+00
 1.00000D+00  0.00000D+00
 0.00000D+00  0.00000D+00  1.00000D+00  0.00000D+00  0.00000D+00  0.00000D+00
 0.00000D+00  0.00000D+00
 0.00000D+00  0.00000D+00  0.00000D+00  0.00000D+00  0.00000D+00  0.00000D+00
 1.00000D+00  0.00000D+00
 0.00000D+00  0.00000D+00  1.00000D+00  0.00000D+00  0.00000D+00  0.00000D+00
 0.00000D+00  0.00000D+00
 0.00000D+00  0.00000D+00  0.00000D+00  0.00000D+00  0.00000D+00  0.00000D+00
 1.00000D+00  0.00000D+00
```

Page 2 of Example AMS Input File

```
 0.00000D+00  0.00000D+00  1.00000D+00  0.00000D+00  0.00000D+00  0.00000D+00
 0.00000D+00  0.00000D+00
 0.00000D+00  0.00000D+00  0.00000D+00  0.00000D+00  0.00000D+00  0.00000D+00
 1.00000D+00  0.00000D+00
 0.00000D+00  0.00000D+00  1.00000D+00  0.00000D+00  0.00000D+00  0.00000D+00
 0.00000D+00  0.00000D+00
 0.00000D+00  0.00000D+00  0.00000D+00  0.00000D+00  0.00000D+00  0.00000D+00
 1.00000D+00  0.00000D+00
 0.00000D+00  0.00000D+00  1.00000D+00  0.00000D+00  0.00000D+00  0.00000D+00
 0.00000D+00  0.00000D+00
 1.00000D+00  0.00000D+00
 0.00000D+00  1.00000D+00
 0.00000D+00  0.00000D+00
 0.00000D+00  1.00000D+00
 0.00000D+00  0.00000D+00
 0.00000D+00  1.00000D+00
 0.00000D+00  0.00000D+00
 0.00000D+00  1.00000D+00
 0.00000D+00  0.00000D+00
 0.00000D+00  1.00000D+00
 0.00000D+00  0.00000D+00
 0.00000D+00  1.00000D+00
 0.00000D+00  0.00000D+00
 0.00000D+00  1.00000D+00
 0.00000D+00  0.00000D+00
 0.00000D+00  1.00000D+00
1 1
0 0
0 0
0 0
0 0
0 0
0 0
0 0
1
1
1
1
1
1
1
1
1
 1.12974D+01  0.00000D+00  3.93156D-01  0.00000D+00  0.00000D+00  0.00000D+00
-1.34829D+01  1.07079D+00
 9.76319D-02  0.00000D+00  0.00000D+00  0.00000D+00  0.00000D+00  0.00000D+00
-1.21290D-01  0.00000D+00
```

Page 3 of Example AMS Input File

```
 0.00000D+00  0.00000D+00  1.34390D+01  0.00000D+00  0.00000D+00  0.00000D+00
 0.00000D+00 -1.68650D+01
 0.00000D+00  0.00000D+00  0.00000D+00  0.00000D+00  0.00000D+00  0.00000D+00
 4.84992D-01  0.00000D+00
 0.00000D+00  0.00000D+00  0.00000D+00  0.00000D+00  0.00000D+00  0.00000D+00
 0.00000D+00  5.53272D-01
 1 0 1 1 0 0 0 1 1 1
 1 1 0 0 1 0 0 0 1 0
 1 0 0 0 1 0 0 0 0 1
 0 0 0 0 0 0 0 0 0 0
```

Page 1 of Example AMS Output File

```
INPUT ANALOG MODEL AND OTHER PARAMETERS
---------------------------------------
IX= 8
IXA= 4
IXC= 2
IU= 5
IU1= 2
IU2= 1
IUC= 2
IWA= 2
TT= 8
MM= 1
TSEC=  2.81250D-02

F MATRIX

          1           2           3           4
1   0.0000D+00  1.0000D+00  0.0000D+00  0.0000D+00
2   0.0000D+00  0.0000D+00  0.0000D+00  0.0000D+00
3   0.0000D+00  0.0000D+00  0.0000D+00  1.0000D+00
4   0.0000D+00  0.0000D+00  0.0000D+00  0.0000D+00

GU MATRIX

          1           2           3
1   0.0000D+00  0.0000D+00  0.0000D+00
2   2.3684D+00 -2.2934D+01 -2.2934D+01
3   0.0000D+00  0.0000D+00  0.0000D+00
4  -1.1428D+00  1.2159D+02  1.2159D+02

GW MATRIX

          1           2
1   0.0000D+00  0.0000D+00
2   2.3684D+00 -2.2934D+01
3   0.0000D+00  0.0000D+00
4  -1.1428D+00  1.2159D+02
```

Page 2 of Example AMS Output File

WA MATRIX

	1	2
1	6.9444D-01	0.0000D+00
2	0.0000D+00	1.0000D-02

QA MATRIX

	1	2	3	4
1	2.1000D-01	0.0000D+00	0.0000D+00	0.0000D+00
2	0.0000D+00	0.0000D+00	0.0000D+00	0.0000D+00
3	0.0000D+00	0.0000D+00	1.8500D+01	0.0000D+00
4	0.0000D+00	0.0000D+00	0.0000D+00	0.0000D+00

RA MATRIX

	1	2	3
1	1.0000D-02	0.0000D+00	0.0000D+00
2	0.0000D+00	6.9444D-01	6.9444D-01
3	0.0000D+00	6.9444D-01	6.9444D-01

ASMC(1)

	1	2	3	4	5	6	7	8
1	1.0000D+00	0.0000D+00	0.0000D+00	0.0000D+00	0.0000D+00	0.0000D+00	0.0000D+00	0.0000D+00
2	0.0000D+00	0.0000D+00	1.0000D+00	0.0000D+00	0.0000D+00	0.0000D+00	0.0000D+00	0.0000D+00

ASMC(2)

	1	2	3	4	5	6	7	8
1	0.0000D+00	0.0000D+00	0.0000D+00	0.0000D+00	0.0000D+00	0.0000D+00	1.0000D+00	0.0000D+00
2	0.0000D+00	0.0000D+00	1.0000D+00	0.0000D+00	0.0000D+00	0.0000D+00	0.0000D+00	0.0000D+00

ASMC(3)

	1	2	3	4	5	6	7	8
1	0.0000D+00	0.0000D+00	0.0000D+00	0.0000D+00	0.0000D+00	0.0000D+00	1.0000D+00	0.0000D+00

Page 3 of Example AMS Output File

```
      2    0.0000D+00  0.0000D+00  1.0000D+00  0.0000D+00  0.0000D+00  0.0000D+00  0.0000D+00  0.0000D+00

ASMC( 4)

                1           2           3           4           5           6           7           8
      1  0.0000D+00  0.0000D+00  0.0000D+00  0.0000D+00  0.0000D+00  0.0000D+00  1.0000D+00  0.0000D+00
      2  0.0000D+00  0.0000D+00  1.0000D+00  0.0000D+00  0.0000D+00  0.0000D+00  0.0000D+00  0.0000D+00

ASMC( 5)

                1           2           3           4           5           6           7           8
      1  0.0000D+00  0.0000D+00  0.0000D+00  0.0000D+00  0.0000D+00  0.0000D+00  1.0000D+00  0.0000D+00
      2  0.0000D+00  0.0000D+00  1.0000D+00  0.0000D+00  0.0000D+00  0.0000D+00  0.0000D+00  0.0000D+00

ASMC( 6)

                1           2           3           4           5           6           7           8
      1  0.0000D+00  0.0000D+00  0.0000D+00  0.0000D+00  0.0000D+00  0.0000D+00  1.0000D+00  0.0000D+00
      2  0.0000D+00  0.0000D+00  1.0000D+00  0.0000D+00  0.0000D+00  0.0000D+00  0.0000D+00  0.0000D+00

ASMC( 7)

                1           2           3           4           5           6           7           8
      1  0.0000D+00  0.0000D+00  0.0000D+00  0.0000D+00  0.0000D+00  0.0000D+00  1.0000D+00  0.0000D+00
      2  0.0000D+00  0.0000D+00  1.0000D+00  0.0000D+00  0.0000D+00  0.0000D+00  0.0000D+00  0.0000D+00

ASMC( 8)

                1           2           3           4           5           6           7           8
      1  0.0000D+00  0.0000D+00  0.0000D+00  0.0000D+00  0.0000D+00  0.0000D+00  1.0000D+00  0.0000D+00
      2  0.0000D+00  0.0000D+00  1.0000D+00  0.0000D+00  0.0000D+00  0.0000D+00  0.0000D+00  0.0000D+00

BSMC( 1)

                1           2
      1  1.0000D+00  0.0000D+00
```

```
      2       0.0000D+00  1.0000D+00

BSMC( 2)

                    1           2
      1       0.0000D+00  0.0000D+00
      2       0.0000D+00  1.0000D+00

BSMC( 3)

                    1           2
      1       0.0000D+00  0.0000D+00
      2       0.0000D+00  1.0000D+00

BSMC( 4)

                    1           2
      1       0.0000D+00  0.0000D+00
      2       0.0000D+00  1.0000D+00

BSMC( 5)

                    1           2
      1       0.0000D+00  0.0000D+00
      2       0.0000D+00  1.0000D+00

BSMC( 6)

                    1           2
      1       0.0000D+00  0.0000D+00
      2       0.0000D+00  1.0000D+00

BSMC( 7)

                    1           2
      1       0.0000D+00  0.0000D+00
```

```
      2       0.0000D+00  1.0000D+00


BSMC( 8)

                  1           2
      1       0.0000D+00  0.0000D+00
      2       0.0000D+00  1.0000D+00


STBL
(A 1(0) AT POSITION I,J INDICATES THAT THE JTH CONTROL IS
SAMPLED AND HELD(JUST HELD) AT THE BEGINNING OF THE ITH STP.)

 1 1
 0 0
 0 0
 0 0
 0 0
 0 0
 0 0
 0 0


ALPHA TABLE
(A 1(0) AT POSITION I,J INDICATES THAT THE JTH FEEDBACK
MATRIX IS ACTIVE(INACTIVE) DURING THE ITH STP.)

 1
 1
 1
 1
 1
 1
 1
 1


FGM( 1)

                  1           2           3           4           5           6           7           8
      1       1.1297D+01  0.0000D+00  3.9316D-01  0.0000D+00  0.0000D+00  0.0000D+00 -1.3483D+01  1.0708D+00
```

Page 6 of Example AMS Output File

2	9.7632D-02	0.0000D+00	0.0000D+00	0.0000D+00	0.0000D+00	0.0000D+00	-1.2129D-01	0.0000D+00
3	0.0000D+00	0.0000D+00	1.3439D+01	0.0000D+00	0.0000D+00	0.0000D+00	0.0000D+00	-1.6865D+01
4	0.0000D+00	0.0000D+00	0.0000D+00	0.0000D+00	0.0000D+00	0.0000D+00	4.8499D-01	0.0000D+00
5	0.0000D+00	0.0000D+00	0.0000D+00	0.0000D+00	0.0000D+00	0.0000D+00	0.0000D+00	5.5327D-01

NOGRDF(1)
(A 1(O) INDICATES THAT THE CORRESPONDING ELEMENT OF FGM(1)
IS UNCONSTRAINED(CONSTRAINED TO BE FIXED))

1 0 1 0 0 0 1 1
1 0 0 0 0 0 1 0
0 0 1 0 0 0 0 1
0 0 0 0 0 0 1 0
0 0 0 0 0 0 0 1

Page 7 of Example AMS Output File

```
DISCRETE STATE MODEL AND COST FUNCTION AND OTHER PARAMETERS
-----------------------------------------------------------

TT= 8
IX= 8
IU= 5
MM= 1
NN=  10000
NITRMX=  10
TOL=1.0000D-05
COST=0.000000D+00
FPZ=2.2204D-16
XFLG= F
GLOBAL= F
HESFLG= F
ETA=2.0000D-01
STEPMX=1.0000D+01
```

ASM(1)

	1	2	3	4	5	6	7	8
1	1.0000D+00	2.8125D-02	0.0000D+00	0.0000D+00	0.0000D+00	0.0000D+00	0.0000D+00	0.0000D+00
2	0.0000D+00	1.0000D+00	0.0000D+00	0.0000D+00	0.0000D+00	0.0000D+00	0.0000D+00	0.0000D+00
3	0.0000D+00	0.0000D+00	1.0000D+00	2.8125D-02	0.0000D+00	0.0000D+00	0.0000D+00	0.0000D+00
4	0.0000D+00	0.0000D+00	0.0000D+00	1.0000D+00	0.0000D+00	0.0000D+00	0.0000D+00	0.0000D+00
5	0.0000D+00	0.0000D+00	0.0000D+00	0.0000D+00	0.0000D+00	0.0000D+00	0.0000D+00	0.0000D+00
6	0.0000D+00	0.0000D+00	0.0000D+00	0.0000D+00	0.0000D+00	0.0000D+00	0.0000D+00	0.0000D+00
7	1.0000D+00	0.0000D+00	0.0000D+00	0.0000D+00	0.0000D+00	0.0000D+00	0.0000D+00	0.0000D+00
8	0.0000D+00	0.0000D+00	1.0000D+00	0.0000D+00	0.0000D+00	0.0000D+00	0.0000D+00	0.0000D+00

ASM(2)

	1	2	3	4	5	6	7	8
1	1.0000D+00	2.8125D-02	0.0000D+00	0.0000D+00	9.3672D-04	-9.0706D-03	0.0000D+00	0.0000D+00
2	0.0000D+00	1.0000D+00	0.0000D+00	0.0000D+00	6.6612D-02	-6.4502D-01	0.0000D+00	0.0000D+00
3	0.0000D+00	0.0000D+00	1.0000D+00	2.8125D-02	-4.5197D-04	4.8089D-02	0.0000D+00	0.0000D+00
4	0.0000D+00	0.0000D+00	0.0000D+00	1.0000D+00	-3.2140D-02	3.4196D+00	0.0000D+00	0.0000D+00
5	0.0000D+00	0.0000D+00	0.0000D+00	0.0000D+00	1.0000D+00	0.0000D+00	0.0000D+00	0.0000D+00
6	0.0000D+00	0.0000D+00	0.0000D+00	0.0000D+00	0.0000D+00	1.0000D+00	0.0000D+00	0.0000D+00
7	0.0000D+00	0.0000D+00	0.0000D+00	0.0000D+00	0.0000D+00	0.0000D+00	1.0000D+00	0.0000D+00

Page 8 of Example AMS Output File

8	0.0000D+00	0.0000D+00	1.0000D+00	0.0000D+00	0.0000D+00	0.0000D+00	0.0000D+00	0.0000D+00

ASM(3)

	1	2	3	4	5	6	7	8
1	1.0000D+00	2.8125D-02	0.0000D+00	0.0000D+00	9.3672D-04	-9.0706D-03	0.0000D+00	0.0000D+00
2	0.0000D+00	1.0000D+00	0.0000D+00	0.0000D+00	6.6612D-02	-6.4502D-01	0.0000D+00	0.0000D+00
3	0.0000D+00	0.0000D+00	1.0000D+00	2.8125D-02	-4.5197D-04	4.8089D-02	0.0000D+00	0.0000D+00
4	0.0000D+00	0.0000D+00	0.0000D+00	1.0000D+00	-3.2140D-02	3.4196D+00	0.0000D+00	0.0000D+00
5	0.0000D+00	0.0000D+00	0.0000D+00	0.0000D+00	1.0000D+00	0.0000D+00	0.0000D+00	0.0000D+00
6	0.0000D+00	0.0000D+00	0.0000D+00	0.0000D+00	0.0000D+00	1.0000D+00	0.0000D+00	0.0000D+00
7	0.0000D+00	0.0000D+00	0.0000D+00	0.0000D+00	0.0000D+00	0.0000D+00	1.0000D+00	0.0000D+00
8	0.0000D+00	0.0000D+00	1.0000D+00	0.0000D+00	0.0000D+00	0.0000D+00	0.0000D+00	0.0000D+00

ASM(4)

	1	2	3	4	5	6	7	8
1	1.0000D+00	2.8125D-02	0.0000D+00	0.0000D+00	9.3672D-04	-9.0706D-03	0.0000D+00	0.0000D+00
2	0.0000D+00	1.0000D+00	0.0000D+00	0.0000D+00	6.6612D-02	-6.4502D-01	0.0000D+00	0.0000D+00
3	0.0000D+00	0.0000D+00	1.0000D+00	2.8125D-02	-4.5197D-04	4.8089D-02	0.0000D+00	0.0000D+00
4	0.0000D+00	0.0000D+00	0.0000D+00	1.0000D+00	-3.2140D-02	3.4196D+00	0.0000D+00	0.0000D+00
5	0.0000D+00	0.0000D+00	0.0000D+00	0.0000D+00	1.0000D+00	0.0000D+00	0.0000D+00	0.0000D+00
6	0.0000D+00	0.0000D+00	0.0000D+00	0.0000D+00	0.0000D+00	1.0000D+00	0.0000D+00	0.0000D+00
7	0.0000D+00	0.0000D+00	0.0000D+00	0.0000D+00	0.0000D+00	0.0000D+00	1.0000D+00	0.0000D+00
8	0.0000D+00	0.0000D+00	1.0000D+00	0.0000D+00	0.0000D+00	0.0000D+00	0.0000D+00	0.0000D+00

ASM(5)

	1	2	3	4	5	6	7	8
1	1.0000D+00	2.8125D-02	0.0000D+00	0.0000D+00	9.3672D-04	-9.0706D-03	0.0000D+00	0.0000D+00
2	0.0000D+00	1.0000D+00	0.0000D+00	0.0000D+00	6.6612D-02	-6.4502D-01	0.0000D+00	0.0000D+00
3	0.0000D+00	0.0000D+00	1.0000D+00	2.8125D-02	-4.5197D-04	4.8089D-02	0.0000D+00	0.0000D+00
4	0.0000D+00	0.0000D+00	0.0000D+00	1.0000D+00	-3.2140D-02	3.4196D+00	0.0000D+00	0.0000D+00
5	0.0000D+00	0.0000D+00	0.0000D+00	0.0000D+00	1.0000D+00	0.0000D+00	0.0000D+00	0.0000D+00
6	0.0000D+00	0.0000D+00	0.0000D+00	0.0000D+00	0.0000D+00	1.0000D+00	0.0000D+00	0.0000D+00
7	0.0000D+00	0.0000D+00	0.0000D+00	0.0000D+00	0.0000D+00	0.0000D+00	1.0000D+00	0.0000D+00
8	0.0000D+00	0.0000D+00	1.0000D+00	0.0000D+00	0.0000D+00	0.0000D+00	0.0000D+00	0.0000D+00

Page 9 of Example AMS Output File

ASM(6)

	1	2	3	4	5	6	7	8
1	1.0000D+00	2.8125D-02	0.0000D+00	0.0000D+00	9.3672D-04	-9.0706D-03	0.0000D+00	0.0000D+00
2	0.0000D+00	1.0000D+00	0.0000D+00	0.0000D+00	6.6612D-02	-6.4502D-01	0.0000D+00	0.0000D+00
3	0.0000D+00	0.0000D+00	1.0000D+00	2.8125D-02	-4.5197D-04	4.8089D-02	0.0000D+00	0.0000D+00
4	0.0000D+00	0.0000D+00	0.0000D+00	1.0000D+00	-3.2140D-02	3.4196D+00	0.0000D+00	0.0000D+00
5	0.0000D+00	0.0000D+00	0.0000D+00	0.0000D+00	1.0000D+00	0.0000D+00	0.0000D+00	0.0000D+00
6	0.0000D+00	0.0000D+00	0.0000D+00	0.0000D+00	0.0000D+00	1.0000D+00	0.0000D+00	0.0000D+00
7	0.0000D+00	0.0000D+00	0.0000D+00	0.0000D+00	0.0000D+00	0.0000D+00	1.0000D+00	0.0000D+00
8	0.0000D+00	0.0000D+00	1.0000D+00	0.0000D+00	0.0000D+00	0.0000D+00	0.0000D+00	0.0000D+00

ASM(7)

	1	2	3	4	5	6	7	8
1	1.0000D+00	2.8125D-02	0.0000D+00	0.0000D+00	9.3672D-04	-9.0706D-03	0.0000D+00	0.0000D+00
2	0.0000D+00	1.0000D+00	0.0000D+00	0.0000D+00	6.6612D-02	-6.4502D-01	0.0000D+00	0.0000D+00
3	0.0000D+00	0.0000D+00	1.0000D+00	2.8125D-02	-4.5197D-04	4.8089D-02	0.0000D+00	0.0000D+00
4	0.0000D+00	0.0000D+00	0.0000D+00	1.0000D+00	-3.2140D-02	3.4196D+00	0.0000D+00	0.0000D+00
5	0.0000D+00	0.0000D+00	0.0000D+00	0.0000D+00	1.0000D+00	0.0000D+00	0.0000D+00	0.0000D+00
6	0.0000D+00	0.0000D+00	0.0000D+00	0.0000D+00	0.0000D+00	1.0000D+00	0.0000D+00	0.0000D+00
7	0.0000D+00	0.0000D+00	0.0000D+00	0.0000D+00	0.0000D+00	0.0000D+00	1.0000D+00	0.0000D+00
8	0.0000D+00	0.0000D+00	1.0000D+00	0.0000D+00	0.0000D+00	0.0000D+00	0.0000D+00	0.0000D+00

ASM(8)

	1	2	3	4	5	6	7	8
1	1.0000D+00	2.8125D-02	0.0000D+00	0.0000D+00	9.3672D-04	-9.0706D-03	0.0000D+00	0.0000D+00
2	0.0000D+00	1.0000D+00	0.0000D+00	0.0000D+00	6.6612D-02	-6.4502D-01	0.0000D+00	0.0000D+00
3	0.0000D+00	0.0000D+00	1.0000D+00	2.8125D-02	-4.5197D-04	4.8089D-02	0.0000D+00	0.0000D+00
4	0.0000D+00	0.0000D+00	0.0000D+00	1.0000D+00	-3.2140D-02	3.4196D+00	0.0000D+00	0.0000D+00
5	0.0000D+00	0.0000D+00	0.0000D+00	0.0000D+00	1.0000D+00	0.0000D+00	0.0000D+00	0.0000D+00
6	0.0000D+00	0.0000D+00	0.0000D+00	0.0000D+00	0.0000D+00	1.0000D+00	0.0000D+00	0.0000D+00
7	0.0000D+00	0.0000D+00	0.0000D+00	0.0000D+00	0.0000D+00	0.0000D+00	1.0000D+00	0.0000D+00
8	0.0000D+00	0.0000D+00	1.0000D+00	0.0000D+00	0.0000D+00	0.0000D+00	0.0000D+00	0.0000D+00

BSM(1)

1	2	3	4	5

Page 10 of Example AMS Output File

1	9.3672D-04	-9.0706D-03	-9.0706D-03	0.0000D+00	0.0000D+00
2	6.6612D-02	-6.4502D-01	-6.4502D-01	0.0000D+00	0.0000D+00
3	-4.5197D-04	4.8089D-02	4.8089D-02	0.0000D+00	0.0000D+00
4	-3.2140D-02	3.4196D+00	3.4196D+00	0.0000D+00	0.0000D+00
5	1.0000D+00	0.0000D+00	0.0000D+00	0.0000D+00	0.0000D+00
6	0.0000D+00	1.0000D+00	0.0000D+00	0.0000D+00	0.0000D+00
7	0.0000D+00	0.0000D+00	0.0000D+00	1.0000D+00	0.0000D+00
8	0.0000D+00	0.0000D+00	0.0000D+00	0.0000D+00	1.0000D+00

BSM(2)

	1	2	3	4	5
1	0.0000D+00	0.0000D+00	-9.0706D-03	0.0000D+00	0.0000D+00
2	0.0000D+00	0.0000D+00	-6.4502D-01	0.0000D+00	0.0000D+00
3	0.0000D+00	0.0000D+00	4.8089D-02	0.0000D+00	0.0000D+00
4	0.0000D+00	0.0000D+00	3.4196D+00	0.0000D+00	0.0000D+00
5	0.0000D+00	0.0000D+00	0.0000D+00	0.0000D+00	0.0000D+00
6	0.0000D+00	0.0000D+00	0.0000D+00	0.0000D+00	0.0000D+00
7	0.0000D+00	0.0000D+00	0.0000D+00	0.0000D+00	0.0000D+00
8	0.0000D+00	0.0000D+00	0.0000D+00	0.0000D+00	1.0000D+00

BSM(3)

	1	2	3	4	5
1	0.0000D+00	0.0000D+00	-9.0706D-03	0.0000D+00	0.0000D+00
2	0.0000D+00	0.0000D+00	-6.4502D-01	0.0000D+00	0.0000D+00
3	0.0000D+00	0.0000D+00	4.8089D-02	0.0000D+00	0.0000D+00
4	0.0000D+00	0.0000D+00	3.4196D+00	0.0000D+00	0.0000D+00
5	0.0000D+00	0.0000D+00	0.0000D+00	0.0000D+00	0.0000D+00
6	0.0000D+00	0.0000D+00	0.0000D+00	0.0000D+00	0.0000D+00
7	0.0000D+00	0.0000D+00	0.0000D+00	0.0000D+00	0.0000D+00
8	0.0000D+00	0.0000D+00	0.0000D+00	0.0000D+00	1.0000D+00

BSM(4)

	1	2	3	4	5
1	0.0000D+00	0.0000D+00	-9.0706D-03	0.0000D+00	0.0000D+00
2	0.0000D+00	0.0000D+00	-6.4502D-01	0.0000D+00	0.0000D+00
3	0.0000D+00	0.0000D+00	4.8089D-02	0.0000D+00	0.0000D+00

Page 11 of Example AMS Output File

```
      4    0.0000D+00  0.0000D+00  3.4196D+00  0.0000D+00  0.0000D+00
      5    0.0000D+00  0.0000D+00  0.0000D+00  0.0000D+00  0.0000D+00
      6    0.0000D+00  0.0000D+00  0.0000D+00  0.0000D+00  0.0000D+00
      7    0.0000D+00  0.0000D+00  0.0000D+00  0.0000D+00  0.0000D+00
      8    0.0000D+00  0.0000D+00  0.0000D+00  0.0000D+00  1.0000D+00

BSM( 5)

           1           2           3           4           5
      1    0.0000D+00  0.0000D+00 -9.0706D-03  0.0000D+00  0.0000D+00
      2    0.0000D+00  0.0000D+00 -6.4502D-01  0.0000D+00  0.0000D+00
      3    0.0000D+00  0.0000D+00  4.8089D-02  0.0000D+00  0.0000D+00
      4    0.0000D+00  0.0000D+00  3.4196D+00  0.0000D+00  0.0000D+00
      5    0.0000D+00  0.0000D+00  0.0000D+00  0.0000D+00  0.0000D+00
      6    0.0000D+00  0.0000D+00  0.0000D+00  0.0000D+00  0.0000D+00
      7    0.0000D+00  0.0000D+00  0.0000D+00  0.0000D+00  0.0000D+00
      8    0.0000D+00  0.0000D+00  0.0000D+00  0.0000D+00  1.0000D+00

BSM( 6)

           1           2           3           4           5
      1    0.0000D+00  0.0000D+00 -9.0706D-03  0.0000D+00  0.0000D+00
      2    0.0000D+00  0.0000D+00 -6.4502D-01  0.0000D+00  0.0000D+00
      3    0.0000D+00  0.0000D+00  4.8089D-02  0.0000D+00  0.0000D+00
      4    0.0000D+00  0.0000D+00  3.4196D+00  0.0000D+00  0.0000D+00
      5    0.0000D+00  0.0000D+00  0.0000D+00  0.0000D+00  0.0000D+00
      6    0.0000D+00  0.0000D+00  0.0000D+00  0.0000D+00  0.0000D+00
      7    0.0000D+00  0.0000D+00  0.0000D+00  0.0000D+00  0.0000D+00
      8    0.0000D+00  0.0000D+00  0.0000D+00  0.0000D+00  1.0000D+00

BSM( 7)

           1           2           3           4           5
      1    0.0000D+00  0.0000D+00 -9.0706D-03  0.0000D+00  0.0000D+00
      2    0.0000D+00  0.0000D+00 -6.4502D-01  0.0000D+00  0.0000D+00
      3    0.0000D+00  0.0000D+00  4.8089D-02  0.0000D+00  0.0000D+00
      4    0.0000D+00  0.0000D+00  3.4196D+00  0.0000D+00  0.0000D+00
      5    0.0000D+00  0.0000D+00  0.0000D+00  0.0000D+00  0.0000D+00
      6    0.0000D+00  0.0000D+00  0.0000D+00  0.0000D+00  0.0000D+00
```

Page 12 of Example AMS Output File

7	0.0000D+00	0.0000D+00	0.0000D+00	0.0000D+00	0.0000D+00
8	0.0000D+00	0.0000D+00	0.0000D+00	0.0000D+00	1.0000D+00

BSM(8)

	1	2	3	4	5
1	0.0000D+00	0.0000D+00	-9.0706D-03	0.0000D+00	0.0000D+00
2	0.0000D+00	0.0000D+00	-6.4502D-01	0.0000D+00	0.0000D+00
3	0.0000D+00	0.0000D+00	4.8089D-02	0.0000D+00	0.0000D+00
4	0.0000D+00	0.0000D+00	3.4196D+00	0.0000D+00	0.0000D+00
5	0.0000D+00	0.0000D+00	0.0000D+00	0.0000D+00	0.0000D+00
6	0.0000D+00	0.0000D+00	0.0000D+00	0.0000D+00	0.0000D+00
7	0.0000D+00	0.0000D+00	0.0000D+00	0.0000D+00	0.0000D+00
8	0.0000D+00	0.0000D+00	0.0000D+00	0.0000D+00	1.0000D+00

GWG(1)

	1	2	3	4	5	6	7	8
1	6.7892D-05	3.6209D-03	-2.2073D-04	-1.1772D-02	0.0000D+00	0.0000D+00	0.0000D+00	0.0000D+00
2	3.6209D-03	2.5749D-01	-1.1772D-02	-8.3712D-01	0.0000D+00	0.0000D+00	0.0000D+00	0.0000D+00
3	-2.2073D-04	-1.1772D-02	1.1030D-03	5.8828D-02	0.0000D+00	0.0000D+00	0.0000D+00	0.0000D+00
4	-1.1772D-02	-8.3712D-01	5.8828D-02	4.1833D+00	0.0000D+00	0.0000D+00	0.0000D+00	0.0000D+00
5	0.0000D+00	0.0000D+00	0.0000D+00	0.0000D+00	0.0000D+00	0.0000D+00	0.0000D+00	0.0000D+00
6	0.0000D+00	0.0000D+00	0.0000D+00	0.0000D+00	0.0000D+00	0.0000D+00	0.0000D+00	0.0000D+00
7	0.0000D+00	0.0000D+00	0.0000D+00	0.0000D+00	0.0000D+00	0.0000D+00	0.0000D+00	0.0000D+00
8	0.0000D+00	0.0000D+00	0.0000D+00	0.0000D+00	0.0000D+00	0.0000D+00	0.0000D+00	0.0000D+00

GWG(2)

	1	2	3	4	5	6	7	8
1	6.7892D-05	3.6209D-03	-2.2073D-04	-1.1772D-02	0.0000D+00	0.0000D+00	0.0000D+00	0.0000D+00
2	3.6209D-03	2.5749D-01	-1.1772D-02	-8.3712D-01	0.0000D+00	0.0000D+00	0.0000D+00	0.0000D+00
3	-2.2073D-04	-1.1772D-02	1.1030D-03	5.8828D-02	0.0000D+00	0.0000D+00	0.0000D+00	0.0000D+00
4	-1.1772D-02	-8.3712D-01	5.8828D-02	4.1833D+00	0.0000D+00	0.0000D+00	0.0000D+00	0.0000D+00
5	0.0000D+00	0.0000D+00	0.0000D+00	0.0000D+00	0.0000D+00	0.0000D+00	0.0000D+00	0.0000D+00
6	0.0000D+00	0.0000D+00	0.0000D+00	0.0000D+00	0.0000D+00	0.0000D+00	0.0000D+00	0.0000D+00
7	0.0000D+00	0.0000D+00	0.0000D+00	0.0000D+00	0.0000D+00	0.0000D+00	0.0000D+00	0.0000D+00
8	0.0000D+00	0.0000D+00	0.0000D+00	0.0000D+00	0.0000D+00	0.0000D+00	0.0000D+00	0.0000D+00

Page 13 of Example AMS Output File

GWG(3)

	1	2	3	4	5	6	7	8
1	6.7892D-05	3.6209D-03	-2.2073D-04	-1.1772D-02	0.0000D+00	0.0000D+00	0.0000D+00	0.0000D+00
2	3.6209D-03	2.5749D-01	-1.1772D-02	-8.3712D-01	0.0000D+00	0.0000D+00	0.0000D+00	0.0000D+00
3	-2.2073D-04	-1.1772D-02	1.1030D-03	5.8828D-02	0.0000D+00	0.0000D+00	0.0000D+00	0.0000D+00
4	-1.1772D-02	-8.3712D-01	5.8828D-02	4.1833D+00	0.0000D+00	0.0000D+00	0.0000D+00	0.0000D+00
5	0.0000D+00	0.0000D+00	0.0000D+00	0.0000D+00	0.0000D+00	0.0000D+00	0.0000D+00	0.0000D+00
6	0.0000D+00	0.0000D+00	0.0000D+00	0.0000D+00	0.0000D+00	0.0000D+00	0.0000D+00	0.0000D+00
7	0.0000D+00	0.0000D+00	0.0000D+00	0.0000D+00	0.0000D+00	0.0000D+00	0.0000D+00	0.0000D+00
8	0.0000D+00	0.0000D+00	0.0000D+00	0.0000D+00	0.0000D+00	0.0000D+00	0.0000D+00	0.0000D+00

GWG(4)

	1	2	3	4	5	6	7	8
1	6.7892D-05	3.6209D-03	-2.2073D-04	-1.1772D-02	0.0000D+00	0.0000D+00	0.0000D+00	0.0000D+00
2	3.6209D-03	2.5749D-01	-1.1772D-02	-8.3712D-01	0.0000D+00	0.0000D+00	0.0000D+00	0.0000D+00
3	-2.2073D-04	-1.1772D-02	1.1030D-03	5.8828D-02	0.0000D+00	0.0000D+00	0.0000D+00	0.0000D+00
4	-1.1772D-02	-8.3712D-01	5.8828D-02	4.1833D+00	0.0000D+00	0.0000D+00	0.0000D+00	0.0000D+00
5	0.0000D+00	0.0000D+00	0.0000D+00	0.0000D+00	0.0000D+00	0.0000D+00	0.0000D+00	0.0000D+00
6	0.0000D+00	0.0000D+00	0.0000D+00	0.0000D+00	0.0000D+00	0.0000D+00	0.0000D+00	0.0000D+00
7	0.0000D+00	0.0000D+00	0.0000D+00	0.0000D+00	0.0000D+00	0.0000D+00	0.0000D+00	0.0000D+00
8	0.0000D+00	0.0000D+00	0.0000D+00	0.0000D+00	0.0000D+00	0.0000D+00	0.0000D+00	0.0000D+00

GWG(5)

	1	2	3	4	5	6	7	8
1	6.7892D-05	3.6209D-03	-2.2073D-04	-1.1772D-02	0.0000D+00	0.0000D+00	0.0000D+00	0.0000D+00
2	3.6209D-03	2.5749D-01	-1.1772D-02	-8.3712D-01	0.0000D+00	0.0000D+00	0.0000D+00	0.0000D+00
3	-2.2073D-04	-1.1772D-02	1.1030D-03	5.8828D-02	0.0000D+00	0.0000D+00	0.0000D+00	0.0000D+00
4	-1.1772D-02	-8.3712D-01	5.8828D-02	4.1833D+00	0.0000D+00	0.0000D+00	0.0000D+00	0.0000D+00
5	0.0000D+00	0.0000D+00	0.0000D+00	0.0000D+00	0.0000D+00	0.0000D+00	0.0000D+00	0.0000D+00
6	0.0000D+00	0.0000D+00	0.0000D+00	0.0000D+00	0.0000D+00	0.0000D+00	0.0000D+00	0.0000D+00
7	0.0000D+00	0.0000D+00	0.0000D+00	0.0000D+00	0.0000D+00	0.0000D+00	0.0000D+00	0.0000D+00
8	0.0000D+00	0.0000D+00	0.0000D+00	0.0000D+00	0.0000D+00	0.0000D+00	0.0000D+00	0.0000D+00

GWG(6)

	1	2	3	4	5	6	7	8
1	6.7892D-05	3.6209D-03	-2.2073D-04	-1.1772D-02	0.0000D+00	0.0000D+00	0.0000D+00	0.0000D+00
2	3.6209D-03	2.5749D-01	-1.1772D-02	-8.3712D-01	0.0000D+00	0.0000D+00	0.0000D+00	0.0000D+00
3	-2.2073D-04	-1.1772D-02	1.1030D-03	5.8828D-02	0.0000D+00	0.0000D+00	0.0000D+00	0.0000D+00
4	-1.1772D-02	-8.3712D-01	5.8828D-02	4.1833D+00	0.0000D+00	0.0000D+00	0.0000D+00	0.0000D+00
5	0.0000D+00	0.0000D+00	0.0000D+00	0.0000D+00	0.0000D+00	0.0000D+00	0.0000D+00	0.0000D+00
6	0.0000D+00	0.0000D+00	0.0000D+00	0.0000D+00	0.0000D+00	0.0000D+00	0.0000D+00	0.0000D+00
7	0.0000D+00	0.0000D+00	0.0000D+00	0.0000D+00	0.0000D+00	0.0000D+00	0.0000D+00	0.0000D+00
8	0.0000D+00	0.0000D+00	0.0000D+00	0.0000D+00	0.0000D+00	0.0000D+00	0.0000D+00	0.0000D+00

GWG(7)

	1	2	3	4	5	6	7	8
1	6.7892D-05	3.6209D-03	-2.2073D-04	-1.1772D-02	0.0000D+00	0.0000D+00	0.0000D+00	0.0000D+00
2	3.6209D-03	2.5749D-01	-1.1772D-02	-8.3712D-01	0.0000D+00	0.0000D+00	0.0000D+00	0.0000D+00
3	-2.2073D-04	-1.1772D-02	1.1030D-03	5.8828D-02	0.0000D+00	0.0000D+00	0.0000D+00	0.0000D+00
4	-1.1772D-02	-8.3712D-01	5.8828D-02	4.1833D+00	0.0000D+00	0.0000D+00	0.0000D+00	0.0000D+00
5	0.0000D+00	0.0000D+00	0.0000D+00	0.0000D+00	0.0000D+00	0.0000D+00	0.0000D+00	0.0000D+00
6	0.0000D+00	0.0000D+00	0.0000D+00	0.0000D+00	0.0000D+00	0.0000D+00	0.0000D+00	0.0000D+00
7	0.0000D+00	0.0000D+00	0.0000D+00	0.0000D+00	0.0000D+00	0.0000D+00	0.0000D+00	0.0000D+00
8	0.0000D+00	0.0000D+00	0.0000D+00	0.0000D+00	0.0000D+00	0.0000D+00	0.0000D+00	0.0000D+00

GWG(8)

	1	2	3	4	5	6	7	8
1	6.7892D-05	3.6209D-03	-2.2073D-04	-1.1772D-02	0.0000D+00	0.0000D+00	0.0000D+00	0.0000D+00
2	3.6209D-03	2.5749D-01	-1.1772D-02	-8.3712D-01	0.0000D+00	0.0000D+00	0.0000D+00	0.0000D+00
3	-2.2073D-04	-1.1772D-02	1.1030D-03	5.8828D-02	0.0000D+00	0.0000D+00	0.0000D+00	0.0000D+00
4	-1.1772D-02	-8.3712D-01	5.8828D-02	4.1833D+00	0.0000D+00	0.0000D+00	0.0000D+00	0.0000D+00
5	0.0000D+00	0.0000D+00	0.0000D+00	0.0000D+00	0.0000D+00	0.0000D+00	0.0000D+00	0.0000D+00
6	0.0000D+00	0.0000D+00	0.0000D+00	0.0000D+00	0.0000D+00	0.0000D+00	0.0000D+00	0.0000D+00
7	0.0000D+00	0.0000D+00	0.0000D+00	0.0000D+00	0.0000D+00	0.0000D+00	0.0000D+00	0.0000D+00
8	0.0000D+00	0.0000D+00	0.0000D+00	0.0000D+00	0.0000D+00	0.0000D+00	0.0000D+00	0.0000D+00

QCST(1)

	1	2	3	4	5	6	7	8
1	5.9062D-03	8.3057D-05	0.0000D+00	0.0000D+00	0.0000D+00	0.0000D+00	0.0000D+00	0.0000D+00
2	8.3057D-05	1.5573D-06	0.0000D+00	0.0000D+00	0.0000D+00	0.0000D+00	0.0000D+00	0.0000D+00

Page 15 of Example AMS Output File

3	0.0000D+00	0.0000D+00	5.2031D-01	7.3169D-03	0.0000D+00	0.0000D+00	0.0000D+00	0.0000D+00
4	0.0000D+00	0.0000D+00	7.3169D-03	1.3719D-04	0.0000D+00	0.0000D+00	0.0000D+00	0.0000D+00
5	0.0000D+00	0.0000D+00	0.0000D+00	0.0000D+00	0.0000D+00	0.0000D+00	0.0000D+00	0.0000D+00
6	0.0000D+00	0.0000D+00	0.0000D+00	0.0000D+00	0.0000D+00	0.0000D+00	0.0000D+00	0.0000D+00
7	0.0000D+00	0.0000D+00	0.0000D+00	0.0000D+00	0.0000D+00	0.0000D+00	0.0000D+00	0.0000D+00
8	0.0000D+00	0.0000D+00	0.0000D+00	0.0000D+00	0.0000D+00	0.0000D+00	0.0000D+00	0.0000D+00

QCST(2)

	1	2	3	4	5	6	7	8
1	5.9062D-03	8.3057D-05	0.0000D+00	0.0000D+00	1.8442D-06	-1.7858D-05	0.0000D+00	0.0000D+00
2	8.3057D-05	1.5573D-06	0.0000D+00	0.0000D+00	3.8901D-08	-3.7669D-07	0.0000D+00	0.0000D+00
3	0.0000D+00	0.0000D+00	5.2031D-01	7.3169D-03	-7.8389D-05	8.3404D-03	0.0000D+00	0.0000D+00
4	0.0000D+00	0.0000D+00	7.3169D-03	1.3719D-04	-1.6535D-06	1.7593D-04	0.0000D+00	0.0000D+00
5	1.8442D-06	3.8901D-08	-7.8389D-05	-1.6535D-06	2.8127D-04	-2.2718D-06	0.0000D+00	0.0000D+00
6	-1.7858D-05	-3.7669D-07	8.3404D-03	1.7593D-04	-2.2718D-06	1.9772D-02	0.0000D+00	0.0000D+00
7	0.0000D+00	0.0000D+00	0.0000D+00	0.0000D+00	0.0000D+00	0.0000D+00	0.0000D+00	0.0000D+00
8	0.0000D+00	0.0000D+00	0.0000D+00	0.0000D+00	0.0000D+00	0.0000D+00	0.0000D+00	0.0000D+00

QCST(3)

	1	2	3	4	5	6	7	8
1	5.9062D-03	8.3057D-05	0.0000D+00	0.0000D+00	1.8442D-06	-1.7858D-05	0.0000D+00	0.0000D+00
2	8.3057D-05	1.5573D-06	0.0000D+00	0.0000D+00	3.8901D-08	-3.7669D-07	0.0000D+00	0.0000D+00
3	0.0000D+00	0.0000D+00	5.2031D-01	7.3169D-03	-7.8389D-05	8.3404D-03	0.0000D+00	0.0000D+00
4	0.0000D+00	0.0000D+00	7.3169D-03	1.3719D-04	-1.6535D-06	1.7593D-04	0.0000D+00	0.0000D+00
5	1.8442D-06	3.8901D-08	-7.8389D-05	-1.6535D-06	2.8127D-04	-2.2718D-06	0.0000D+00	0.0000D+00
6	-1.7858D-05	-3.7669D-07	8.3404D-03	1.7593D-04	-2.2718D-06	1.9772D-02	0.0000D+00	0.0000D+00
7	0.0000D+00	0.0000D+00	0.0000D+00	0.0000D+00	0.0000D+00	0.0000D+00	0.0000D+00	0.0000D+00
8	0.0000D+00	0.0000D+00	0.0000D+00	0.0000D+00	0.0000D+00	0.0000D+00	0.0000D+00	0.0000D+00

QCST(4)

	1	2	3	4	5	6	7	8
1	5.9062D-03	8.3057D-05	0.0000D+00	0.0000D+00	1.8442D-06	-1.7858D-05	0.0000D+00	0.0000D+00
2	8.3057D-05	1.5573D-06	0.0000D+00	0.0000D+00	3.8901D-08	-3.7669D-07	0.0000D+00	0.0000D+00
3	0.0000D+00	0.0000D+00	5.2031D-01	7.3169D-03	-7.8389D-05	8.3404D-03	0.0000D+00	0.0000D+00
4	0.0000D+00	0.0000D+00	7.3169D-03	1.3719D-04	-1.6535D-06	1.7593D-04	0.0000D+00	0.0000D+00
5	1.8442D-06	3.8901D-08	-7.8389D-05	-1.6535D-06	2.8127D-04	-2.2718D-06	0.0000D+00	0.0000D+00

6	-1.7858D-05	-3.7669D-07	8.3404D-03	1.7593D-04	-2.2718D-06	1.9772D-02	0.0000D+00	0.0000D+00
7	0.0000D+00	0.0000D+00	0.0000D+00	0.0000D+00	0.0000D+00	0.0000D+00	0.0000D+00	0.0000D+00
8	0.0000D+00	0.0000D+00	0.0000D+00	0.0000D+00	0.0000D+00	0.0000D+00	0.0000D+00	0.0000D+00

QCST(5)

	1	2	3	4	5	6	7	8
1	5.9062D-03	8.3057D-05	0.0000D+00	0.0000D+00	1.8442D-06	-1.7858D-05	0.0000D+00	0.0000D+00
2	8.3057D-05	1.5573D-06	0.0000D+00	0.0000D+00	3.8901D-08	-3.7669D-07	0.0000D+00	0.0000D+00
3	0.0000D+00	0.0000D+00	5.2031D-01	7.3169D-03	-7.8389D-05	8.3404D-03	0.0000D+00	0.0000D+00
4	0.0000D+00	0.0000D+00	7.3169D-03	1.3719D-04	-1.6535D-06	1.7593D-04	0.0000D+00	0.0000D+00
5	1.8442D-06	3.8901D-08	-7.8389D-05	-1.6535D-06	2.8127D-04	-2.2718D-06	0.0000D+00	0.0000D+00
6	-1.7858D-05	-3.7669D-07	8.3404D-03	1.7593D-04	-2.2718D-06	1.9772D-02	0.0000D+00	0.0000D+00
7	0.0000D+00	0.0000D+00	0.0000D+00	0.0000D+00	0.0000D+00	0.0000D+00	0.0000D+00	0.0000D+00
8	0.0000D+00	0.0000D+00	0.0000D+00	0.0000D+00	0.0000D+00	0.0000D+00	0.0000D+00	0.0000D+00

QCST(6)

	1	2	3	4	5	6	7	8
1	5.9062D-03	8.3057D-05	0.0000D+00	0.0000D+00	1.8442D-06	-1.7858D-05	0.0000D+00	0.0000D+00
2	8.3057D-05	1.5573D-06	0.0000D+00	0.0000D+00	3.8901D-08	-3.7669D-07	0.0000D+00	0.0000D+00
3	0.0000D+00	0.0000D+00	5.2031D-01	7.3169D-03	-7.8389D-05	8.3404D-03	0.0000D+00	0.0000D+00
4	0.0000D+00	0.0000D+00	7.3169D-03	1.3719D-04	-1.6535D-06	1.7593D-04	0.0000D+00	0.0000D+00
5	1.8442D-06	3.8901D-08	-7.8389D-05	-1.6535D-06	2.8127D-04	-2.2718D-06	0.0000D+00	0.0000D+00
6	-1.7858D-05	-3.7669D-07	8.3404D-03	1.7593D-04	-2.2718D-06	1.9772D-02	0.0000D+00	0.0000D+00
7	0.0000D+00	0.0000D+00	0.0000D+00	0.0000D+00	0.0000D+00	0.0000D+00	0.0000D+00	0.0000D+00
8	0.0000D+00	0.0000D+00	0.0000D+00	0.0000D+00	0.0000D+00	0.0000D+00	0.0000D+00	0.0000D+00

QCST(7)

	1	2	3	4	5	6	7	8
1	5.9062D-03	8.3057D-05	0.0000D+00	0.0000D+00	1.8442D-06	-1.7858D-05	0.0000D+00	0.0000D+00
2	8.3057D-05	1.5573D-06	0.0000D+00	0.0000D+00	3.8901D-08	-3.7669D-07	0.0000D+00	0.0000D+00
3	0.0000D+00	0.0000D+00	5.2031D-01	7.3169D-03	-7.8389D-05	8.3404D-03	0.0000D+00	0.0000D+00
4	0.0000D+00	0.0000D+00	7.3169D-03	1.3719D-04	-1.6535D-06	1.7593D-04	0.0000D+00	0.0000D+00
5	1.8442D-06	3.8901D-08	-7.8389D-05	-1.6535D-06	2.8127D-04	-2.2718D-06	0.0000D+00	0.0000D+00
6	-1.7858D-05	-3.7669D-07	8.3404D-03	1.7593D-04	-2.2718D-06	1.9772D-02	0.0000D+00	0.0000D+00
7	0.0000D+00	0.0000D+00	0.0000D+00	0.0000D+00	0.0000D+00	0.0000D+00	0.0000D+00	0.0000D+00
8	0.0000D+00	0.0000D+00	0.0000D+00	0.0000D+00	0.0000D+00	0.0000D+00	0.0000D+00	0.0000D+00

QCST(8)

	1	2	3	4	5	6	7	8
1	5.9062D-03	8.3057D-05	0.0000D+00	0.0000D+00	1.8442D-06	-1.7858D-05	0.0000D+00	0.0000D+00
2	8.3057D-05	1.5573D-06	0.0000D+00	0.0000D+00	3.8901D-08	-3.7669D-07	0.0000D+00	0.0000D+00
3	0.0000D+00	0.0000D+00	5.2031D-01	7.3169D-03	-7.8389D-05	8.3404D-03	0.0000D+00	0.0000D+00
4	0.0000D+00	0.0000D+00	7.3169D-03	1.3719D-04	-1.6535D-06	1.7593D-04	0.0000D+00	0.0000D+00
5	1.8442D-06	3.8901D-08	-7.8389D-05	-1.6535D-06	2.8127D-04	-2.2718D-06	0.0000D+00	0.0000D+00
6	-1.7858D-05	-3.7669D-07	8.3404D-03	1.7593D-04	-2.2718D-06	1.9772D-02	0.0000D+00	0.0000D+00
7	0.0000D+00	0.0000D+00	0.0000D+00	0.0000D+00	0.0000D+00	0.0000D+00	0.0000D+00	0.0000D+00
8	0.0000D+00	0.0000D+00	0.0000D+00	0.0000D+00	0.0000D+00	0.0000D+00	0.0000D+00	0.0000D+00

NCST(1)

	1	2	3	4	5
1	1.8442D-06	-1.7858D-05	-1.7858D-05	0.0000D+00	0.0000D+00
2	3.8901D-08	-3.7669D-07	-3.7669D-07	0.0000D+00	0.0000D+00
3	-7.8389D-05	8.3404D-03	8.3404D-03	0.0000D+00	0.0000D+00
4	-1.6535D-06	1.7593D-04	1.7593D-04	0.0000D+00	0.0000D+00
5	0.0000D+00	0.0000D+00	0.0000D+00	0.0000D+00	0.0000D+00
6	0.0000D+00	0.0000D+00	0.0000D+00	0.0000D+00	0.0000D+00
7	0.0000D+00	0.0000D+00	0.0000D+00	0.0000D+00	0.0000D+00
8	0.0000D+00	0.0000D+00	0.0000D+00	0.0000D+00	0.0000D+00

C-3

NCST(2)

	1	2	3	4	5
1	0.0000D+00	0.0000D+00	-1.7858D-05	0.0000D+00	0.0000D+00
2	0.0000D+00	0.0000D+00	-3.7669D-07	0.0000D+00	0.0000D+00
3	0.0000D+00	0.0000D+00	8.3404D-03	0.0000D+00	0.0000D+00
4	0.0000D+00	0.0000D+00	1.7593D-04	0.0000D+00	0.0000D+00
5	0.0000D+00	0.0000D+00	-2.2718D-06	0.0000D+00	0.0000D+00
6	0.0000D+00	0.0000D+00	1.9772D-02	0.0000D+00	0.0000D+00
7	0.0000D+00	0.0000D+00	0.0000D+00	0.0000D+00	0.0000D+00
8	0.0000D+00	0.0000D+00	0.0000D+00	0.0000D+00	0.0000D+00

NCST(3)

Page 18 of Example AMS Output File

	1	2	3	4	5
1	0.0000D+00	0.0000D+00	-1.7858D-05	0.0000D+00	0.0000D+00
2	0.0000D+00	0.0000D+00	-3.7669D-07	0.0000D+00	0.0000D+00
3	0.0000D+00	0.0000D+00	8.3404D-03	0.0000D+00	0.0000D+00
4	0.0000D+00	0.0000D+00	1.7593D-04	0.0000D+00	0.0000D+00
5	0.0000D+00	0.0000D+00	-2.2718D-06	0.0000D+00	0.0000D+00
6	0.0000D+00	0.0000D+00	1.9772D-02	0.0000D+00	0.0000D+00
7	0.0000D+00	0.0000D+00	0.0000D+00	0.0000D+00	0.0000D+00
8	0.0000D+00	0.0000D+00	0.0000D+00	0.0000D+00	0.0000D+00

NCST(4)

	1	2	3	4	5
1	0.0000D+00	0.0000D+00	-1.7858D-05	0.0000D+00	0.0000D+00
2	0.0000D+00	0.0000D+00	-3.7669D-07	0.0000D+00	0.0000D+00
3	0.0000D+00	0.0000D+00	8.3404D-03	0.0000D+00	0.0000D+00
4	0.0000D+00	0.0000D+00	1.7593D-04	0.0000D+00	0.0000D+00
5	0.0000D+00	0.0000D+00	-2.2718D-06	0.0000D+00	0.0000D+00
6	0.0000D+00	0.0000D+00	1.9772D-02	0.0000D+00	0.0000D+00
7	0.0000D+00	0.0000D+00	0.0000D+00	0.0000D+00	0.0000D+00
8	0.0000D+00	0.0000D+00	0.0000D+00	0.0000D+00	0.0000D+00

NCST(5)

	1	2	3	4	5
1	0.0000D+00	0.0000D+00	-1.7858D-05	0.0000D+00	0.0000D+00
2	0.0000D+00	0.0000D+00	-3.7669D-07	0.0000D+00	0.0000D+00
3	0.0000D+00	0.0000D+00	8.3404D-03	0.0000D+00	0.0000D+00
4	0.0000D+00	0.0000D+00	1.7593D-04	0.0000D+00	0.0000D+00
5	0.0000D+00	0.0000D+00	-2.2718D-06	0.0000D+00	0.0000D+00
6	0.0000D+00	0.0000D+00	1.9772D-02	0.0000D+00	0.0000D+00
7	0.0000D+00	0.0000D+00	0.0000D+00	0.0000D+00	0.0000D+00
8	0.0000D+00	0.0000D+00	0.0000D+00	0.0000D+00	0.0000D+00

NCST(6)

	1	2	3	4	5
1	0.0000D+00	0.0000D+00	-1.7858D-05	0.0000D+00	0.0000D+00

Page 19 of Example AMS Output File

2	0.0000D+00	0.0000D+00	-3.7669D-07	0.0000D+00	0.0000D+00
3	0.0000D+00	0.0000D+00	8.3404D-03	0.0000D+00	0.0000D+00
4	0.0000D+00	0.0000D+00	1.7593D-04	0.0000D+00	0.0000D+00
5	0.0000D+00	0.0000D+00	-2.2718D-06	0.0000D+00	0.0000D+00
6	0.0000D+00	0.0000D+00	1.9772D-02	0.0000D+00	0.0000D+00
7	0.0000D+00	0.0000D+00	0.0000D+00	0.0000D+00	0.0000D+00
8	0.0000D+00	0.0000D+00	0.0000D+00	0.0000D+00	0.0000D+00

NCST(7)

	1	2	3	4	5
1	0.0000D+00	0.0000D+00	-1.7858D-05	0.0000D+00	0.0000D+00
2	0.0000D+00	0.0000D+00	-3.7669D-07	0.0000D+00	0.0000D+00
3	0.0000D+00	0.0000D+00	8.3404D-03	0.0000D+00	0.0000D+00
4	0.0000D+00	0.0000D+00	1.7593D-04	0.0000D+00	0.0000D+00
5	0.0000D+00	0.0000D+00	-2.2718D-06	0.0000D+00	0.0000D+00
6	0.0000D+00	0.0000D+00	1.9772D-02	0.0000D+00	0.0000D+00
7	0.0000D+00	0.0000D+00	0.0000D+00	0.0000D+00	0.0000D+00
8	0.0000D+00	0.0000D+00	0.0000D+00	0.0000D+00	0.0000D+00

NCST(8)

	1	2	3	4	5
1	0.0000D+00	0.0000D+00	-1.7858D-05	0.0000D+00	0.0000D+00
2	0.0000D+00	0.0000D+00	-3.7669D-07	0.0000D+00	0.0000D+00
3	0.0000D+00	0.0000D+00	8.3404D-03	0.0000D+00	0.0000D+00
4	0.0000D+00	0.0000D+00	1.7593D-04	0.0000D+00	0.0000D+00
5	0.0000D+00	0.0000D+00	-2.2718D-06	0.0000D+00	0.0000D+00
6	0.0000D+00	0.0000D+00	1.9772D-02	0.0000D+00	0.0000D+00
7	0.0000D+00	0.0000D+00	0.0000D+00	0.0000D+00	0.0000D+00
8	0.0000D+00	0.0000D+00	0.0000D+00	0.0000D+00	0.0000D+00

RCST(1)

	1	2	3	4	5
1	2.8127D-04	-2.2718D-06	-2.2718D-06	0.0000D+00	0.0000D+00
2	-2.2718D-06	1.9772D-02	1.9772D-02	0.0000D+00	0.0000D+00
3	-2.2718D-06	1.9772D-02	1.9772D-02	0.0000D+00	0.0000D+00
4	0.0000D+00	0.0000D+00	0.0000D+00	0.0000D+00	0.0000D+00

Page 20 of Example AMS Output File

5	0.0000D+00	0.0000D+00	0.0000D+00	0.0000D+00	0.0000D+00

RCST(2)

	1	2	3	4	5
1	0.0000D+00	0.0000D+00	0.0000D+00	0.0000D+00	0.0000D+00
2	0.0000D+00	0.0000D+00	0.0000D+00	0.0000D+00	0.0000D+00
3	0.0000D+00	0.0000D+00	1.9772D-02	0.0000D+00	0.0000D+00
4	0.0000D+00	0.0000D+00	0.0000D+00	0.0000D+00	0.0000D+00
5	0.0000D+00	0.0000D+00	0.0000D+00	0.0000D+00	0.0000D+00

RCST(3)

	1	2	3	4	5
1	0.0000D+00	0.0000D+00	0.0000D+00	0.0000D+00	0.0000D+00
2	0.0000D+00	0.0000D+00	0.0000D+00	0.0000D+00	0.0000D+00
3	0.0000D+00	0.0000D+00	1.9772D-02	0.0000D+00	0.0000D+00
4	0.0000D+00	0.0000D+00	0.0000D+00	0.0000D+00	0.0000D+00
5	0.0000D+00	0.0000D+00	0.0000D+00	0.0000D+00	0.0000D+00

RCST(4)

	1	2	3	4	5
1	0.0000D+00	0.0000D+00	0.0000D+00	0.0000D+00	0.0000D+00
2	0.0000D+00	0.0000D+00	0.0000D+00	0.0000D+00	0.0000D+00
3	0.0000D+00	0.0000D+00	1.9772D-02	0.0000D+00	0.0000D+00
4	0.0000D+00	0.0000D+00	0.0000D+00	0.0000D+00	0.0000D+00
5	0.0000D+00	0.0000D+00	0.0000D+00	0.0000D+00	0.0000D+00

RCST(5)

	1	2	3	4	5
1	0.0000D+00	0.0000D+00	0.0000D+00	0.0000D+00	0.0000D+00
2	0.0000D+00	0.0000D+00	0.0000D+00	0.0000D+00	0.0000D+00
3	0.0000D+00	0.0000D+00	1.9772D-02	0.0000D+00	0.0000D+00
4	0.0000D+00	0.0000D+00	0.0000D+00	0.0000D+00	0.0000D+00
5	0.0000D+00	0.0000D+00	0.0000D+00	0.0000D+00	0.0000D+00

Page 21 of Example AMS Output File

RCST(6)

	1	2	3	4	5
1	0.0000D+00	0.0000D+00	0.0000D+00	0.0000D+00	0.0000D+00
2	0.0000D+00	0.0000D+00	0.0000D+00	0.0000D+00	0.0000D+00
3	0.0000D+00	0.0000D+00	1.9772D-02	0.0000D+00	0.0000D+00
4	0.0000D+00	0.0000D+00	0.0000D+00	0.0000D+00	0.0000D+00
5	0.0000D+00	0.0000D+00	0.0000D+00	0.0000D+00	0.0000D+00

RCST(7)

	1	2	3	4	5
1	0.0000D+00	0.0000D+00	0.0000D+00	0.0000D+00	0.0000D+00
2	0.0000D+00	0.0000D+00	0.0000D+00	0.0000D+00	0.0000D+00
3	0.0000D+00	0.0000D+00	1.9772D-02	0.0000D+00	0.0000D+00
4	0.0000D+00	0.0000D+00	0.0000D+00	0.0000D+00	0.0000D+00
5	0.0000D+00	0.0000D+00	0.0000D+00	0.0000D+00	0.0000D+00

RCST(8)

	1	2	3	4	5
1	0.0000D+00	0.0000D+00	0.0000D+00	0.0000D+00	0.0000D+00
2	0.0000D+00	0.0000D+00	0.0000D+00	0.0000D+00	0.0000D+00
3	0.0000D+00	0.0000D+00	1.9772D-02	0.0000D+00	0.0000D+00
4	0.0000D+00	0.0000D+00	0.0000D+00	0.0000D+00	0.0000D+00
5	0.0000D+00	0.0000D+00	0.0000D+00	0.0000D+00	0.0000D+00

ALPHA TABLE
(A 1(0) AT POSITION I,J INDICATES THAT THE JTH FEEDBACK
MATRIX IS ACTIVE(INACTIVE) DURING THE ITH STP.)

1
1
1
1
1
1
1

1

NOGRDF(1)
(A 1(0) INDICATES THAT THE CORRESPONDING ELEMENT OF FGM(1)
IS UNCONSTRAINED(CONSTRAINED TO BE FIXED))

```
 1 0 1 0 0 0 1 1
 1 0 0 0 0 0 1 0
 0 0 1 0 0 0 0 1
 0 0 0 0 0 0 1 0
 0 0 0 0 0 0 0 1
```

FGM(1)

	1	2	3	4	5	6	7	8
1	1.1297D+01	0.0000D+00	3.9316D-01	0.0000D+00	0.0000D+00	0.0000D+00	-1.3483D+01	1.0708D+00
2	9.7632D-02	0.0000D+00	0.0000D+00	0.0000D+00	0.0000D+00	0.0000D+00	-1.2129D-01	0.0000D+00
3	0.0000D+00	0.0000D+00	1.3439D+01	0.0000D+00	0.0000D+00	0.0000D+00	0.0000D+00	-1.6865D+01
4	0.0000D+00	0.0000D+00	0.0000D+00	0.0000D+00	0.0000D+00	0.0000D+00	4.8499D-01	0.0000D+00
5	0.0000D+00	0.0000D+00	0.0000D+00	0.0000D+00	0.0000D+00	0.0000D+00	0.0000D+00	5.5327D-01

Page 23 of Example AMS Output File

```
**********************************************************
*                                                        *
*  QNMDER STATISTICS FOR NN=   10000  ITERATION   1     *
*                                                        *
**********************************************************

CONVERGENCE PARAMETER=  2.47637D-05
COST= 6.9047024369417247D-02
NUMBER OF COST EVALUATIONS=   3
NUMBER OF GRADIENT EVALUATIONS=   3
LINEAR SEARCH STEP SIZE=  1.72704D-06
PERCENT COST REDUCTION=  6.95304D-10

FGM( 1)

          1          2          3          4          5          6          7          8
1  1.1297D+01 0.0000D+00 3.9316D-01 0.0000D+00 0.0000D+00 0.0000D+00 -1.3483D+01 1.0708D+00
2  9.7632D-02 0.0000D+00 0.0000D+00 0.0000D+00 0.0000D+00 0.0000D+00 -1.2129D-01 0.0000D+00
3  0.0000D+00 0.0000D+00 1.3439D+01 0.0000D+00 0.0000D+00 0.0000D+00 0.0000D+00 -1.6865D+01
4  0.0000D+00 0.0000D+00 0.0000D+00 0.0000D+00 0.0000D+00 0.0000D+00 4.8499D-01 0.0000D+00
5  0.0000D+00 0.0000D+00 0.0000D+00 0.0000D+00 0.0000D+00 0.0000D+00 0.0000D+00 5.5327D-01

GRDF( 1)

          1          2          3          4          5          6          7          8
1 -6.5940D-08 0.0000D+00 1.0278D-09 0.0000D+00 0.0000D+00 0.0000D+00 -4.4724D-08 5.3800D-10
2  3.8606D-08 0.0000D+00 0.0000D+00 0.0000D+00 0.0000D+00 0.0000D+00 3.8849D-08 0.0000D+00
3  0.0000D+00 0.0000D+00 -1.2723D-07 0.0000D+00 0.0000D+00 0.0000D+00 0.0000D+00 -6.3859D-08
4  0.0000D+00 0.0000D+00 0.0000D+00 0.0000D+00 0.0000D+00 0.0000D+00 -3.3318D-07 0.0000D+00
5  0.0000D+00 0.0000D+00 0.0000D+00 0.0000D+00 0.0000D+00 0.0000D+00 0.0000D+00 -4.1106D-07

GNORM( 1)

          1          2          3          4          5          6          7          8
1 -1.0789D-05 0.0000D+00 5.8522D-09 0.0000D+00 0.0000D+00 0.0000D+00 8.7334D-06 8.3434D-09
2  5.4589D-08 0.0000D+00 0.0000D+00 0.0000D+00 0.0000D+00 0.0000D+00 -6.8244D-08 0.0000D+00
3  0.0000D+00 0.0000D+00 -2.4764D-05 0.0000D+00 0.0000D+00 0.0000D+00 0.0000D+00 1.5598D-05
4  0.0000D+00 0.0000D+00 0.0000D+00 0.0000D+00 0.0000D+00 0.0000D+00 -2.3403D-06 0.0000D+00
5  0.0000D+00 0.0000D+00 0.0000D+00 0.0000D+00 0.0000D+00 0.0000D+00 0.0000D+00 -3.2938D-06
```

Page 24 of Example AMS Output File

```
**********************************************************
*                                                        *
*  QNMDER STATISTICS FOR NN=   10000  ITERATION   2     *
*                                                        *
**********************************************************

CONVERGENCE PARAMETER=  1.30228D-05
COST= 6.9047024368937161D-02
NUMBER OF COST EVALUATIONS=   6
NUMBER OF GRADIENT EVALUATIONS=   6
LINEAR SEARCH STEP SIZE=  4.67128D-06
PERCENT COST REDUCTION=  1.05897D-09
```

FGM(1)

	1	2	3	4	5	6	7	8
1	1.1297D+01	0.0000D+00	3.9316D-01	0.0000D+00	0.0000D+00	0.0000D+00	-1.3483D+01	1.0708D+00
2	9.7632D-02	0.0000D+00	0.0000D+00	0.0000D+00	0.0000D+00	0.0000D+00	-1.2129D-01	0.0000D+00
3	0.0000D+00	0.0000D+00	1.3439D+01	0.0000D+00	0.0000D+00	0.0000D+00	0.0000D+00	-1.6865D+01
4	0.0000D+00	0.0000D+00	0.0000D+00	0.0000D+00	0.0000D+00	0.0000D+00	4.8499D-01	0.0000D+00
5	0.0000D+00	0.0000D+00	0.0000D+00	0.0000D+00	0.0000D+00	0.0000D+00	0.0000D+00	5.5327D-01

GRDF(1)

	1	2	3	4	5	6	7	8
1	-5.8243D-08	0.0000D+00	5.8517D-10	0.0000D+00	0.0000D+00	0.0000D+00	-3.8098D-08	2.3780D-10
2	1.0097D-08	0.0000D+00	0.0000D+00	0.0000D+00	0.0000D+00	0.0000D+00	2.5627D-08	0.0000D+00
3	0.0000D+00	0.0000D+00	-6.6909D-08	0.0000D+00	0.0000D+00	0.0000D+00	0.0000D+00	-1.3731D-08
4	0.0000D+00	0.0000D+00	0.0000D+00	0.0000D+00	0.0000D+00	0.0000D+00	-2.6213D-07	0.0000D+00
5	0.0000D+00	0.0000D+00	0.0000D+00	0.0000D+00	0.0000D+00	0.0000D+00	0.0000D+00	2.5277D-07

GNORM(1)

	1	2	3	4	5	6	7	8
1	-9.5296D-06	0.0000D+00	3.3320D-09	0.0000D+00	0.0000D+00	0.0000D+00	7.4394D-06	3.6878D-09
2	1.4277D-08	0.0000D+00	0.0000D+00	0.0000D+00	0.0000D+00	0.0000D+00	-4.5017D-08	0.0000D+00
3	0.0000D+00	0.0000D+00	-1.3023D-05	0.0000D+00	0.0000D+00	0.0000D+00	0.0000D+00	3.3537D-06
4	0.0000D+00	0.0000D+00	0.0000D+00	0.0000D+00	0.0000D+00	0.0000D+00	-1.8412D-06	0.0000D+00
5	0.0000D+00	0.0000D+00	0.0000D+00	0.0000D+00	0.0000D+00	0.0000D+00	0.0000D+00	2.0254D-06

Page 25 of Example AMS Output File

```
**********************************************************
*                                                        *
*  QNMDER STATISTICS FOR NN=   10000  ITERATION   3     *
*                                                        *
**********************************************************

CONVERGENCE PARAMETER=  1.61995D-05
COST= 6.90470243682O5973D-02
NUMBER OF COST EVALUATIONS=  10
NUMBER OF GRADIENT EVALUATIONS=  10
LINEAR SEARCH STEP SIZE=  3.29654D-06
PERCENT COST REDUCTION=  2.51288D-10
```

FGM(1)

	1	2	3	4	5	6	7	8
1	1.1297D+01	0.0000D+00	3.9316D-01	0.0000D+00	0.0000D+00	0.0000D+00	-1.3483D+01	1.0708D+00
2	9.7631D-02	0.0000D+00	0.0000D+00	0.0000D+00	0.0000D+00	0.0000D+00	-1.2129D-01	0.0000D+00
3	0.0000D+00	0.0000D+00	1.3439D+01	0.0000D+00	0.0000D+00	0.0000D+00	0.0000D+00	-1.6865D+01
4	0.0000D+00	0.0000D+00	0.0000D+00	0.0000D+00	0.0000D+00	0.0000D+00	4.8500D-01	0.0000D+00
5	0.0000D+00	0.0000D+00	0.0000D+00	0.0000D+00	0.0000D+00	0.0000D+00	0.0000D+00	5.5327D-01

GRDF(1)

	1	2	3	4	5	6	7	8
1	-2.7305D-08	0.0000D+00	8.7820D-10	0.0000D+00	0.0000D+00	0.0000D+00	-1.1057D-08	4.4267D-10
2	-5.6907D-08	0.0000D+00	0.0000D+00	0.0000D+00	0.0000D+00	0.0000D+00	-1.9219D-08	0.0000D+00
3	0.0000D+00	0.0000D+00	-8.3230D-08	0.0000D+00	0.0000D+00	0.0000D+00	0.0000D+00	-2.9995D-08
4	0.0000D+00	0.0000D+00	0.0000D+00	0.0000D+00	0.0000D+00	0.0000D+00	2.9651D-08	0.0000D+00
5	0.0000D+00	0.0000D+00	0.0000D+00	0.0000D+00	0.0000D+00	0.0000D+00	0.0000D+00	-7.2242D-10

GNORM(1)

	1	2	3	4	5	6	7	8
1	-4.4677D-06	0.0000D+00	5.0005D-09	0.0000D+00	0.0000D+00	0.0000D+00	2.1590D-06	6.8650D-09
2	-8.0466D-08	0.0000D+00	0.0000D+00	0.0000D+00	0.0000D+00	0.0000D+00	3.3761D-08	0.0000D+00
3	0.0000D+00	0.0000D+00	-1.6199D-05	0.0000D+00	0.0000D+00	0.0000D+00	0.0000D+00	7.3264D-06
4	0.0000D+00	0.0000D+00	0.0000D+00	0.0000D+00	0.0000D+00	0.0000D+00	2.0827D-07	0.0000D+00
5	0.0000D+00	0.0000D+00	0.0000D+00	0.0000D+00	0.0000D+00	0.0000D+00	0.0000D+00	-5.7888D-09

```
**********************************************************
*                                                        *
*  QNMDER STATISTICS FOR NN=   10000  ITERATION   4      *
*                                                        *
**********************************************************

CONVERGENCE PARAMETER=  1.15368D-05
COST= 6.9047024368032466D-02
NUMBER OF COST EVALUATIONS=  12
NUMBER OF GRADIENT EVALUATIONS=  12
LINEAR SEARCH STEP SIZE=  1.41159D-06
PERCENT COST REDUCTION=  1.01874D-10

FGM( 1)

          1           2           3           4           5           6           7           8
1  1.1297D+01  0.0000D+00  3.9316D-01  0.0000D+00  0.0000D+00  0.0000D+00 -1.3483D+01  1.0708D+00
2  9.7633D-02  0.0000D+00  0.0000D+00  0.0000D+00  0.0000D+00  0.0000D+00 -1.2129D-01  0.0000D+00
3  0.0000D+00  0.0000D+00  1.3439D+01  0.0000D+00  0.0000D+00  0.0000D+00  0.0000D+00 -1.6865D+01
4  0.0000D+00  0.0000D+00  0.0000D+00  0.0000D+00  0.0000D+00  0.0000D+00  4.8500D-01  0.0000D+00
5  0.0000D+00  0.0000D+00  0.0000D+00  0.0000D+00  0.0000D+00  0.0000D+00  0.0000D+00  5.5327D-01

GRDF( 1)

          1           2           3           4           5           6           7           8
1 -2.4289D-08  0.0000D+00  8.0967D-10  0.0000D+00  0.0000D+00  0.0000D+00 -8.5083D-09  4.0883D-10
2  9.7452D-08  0.0000D+00  0.0000D+00  0.0000D+00  0.0000D+00  0.0000D+00  8.3942D-08  0.0000D+00
3  0.0000D+00  0.0000D+00 -5.9274D-08  0.0000D+00  0.0000D+00  0.0000D+00  0.0000D+00 -1.4979D-08
4  0.0000D+00  0.0000D+00  0.0000D+00  0.0000D+00  0.0000D+00  0.0000D+00  6.2237D-08  0.0000D+00
5  0.0000D+00  0.0000D+00  0.0000D+00  0.0000D+00  0.0000D+00  0.0000D+00  0.0000D+00  1.3051D-07

GNORM( 1)

          1           2           3           4           5           6           7           8
1 -3.9741D-06  0.0000D+00  4.6103D-09  0.0000D+00  0.0000D+00  0.0000D+00  1.6614D-06  6.3402D-09
2  1.3780D-07  0.0000D+00  0.0000D+00  0.0000D+00  0.0000D+00  0.0000D+00 -1.4745D-07  0.0000D+00
3  0.0000D+00  0.0000D+00 -1.1537D-05  0.0000D+00  0.0000D+00  0.0000D+00  0.0000D+00  3.6587D-06
4  0.0000D+00  0.0000D+00  0.0000D+00  0.0000D+00  0.0000D+00  0.0000D+00  4.3716D-07  0.0000D+00
5  0.0000D+00  0.0000D+00  0.0000D+00  0.0000D+00  0.0000D+00  0.0000D+00  0.0000D+00  1.0458D-06
```

Page 27 of Example AMS Output File

```
**********************************************************
*                                                        *
*  QNMDER STATISTICS FOR NN=   10000  ITERATION   5      *
*                                                        *
**********************************************************

CONVERGENCE PARAMETER=  1.46198D-05
COST= 6.9047024367962125D-02
NUMBER OF COST EVALUATIONS=  15
NUMBER OF GRADIENT EVALUATIONS=  15
LINEAR SEARCH STEP SIZE=  1.49819D-05
PERCENT COST REDUCTION=  1.14138D-09

FGM( 1)

          1           2           3           4           5           6           7           8
1  1.1297D+01  0.0000D+00  3.9316D-01  0.0000D+00  0.0000D+00  0.0000D+00 -1.3483D+01  1.0708D+00
2  9.7633D-02  0.0000D+00  0.0000D+00  0.0000D+00  0.0000D+00  0.0000D+00 -1.2129D-01  0.0000D+00
3  0.0000D+00  0.0000D+00  1.3439D+01  0.0000D+00  0.0000D+00  0.0000D+00  0.0000D+00 -1.6865D+01
4  0.0000D+00  0.0000D+00  0.0000D+00  0.0000D+00  0.0000D+00  0.0000D+00  4.8500D-01  0.0000D+00
5  0.0000D+00  0.0000D+00  0.0000D+00  0.0000D+00  0.0000D+00  0.0000D+00  0.0000D+00  5.5327D-01

GRDF( 1)

          1           2           3           4           5           6           7           8
1 -2.6926D-08  0.0000D+00  9.6745D-10  0.0000D+00  0.0000D+00  0.0000D+00 -1.0879D-08  5.2206D-10
2  1.3739D-07  0.0000D+00  0.0000D+00  0.0000D+00  0.0000D+00  0.0000D+00  1.0721D-07  0.0000D+00
3  0.0000D+00  0.0000D+00 -7.5114D-08  0.0000D+00  0.0000D+00  0.0000D+00  0.0000D+00 -3.0436D-08
4  0.0000D+00  0.0000D+00  0.0000D+00  0.0000D+00  0.0000D+00  0.0000D+00  3.6294D-08  0.0000D+00
5  0.0000D+00  0.0000D+00  0.0000D+00  0.0000D+00  0.0000D+00  0.0000D+00  0.0000D+00 -1.0595D-07

GNORM( 1)

          1           2           3           4           5           6           7           8
1 -4.4057D-06  0.0000D+00  5.5087D-09  0.0000D+00  0.0000D+00  0.0000D+00  2.1244D-06  8.0962D-09
2  1.9427D-07  0.0000D+00  0.0000D+00  0.0000D+00  0.0000D+00  0.0000D+00 -1.8833D-07  0.0000D+00
3  0.0000D+00  0.0000D+00 -1.4620D-05  0.0000D+00  0.0000D+00  0.0000D+00  0.0000D+00  7.4341D-06
4  0.0000D+00  0.0000D+00  0.0000D+00  0.0000D+00  0.0000D+00  0.0000D+00  2.5493D-07  0.0000D+00
5  0.0000D+00  0.0000D+00  0.0000D+00  0.0000D+00  0.0000D+00  0.0000D+00  0.0000D+00 -8.4896D-07
```

Page 28 of Example AMS Output File

```
**************************************************
* QNMDER HAS SATISFIED THE TEST FOR CONVERGENCE *
**************************************************
```

Page 29 of Example AMS Output File

```
*********************************************
*                                           *
*  FINAL QNMDER STATISTICS FOR NN=   10000  *
*                                           *
*********************************************

CONVERGENCE PARAMETER=  3.96248D-06
COST= 6.9047024367174034D-02
```

FGM(1)

	1	2	3	4	5	6	7	8
1	1.1297D+01	0.0000D+00	3.9316D-01	0.0000D+00	0.0000D+00	0.0000D+00	-1.3483D+01	1.0708D+00
2	9.7634D-02	0.0000D+00	0.0000D+00	0.0000D+00	0.0000D+00	0.0000D+00	-1.2129D-01	0.0000D+00
3	0.0000D+00	0.0000D+00	1.3439D+01	0.0000D+00	0.0000D+00	0.0000D+00	0.0000D+00	-1.6865D+01
4	0.0000D+00	0.0000D+00	0.0000D+00	0.0000D+00	0.0000D+00	0.0000D+00	4.8500D-01	0.0000D+00
5	0.0000D+00	0.0000D+00	0.0000D+00	0.0000D+00	0.0000D+00	0.0000D+00	0.0000D+00	5.5327D-01

GRDF(1)

	1	2	3	4	5	6	7	8
1	-2.4218D-08	0.0000D+00	8.3609D-10	0.0000D+00	0.0000D+00	0.0000D+00	-1.0283D-08	5.0340D-10
2	1.9081D-08	0.0000D+00	0.0000D+00	0.0000D+00	0.0000D+00	0.0000D+00	7.6964D-09	0.0000D+00
3	0.0000D+00	0.0000D+00	-3.6172D-09	0.0000D+00	0.0000D+00	0.0000D+00	0.0000D+00	3.9489D-09
4	0.0000D+00	0.0000D+00	0.0000D+00	0.0000D+00	0.0000D+00	0.0000D+00	9.6670D-09	0.0000D+00
5	0.0000D+00	0.0000D+00	0.0000D+00	0.0000D+00	0.0000D+00	0.0000D+00	0.0000D+00	1.7738D-09

GNORM(1)

	1	2	3	4	5	6	7	8
1	-3.9625D-06	0.0000D+00	4.7607D-09	0.0000D+00	0.0000D+00	0.0000D+00	2.0080D-06	7.8067D-09
2	2.6981D-08	0.0000D+00	0.0000D+00	0.0000D+00	0.0000D+00	0.0000D+00	-1.3520D-08	0.0000D+00
3	0.0000D+00	0.0000D+00	-7.0403D-07	0.0000D+00	0.0000D+00	0.0000D+00	0.0000D+00	-9.6453D-07
4	0.0000D+00	0.0000D+00	0.0000D+00	0.0000D+00	0.0000D+00	0.0000D+00	6.7902D-08	0.0000D+00
5	0.0000D+00	0.0000D+00	0.0000D+00	0.0000D+00	0.0000D+00	0.0000D+00	0.0000D+00	1.4214D-08

Page 30 of Example AMS Output File

FINAL CLOSED-LOOP BTP EIGENVALUES

Z-PLANE		EQUIVALENT S-PLANE (TSEC=2.2500D-01)			
REAL	IMAGINARY	REAL	IMAGINARY	DAMPING	FREQUENCY (HZ)
0.0000D+00	0.0000D+00				
0.0000D+00	0.0000D+00				
5.1923D-01	2.9022D-01	-2.3088D+00	2.2652D+00	0.7138	5.1478D-01
5.1923D-01	-2.9022D-01	-2.3088D+00	-2.2652D+00	0.7138	5.1478D-01
-1.4307D-01	0.0000D+00	-8.6417D+00	1.3963D+01	0.5263	2.6134D+00
-8.5297D-03	1.8911D-02	-1.7224D+01	8.8646D+00	0.8892	3.0831D+00
-8.5297D-03	-1.8911D-02	-1.7224D+01	-8.8646D+00	0.8892	3.0831D+00
4.7643D-04	0.0000D+00	-3.3996D+01	0.0000D+00	1.0000	5.4107D+00

Page 1 of Example AMS Save File

1.12974D+01	0.00000D+00	3.93156D-01	0.00000D+00	0.00000D+00	0.00000D+00
-1.34829D+01	1.07079D+00				
9.76338D-02	0.00000D+00	0.00000D+00	0.00000D+00	0.00000D+00	0.00000D+00
-1.21293D-01	0.00000D+00				
0.00000D+00	0.00000D+00	1.34390D+01	0.00000D+00	0.00000D+00	0.00000D+00
0.00000D+00	-1.68650D+01				
0.00000D+00	0.00000D+00	0.00000D+00	0.00000D+00	0.00000D+00	0.00000D+00
4.84996D-01	0.00000D+00				
0.00000D+00	0.00000D+00	0.00000D+00	0.00000D+00	0.00000D+00	0.00000D+00
0.00000D+00	5.53271D-01				
8.85581D-01	3.98000D-01	1.00000D+00	1.00000D+00	1.00000D+00	1.00000D+00
1.00000D+00	1.00000D+00	1.00000D+00	1.00000D+00	9.99901D-01	1.00000D+00
1.49946D-01	1.00000D+00	1.00000D+00	1.00000D+00	1.00000D+00	1.00000D+00
1.00000D+00	1.00000D+00	1.00000D+00	1.00000D+00	1.00000D+00	1.00000D+00
1.00000D+00	1.00000D+00	1.00000D+00	1.00000D+00	1.00000D+00	1.00000D+00
8.28603D-01	3.18379D-01	1.00000D+00	6.79913D-02	1.00000D+00	9.99773D-01
1.00000D+00	9.01485D-02	1.00000D+00	2.41873D-01		
-1.17934D-02	0.00000D+00	0.00000D+00	0.00000D+00	0.00000D+00	0.00000D+00
0.00000D+00	0.00000D+00	0.00000D+00	0.00000D+00	0.00000D+00	0.00000D+00
0.00000D+00	0.00000D+00	0.00000D+00	0.00000D+00	0.00000D+00	0.00000D+00
0.00000D+00	0.00000D+00	0.00000D+00	0.00000D+00	0.00000D+00	0.00000D+00
0.00000D+00	0.00000D+00	0.00000D+00	0.00000D+00	0.00000D+00	0.00000D+00
0.00000D+00	0.00000D+00	0.00000D+00	0.00000D+00	0.00000D+00	0.00000D+00
0.00000D+00	0.00000D+00	0.00000D+00	0.00000D+00	0.00000D+00	0.00000D+00
0.00000D+00	0.00000D+00	0.00000D+00	3.38633D-03	8.15820D-04	0.00000D+00
0.00000D+00	0.00000D+00	0.00000D+00	0.00000D+00	0.00000D+00	0.00000D+00
0.00000D+00	0.00000D+00	0.00000D+00	0.00000D+00	0.00000D+00	0.00000D+00
0.00000D+00	0.00000D+00	0.00000D+00	0.00000D+00	0.00000D+00	0.00000D+00
-3.16868D-01	-2.23406D-01	0.00000D+00	0.00000D+00	0.00000D+00	0.00000D+00
0.00000D+00	0.00000D+00	0.00000D+00	0.00000D+00	9.10414D-03	0.00000D+00
0.00000D+00	0.00000D+00	0.00000D+00	0.00000D+00	0.00000D+00	0.00000D+00
0.00000D+00	0.00000D+00	0.00000D+00	0.00000D+00	0.00000D+00	0.00000D+00
0.00000D+00	0.00000D+00	0.00000D+00	0.00000D+00	0.00000D+00	0.00000D+00
0.00000D+00	0.00000D+00	0.00000D+00	0.00000D+00	0.00000D+00	0.00000D+00
0.00000D+00	0.00000D+00	0.00000D+00	0.00000D+00	0.00000D+00	0.00000D+00
0.00000D+00	0.00000D+00	0.00000D+00	0.00000D+00	0.00000D+00	0.00000D+00
0.00000D+00	0.00000D+00	0.00000D+00	0.00000D+00	0.00000D+00	0.00000D+00
0.00000D+00	0.00000D+00	0.00000D+00	0.00000D+00	0.00000D+00	0.00000D+00
0.00000D+00	0.00000D+00	0.00000D+00	0.00000D+00	0.00000D+00	0.00000D+00
0.00000D+00	0.00000D+00	0.00000D+00	0.00000D+00	0.00000D+00	0.00000D+00
0.00000D+00	0.00000D+00	0.00000D+00	0.00000D+00	0.00000D+00	0.00000D+00
0.00000D+00	0.00000D+00	0.00000D+00	0.00000D+00	0.00000D+00	0.00000D+00
0.00000D+00	0.00000D+00	0.00000D+00	0.00000D+00	0.00000D+00	0.00000D+00
0.00000D+00	0.00000D+00	0.00000D+00	0.00000D+00	0.00000D+00	0.00000D+00
0.00000D+00	0.00000D+00	0.00000D+00	0.00000D+00	0.00000D+00	0.00000D+00
0.00000D+00	0.00000D+00	0.00000D+00	0.00000D+00	0.00000D+00	0.00000D+00

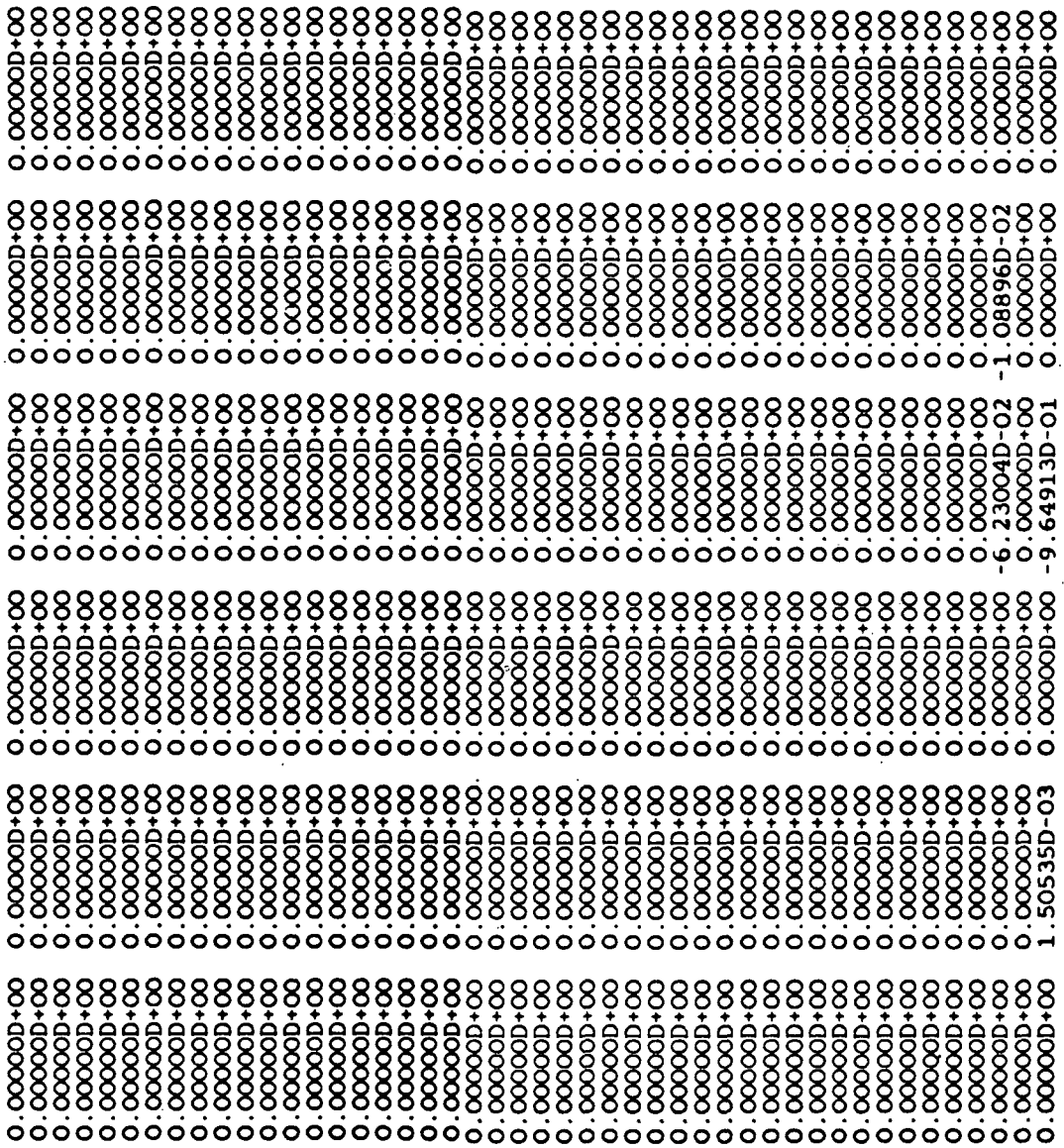
Page 2 of Example AMS Save File

Page 3 of Example AMS Save File

```
0.00000D+00  0.00000D+00  0.00000D+00  0.00000D+00  0.00000D+00  0.00000D+00
0.00000D+00  0.00000D+00  0.00000D+00  0.00000D+00  0.00000D+00  0.00000D+00
0.00000D+00  0.00000D+00  0.00000D+00  6.37469D-02 -9.69060D-01  0.00000D+00
0.00000D+00  0.00000D+00  0.00000D+00  0.00000D+00  0.00000D+00  0.00000D+00
0.00000D+00 -1.54190D-03  0.00000D+00  2.87716D-01  0.00000D+00  0.00000D+00
0.00000D+00  0.00000D+00  0.00000D+00  0.00000D+00  0.00000D+00  0.00000D+00
0.00000D+00  0.00000D+00  0.00000D+00  0.00000D+00  0.00000D+00  0.00000D+00
0.00000D+00  0.00000D+00  0.00000D+00  8.02381D-02  0.00000D+00  0.00000D+00
0.00000D+00  0.00000D+00  0.00000D+00  0.00000D+00  0.00000D+00  0.00000D+00
0.00000D+00  0.00000D+00  0.00000D+00  0.00000D+00  0.00000D+00  0.00000D+00
0.00000D+00  0.00000D+00  0.00000D+00  0.00000D+00  0.00000D+00  0.00000D+00
0.00000D+00  0.00000D+00  0.00000D+00  0.00000D+00  0.00000D+00  0.00000D+00
0.00000D+00  0.00000D+00  0.00000D+00  0.00000D+00  0.00000D+00  0.00000D+00
-7.78171D-02  8.11436D-03  0.00000D+00  0.00000D+00  0.00000D+00  0.00000D+00
0.00000D+00  0.00000D+00  0.00000D+00  0.00000D+00 -9.49041D-04  0.00000D+00
9.46933D-02  0.00000D+00  0.00000D+00  0.00000D+00  0.00000D+00  0.00000D+00
0.00000D+00  0.00000D+00  0.00000D+00  0.00000D+00  0.00000D+00  0.00000D+00
0.00000D+00  0.00000D+00  0.00000D+00  0.00000D+00  0.00000D+00  0.00000D+00
-7.53154D-02 -2.85403D-02  0.00000D+00  0.00000D+00  0.00000D+00  0.00000D+00
0.00000D+00  0.00000D+00  0.00000D+00  0.00000D+00  0.00000D+00  0.00000D+00
0.00000D+00  0.00000D+00  0.00000D+00  0.00000D+00  0.00000D+00  0.00000D+00
0.00000D+00  0.00000D+00  0.00000D+00  0.00000D+00  0.00000D+00  0.00000D+00
0.00000D+00  0.00000D+00  0.00000D+00  0.00000D+00  0.00000D+00  0.00000D+00
0.00000D+00  0.00000D+00  0.00000D+00  0.00000D+00  0.00000D+00  0.00000D+00
0.00000D+00  1.70167D-03  2.43832D-04  0.00000D+00  0.00000D+00  0.00000D+00
0.00000D+00  0.00000D+00  0.00000D+00  0.00000D+00  0.00000D+00 -5.03107D-05
0.00000D+00  3.05957D-02  0.00000D+00  0.00000D+00  0.00000D+00  0.00000D+00
0.00000D+00  0.00000D+00  0.00000D+00  0.00000D+00  0.00000D+00  0.00000D+00
0.00000D+00  0.00000D+00  0.00000D+00  0.00000D+00  0.00000D+00  0.00000D+00
0.00000D+00  6.24896D-03 -8.24501D-03  0.00000D+00 -1.03295D-02  0.00000D+00
0.00000D+00  0.00000D+00  0.00000D+00  0.00000D+00  0.00000D+00  0.00000D+00
0.00000D+00  0.00000D+00  0.00000D+00  0.00000D+00  0.00000D+00  0.00000D+00
0.00000D+00  0.00000D+00  0.00000D+00  0.00000D+00  0.00000D+00  0.00000D+00
0.00000D+00  0.00000D+00  0.00000D+00  0.00000D+00  0.00000D+00  0.00000D+00
0.00000D+00  0.00000D+00  0.00000D+00  0.00000D+00  0.00000D+00  0.00000D+00
0.00000D+00  0.00000D+00  0.00000D+00  0.00000D+00  0.00000D+00  0.00000D+00
-1.12038D-01 -8.82549D-02  0.00000D+00  0.00000D+00  0.00000D+00  0.00000D+00
0.00000D+00  0.00000D+00  0.00000D+00  0.00000D+00  3.22818D-03  0.00000D+00
-2.01716D+00  0.00000D+00  0.00000D+00  0.00000D+00  0.00000D+00  0.00000D+00
0.00000D+00  0.00000D+00  0.00000D+00  0.00000D+00  0.00000D+00  0.00000D+00
0.00000D+00  0.00000D+00  0.00000D+00  0.00000D+00  0.00000D+00  0.00000D+00
-4.14142D-01  3.87361D-01  0.00000D+00  1.27504D-01  0.00000D+00  1.41367D-02
0.00000D+00  0.00000D+00  0.00000D+00  0.00000D+00  0.00000D+00  0.00000D+00
0.00000D+00  0.00000D+00  0.00000D+00  0.00000D+00  0.00000D+00  0.00000D+00
0.00000D+00  0.00000D+00  0.00000D+00  0.00000D+00  0.00000D+00  0.00000D+00
0.00000D+00  0.00000D+00  0.00000D+00  0.00000D+00  0.00000D+00  0.00000D+00
```

Page 4 of Example AMS Save File

```
 0.00000D+00  0.00000D+00  0.00000D+00  0.00000D+00  0.00000D+00  0.00000D+00
 0.00000D+00  0.00000D+00  0.00000D+00  0.00000D+00  0.00000D+00  0.00000D+00
 0.00000D+00  0.00000D+00  0.00000D+00  3.40278D-02  2.44561D-02  0.00000D+00
 0.00000D+00  0.00000D+00  0.00000D+00  0.00000D+00  0.00000D+00  0.00000D+00
 0.00000D+00 -6.20595D-04  0.00000D+00  3.54077D-01  0.00000D+00  0.00000D+00
 0.00000D+00  0.00000D+00  0.00000D+00  0.00000D+00  0.00000D+00  0.00000D+00
 0.00000D+00  0.00000D+00  0.00000D+00  0.00000D+00  0.00000D+00  0.00000D+00
 0.00000D+00  0.00000D+00  0.00000D+00  8.06834D-02 -9.66875D-02  0.00000D+00
-2.98309D-02  0.00000D+00 -2.56180D-03  0.00000D+00  1.61082D+00  0.00000D+00
```

References

1. Albanes, W., *"Design of Guidance and Control Digital Autopilots"*, AIAA Journal of Guidance and Control, Vol. 4, No. 2, March-April 1981.

2. Amit, N., *"Optimal Control of Multirate Digital Control Systems"*, Ph. D. Thesis, Stanford University Department of Aeronautics and Astronautics, Stanford, California, SUDAAR No. 523, July 1980.

3. Amit, N. and Powell, J. D., *"Optimal Control of Mutirate Systems"*, Proceedings of the AIAA Guidance and Control Conference, Albuquerque, New Mexico, Paper No. 81-1797, August 1981.

4. Broussard, J. R. and Halyo, N., *"Optimal Multi-Rate Output Feedback"*, Proceedings of the 23rd Conference on Decision and Control, Las Vegas, Nevada, December 1984.

5. Bryson, Jr., A. E. and Ho, Y. C., Applied Optimal Control, Hemisphere Publishing Company, Washington, D. C., 1975.

6. Bryson, Jr., A. E., Personal Communications, March 1986.

7. Chiang, W. W., *"Rapid Precise End Point Control of a Wrist Carried by a Flexible Manipulator"*, Ph. D. Thesis, Stanford University Department of Aeronautics and Astronautics, Stanford, California, SUDAAR No. 550, Work in Progress.

8. Chrétien, J. P., Reboulet, C., Rodrigo, P. and Maurette, M., *"Attitude Control of a Satellite with a Rotating Solar Array"*, AIAA Journal of Guidance and

Control, Vol. 5, No 6, November-December 1982.

9. Franklin, G. F. and Powell, J. D., Digital Control of Dynamic Systems, Addison-Wesley Publishing Company, Reading, Massachusetts, 1980.

10. Gill, P. E. and Murray, W., *"Quasi-Newton Methods for Unconstrained Optimization"*, Journal of Mathematics and Its Applications, Vol. 9, 1972.

11. Gill, P. E., Murray, W. and Wright, M., Practical Optimization, Academic Press, 1981.

12. Glasson, D. P. and Broussard, J. R., *"Design of Optimal Multirate Estimators and Controllers—Preliminary Results"*, Report No. TIM-1356-1, The Analytical Sciences Corporation, Reading, Massachusetts, 1979.

13. Glasson, D. P., *"Research in Multirate Estimation and Control"*, Report No. TR-1356-1, The Analytic Sciences Corporation, Reading, Massachusetts, 1980.

14. Glasson, D. P. and Dowd, J., *"Research in Multirate Estimation and Control Sample Rate Selection"*, Report No. TR-1356-2, The Analytic Sciences Corporation, Reading, Massachusetts, 1981.

15. Glasson, D. P., *"A New Technique for Multirate Digital Control Design and Sample Rate Selection"*, AIAA Journal of Guidance and Control, Vol. 5, July-August 1982.

16. Gradshteyn, I. S. and Ryzhik, I. M., Table of Integrals, Series and Products, Academic Press, New York, 1980.

17. Johnson, T. L. and Athans, M., *"On the Design of Optimal Constrained Dynamic Compensators for Linear Constant Systems"*, IEEE Transactions on Automatic Control, Vol. AC-15, December 1970.

18. Kalman, R. E. and Bertram, J., *"A Unified Approach to the Theory of Sampling Systems"*, Journal of the Franklin Institute, Vol. 267, May 1959.

19. Kane, T. R., Dynamics, Published by T. R. Kane, Stanford University, Stanford, California, 1972.

20. Katz, P., *"Selection of Sampling Rate for Digital Control of Aircrafts"*, Ph. D. Thesis, Stanford University Department of Aeronautics and Astronautics, Stanford, California, SUDAAR No. 486, September 1974.

21. Kleinman, D. L., Fortman, T. and Athans, M., *"On the Design of Linear Systems with Piecewise-Constant Feedback Gains"*, IEEE Transactions on Automatic Control, Vol. AC-13, No. 4, August 1968.

22. Kranc, G. M., *"The Analysis of Multiple-Rate Sampled Systems"*, Technical Report T-11/B, Electronics Research Lab., Department of Electrical Engineering, Columbia University, New York, November 1955.

23. Kranc, G. M., *"Multirate Sampled Systems"*, Technical Report T-14/B, Electronics Research Lab., Department of Electrical Engineering, Columbia University, New York, May 1956.

24. Kranc, G. M., *"Compensation of an Error Sampled System by a Multirate Controller"*, Part II, AIEE Transactions, Vol. 76, July 1957.

25. Kranc, G. M., *"Input-Output Analysis of Multirate Feedback Systems"*, IRE Transactions on Automatic Control, Vol. AC-3, November 1957.

26. Kranc, G. M., *"Additional Techniques for Sampled Data Feedback Problems"*, 1957 IRE Wescon Convention Record, Part IV, 1957.

27. Levine, W. S. and Athans, M., *"On the Determination of the Optimal Constant Output Feedback Gains for Linear Multivariable Systems"*, IEEE Transactions on Automatic Control, Vol. AC-15, February 1970.

28. Ly, U. L., *"A Design Algorithm for Robust Low-Order Controllers"*, Ph. D. Thesis, Stanford University Department of Aeronautics and Astronautics, Stanford, California, SUDAAR No. 536, November 1982.

29. Parsons, E., *"Efficient Sampling Rates for Digital Controllers and Pointing Systems with Digital Solid-State Dectectors,"* Ph. D. Thesis, Stanford University Department of Aeronautics and Astronautics, Stanford, California, SUDAAR No. 533, June 1982.

30. Penchuk, A. and Croopnik, S., *"Digital Autopilot for Thrust Vector Control of the Shuttle Orbital Maneuvering System"*, AIAA Journal of Guidance and Control, Vol. 6, No. 6, November-December 1983.

31. Ragazzini, J. R. and Franklin, G. F., Sampled Data Control Systems, McGraw-Hill, New York, 1958.

32. Rao, G. V., Complex Digital Control Systems, Chapters 1 and 3, Van Nostrand

Reinhold Company, New York, 1979.

33. Schmidt, E., *"Experiments on the End Point Position Control of a One Link Very Flexible Manipulator"*, Ph. D. Thesis, Stanford University Department of Aeronautics and Astronautics, Stanford, California, SUDAAR No. 548, July 1985.

34. Sklansky, J., *"Network Compensation of Error-Sampled Feedback Systems"*, Ph.D. Thesis, Department of Electrical Engineering, Columbia University, New York, 1955.

35. Sklansky, J. and Ragazzini, J. R., *"Analysis of Errors in Sampled-Data Feedback Systems"*, Part II AIEE Transactions, Vol. 74, May 1955.

36. Sun, J., Ph. D. Thesis, Stanford University Department of Aeronautics and Astronautics, Stanford, California, Work in Progress.

37. Thompson, P. M., Stein, G. and Athans, M., *"Conic Sectors for Sampled-Data Feedback Systems"*, Systems and Control Letters, Vol. 3, No. 2, July 1983.

38. Van Loan, C. F., *"Computing Integrals Involving the Matrix Exponential"*, IEEE Transactions on Automatic Control, Vol. AC-23, June 1978.

39. Walton, V. M., *"State Space Stability Analysis of Multirate-Multiloop Sampled Data Systems"*, AAS/AIAA Astrodynamics Specialist Conference, Paper No. 81-201, August 1981.

40. Whitbeck, R. F. and Didaleusky, D. G. J., *"Multirate Digital Control Systems with Simulation Applications"*, Vol. I, II, III, Technical Report, Computer Algorithms, Source Listing, No. AFWAL-TR-80-3031, Systems Technology, Inc., Hawthorne, California, 1980.

41. Whitbeck, R. F., Didaleusky, D. G. J. and Hofman, L. G., *"Frequency Response of Digitally Controlled Systems"*, AIAA Journal of Guidance and Control, Vol. 4, No. 4, July-August 1981.